Timur Bikmukhametov

Machine Learning and First Principles Modeling Applied to Multiphase Flow Estimation

with a focus on the oil and gas industry

Thesis for the degree of Philosophiae Doctor

Trondheim, December 2020

Norwegian University of Science and Technology
Faculty of Natural Sciences
Department of Chemical Engineering

NTNU

Norwegian University of Science and Technology

Thesis for the degree of Philosophiae Doctor

Faculty of Natural Sciences
Department of Chemical Engineering

ISBN (printed version)
ISBN (electronic version)
ISSN 1503-8181

Doctoral theses at NTNU,

Printed by NTNU-trykk

Contents

Abstract

Accurate knowledge of multiphase flowrates produced by each well in an oil and gas production system is important for performing production optimization, flow assurance and reservoir management. Among the alternatives, estimation methods, often referred as Virtual Flow Metering, are promising in terms of high level of accuracy given the low cost of the solution. Virtual Flow Metering systems use readily available field measurements and estimate multiphase flowrates by means of mathematical modeling of a production system.

The main objective of this work is to review the current state-of-the-art multiphase flowrate estimation methods and further develop new estimation solutions based on combining physical knowledge about petroleum production systems and machine learning techniques.

The literature review shows that current approaches for creating Virtual Flow Metering systems mostly rely on first principles models of petroleum production system parts. However, despite the reasonable accuracy of these models, their estimation uncertainty and sensitivity to erroneous field measurements has not been studied in detail yet. We address this issue in Chapter 4, where, in the first part, we create a first principles Virtual Flow Metering system based on a commercial multiphase flow software and optimization engine and study the sensitivity of the resulting solution to erroneous field measurements. In the second part, we investigate how Bayesian Machine Learning can help in uncertainty estimation of first principles multiphase flow models based on the available field data.

In addition, the literature review shows that applications of machine learning to multiphase flowrate estimation problems are promising and have been gaining momentum in the last several years. However, in the vast majority of cases, the created machine learning Virtual Flow Metering solutions are based on feed-forward

neural networks which use raw field data without any multiphase flow physics consideration. This results in black-box solutions which are hardly used in industry because productions engineers do not trust the produced results. We address this problem in Chapter 3, where, in addition to feed-forward neural networks, we investigate capabilities of gradient boosting machine learning algorithm and recurrent neural networks, and combine them with multiphase flow physics to create accurate and explainable data-driven Virtual Flow Metering solutions.

The results of this work show that first principles Virtual Flow Metering systems are very sensitive to measurement drift, and production engineers must carefully address this issue when tuning the software to the available field measurements. In addition, it was revealed that by combining Bayesian machine learning methods with first principles modeling, it is possible not only to tune first principles models to field conditions accurately, but also quantify the estimation uncertainty depending on the distribution of the historical data as well as process conditions. As a result, it becomes possible to understand when there is a need for model recalibration or performing condition maintenance.

This work also demonstrates that by combining machine learning with first principles models, it is possible to create robust hybrid multiphase flow estimation solutions with enhanced accuracy and explainability of the resulting data-driven models.

The results from this work can further be extended towards more advanced combinations of machine learning methods and first principles models, especially for dynamic process conditions. In addition, various combinations of Bayesian machine learning approaches with first principles modeling can further be developed in order to create a basis for robust, trustworthy and auto-tunable models applied to multiphase flowrate estimation tasks.

Acknowledgments

Pursuing a PhD degree at NTNU was one the best decisions in my life. To be precise, it was not even a decision but an opportunity that I was given by professor Johannes Jäschke. I was checking-in at a hotel in Vienna during a business trip, working for a good company with great people but doing a job that I never liked. I was entering the hotel room when I received the e-mail with the offer from Johannes. Since then my life has changed completely, and now I am following the career and life path that I have never dreamed of. As such, I would like to thank my supervisor Johannes Jäschke for giving me such a great project and an opportunity to choose the research directions and methods I was interested in. Our collaboration has been converging to the global optimum over the years, sometimes jumping over but finally finding it by the last year of the PhD. I truly believe that it is not the end, and we will have a chance for working together and continue our fruitful discussions and existing work in the future. Thank you for everything and more.

I also want to thank professor Milan Stanko for great discussions and collaboration throughout my PhD time. You always had your doors open since my Master's time at NTNU, and it was always a pleasure to work with and learn from you. It was also great to supervise brilliant students together and feel engaged in their development.

I am very much grateful to SUBPRO for the financial support, opportunity to travel anywhere I wanted to and the great events we had together. I am also thankful to the SUBPRO industry partners, especially to Equinor and Audun Faanes, for the constant support, field data providing and opportunities to present my work and discuss the results in the industrial environment.

I also would like to thank the process engineering group which I was lucky to be part of. I felt privileged to share my office with brilliant researchers and great people as Dinesh, Adriaen, Christoph, Jose, Eka, Ana, Allyne and Tamal. It was

great to had lunches, group meetings, conferences and talks together with Mandar, Christina, Fabienne, Adriana, Julian, Bahareh, Pedro, Haakon, Brian, Tobias, Cansu, David, Lucas, Andrea and Zawadi. Thank you all for making my stay in the group fun and happy.

I am extremely grateful to my parents, Ildar and Galina, for their constant support and everything they have done for me. All I have now is because of you. Thanks to my sister, Kate, for her love and care, and especially for hosting me at 4 a.m. every time when coming from Trondheim to Moscow.

Finally, I want to thank my amazing wife, Svetlana, for being my love, my life and my friend. Far away in Russia or in our cozy place in Trondheim, at any single hard moment, over all these years, your smile, care and love helped me to keep my head up and look ahead with confidence. You are the greatest win of my life.

Chapter 1

Introduction

This chapter gives an introduction and motivation for the conducted PhD work. Also, the structure of the thesis is presented. The journal and conference publications are listed together with the list of presentations and poster contributions given by the author during the PhD time.

1.1 Motivation

Oil and gas are still among major energy resources and this situation is not going to be changed significantly in the near future (Zou et al. (2016)). As such, oil and gas companies become more and more concerned about safe, reliable and efficient operation of petroleum fields to stay competitive on the energy resources market to extend this trend. However, in practice, it is often difficult to maintain efficient operation of petroleum systems because it includes handling various complex physical phenomena. It is even more difficult in offshore and subsea environment due to the difficulty of the production facility access, high cost of the operation and influence of the sea conditions, for instance, low temperature and high loads on the infrastructure. A typical offshore production system with subsea wells is shown in Figure 1.1.

In the shown system, typically, the produced petroleum fluid has the form of a multiphase flow which can consist of oil, gas and water (Bendiksen et al. (1991)). In many cases, sand and other solid particles may exist in the flow (Leporini et al. (2019)). In order to produce oil and gas from a reservoir in a safe, reliable and efficient manner, it is essential to know the produced multiphase volumetric flowrates in the real time or close to the real time scale. This is because it enables identification of unstable well behavior, efficient reservoir management and production

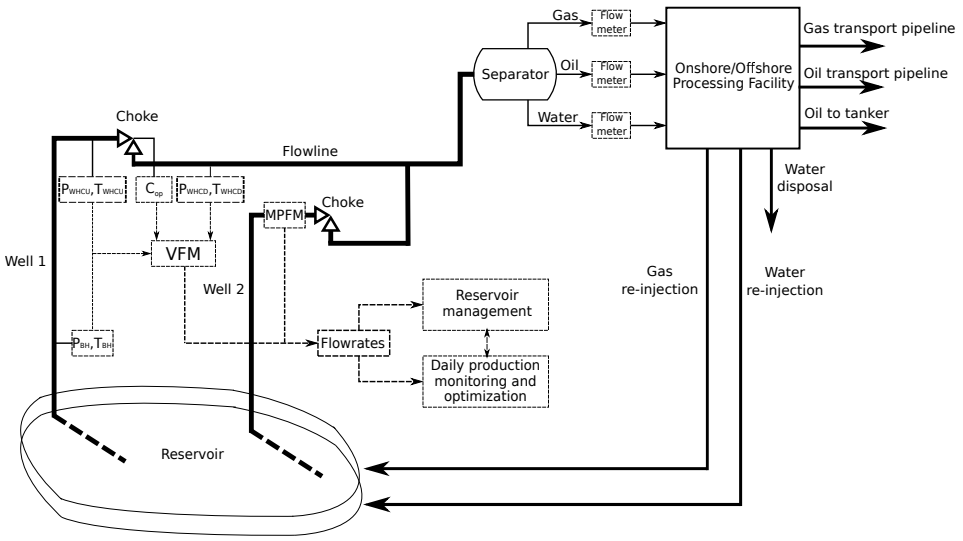

Figure 1.1: Schematic representation of a typical offshore production system with subsea wells with a multiphase flow meter (MPFM) and a Virtual Flow Meter (VFM) together with available measurements and typical production and processing stages. In the measurements, P denotes the pressure, T- the temperature, BH - bottomhole, WHCU - wellhead choke upstream, WHCD - wellhead choke downstream, C_{op} - the choke opening.

optimization (Falcone et al. (2001; 2009)). Apart from that, multiphase flowrates are typically used as boundary conditions to fluid dynamics and flow assurance models. These models are used to describe undesirable situations in production systems and prevent them when possible (Bendiksen et al. (1991)).

In addition to the technical side, for small petroleum fields which are tied-in to existing infrastructures, it is crucial to know by which margin they increase the overall produced volume which is measured by fiscal meters at the offshore platform outlet. This is because it will largely impact the income of the assets owners.

One of the main solutions to the multiphase flow production monitoring problem is installation of hardware multiphase flow meters (MPFMs), shown in Figure 1.1, installed at the well on the right (Well 2). This is a special device which measures the gas, oil and water flowrates in real time using various techniques, for instance, gamma-rays. Such measurements are then used in correlations together with fluid properties, so called Pressure-Volume-Temperature (PVT) data, to estimate the flowrates of each multiphase flow phase (Falcone et al. (2009)).

Despite being a relatively accurate source of multiphase flowrate estimates, MP-

FMs are prone to degradation, drifting and have a certain limited operational envelope (Falcone et al. (2009)). As such, they require expensive calibrations using test separators. The frequency of the calibration varies from 3 to 12 months depending on the field conditions. However, the main drawback of MPFMs is the price which varies from 0.5 to 1.5 million dollars depending on if it is supposed to be installed onshore or subsea.

An alternative to MPFMs is a mathematical model which estimates the flowrates. Such a multiphase flowrate estimation tool is usually called Virtual Flow Meter (VFM) (Parthasarathy et al. (2016)), shown in Figure 1.1, applied at the well on the left (Well 1). A Virtual Flow Meter uses sensors already installed in the field (examples of the sensors are shown in Figure 1.1) and some historical flowrate measurements produced by test separators or any other reliable source of flow information in order to construct and tune the mathematical model. The main advantage of using a Virtual Flow Meter instead of a MPFM is the cost reduction of the multiphase flow monitoring system.

Despite the fact that Virtual Flow Metering technology has been being developed for almost 25 years, there has not been done a comprehensive review on this topic which resulted in the fact that it is still unclear how to construct a model of an oil and gas field which gives robust and accurate estimates of the flowrates. This is especially challenging under conditions when the measurements, which VFM systems rely on, degrade over time. In this case, VFM systems will typically become biased until tuned against the separator measurements. All this was the reason for performing a detailed literature review on the multiphase flowrate estimation topic and identifying directions for future development of accurate and robust multiphase flowrate estimation systems for oil and gas production fields.

Nowadays, in the era of machine learning being applied to many process engineering problems, it is very interesting to investigate how these techniques can help us to construct multiphase flow estimation tools which produce accurate estimates. It is also interesting to see if we are able to include knowledge of multiphase flow modeling into machine learning techniques to make flowrate estimates more accurate. Such a promising research direction at the border of mechanistic and data-driven modeling has formed the second motivation for performing this work.

Another issue that has not been well addressed so far is investigation of sensitivity of first principles Virtual Flow Metering systems to degraded field measurements and the associated estimation uncertainty. Moreover, the general problem of uncertainty estimation of first principles multiphase flows models that are tuned to field conditions has not been well described yet. These facts gave motivation to explore this problem in this work and address it using Bayesian Machine Learning

techniques.

1.2 Main contributions and the thesis structure

The thesis is organized in a paper-based format and includes five chapters. In Chapter 1, motivation for performing this PhD work is described. The other chapters present the main contributions of the work which are the following:

1. A comprehensive overview of the currently available methods on the topic of multiphase flow estimation. This is presented in Chapter 2.
2. Development and investigation of new Virtual Flow Metering solutions that are based on combinations of first principles and machine learning modeling which result in accurate and explainable data-driven solutions. This part of the work is described in Chapter 3.
3. Methods for uncertainty estimation of first principles and hybrid data-driven multiphase flow models, applied to multiphase flow modeling and estimation based on sensitivity analysis and Bayesian Machine Learning techniques. This contribution is presented in Chapter 4.

Finally, in Chapter 5, concluding remarks are made and recommendations for future work are suggested.

1.3 List of publications

I Bikmukhametov, T. and Jäschke, J. (2019). First principles and machine learning virtual flow metering: a literature review. *Journal of Petroleum Science and Engineering*, Volume 184, 106487, 3037–3043, doi.org/10.1016/j.petrol.2019.106487

II Bikmukhametov, T., and Jäschke, J. (2019). Oil Production Monitoring using Gradient Boosting Machine Learning Algorithm. *IFAC-PapersOnLine*, Volume 52(1), 514-519, doi.org/10.1016/j.ifacol.2019.06.114

III Bikmukhametov, T., and Jäschke, J. (2020). Combining Machine Learning and Process Engineering Physics Towards Enhanced Accuracy and Explainability of Data-Driven Models. *Computers and Chemical Engineering*, Volume 138, 10683, doi.org/10.1016/j.compchemeng.2020.106834

IV Bikmukhametov, T., Stanko, M., and Jäschke, J. (2018). Statistical Analysis of Effect of Sensor Degradation and Heat Transfer Modeling on Multiphase Flowrate Estimates from a Virtual Flow Meter. *In SPE Asia Pacific*

Oil and Gas Conference and Exhibition. Society of Petroleum Engineers, doi.org/10.2118/191962-MS

V Bikmukhametov, T., and Jäschke, J. Uncertainty Estimation of Mechanistic First Principles Models and Digital Twins Using Bayesian Machine Learning. *Submitted to Engineering Applications of Artificial Intelligence, 2020.*

1.4 List of conference and workshop presentations and poster contributions

Bikmukhametov T. and Jäschke J. (2018). *Analysis of Influence of Sensor Degradation on Flowrate Estimates by Virtual Flow Metering Systems*. Presentation at Nordic Process Control Conference. Abo Akademi, Finland

Bikmukhametov T. and Jäschke J. (2019) *Physics-Aware Machine Learning Algorithms with Improved Accuracy and Explainability Applied to Multiphase Flowrate Estimation*. AIChE Annual Meeting, Orlando, USA.

Bikmukhametov T., Jäschke J. (2019) *Physics-Aware Machine Learning in Multiphase Flow Estimation*. Poster at Nordic Process Control Conference. Technical University of Denmark, Denmark

Bikmukhametov T. (2019). *Using First Principles Modeling in Machine Learning VFM*. Presentation at IOC and BP workshop on daily production optimization. Rio de Janeiro, Brazil.

References

Bendiksen, K.H., Maines, D., Moe, R., Nuland, S., et al., 1991. The dynamic two-fluid model olga: Theory and application. SPE production engineering 6, 171–180.

Falcone, G., Hewitt, G., Alimonti, C., 2009. Multiphase flow metering: principles and applications. volume 54. Elsevier.

Falcone, G., Hewitt, G., Alimonti, C., Harrison, B., et al., 2001. Multiphase flow metering: current trends and future developments, in: SPE annual technical conference and exhibition, Society of Petroleum Engineers.

Leporini, M., Marchetti, B., Corvaro, F., di Giovine, G., Polonara, F., Terenzi, A., 2019. Sand transport in multiphase flow mixtures in a horizontal pipeline: An experimental investigation. Petroleum 5, 161–170.

Parthasarathy, P., Mai, M., et al., 2016. Bridging the gap between design world and online, real-time, dynamic simulation world, in: Offshore Technology Conference, Offshore Technology Conference.

Zou, C., Zhao, Q., Zhang, G., Xiong, B., 2016. Energy revolution: From a fossil energy era to a new energy era. Natural Gas Industry B 3, 1–11.

Chapter 2

Literature Review of Multiphase Flowrate Estimation Methods (Paper I)

This chapter consists of Paper I, which is a comprehensive review of multiphase flow estimation methods referred as Virtual Flow Metering technology. It gives an overview of the applied methods, which have been reported in the literature, commercial products, field experience, comparison between different flow estimation methods and future directions for the research and development of the technology.

Bikmukhametov, T. and Jäschke, J. (2019). First principles and machine learning virtual flow metering: a literature review. Journal of Petroleum Science and Engineering, Volume 184, 106487, 3037–3043, doi.org/10.1016/j.petrol.2019.106487

Journal of Petroleum Science and Engineering 184 (2020) 106487

Contents lists available at ScienceDirect

Journal of Petroleum Science and Engineering

journal homepage: www.elsevier.com/locate/petrol

First Principles and Machine Learning Virtual Flow Metering: A Literature Review

Timur Bikmukhametov, Johannes Jäschke*

Department of Chemical Engineering, Norwegian University of Science and Technology, 7034, Sem Sælandsvei 4, Trondheim, Norway

ARTICLE INFO

Keywords:
Virtual flow metering
Multiphase flow modeling and estimation
Machine learning
Oil and gas production monitoring

ABSTRACT

Virtual Flow Metering (VFM) is an increasingly attractive method for estimation of multiphase flowrates in oil and gas production systems. Instead of using expensive hardware metering devices, numerical models are used to compute the flowrates by using readily available field measurements such as pressure and temperature. Currently, several VFM methods and software are developed which differ by their methodological nature and the industry use. In this paper, we review the state-of-the-art of VFM methods, the applied numerical models, field experience and current research activity. In addition, we identify gaps for future VFM research and development. The review shows that VFM is an active field of research, which has the potential to be used as a standalone metering solution or as a back-up for physical multiphase flow meters. However, to increase the value of VFM technology for oil and gas operators, future research should focus on developing auto-tuning and calibration methods which account for changes of fluid properties and operation conditions. In addition, the review shows that the potential of machine learning methods in VFM is not fully revealed, and future research should focus on developing robust methods which are able to quantify flow estimation uncertainties and incorporate first principle models that will result in more accurate and robust hybrid VFM systems. Finally, our review reveals that dynamic state estimation methods combined with first principles and machine learning models could further improve the VFM accuracy, especially under transient conditions, but implementation of these methods can be challenging, and further research is required to make them robust.

1. Introduction

An oil and gas production system typically consists of a number of wells which are connected to a flowline which carries the produced fluid from wellheads to an inlet separator of a processing facility. If the field is subsea, the flowline is connected with the inlet separator via a riser. The flowrate of the produced fluid is controlled by choke valves installed at the wellheads. A schematic representation of a typical subsea production system is shown in Fig. 1, where an example with two wells is shown for simplicity. In the vast majority of cases the production field consists of more wells. In this example, we also include an electric submersible pump (ESP) as an example of artificial lift, however, other methods may also be used for this purpose, for instance, gas lift (Rashid et al., 2012). Typically, the produced fluid is a multiphase mixture of oil, gas, water and solids such as sand or asphaltenes (Falcone et al., 2009). This mixture is split into single phases in the inlet separator and further processed at a processing facility.

For economic operation of the production systems, it is important to know the oil, gas and water flowrates from each well. It allows operators to make critical decisions in production optimization, rate allocation, reservoir management and predict the future performance of the field (Retnanto et al., 2001; Morra et al., 2014; Falcone et al., 2001). At the early stage of the industry, the main method to estimate well flowrates was well testing. Here, a well stream is directed into a test separator where it is split into oil, gas and water. These flow streams are then measured by single-phase meters at the separator outlet (Corneliussen et al., 2005). The test separators require a separate flowline, so that each well can be routed to the test separator and tested without shutting-down the entire field. As an alternative, the flowrates can be estimated by the use of an inlet separator. In this case, two options are possible. The first option is to shut-down all the wells except the tested one, so that the flowrates of this well can be estimated. This option is associated with a large production loss and often economically undesirable. Another possibility is to close the well of interest, measure the flowrates of the producing wells at the separator conditions and then back-calculate the flowrates of the closed well. This is done by subtracting the obtained flowrates from the ones recorded before the well test. This method is called deduction well testing (Idso et al.,

* Corresponding author.
E-mail address: johannes.jaschke@ntnu.no (J. Jäschke).

https://doi.org/10.1016/j.petrol.2019.106487
Received 1 March 2019; Received in revised form 5 July 2019; Accepted 9 September 2019
Available online 10 September 2019

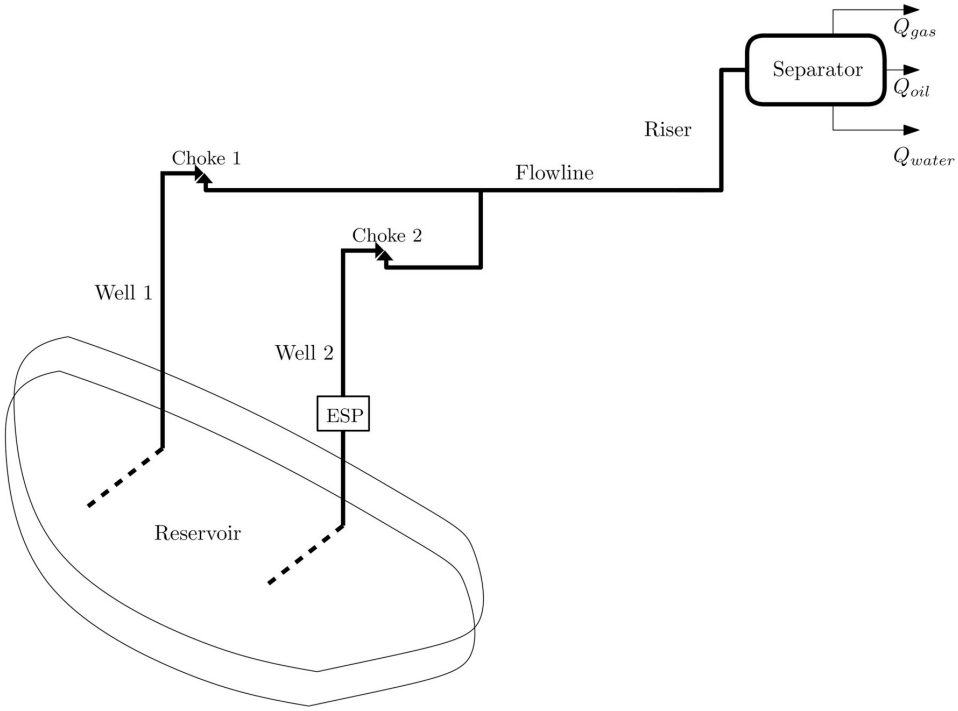

Fig. 1. Schematic representation of a typical subsea oil and gas production system.

2014). In all the described options, stable operating conditions need to be achieved in order to measure the flowrates, which might require several hours depending on the distance between the well and separator. In addition, the act of closing one well affects the performance of other wells which may result in inaccurate flowrate estimations (Falcone et al., 2001; Idso et al., 2014).

Over the last 25 years, physical multiphase flow meters (MPFMs) have been developed as an alternative solution to well testing to measure well multiphase flowrates and were first commercialized in the early 1990s (Falcone et al., 2001). The core idea behind MPFMs is to estimate oil, gas and water flowrates without separating the phases. These meters are usually installed at the wellhead, so that the multiphase flowrates from a particular well can be tracked in real-time. The flowrates are calculated indirectly using supplementary measurements of fluid phase properties such as velocities and phase fractions inside the device (Falcone et al., 2001; Gryzlov, 2011). An extensive effort was made to develop accurate multiphase flow meters and several technologies have been used for this purpose such as acoustic attenuation, impedance and gamma densitometers (Falcone et al., 2001). A number of review articles exist, in which the applied methods, principles, governing equations and measurement strategies are discussed in details (Corneliussen et al., 2005; Falcone et al., 2009; Thorn et al., 2013).

Both aforementioned flowrate measurement techniques have their advantages and disadvantages. First of all, well testing requires a separate flowline and a separator, which results in high capital costs of the field development (Falcone et al., 2001). If the inlet separator is used as a test separator, the cost associated with the production loss can be significant due to closing the well of interest. Sometimes, deduction testing may be impossible to perform due to potential flow assurance problems (Melbø et al., 2003). Despite these facts, well testing measurements are still widely used in oil and gas production monitoring, even if multiphase flow meters are installed in the field. The reason for this is that the flowrate measurements from well tests are used as a reference to calibrate multiphase flow meters and extract information about the fluid properties (Corneliussen et al., 2005).

In contrast to well testing, MPFMs provide real-time information about the well flowrates. This is definitely advantageous from an operational point of view. However, MPFMs are quite expensive and require an intervention in case of a failure, which adds a significant operational cost (Falcone et al., 2001; Patel et al., 2014). Moreover, MPFMs have a specific operation range beyond which the accuracy of the flowrate estimates can decrease significantly. Apart from this, the meters may face degradation due to sand erosion or partial blockage which also has an impact on the measurement accuracy (Marshall and Thomas, 2015).

Considering the discussed challenges as well as associated costs for both flow measurement approaches, an alternative solution is Virtual Flow Metering (VFM). The idea behind VFM is to collect available field data and use it in a numerical model to estimate flowrates (Rasmussen, 2004; Toskey, 2011). The measurement data usually include:

- Bottomhole pressure and temperature (P_{BH} and T_{BH}).
- Wellhead pressure and temperature upstream of the choke (P_{WHCU} and T_{WHCU}).
- Wellhead pressure and temperature downstream of the choke (P_{WHCD} and T_{WHCD}).
- Choke opening (C_{op}).

In contrast to well testing and MPFMs, VFM systems do not require installation of an additional hardware, as such they can reduce the capital and operational costs of the field development. At the same time, VFM systems have capabilities to estimate the flowrates in real time and reflect changes of flow conditions accordingly. This is a clear advantage compared to the well testing approach which assumes constant well flowrates between the tests (Marshall and Thomas, 2015). Moreover, VFM can be used as a standalone solution, or in a

combination with a MPFM as a back-up system such that it can use the information from a MPFM to further improve the flowrate estimates (Holmås et al., 2013).

Despite the amount of work done on Virtual Flow Metering and the diversity of applicable methods and models, there is a lack of an overview of this. In this paper, we fill this gap and cover the following objectives:

- Summarize and classify VFM methods, models and computational procedures.
- Distinguish the differences among the VFM vendors based on publicly available resources.
- Review the reported VFM field experience and the research activity.
- Identify gaps and propose directions for future VFM research and development.

We believe that this paper will be an asset for readers who want to get an overview of available VFM solutions, implement the existing commercial VFM solutions in the field, construct an own VFM or improve the already created one.

Our paper is organized as follows. First, we introduce the main VFM approaches which are applied in industry or developed for research purposes. Then, we explain each VFM method in detail by providing the main concepts behind it, the models used, the available market products as well as reported field experience and the current status of the academic research. Finally, we compare the methods and specify their advantages and disadvantages and propose directions for the future research and development of the VFM systems.

2. VFM methods

Over the last 20 years, the concept development of VFM resulted in various methods to estimate the multiphase flowrates using available field data, and several companies have developed commercial VFM systems which are used by oil and gas operators around the world. Some methods are currently emerging and aiming to improve the accuracy of the flowrate predictions, while yet other methods are currently not used in the industry but have a good potential to move the VFM development forward in the future.

Based on modeling paradigms, two main Virtual Flow Metering approaches can be distinguished:

- First principles VFM
- Data-driven VFM

The first principles VFM systems are based on mechanistic modeling of multiphase flows in the near-well region, wells, pipelines and production chokes (Holmås and Løvli, 2011). The models are used together with the measurements such as pressure and temperature to find accurate estimates of the flowrates. An optimization algorithm adjusts the flowrates and other tuning parameters to minimize the mismatch between the model predictions and real measurements (Holmås and Løvli, 2011). The production system can be modelled as a whole from the reservoir to the processing facility, or it can be separated into submodels depending on the available measurement data. First principles models are currently used in most commercial Virtual Flow Metering systems.

The data-driven VFM approach is based on collecting the field data and fitting a mathematical model to it without the exact description of the physical parameters of the production system such as a wellbore and choke geometry, flowline wall thickness, etc. This approach is also referred to as “machine learning” modeling and it has become very popular in the past several years, not only for oil and gas applications but for many other applications as well. In this paper, we will call this approach “data-driven” modeling because in many VFM related publications it was named with this definition. In data-driven modeling, the fitting process is often called training (Hastie et al., 2009). If the model is well trained and the exposed conditions are within the range used for the training, the data-driven model can perform fast and accurate real-time metering. In this approach, deep domain knowledge of production engineering is not as important as in the first principles models and the model can be constructed at a lower cost.

In addition to the classification based on the modeling principles, we may classify approaches based on how time dependency is included in the model. Based on this, the following sub-classification can be performed:

- First principles VFM – steady state and dynamic models
- Data-driven VFM – steady state and dynamic models

In the first principles VFM, conservation equations often have a dynamic form, however, the formulation of the optimization problem is steady state or quasi-steady state, so that an optimization solver finds the solution for only one point in time or takes the solution from the last step as an initial guess for the current time step prediction. In some cases, even the conservation equations take steady state form or do not consider time because of its nature, for instance, a choke model (Perkins, 1993). While it is possible to formulate the VFM optimization problem in a dynamic way, in the available literature on the first principles VFM does not consider this approach. The main reason for this may be the fact that dynamic optimization for first principles VFM systems is computationally very expensive (Lew and Mauch, 2006). On the other hand, such methods may have been utilized but not discussed in the literature.

Apart from dynamic optimization, state estimation techniques such as Kalman filter approaches can be used in order to create a dynamic VFM (De Kruif et al., 2008). This approach has been covered in the research as we will show in the future sections, however, it is not implemented in the commercial software yet. The main reason for this may be that it requires a high expertise for setting up and using, and it can be difficult to tune in a robust manner for real field data.

For the large majority of data-driven algorithms used for VFM, the model formulation is steady state, so that the algorithms consider pressure and temperature measurements in one point in time to predict the flowrates at the same time step. At the same time, there are data-driven algorithm structures which have a dynamic formulation, so that measurements from the past may also be used to estimate the flowrate at the current time step and some of these algorithms have recently been studied for VFM applications. In the next sections, we consider each VFM paradigm in more detail and explain the considerations of dynamic system behavior by each method based on the used models and algorithms.

3. First principles VFM systems

3.1. An overview of the concept

The first principles VFM systems are the most widely used Virtual Flow Meters in the industry. This is because a tremendous effort was made over the past 50 years in order to describe each part of this VFM approach. This resulted in a quite good understanding of the mechanistic modeling of production systems, fluid properties and optimization techniques. As such, first principles modeling can be considered as a reliable way to describe the production system behavior in general, and multiphase flow phenomena in particular. In this section, we will describe the main concept behind the first principles VFM. In the later sections, each model used in the concept is discussed in more detail.

A current state-of-the-art first principles VFM system consists of the following main components:

- Fluid properties model.
- Production system model including:

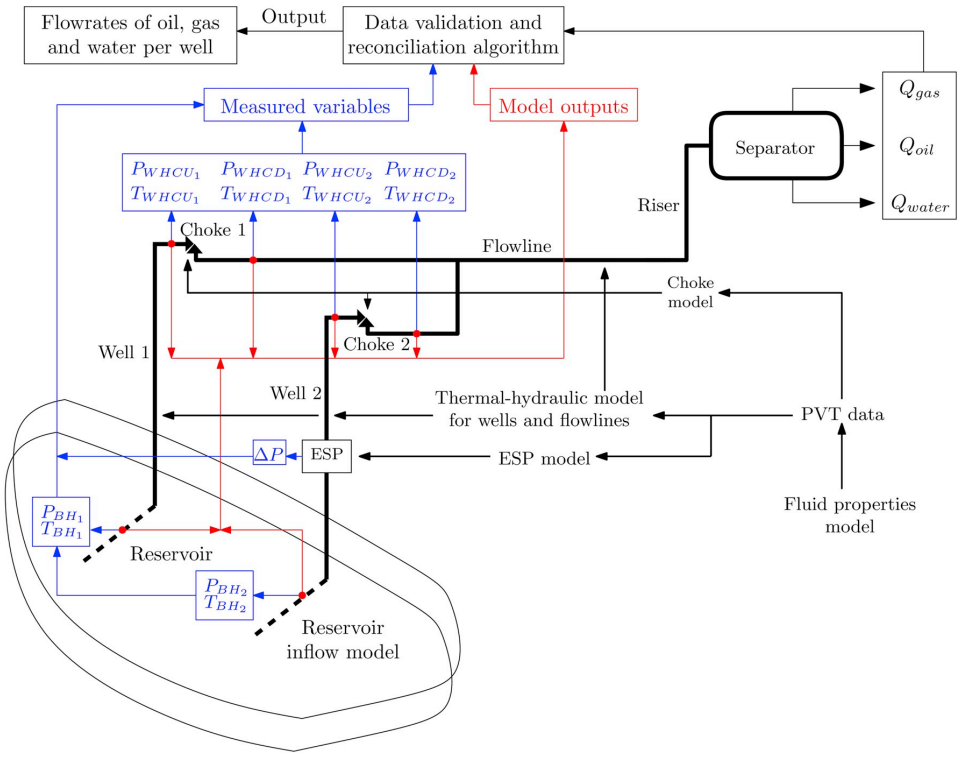

Fig. 2. Schematic overview of a first principles Virtual Flow Metering system. Thermal-hydraulic, choke, ESP and reservoir inflow models use pre-generated PVT data in order to predict the system variables such as pressures and temperatures along the system. The data validation and reconciliation algorithm adjusts the model parameters (flowrates, choke discharge coefficient, etc.) such that the model outputs (red color) match the measurements from the physical system (blue color) and the overall material balance (flowrates measured at the separator outlet). (For interpretation of the references to color in this figure legend, the reader is referred to the Web version of this article.)

- Reservoir inflow model
- Thermal-hydraulic model
- Choke model
- Electric submersible pump (ESP) model

• Data validation and reconciliation (DVR) algorithm.

The main idea behind the first principles VFM system is depicted in Fig. 2 where the concept is applied for the production system shown in Fig. 1. First, the thermal-hydraulic, choke, ESP and reservoir inflow models produce model outputs which can be pressures and temperatures along the production system. To do that, the models require pre-generated pressure-volume-temperature (PVT) data which describe the fluid properties under given conditions and generated using fluid properties models. The popular forms of the fluid properties model are Equations of State (EoS) and Black Oil model (BOM) which will be described further below.

Next, the measured field data is processed by the data validation and reconciliation algorithm. In the DVR, first, the data are validated which can include removal of outliers and noise filtering. Then, in the reconciliation step the model parameters (e.g. flowrates, choke discharge coefficient, gas and water fractions, friction and heat transfer coefficients, slip relation, etc.) are adjusted such that the model outputs (in red in Fig. 2) match the measurements from the physical system (in blue in Fig. 2) and the overall material balance (flowrates measured at the separator outlet).

In summary, for VFM using the first principles models, the following steps are taken:

1 Create a fluid properties model which represents the fluid data accurately.
2 Choose appropriate production system models based on the available measurements.
3 Read and validate the measurement data, remove outliers and filter noise.
4. Select appropriate tuning parameters, for instance, flowrates, choke discharge and heat transfer coefficients, etc. and make a guess of the initial parameter values.
5. Simulate the models selected at step 2 using the fluid properties from step 1 and initial values of the tuning parameters from step 4.
6. Select the model outputs from step 5 for which the measurements are available, for instance, pressures and temperatures at the bottomhole and the wellhead.
7. Run the data reconciliation algorithm to minimize the mismatch between the model outputs from step 6 and the validated measurement data from step 3 by adjusting the tuning parameters selected at step 4.
8. Report the oil, gas and water flowrates for each well from the solution from step 7.

3.2. Commercial first principles VFM systems

To discuss the details behind each component of the first principles VFM, we consider commercial VFM systems which are based on this approach. The reason for this is that these systems use the most advanced methods and models which are currently applied in VFM

Table 1
Commercial first principles VFM systems.

Virtual Flow Metering system	Vendor
OLGA Online	Schlumberger
K-Spice Meter (K-Spice + LedaFlow)	KONGSBERG
FlowManager	FMC
Well Monitoring System (WMS)	ABB
Virtuoso	WoodGroup
FieldWatch + METTE	Roxar
ValiPerformance	Belsim
Rate&Phase	BP

technology. At the same time, the discussion gives an overview of the model variations among the software as well as the available products on the market. As such, we believe by describing the models and capabilities of the commercial software, we will be able to better evaluate the current state of the VFM technology development.

In our review, we will consider the methods and models of the commercial VFM systems listed in Table 1. All these products have conceptually the same structure, i.e. utilize fluid properties and production system models together with the data validation and reconciliation algorithm to estimate the multiphase flowrates. It is also important to mention other VFM suppliers which are not included in the list. Ensys Yocum delivers VMSS3 Virtual Flow Meter but the information about it in the literature is very limited, so that it is hard to evaluate software's features precisely. TurbulentFlux is currently an emerging company which supplies a state-of-the-art VFM product. As the company is at the starting phase, the information about the software is not publicly available yet, as such we do not consider it in the further analysis.

In addition to the listed software, there are several other software which could potentially be considered as a VFM system, but they are not considered in this paper in details. For instance, Amin (2015) used Prosper (PETEX, 2017) as a Virtual Flow Meter. Prosper is a software which describes performance of wells and production systems under various conditions and extensively used in the petroleum industry. The software has a variety of reservoir inflow, choke and hydrodynamic models linked to PVT data to evaluate production performance of wells (PETEX, 2017) However, in this paper we do not consider Prosper as a fully integrated VFM system because, according to the software description, it does not include the DVR algorithm to fit specific field measurement conditions. In addition, there are no other studies or papers which evaluate Prosper as a VFM system. Mokhtari and Waltrich (2016) used PIPESIM as a Virtual Flow Metering system to evaluate different models for VFM purposes. PIPESIM is a steady state multiphase flow simulator supplied by Schlumberger which delivers OLGA Online as a VFM product which we consider in this study. As such, PIPESIM is not considered as Schlumberger's VFM system in this study, but potentially can be utilized for VFM purposes.

In the next section, we will consider the components of the first principles VFM products from Table 1 in more detail. More specifically, we will emphasize the mathematical description of the models and the usage of a particular model type in a particular VFM product.

3.3. Description of the first principles VFM components and applied methods

In this section, we consider the components of the first principles VFM systems in more detail. First, we will discuss the fluid properties model together with subsequent PVT data generation. Then, we will show what the principles behind the production system models are and how the PVT data is used for in these models. Finally, we will discuss how the data validation and reconciliation algorithm finds optimum flowrate estimates. Throughout the description of the models, we will discuss its implementation in the commercial VFM products.

3.3.1. Fluid properties model

Hydrocarbon mixtures are complex substances whose properties vary with local pressure and temperature conditions along the production system. In order to take these variations into account, fluid characterization is carried out based on fluid samples taken at different points such as downhole or at the separator (Whitson and Brule, 2000). Based on the characterized fluid, a pressure-volume-temperature (PVT) data can be generated which is then used by VFM systems for two purposes (Falcone et al., 2009):

- Calculating local phase properties of the hydrocarbon mixtures such as density, viscosity, thermal conductivity, etc. for using in the first principles models.
- Reconciling reference flowrate measurements (e.g. at separator or standard conditions) with flowrate measurements/estimates at local conditions (e.g. at the wellhead).

As for the first point, the local fluid properties have a direct influence on the flowrate predictions by a VFM system because they are included in thermal-hydraulic conservation equations as well as the models of choke, ESP and reservoir inflow. As such, giving incorrect phase densities or enthalpies for certain pressures and temperatures to the VFM system will result in deviations between the predicted and actual flowrates. This in turn will cause problems in finding a good solution by the data validation and reconciliation algorithm when tuning flowrates and other model parameters.

Regarding the second point, when the local flowrates are calculated, they are usually reported at reference conditions for reconciliation, production and sales reporting purposes (Pinguet et al., 2005). Reconciliation is especially important in fields with commingled wells, so that the overall measured production rates at the separator conditions can be back-allocated (reconciled) to the individual wells as shown in Fig. 2.

Fluid characterization is typically done by two approaches separator (Whitson and Brule, 2000; Falcone et al., 2009):

- Black Oil model.
- Compositional model.

These two models are discussed below.

3.3.1.1. Black Oil Model (BOM). Black Oil model is a simple, yet useful approach for petroleum fluid characterization. In this approach, oil and gas are treated as two separate substances and their properties are calculated based on correlations (Whitson and Brule, 2000). In the traditional formulation of the BOM, three main PVT properties are considered: oil formation volume factor, gas formation volume factor and solution gas-oil ratio. For volatile hydrocarbon mixtures, modified Black Oil models (MBOM) are developed which introduce another core variable called solution oil-gas ratio. If water is present in the produced fluid, additional properties such as water formation volume factor, solution gas-water ratio and water content in gas are introduced into calculations. The full description of both traditional and modified black oil models for volatile oils and water/hydrocarbon systems are well described in the SPE monograph by Whitson and Brule (2000).

3.3.1.2. Compositional model. A compositional fluid model is described by Equations of State (EoS) which are relations between pressure, volume and temperature which is a basis for calculating phase and volumetric behavior of the produced fluid (Whitson and Brule, 2000). The history of the EoS development starts from the fundamental work by Van der Waals (1870). Later, various modifications and improvements of the van der Waals' equation were proposed. For the majority of oil and gas applications, the following modifications are used (Whitson and Brule, 2000; Falcone et al., 2009):

- Peng-Robinson (PR) (Peng and Robinson, 1976).
- Redlich-Kwong (RK) (Redlich and Kwong, 1949).
- Soave-Redlich-Kwong (SRK) (Soave, 1972).

State-of-the-art VFM systems support both compositional and BOM approaches for PVT modeling (Bendiksen et al., 1991; Haldipur and Metcalf, 2008; Kongsberg, 2016; Løvli and Amaya, 2016; Melbø et al., 2003). Even though the current trend in the first principles VFM is to use the compositional approach [e.g. VFM evaluation study by Letton-Hall Group (Toskey, 2011)], simplified VFM systems based only on one model (e.g. choke/orifice model) tend to utilize the Black Oil model because of its simplicity (Campos et al., 2014; Da Paz et al., 2010).

3.3.1.3. PVT data development. In order to simplify the simulation process, the obtained fluid properties models (BOM or compositional model) are typically stored in the form of PVT tables which are then used by the VFM models. In principle, the fluid properties models could be used directly in the VFM systems, however, this would lead to a high computational cost. Therefore, before performing the simulations, the fluid properties data are stored in PVT tables which are then used by the models to find the fluid properties values by interpolating between the generated data points.

Prior to the PVT table construction, it is first required to tune the fluid properties models to the specific petroleum fluid. This is because the default model parameters usually do not predict precisely the fluid properties from a specific field (Coats and Smart, 1986). Moreover, during the field life-cycle, fluid properties are changing which also require model calibration (Falcone et al., 2009). This tuning/calibration can be performed by applying non-linear regression (Agarwal et al., 1990; Coats and Smart, 1986) or by an iterative adjustment of EoS parameters (Pedersen et al., 1988; Whitson and Torp, 1983). The calibration is performed based on the data obtained in the laboratory tests. For the EoS model, the tests may include compositional analysis (gas chromatography), constant composition expansion, multistage surface separation, constant volume depletion and differential liberation expansion (Whitson and Brule, 2000). If BOM is used, the laboratory tests are used in order to estimate the main model parameters. An example of BOM parameters estimation based on the lab data is Whitson-Torp method (Whitson and Torp, 1983).

When the fluid models are tuned to the specific fluid properties, the PVT tables for the expected range of pressure and temperature conditions is generated and uploaded into a VFM system. Using these data, the system can interpolate the computed properties (e.g. phase density and viscosity) to local pressure and temperature (e.g. at the wellhead) based on the specified table values (Bendiksen et al., 1991).

3.3.1.4. Importance of fluid properties model tuning. Regardless the fluid model used for the PVT properties characterization, the fluid properties model accuracy has to be addressed with a particular attention. PVT related deviations in flowrate metering have been typically observed in MPFMs which have been found to be very sensitive to PVT data (AlDabbous et al., 2015). The sources of the PVT related deviations in MPFMs may originate from incorrect phase properties estimation or inaccurate usage of EoS (Åbro et al., 2017). EoS estimates of the fluid properties are consistent only within the tuning range of pressures and temperatures. If the fluid properties values are extrapolated outside the tuning range, the error of the estimates may be significant (Joshi and Joshi, 2007).

Similar to MPFMs, first principles VFM systems strongly rely on the PVT data. This means that accurate flowrate estimations require well characterized fluid properties data (Petukhov et al., 2011; Zhang et al., 2017). It has been found that when VFM is applied in a pilot case study or a field, PVT data is one of the most critical system parameters (Haouche et al., 2012a). Inaccurate PVT characterization results in the increase of the uncertainty of the VFM estimates (Ausen et al., 2017). The reason for such a large influence is the fact that the PVT data defines the local fluid properties, hence the discrepancies in fluid properties will directly influence the local flowrate estimates. Also, it will affect the reconciliation algorithm outputs because the fluid properties are directly involved in converting the rates from local to reference conditions which are used in the algorithm.

3.3.2. Production system model

The production system model typically consists of different components that are given by the measurements available in the field as well as the installed equipment. Below, we present the most relevant models which may be included into the first principles VFM system.

3.3.2.1. Reservoir inflow model. The reservoir inflow model is usually represented by an Inflow Performance Relationship (IPR) model which defines the well production rate as a function of pressure difference at reservoir and bottomhole conditions. The data for IPR curves are collected during multi-rate well testing (Golan and Whitson, 1991). This method has been extensively used in the industry to calculate the performance and production potential of wells and many models have been developed which are currently implemented in the state-of-the-art VFM systems. The most frequently used models are:

- Linear
- Backpressure/Backpressure normalized
- Undersaturated
- Vogel
- IPR table
- Forchheimer/Single Forchheimer

The linear model assumes that the well rate is proportional to the pressure difference between the reservoir and bottomhole (Bradley, 1987). This model is typically used for undersaturated oil wells and can be expressed in the following form (Cholet, 2008; Schlumberger Limited., 2014):

$$q_0 = PI \cdot (P_R - P_{BH}) \tag{1}$$

where q_0 denotes the oil flowrate, PI– the productivity index, P_R – the reservoir pressure, P_{BH} – the bottomhole pressure. The productivity index PI is estimated during a well test and then used in subsequent calculations.

The backpressure model is suitable for gas wells and can be written as follows:

$$q_g = C_b (P_R^2 - P_{BH}^2)^n \tag{2}$$

where q_g denotes the gas flowrate, C_b and n – the tuning coefficients which are estimated during well tests.

A normalized form of Eq. (2) is used for saturated oil wells and can be expressed as:

$$q_o = q_{o,\max} \left[1 - \left(\frac{P_{BH}}{P_R} \right)^2 \right]^n \tag{3}$$

where $q_{o,\max}$ denotes the maximum oil flowrate.

For the full description of the backpressure model, please see Bradley (1987).

The undersaturated model is often used to model oil wells with the static reservoir pressure for which the bottomhole pressure drops below the bubble point during production (Schlumberger Limited., 2014).

$$q_o = PI \cdot (P_R - P_B) + \left(\frac{PI}{2P_B} \right) (P_B^2 - P_{BH}^2) \tag{4}$$

where P_B denotes the bubble point pressure.

The Vogel model (Vogel, 1968) is commonly used in solution-gas-drive reservoirs and expressed as the following:

$$q_o = q_{o,\max} \left[1 - 0.2 \left(\frac{P_{BH}}{P_R} \right) - \left(\frac{P_{BH}}{P_R} \right)^2 \right] \tag{5}$$

To compute the gas flowrate using the equations above, the obtained flowrate must be multiplied by GOR.

IPR table, as the name states, represents the tabulated relationship between the flowrate and pressure difference. Based on the user-specified data and a calculated pressure difference value, the flowrate is interpolated by a linear or polynomial method (Schlumberger Limited., 2014).

For gas reservoirs with high flowrates, the inertial effect can be important to be accounted. In this case, a non-Darcy's law model called Forchheimer model is applicable (Bradley, 1987) which has the following form (Schlumberger Limited., 2014):

$$P_R^2 - P_{BH}^2 = B_f q_g + C_f q_g^2 \tag{6}$$

where B_f and C_f denote the tuning coefficients, which are estimated during well tests.

In case of high pressure gas wells, the single Forchheimer model can be used instead. It has a linear form of the pressure difference as follows:

$$P_R - P_{BH} = B_f q_g + C_f q_g^2 \tag{7}$$

Except for the Forchheimer's models, all the models are currently implemented in K-Spice Meter, while OLGA-Online currently incorporates all the listed models (Kongsberg, 2016; Schlumberger Limited., 2014). For other VFM software the information about implemented IPR models is rather limited. In ValiPerformance (Belsim), Vogel's model was utilized and tested (Haouche et al., 2012a, 2012b), while in Petukhov et al. (2011) and Wising et al. (2009). IPR model is mentioned as a part of the system but the type is not specified. In both FieldWatch and FlowManager, the reservoir inflow model can be specified by IPR tables (Gunnerud, 2011; Roxar, 2015). WoodGroup's Virtuoso and BP's Rate&Phase also use the IPR models, however, the exact models are not specified (Haldipur and Metcalf, 2008; Heddle et al., 2012).

As we can see, the IPR models have variety of forms depending on the well production conditions. In VFM, IPR models can be used in different purposes. First, it can be used as a separate model to estimate the production potential of a well. Secondly, the IPR models can be used in a combination with the thermal-hydraulic and choke models as a boundary condition of the system representing reservoir inflow to the well. In this case, it adds additional variables to the tuning process described in Fig. 2 which can further be used to tune the VFM system to the historical data. Apart from that, IPR equation can be combined with a thermal-hydraulic model (vertical lift performance curve) to estimate multiphase flowrate under steady state conditions, please, see, for instance, Lansagan (2012).

3.3.2.2. Thermal-hydraulic model. Multiphase flows in wells and pipelines in oil and gas fields have existed for more than a hundred years (Shippen and Bailey, 2012). The first attempt to model the multiphase flow was made by Lockhart and Martinelli (1949). At that time, the approach for multiphase flow modeling was based on empirical correlations obtained from experiments and available field data. With time, a more fundamental modeling approach replaced pure empirical models by including the physics behind the multiphase flow phenomena. An excellent review of the history of multiphase flow models development can be found in Shippen and Bailey (2012).

In this work, we will focus on the models currently used in commercial Virtual Flow Metering systems. Based on the literature, the following types of thermal-hydraulic multiphase models are currently implemented in the first principles VFM products:

- Two-fluid model.
- Drift-flux model.
- Steady state mechanistic model.

In the two-fluid model (often referred as the multi-fluid model), the conservation equations are written for each phase which can be continuous or dispersed. In a simplified manner, the general form of mass, momentum and energy equations respectively can be written as follows (Goldszal et al., 2007; Nydal, 2012):

$$\frac{\partial \alpha_k \rho_k}{\partial t} + \frac{\partial \alpha_k \rho_k u_k}{\partial x} = \Psi \tag{8}$$

$$\frac{\partial \alpha_k \rho_k u_k}{\partial t} + \frac{\partial \alpha_k \rho_k u_k u_k}{\partial x} = -\frac{\partial \alpha_k p_k}{\partial x} - \alpha_k \rho_k g \sin\theta - F_{kw} \pm F_{ki} + O_k \tag{9}$$

$$\frac{\partial \alpha_k \rho_k h_k}{\partial t} + \frac{\partial \alpha_k \rho_k u_k h_k}{\partial x} = \frac{\partial}{\partial x}\alpha_k k_k \frac{\partial}{\partial x} T_k + \alpha_k \frac{Dp}{Dx} + Q_{kw} + \sum_{i \neq k} Q_{ki} + Q_{ext} \tag{10}$$

where α_k denotes the phase volume fraction, ρ_k – the phase density, t – the time, u_k – the phase velocity, x – the pipe axial dimension,Ψ – the mass transfer sources (e.g. phase change and mixing), p_k – the phase pressure, θ – the pipe inclination angle, F_{kw} – the wall friction, F_{ki} – the interphase friction, O_k – the other momentum exchange terms (e.g. phase change, droplet-exchange, level-gradient term), p – the system pressure, k_k – the effective phase thermal conductivity, Q_{kw} – the phase transfer rate at pipe wall, Q_{ki} – the interfacial heat transfer rate of k-phase with other fields, Q_{ext} – the other net external heat transfer sources.

In the drift-flux model, the momentum and energy equations are written for the mixture while the mass conservation equations can be written for each phase. It can be expressed as the following (Holmås and Løvli, 2011):

$$\frac{\partial \alpha_k \rho_k}{\partial t} + \frac{\partial \alpha_k \rho_k u_k}{\partial x} = \Psi \tag{11}$$

$$\frac{\partial}{\partial t}\sum_k \alpha_k \rho_k u_k + \frac{\partial}{\partial x}\sum_k \alpha_k \rho_k u_k u_k + \sum_K \alpha_k \rho_k g + \frac{\partial p}{\partial x} = -F_{tot} - O_{tot} \tag{12}$$

$$\frac{\partial}{\partial t}\sum_k \alpha_k \rho_k E_k + \frac{\partial}{\partial x}\sum_k \alpha_k \rho_k u_k E_k + \frac{\partial}{\partial x}\sum_k \alpha_k \rho_k p + U_{tot} = 0 \tag{13}$$

where F_{tot} denotes the total wall friction, O_{tot} – the source term,E_k – the total energy, U_{tot} – the total source term including wall heat transfer, mass transfer and sources.

The drift-flux model requires a slip relation in order to take the difference between the phase velocities into account. The most famous and commonly used form is developed by Zuber and Findlay (1965):

$$u_g = C_0 u_m + u_d \tag{14}$$

where u_g denotes the gas velocity, u_m – the mixture velocity, u_d – the drift velocity, C_0 – the profile parameter.

Both multiphase flow model formulations above are transient which means they reconstruct the flow behavior in space and time. If the time derivative term $\frac{\partial}{\partial t}$ is set to zero, the model becomes steady state and resolved only in space. With a steady state model, it is not possible to properly describe an unstable behavior in wells, for instance, liquid loading or severe slugging as it is transient in nature (Waltrich and Barbosa, 2011).

Some VFM systems use only one specific formulation of the thermal-hydraulic model, while others utilize a combination of them. For instance, in OLGA the two-fluid formulation of the momentum equation is combined with a mixture energy equation (Nydal, 2012). In total, OLGA includes five mass and three momentum equations as well as one mixture energy equation (Shippen and Bailey, 2012). In K-Spice Meter which uses LedaFlow for resolving multiphase flows in wells, nine mass, three momentum and three energy equations are used (Kongsberg, 2016; Shippen and Bailey, 2012). As such, it is classified as a two-fluid model which have nine fields: 3 continuous and 6 dispersed.

In contrast to OLGA and K-Spice Meter, FlowManager utilizes the transient drift-flux model with one mixture momentum and one energy equation. The mass balances are solved for each phase (Holmås and Løvli, 2011). A similar approach is used in METTE which is a

multiphase flow solver in FieldWatch. The software uses the transient drift-flux model with the mixture momentum and energy equations with a possibility to include and exclude the slip effect between the phases (Roxar, 2015).

Based on the literature available on Well Monitoring System by ABB, it is difficult to relate the software model to any of the formulations above. van der Geest et al. (2000) formulated the momentum equation in a very generic way as the following:

$$-\frac{dp}{dx} = f_{fric}\frac{2\rho u^2}{D} + \rho g \sin\theta \tag{15}$$

where p denotes the system pressure, f_{fric} – the friction factor, u – the fluid velocity, ρ – the fluid density, D – the pipe diameter, x – the pipe axial dimension, θ – the pipe inclination angle.

The equation basically states that the pressure drop along the well depends on friction and gravity. In this case, the multiphase flow is resolved as follows. First, the flow pattern is identified based on the method developed by Barnea (1987). Based on the local flow pattern, the respective closure laws and correlations are identified and the momentum equation is solved. Given the solution of the momentum equation, the temperature gradient is solved which has the following form (van der Geest et al., 2000):

$$\frac{dT}{dx} = \frac{\frac{e+w}{dx} - u\frac{du}{dx} - g\sin\theta - \frac{\partial h}{\partial P}\frac{dp}{dx}}{\frac{\partial h}{\partial T}} \tag{16}$$

where e denotes the specific heat exchange with the environment, T – the fluid temperature, h – the specific fluid enthalpy, w – the specific work done on the system.

This is a similar approach to the Unified Model developed at the University of Tulsa, see Zhang et al. (2003). However, since the literature on the model applied in Well Monitoring System is limited, it is not possible to surely state that the Unified Model is applied. On the other hand, it is possible to conclude that this model uses a mechanistic steady state approach as there is no time derivative in the model as well as flow is modelled based on the physics behind including force balances and correlations based on the flow pattern. This classification is also in correspondence with the one provided by Shippen and Bailey (2012).

As for the rest of the commercial VFM systems, based on the available sources, we have not been able to identify the type of the implemented thermal-hydraulic model. However, the software definitely use one, please see Haouche et al. (2012b) for Vali-Performance, Haldipur and Metcalf (2008) for Virtuoso and Heddle et al. (2012) for Rate&Phase.

3.3.2.3. Choke model. Over many years, choke valves at the wellheads have been used in oil and gas production for safety and control purposes (Buffa and Baliño, 2017). In addition to this, because the pressure drop over the choke depends on the flowrate, the choke valve can be used to estimate the flow. As such, a choke valve model can be considered as a simple Virtual Flow Meter because the flow is not measured directly but rather estimated. However, estimating the flow over the choke is not a straightforward task due to the multiphase flow complexity.

As in many other fluid dynamics applications, the first attempts to estimate the flow through the choke were made using empirical correlations. For example, see the model developed by Gilbert (1954). At the later development stage, mechanistic models were proposed which are currently implemented in Virtual Flow Meters.

Based on the available literature, we found that four models are currently implemented in commercial VFM systems. It can be the case that there are more utilized models, but, unfortunately, the literature published by VFM suppliers on this topic is rather limited.

As for the implemented models, they are:

- Modified Bernoulli
- Hydro (Long and Short)
- Perkins

The Modified Bernoulli model is implemented in Roxar's FieldWatch. The model is derived from the famous Bernoulli equation which was originally applied for a single-phase flow. In order to adjust the model to specific choke parameters, the choke discharge coefficient and mixture density are introduced. The Modified Bernoulli model can be written as follows:

$$\dot{m} = A_1 C_D \left[\frac{2\Delta p \rho_m}{\frac{A_1}{A_2} - 1}\right]^{1/2} \tag{17}$$

where $\dot{m}$ denotes the mass flowrate, C_D – the choke discharge coefficient, A_1 – the inlet choke area, A_2 – the choke throat area, ρ_m – the fluid mixture density, Δp – the pressure drop over the choke.

The Hydro model developed by Selmer-Olsen (1995) is used in OLGA Online. This model has two versions: Long and Short. In the Long version, it is assumed that vena contracta is located inside the throat while in the Short model it is located downstream of the throat. In both models, sub-critical and critical flows are calculated and then the smallest one is selected since the critical flow is the largest possible. In comparison with many other models, the Hydro model considers irreversible losses in the choke in a mechanistic manner, thus, the discharge coefficient is not involved in calculations. For the full Hydro model description with the derivation details, an improved slip relation as well as testing results by experimental data, please see Schüller et al. (2003) and Sampath et al. (2006).

The Perkins model (Perkins, 1993) is implemented in Rate&Phase. The model is derived from the energy equation applied on a control volume of a fluid. It calculates the mass flowrate for sub-critical and critical flows and then adjusts it to the actual flow by multiplying with a discharge coefficient (Perkins, 1993). In contrast to the Hydro model, this model does not consider the slip effect between the phases as well as frictional losses in the throat. However, Sampath et al. (2006) found that this is a disadvantage of this model and that the Hydro model outperforms Perkins model by accounting the slip effect. K-Spice Meter includes both Hydro and Perkins models, so that the user may choose a preferable option (Kongsberg, 2016).

Apart from the models implemented in the commercial simulators, there are many other models suitable for estimating the mass flowrate over the choke. Ashford (1974) derived a model for the total mass flowrate based on the fluid properties, choke size and discharge coefficient. With the computed total mass flowrate, the oil flowrate can be estimated based on Black Oil properties.

By considering a no-slip frozen two-phase flow, Sachdeva et al. (1986) developed a model which has been popular in the literature. As in the Perkins model, they consider the discharge coefficient to adjust the flowrate to the actual conditions. Sampath et al. (2006) showed that the no-slip assumption makes this model to be less accurate than the Hydro model. Despite this drawback, the Sachdeva et al. (1986) model is one of the first mechanistic choke models and often considered in the literature for the analysis and comparison with new models.

Al-Safran and Kelkar (2009) developed a mechanistic choke model which accounts for the slip between phases. The idea behind the model development was to create a simple (as Sachdeva and Perkins) and accurate (as Hydro) model. As such, the basis of the model is taken from Sachdeva and Perkins models with an implementation of the slip model developed by Schüller et al. (2003) for a modified version of the Hydro model (Sampath et al., 2006). Based on experimental tests, Al-Safran and Kelkar model outperformed Sachdeva and Perkins models and decreased the average percent error by 5–10%.

As the field of choke models for flowrate estimation is wide, in addition to the aforementioned models, there are some less popular and general models available in the literature and utilized for real field cases. Several review papers study the history of the choke models' development and evaluate performance of different models. So, if the validation of the discussed models as well as description of other

developed ones is of interest, see the works by Rastoin et al. (1997), Buffa and Baliño (2017) and Sampath et al. (2006).

3.3.2.4. Electric submersible pump (ESP) model. An electric submersible pump is a widely used artificial lift equipment which is used to produce oil where natural production is not possible due to various reasons, for instance, low bottomhole pressure, liquid loading, heavy oil presence, etc. ESPs have a long application history in the oil and gas industry, for example, see Lea and Bearden (1999) for a review of ESP applications in onshore and offshore oil and gas production. Due to its popularity, there have been a numerous amount of attempts to make a first principles model which describes ESP operation which are not possible to cover within this paper. The general idea behind an ESP model is to link the pump pressure increase with the pump inlet pressure, the flow and the pump speed (Schlumberger Limited., 2014):

$$\Delta P = f(q, \xi, \alpha_l, P_{inlet}) \tag{18}$$

where q denotes the flowrate, ξ – the pump speed, α_l – liquid fraction, P_{inlet} – pump inlet pressure.

By measuring the pressure before and after the pump and using a model described in a form of Eq. (18), it becomes possible to compute flowrates of the multiphase flow mixture which is pumped by an ESP. In this paper, we do not describe the exact differences between the models which are used by the commercial VFM systems. First of all, it is in general difficult to group the ESP models as it was done, for instance, for the thermal-hydraulic and choke models. In addition, some VFM suppliers do not provide specifics of the used models and mention only the fact that these models exist. What is important to note is the fact that these systems use ESP models and it can be a good source for multiphase flowrate estimation without additional hardware installations.

3.3.3. Data validation and reconciliation (DVR) algorithm

Another important part of the state-of-the-art first principles VFM systems is a data validation and reconciliation algorithm. In some papers and software, this VFM part is called simply "optimization algorithm" (Heddle et al., 2012; Holmås and Løvli, 2011), while in others it is mentioned as DVR (Haouche et al., 2012a; Patel et al., 2014). In case of Well Monitoring System by ABB, Melbø et al. (2003) defines it as the optimization algorithm, while van der Geest et al. (2001) defines it as DVR. In this paper, we use the term "data validation and reconciliation" to describe the process of adjusting the VFM model parameters such that the VFM model outputs match the measured field data.

As the technique name states, DVR consists of two parts: (1) validation and (2) reconciliation. In the data validation part (1), the goal is to remove erroneous and noisy data. This step can be done by means of statistical analysis and filtering techniques, for example, exponential filters or moving averages (Stanley, 1982).

When the data is validated, the reconciliation part (2) takes place. Here, an optimization algorithm adjusts the model parameters, for instance, flowrates, choke discharge coefficient, gas and water fractions, and friction and heat transfer coefficients such that the model outputs match the validated measured data being constrained to process conditions, for instance, the material balances (Câmara et al., 2017). In Virtual Flow Metering systems, the reconciliation algorithm is often written in the constrained least-squares form (Petukhov et al., 2011):

$$\min_x \sum_i^N \left(\frac{y_{meas\ i} - y_{predicted\ i}}{\sigma_i} \right)^2 \tag{19}$$

subject to the following constraints:

$$F(s, y) = 0 \tag{20}$$

$$y_{\min} \le y_{predicted\ i} \le y_{\max} \tag{21}$$

$$s_{\min} \le s_i \le s_{\max} \tag{22}$$

where i denotes the measurement index, $y_{meas\ i}$ – the measured value, $y_{predicted\ i}$ – the reconciled (predicted) value, σ_i – the measurement uncertainty, s_i – the unmeasured variable, $F(s, y) = 0$ – the process equality constraints (e.g. mass and energy balances).

In VFM applications, the problem formulation is usually non-linear due to the complexity of the system. In order to find the solution of a non-linear data reconciliation problem, different methods can be applied. If inequality constraints are not present, the method of Lagrangian multipliers may be used to obtain the solution (Câmara et al., 2017). If constrains are included, typically gradient based optimization methods are used such as Levenberg-Marquardt, SQP or Gauss-Newton (Câmara et al., 2017; Holmås and Løvli, 2011). In the outcome, the algorithm estimates the flowrates which give a local or global minimum error.

When the reconciliation process is finished, the results can be validated. In this step, statistical tests are conducted in order to further detect unreliable measurements and estimates and probability of a gross error existence. This can be achieved by performing individual (e.g. penalty) and global (e.g. chi-squared) tests (Petukhov et al., 2011).

3.4. Reported field experience with first principles VFM systems

The VFM systems derived from the first principles have been used in the industry as standalone solutions as well as back-up systems for physical multiphase flow meters. Unfortunately, not many examples of using a particular VFM solution are published. Despite this fact, some examples are still available in the open literature and are summarized in this section.

3.4.1. Reported field experience with commercial first principles VFM products

One of the most widely spread first principles VFM systems is Rate& Phase which was reported to be installed in more than 300 production and injection wells by 2011(Heddle et al., 2012). The authors reported that the average error of this VFM is usually recorded at the level of less than 5%.

In 2004, FlowManager was in operation in a subsea field with three wells which had challenges with downhole pressure sensors and unreliable choke information. Despite these difficulties, the software was able to identify erroneous flowrate measurements at the separator that emphasized possible features of the VFM technology (Rasmussen, 2004). FlowManager is also successfully utilized as a flow assurance system in Ormen Lange and Vega fields in the North Sea and used as a back-up system to the MPFMs (Holmås et al., 2013; Holmås and Løvli, 2011). Løvli and Amaya (2016) showed six cases of FlowManager implementation for VFM applications including gas condensate and oil fields. The software was used during normal conditions as well as start-up operations. These examples showed usefulness of VFM not only as a standalone solution but also for performance monitoring of physical flow meters. Overall, by 2018, FlowManager is in operation of 700 wells around the world (Escuer et al., 2018).

Application of Well Monitoring System in the British sector in the North Sea is discussed in Melbø et al. (2003). In this application, the information from the sensors was limited and not reliable but the flowrate estimations were close to the true values. van der Geest et al. (2001) presented the tests of WMS in Troika Field in the Gulf of Mexico and emphasized the ability of the simulator to predict the flowrates as well as other system parameters when necessary. Another example of installation is Bonga field in Nigeria (ABB, 2004; Bringedal et al., 2006).

An example of VFM as a standalone metering solution is the implementation of K-Spice meter in Alta field in Norway which is a small field tied-in to the existing infrastructure (Patel et al., 2014). In this case, the MPFM solution would have significantly increased CAPEX and OPEX, so that it was decided to apply the VFM solution which showed a good performance during the tests.

ValiPerformance was successfully tested and suggested for further use in Ceiba oil field in Equatorial Guinea (Petukhov et al., 2011). It was also installed in an offshore field in the Middle East operated by Total with 16 wells with ESPs (Couput and Renaud, 2010). During the tests and

operation, the ESP model was tested and improved by "density correction factor" (Haouche et al., 2012a, 2012b). Couput et al. (2008) showed examples of the software installation in an onshore field in France and a complex subsea field as a back-up and reduction uncertainty system.

Virtuoso was successfully used as a standalone multiphase flow metering technology in gas condensate and black oil systems in Asia Pacific, the Gulf of Mexico and Southern North Sea (Haldipur and Metcalf, 2008). The system was also linked to the implemented pipeline flow simulators that resulted in an integration flow assurance system used for multiple purposes such as flow metering, detection of hydrates, asphaltene and wax depositions and leak detection. Parthasarathy and Mai (2006) showed two other examples of Virtuoso implementation. In the examples, Virtuoso was used as a back-up for wet gas meters initially but after ones' failure it was used as primary metering information for the flow assurance system. In another example, the software revealed inconsistent performance of topside meters which then was successfully fixed.

Couput et al. (2017) summarized the operational experience with ValiPerformance and K-Spice VFM systems in Total providing examples from Couput and Renaud (2010) and Patel et al. (2014). They emphasized that despite the advantages of the VFM costs, this technology still needs skilled people to tune and calibrate the software which can be a challenge for operator companies.

3.4.2. Reported field experience with patchwork first principles VFM solutions

Apart from the commercial first principles VFM products discussed above, there were several examples of combining commercial software with an optimization algorithm to create a VFM solution. Acuna (2016), Omole et al. (2011) and Ma et al. (2016) combined the software packages Prosper and GAP as an engine for VFM in real field cases and then combined it with external optimization techniques to estimate the flowrates continuously and optimize the field production.

In addition, smaller VFM solutions have also been utilized for flow metering. Usually, these systems rely on a particular model rather than on an integrated approach as the systems described above. For example, Ajayi et al. (2012) and Allen and Smith (2012) used the models of downhole inflow control valves (ICV) to construct a Virtual Flow Metering system. Campos et al. (2010), Hussain et al. (2016), Moreno et al. (2014), Loseto et al. (2010) and Espinoza et al. (2017) used choke valve models in order to estimate the flowrate at the field conditions. Delarolle et al. (2005) and Faluomi et al. (2006) from TEA Sistemi also developed a choke model, validated it with experimental data and CFD analysis and applied the model at field conditions in Italy, North and West Africa and the Gulf of Mexico. They also tried to implement the hydraulic tubing model, but it showed a less accurate performance than the choke model.

Cheng et al. (2018) created a VFM system based on not a particular model but a combination of the discussed models such as IPR, steady state thermal-hydraulic and choke models and successfully applied in real operation of an offshore field in China. Similarly, Mursaliyev (2018) used a steady state thermal-hydraulic model together with tuned PVT model to construct a VFM system and applied it for real time production monitoring in Kashagan field achieving the error of less than 5%.

Apart from the choke model based VFM solutions, the ESP model has also been used for flow metering. Camilleri and Zhou (2011) and Camilleri et al. (2016a, 2016c, 2016b, 2015) showed field case studies in which ESP first principles models act as Virtual Flow Meters and able to estimate the flowrates as well as other production system parameters such as productivity index.

3.5. Evaluation studies of the first principles VFM systems in the literature

In order to improve accuracy of VFM systems, it is important to critically evaluate it against various input data. This is because each single field may differ from one to another in terms of sensor availability and accuracy, frequency of well testing, presence of an additional equipment (e.g. Venturi meters), etc. The critical evaluation of the existing VFM solutions is beneficial for both operators and software vendors. The operators might understand the applicability of VFM systems for a particular case and/or a necessity for installing the required instrumentation to improve the accuracy of the flowrate estimates. The vendors in turn could understand the direction for further improvements of the software.

In the literature, there are several evaluations of the commercial first principles VFM systems. Among the others, the evaluations by Toskey (2011) and Amin (2015) are of a particular interest. This is because they compare several VFM systems and evaluate the relative error depending on the input data. Even though the works are conducted by the same company and within a similar strategy, some major differences exist. Toskey (2011) used OLGA to simulate the field data while Amin (2015) used real field data. For tuning purposes, the vendors in Toskey (2011) were provided with phase flowrates, while in Amin (2015) the vendors were given Water-Liquid-Ratio at first and total mass flowrates with Gas-Volume Fractions later. Last but not least, Amin (2015) also included a short but important study of the VFM products sensitivity to the PVT data. In addition to the mentioned studies, a smaller but similar work was performed by Varyan et al. (2015). They evaluated the performance of FlowManager software using a similar approach, so that some conclusions may be compared with the ones by Toskey (2011) and Amin (2015).

As the studies are extensive, we will not give a thorough description of them here. Instead, we will summarize the main common conclusions and disagreements. From the studies, the following common conclusions can be made:

- VFM tuning is required for accurate estimations.
- Tuning frequency depends on the local field conditions.
- Tuning is essential when the pressure drops below the bubble point at well conditions.
- When GOR increases, more attention must be paid to carefully tune the VFM system
- Total mass flowrate is a reliable tuning parameter.
- Increase in choke opening decreases the estimates accuracy.
- Additional devices such as Venturi, densitometer or partly working MPFM may help to improve the VFM system accuracy.
- Importance of adding measurements to the model depends on the VFM strategy.

At first, the last conclusion may seem not very clear. This is because it comes from a disagreement between the studies. Toskey (2011) concluded that adding bottomhole sensors data to the VFM system does not improve the flowrate predictions while the results from Amin (2015) and Varyan et al. (2015) state opposite conclusions. Comparing these statements and looking at the results, it can be said that the importance of adding the measurements depends on the strategy used for Virtual Flow Metering. This means that if the VFM strategy initially relies on the choke model, then adding the bottomhole measurements will not add much value because the final estimates still rely on the choke model. On the other hand, if adding the measurement adds a separate model into the VFM and the estimates are made based on both the choke and tubing models (e.g. weighted average value), the results might improve.

Another important point is that using the total mass flowrate and mixture densities as tuning parameters may allow some errors in PVT data while still maintaining a high accuracy of the flowrate estimates (Amin, 2015). This is a very important conclusion since it may be the case that the PVT data is tuned with some errors or not being tuned continuously. However, this conclusion is made based only on the case considered in one study and may not be generalized for other cases. Definitely, more studies are needed on this topic.

Finally, an attempt was made to evaluate the sensitivity of the VFM systems to the errors in pressure and temperature readings. Amin (2015) showed that with the measurement error the VFM systems were unable to estimate the flowrate within a high accuracy. Toskey (2011) found that the VFM suppliers were able to eliminate the measurement

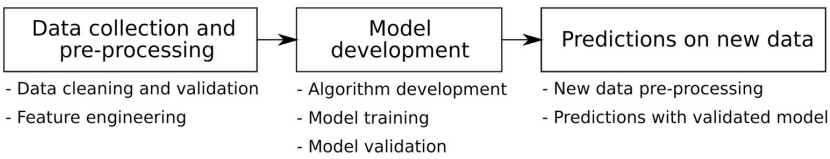

Fig. 3. A typical workflow of data-driven model development.

error and provide accurate estimates. However, both authors concluded that more investigation on this topic is required because these results were highly dependent on the studies conditions.

Additional investigations on the measurement errors influence were conducted by Tangen et al. (2017) and Lansagan (2012). Tangen et al. (2017) used K-Spice meter to test the sensitivity of the VFM software to the errors in the pressure and choke opening measurements as well as in GOR and WC. To do that, a digital twin approach was used where one model represented a plant while the second one represented the VFM model. Lansagan (2012) used two different approaches to test the sensitivity of a VFM system. The first one relies on the intersection method between the inflow and outflow performance of the well while the second one is the same as in Tangen et al. (2017): using a transient multiphase flow simulator. From the studies, some common and distinct conclusions can be drawn:

- Redundant measurements are preferable to improve VFM accuracy.
- Wellhead pressure measurements are more important than bottomhole ones.
- Validated choke model makes the predictions more accurate.
- Oil wells are more sensitive to WC input.
- Gas wells are more sensitive to GOR input.
- Increase in choke opening decreases the estimates accuracy.
- If the intersection method is used, reservoir and bottomhole pressures are more sensitive parameters than wellhead pressures.

Considering all the aforementioned studies on the VFM systems sensitivity, the following general conclusions can be made. First principles VFM is a sophisticated system which aims to simulate complex nonlinear multiphase flow phenomena by combining several computational approaches. This leads to the difficulty of a comprehensive VFM evaluation since it highly depends on the selected strategy and applied computational methods. From the studies we see that some conclusions agree with each other while the others may be totally contradictive. Hence, we conclude that more studies on this topic are required in order to better understand the behavior of the VFM under different conditions. Future studies can take the discussed works into account and go deeper in terms of the evaluation of critical system parameters such as measurements and PVT data. An attempt to address some of these points was done by Bikmukhametov et al. (2018). They conducted a statistical analysis of the sensor degradation effect on a first principles VFM system and revealed that drift errors in pressure and temperature measurements may lead to a big systematic error in flowrate estimated from a VFM system. They also conducted a sensitivity study on heat transfer modeling approaches of the wellbore and found that the detailed heat transfer modeling is not necessary for VFM in oil wells with middle range values of GOR. Despite this attempt, further sensitivities studies are required for a deeper understanding of first principles VFM systems and suggestions for the future work are discussed later in the respective section.

4. Data-driven VFM systems

4.1. An overview of the concept

Data-driven modeling is a technique which is based on analyzing the system data and finding relationships between the system state input and output variables without exact knowledge about the physical behavior of the system (Solomatine et al., 2009). The main advantage of this approach is that it allows to skip the detailed physical modeling of systems or processes for which the exact solution can be difficult to find numerically, for example, multiphase flows in pipes. Data-driven methods rely on the fact that experimental or industrial data represent the system well and attempt to learn the physics relationship which describe the system directly from data. A typical workflow process of data-driven modeling is shown in Fig. 3.

In order to start the modeling process, first, the data must be collected. Any data related to the process can be relevant, for instance, historical system data, current system data or even historical data from a similar system. In the next step, the data must be pre-processed. This may include different operations. First, we ensure that the collected data is suited for modeling by removing outliers, treating missing values or removing noise. Also, additional insights about the information contained in data can be obtained through data transformation and feature engineering. Feature engineering get its name from the fact that in the machine learning community the input data are often called features, so that feature engineering is the process of manipulating the input data to reveal useful information which can help in the model training process.

When the data is pre-processed, the model development is performed. At this step, a data-driven model is developed and trained on the pre-processed data. The training process is basically fitting a mathematical function which describes the data well. In some cases, this function has an analytical form, for instance, in a linear regression model, but it can also be a black-box model, for instance, a neural network (NN). The obtained model must be validated on a separate dataset to ensure the capability of the model of making accurate predictions on the new data. After the model has been validated, it can be used to make predictions on newly obtained data.

In Fig. 4, a schematic overview of the data-driven modeling application for Virtual Flow Metering is shown for the production system shown in Fig. 1. In a data-driven VFM system, the collected data typically includes the pressures and temperatures at the bottomhole and wellhead, the choke opening values as well as the parameters of the ESP and the corresponding measurements of oil, gas and water flowrates. The measurements of the flowrates can come from different sources. One possibility is to use well test data and another possibility is to use the data from hardware multiphase flow meters. In the latter case, if MPFMs are installed at each wellhead, the data-driven model becomes a back-up metering system for each well. However, if one MPFM is installed for a cluster of wells, its data can be used similar to well test and separator data, so that the flowrate measurements from each well are collected according to the well testing schedule. In this case, after training and validation, the data-driven model can be used as a standalone VFM system. In the next section, we will describe the data-driven workflow process in more detail.

4.2. Description of the data-driven VFM components and applied methods

4.2.1. Data collection and pre-processing

Before developing any data-driven model, the data must be collected and pre-processed. In Virtual Flow Metering systems, the data may include sensor readings from wells and processing facilities. In addition, historical data from similar wells or fields can potentially be used for model development. In the next step, the data is pre-processed prior to training. Typically, the collected data are noisy, corrupted, may include missing values, outliers and irrelevant inputs (Famili et al., 1997). As such, the data needs to be cleaned and validated before

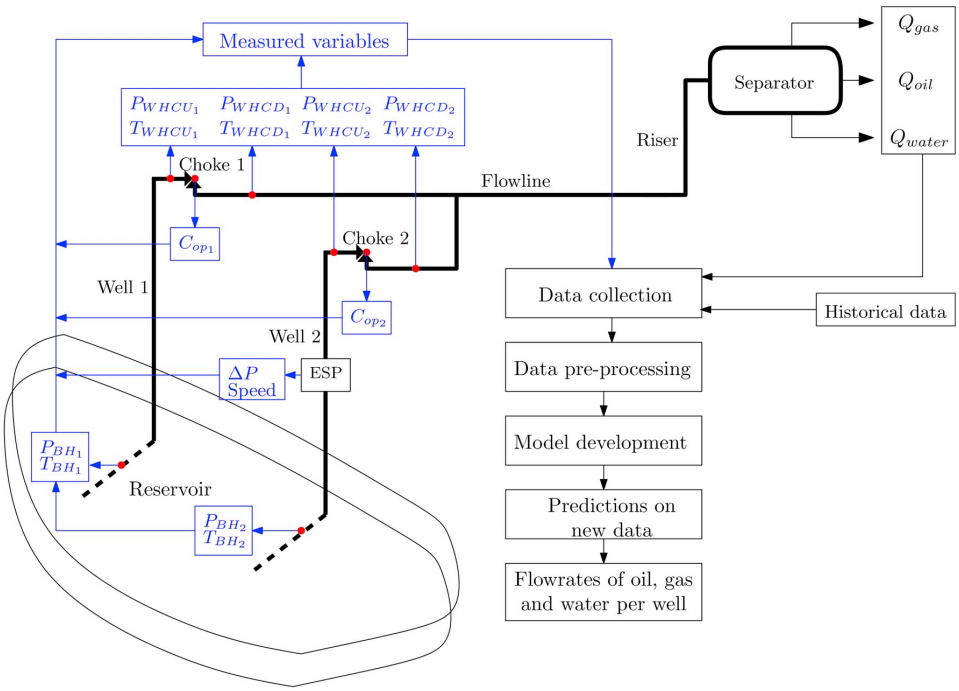

Fig. 4. A schematic overview of a data-driven Virtual Flow Meter. First, the production system data is collected and pre-processed. Then, the pre-processed data is used for model development and validation. When new measurement data is obtained, the validated model is used to estimate the well flowrates of oil, gas and water.

further usage. In principle, this is the same validation process as in the data validation and reconciliation algorithm which is used in the first principles VFM systems discussed before.

In the pre-processing step, data may also be transformed and additional insights about the information contained in the data can be obtained. This process is usually called feature engineering. Typical raw features in VFM are shown in Fig. 4, i.e. pressures and temperatures along the production system, choke openings and the information from the ESP. There are many techniques which are used in feature engineering, for instance, dimensionality reduction algorithms by Principal Component Analysis (PCA), feature selection methods or linear and non-linear combination of the raw features. A good overview of the feature engineering methods is provided by Cunningham (2008). In general, feature engineering may help the data-driven algorithm to find complex relationships between the original data and the output variable or remove redundant features which leads to lower computational cost during training and prediction steps. In most of the cases, domain knowledge of the field of interest is important to construct informative features for further algorithm training and Virtual Flow Metering is not an exception. Creating good features using the input data which can describe the multiphase flow transport process may help to obtain better predictions. However, as we will see in the next sections, in most of the literature resources the production system sensor data are often used as it is and the potential of good feature engineering for VFM applications is not explored yet.

4.2.2. Model development

Model development is the process of developing an algorithm which is able to map input features and output (target) variables. The mapping process is also called training or learning during which the algorithm adjusts the parameters in such a way that it estimates the target variables accurately. The adjusted parameters depend on the algorithm in use. For instance, in case of a neural network, the parameters are typically weights, which connect the neurons, while in case of regression trees the parameter can be the tree depth. The process of training is achieved by minimizing a cost function which is formulated as the difference between the algorithm predictions and true (measured) values. For regression problems as Virtual Flow Metering, the mean squared error (MSE) is often used as a cost function which has the following form:

$$MSE = \frac{1}{N}\sum_{i=1}^{N}(y_{meas\ i} - y_{predicted\ i})^2 \tag{23}$$

where MSE denotes the mean squared error (cost function), $y_{meas\ i}$ – the measured (true) value of the *i-th* training example, $y_{predicted\ i}$ – the predicted value of the *i-th* training example, N – the number of training examples, i – the index of the training example.

This expression resembles Eq. (19) for the data reconciliation algorithm in the first principles VFM systems except for the fact that the data-driven model training is typically an unconstrained optimization problem while in data reconciliation the problem includes constrains as well as uncertainty in the cost function. As such, the main idea behind the first principles and data-driven VFM systems is the same – adjust the model parameters such that the difference between the predictions produced by the mathematical model and the measurement data is small. However, the major difference is the mathematical formulation of the model where the first principles models try to explain the multiphase flow transport using the physics behind the phenomenon while the data-driven models try to learn the multiphase flow behavior directly from data.

After the model is trained, it must be validated and tested on a different dataset to ensure that the trained model will perform well on the data which the model has not seen during the training. The model ability of producing accurate predictions on new data is called model generalization (Abrahart et al., 2008). Another purpose of validation is

to select accurate hyperparameters of the model to fit the data well. Hyperparameters are the model parameters which are set prior to training and are not learned during the training process. For instance, in case of neural networks, the hyperparameters are the number of layers, number of nodes in the hidden layers, regularization parameters, etc. The regularization parameters are the hyperparameters which allow to reduce the effect of noise and outliers on the final algorithm predictions, so that the algorithm does not overfit the data. Bishop (2006) provides a rigorous discussion on the influence of hyperparameters on the model performance including its more detailed definitions.

There are different methods for validation. One of the most widely used approach is standard K-fold cross-validation (Hastie et al., 2009) which is shown in Fig. 5 (left). In this method, the available data is divided into training and test parts. Then, the training set is again divided into K-folds. Prior to training, a set of hyperparameters is selected and then the model is trained with these parameters on K-1 folds and the error between the actual values and the algorithm predictions is checked on the remaining fold. This process is repeated K times and the error is averaged over K folds. The obtained error corresponds to the model error with the selected hyperparameters. Then, the hyperparameters can be changed and the averaged error over K folds is computed again. The best set of hyperparameters is the one which corresponds to the lowest obtained error over K folds. The model with the best hyperparameters set can be re-trained on the entire training set to utilize all the available data.

One of the main assumptions behind the K-fold cross-validation is that the data points are independent from each other. However, in case of Virtual Flow Metering this is an inadequate assumption because, for instance, the bottomhole pressures at time instance *t* are dependent on conditions at time instance *t-1* unless the time difference between the instances is large or during steady state operation with no pressure variations. However, in most of the reported applications of data-driven models in VFM, this fact has not been considered and the standard K-fold cross-validation was performed as shown in Fig. 5 (left), see, for instance, the works by Al-Qutami et al. (2017c, 2017a).

An alternative to the standard K-fold cross-validation can be nested K-fold cross-validation, see Fig. 5 (right). In this case, the training set is again divided into K-folds, however, the model is trained and validated in a nested manner, for instance, trained on fold 1 and validated on fold 2, trained on folds 1 and 2 combined and validated on fold 3. In this case, the algorithm does not use the future data in order to predict the past outputs and misleading conclusions about the model performance can be avoided. An application of the nested K-fold cross-validation in data-driven VFM is described by Bikmukhametov and Jäschke (2019).

Ideally, the performance of the obtained validated model is checked on a separate test dataset to make conclusions about the model generalization. Typically, two situations can happen when testing the model performance:

- The errors on the training and test sets are large.
- The error on the training set is small but large on the test set.

The first situation is called underfitting and often referred as the fact that the trained algorithm has high bias. The second situation is called overfitting and often referred as the fact that the trained algorithm has high variance. In fact, finding an optimum value of both bias and variance is the overall goal of the data-driven algorithm training and called *a bias-variance trade-off* (Hastie et al., 2009). So, in summary, *the validation and testing are conducted in order to find the best set of hyperparameters which provides an optimal value of bias and variance.* In this case, the algorithm has good generalization and can be used for future predictions with greater confidence. For a more detailed explanation and the rigorous mathematical formulation of the data-driven model assessment, we recommend the book by Hastie et al. (2009).

An alternative to K-fold cross-validation is early stopping approach which has been extensively used for data-driven models training including VFM applications (Al-Qutami et al., 2017b; Bikmukhametov and Jäschke, 2019; Prechelt, 2012). In this case, the dataset is divided into training, validation and test sets. During training, the error is monitored on the training and validation sets. The training continues until the error on the validation set keeps increasing a specified number of training steps. The model can be further re-trained on the combination of the training and validation sets and evaluated on the test set. Prechelt (2012) provides a thorough explanation of this approach and the methodology for selecting the stopping criteria.

4.2.3. Applied methods for data-driven VFM systems

Having considered how data-driven model can be developed, in this section, we will discuss data-driven methods which have been reported to be used for VFM systems. Because VFM is a non-linear regression problem, most of the data-driven VFM approaches are based on artificial neural networks alone or with some modifications, for instance, ensemble algorithms. As such, we will separate the ANNs applications from the other used methods. In addition, we distinguish recurrent neural networks which are able to model dynamic problems.

4.2.3.1. Steady state artificial neural network VFM solutions. Feed-forward neural networks (also often referred as Multilayer Perceptrons (MLPs)) are a type of artificial neural networks which aims to approximate a function based on a certain number of input features without any recursive feedback connection between the network outputs and inputs. They are inspired by cognitive abilities of biological neural networks. The network is constructed using interconnected cells (neurons). These neurons are structured in a layered manner, so that the network usually consists of an input, hidden and output layers (Goodfellow et al., 2016). The input layer is required to read the variable (feature) values which are used for

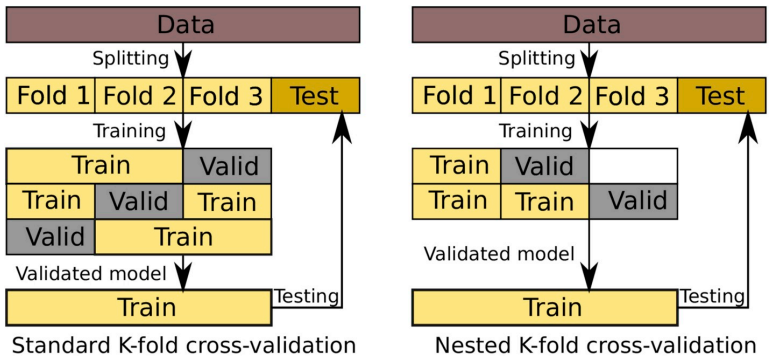

Fig. 5. Standard (left) and nested (right) K-fold cross-validation schemes for data-driven models.

training and for future predictions after training. In a VFM case, this can be pressure and temperature measurements, choke opening or other production system parameters. The hidden layers are used to produce non-linear relationships between the input parameters and approximate the function which describes the system behavior. In the output layer, the values produced in the hidden layer go through an activation function and then the network estimates the output variables (e.g. flowrates). This type of neural networks has been a popular choice for VFM technology because its key advantage is that it can approximate any relationships and patterns between variables, so that it can be considered as a universal approximator (Hornik et al., 1989). However, in case of transient flow behavior, steady state solution provided by a feed-forward neural network may not be accurate (Omrani et al., 2018).

One of the earliest attempts to estimate the multiphase flowrates based on pressure sensor data using neural network models was done by Qiu and Toral (1993). They used laboratory pressure transducers data as an input to the neural network and predicted gas-liquid rates as outputs. Since then, several examples of neural networks for VFM were reported.

A noticeable effort in applying neural networks for Virtual Flow Metering systems is done by Al-Qutami et al. (2018, 2017a, 2017c, 2017b). Al-Qutami et al. (2017b) used a neural network trained by Levenberg-Marquardt optimization algorithm. K-fold cross validation technique was used to select the number of neurons. The model was validated over 1.5 years of well test data. In order to avoid problems with overfitting, the early stopping technique was utilized. In addition to the evaluation of the trained model on the test data set, a sensitivity study was performed. The study revealed that the estimated gas flowrate is the most sensitive to the choke position value while bottomhole pressure is the most critical parameter for the oil flowrate predictions.

Al-Qutami et al. (2017a) discussed a hybrid ensemble learning by combining the neural network and regression tree (RT) approaches (NN-RTE). The idea behind the method is to generate a certain number of learners using different algorithms (in this case NN and RT), use a pruning technique to optimize this number (in this case simulated annealing (SA)) and then use a combining strategy (in this case simple averaging) to produce the final output. The paper compared the hybrid approach (NN-RTE) with homogeneous ensemble approaches (NN and RTE) and revealed a more accurate performance of the hybrid one.

Al-Qutami et al. (2017c) implemented a radial basis function network (RBFN) which uses a Gaussian transfer function in the hidden layer instead of a sigmoid function used in Al-Qutami et al. (2017a). The advantage of this method is the fact that it generally results in a faster training. In order to train the RBFN, Orthogonal Least Squares algorithm was used which is a common technique applied for RBFNs. A sensitivity study was carried out by excluding bottomhole pressure and choke opening form the model inputs. The results showed that the bottomhole pressure did not change much the resulting estimates while the choke opening was crucial for the network performance. This is a similar conclusion to the one in Al-Qutami et al. (2017b) for the gas rate. The authors concluded that further investigations in neural network sensitivity are required to make a solid argument on robustness of the method.

Al-Qutami et al. (2018) considered a modified version of the ensemble learning if compare to Al-Qutami et al. (2017b). In this case, the homogeneous approach with neural network ensemble was used. Instead of using another algorithm for learners, the diversity was achieved by implemented different regularization criteria such as scaled conjugate gradient and Bayesian regulation. In addition to the simple averaging, weighted average and NN meta-learner combining strategies were used. The results were compared before and after adaptive simulated annealing with bagging and stacking ensemble methods.

Omrani et al. (2018) performed a rigorous study of applying feed-forward neural networks to simulated and real field data. First, they considered a NN for predicting oil and gas flowrates in steady state operation and showed that the algorithm produces a good performance while during transient operation the NN may give inaccurate results. In addition, they considered sensitivity studies of the target variables with respect to uncertainty of the input data and revealed that in general NNs are capable to produce accurate flowrate predictions even under noisy input features unless the uncertainty increases dramatically. Finally, they proposed a method for back-allocation of well flowrates using total flow measurements from a separator, and the method showed a reasonable performance and can be addressed in future research.

AlAjmi et al. (2015) used a neural network to predict the oil flowrate through the choke. In addition to pressure, temperature, choke size and WC data, they used some additional parameters for inputs including an empirical correlation for the critical choke flow. When compared with flowrate estimations obtained by using the choke empirical correlations, the NN showed a reasonably better performance. It has to be noted that the choke models used in the study were purely empirical and not mechanistic which usually make better flowrate predictions.

Berneti and Shahbazian (2011) and Ahmadi et al. (2013) compared a conventional neural network approach with a hybrid approach by introducing Imperialist Competitive Algorithm (ICA) to optimize the initial values of weights in the network. Ahmadi et al. (2013) compared also considered Particle Swarm Optimization (PSO) and Genetic Algorithm for this purpose as well as utilized Fuzzy Logic approach to estimate the flows. Based on the study, superior capabilities of NN with ICA were revealed compared to other hybrid methods and the conventional NN training approach.

Zangl et al. (2014) constructed a neural network to estimate oil and water rates by the use of multi-rate well tests. They trained the network with a gradient descent method and the resulted network produced good predictions on a test dataset. A similar work by Hasanvand and Berneti (2015) shows a successful application of a three layers feed-forward neural network trained by Levenberg-Marquardt algorithm to predict oil flowrates using real field well test data from 31 wells collected over 8 years of production.

Xu et al. (2011) and Shaban and Tavoularis (2014) used Principal Component Analysis (PCA) in order to extract features from the experiemntal data sets to produce input variables to neural networks. The output flowrate estimates from the networks were in a good agreement with the measured values.

In addition to the research oriented neural network VFM applications, Baker Hughes has developed NeuraFlow software which is based on the neural network model (Baker Huges, 2014; Denney et al., 2013). This software is used to estimate the flowrates in systems with electric submersible pumps by applying the neural network approach. Similar to the previously discussed NNs, this system takes pump intake and discharge pressures as well as other measured parameters such as pump frequency as an input and produces the flowrate estimates as the network output.

4.2.3.2. Dynamic artificial neural network VFM solutions. In addition to the steady state feed-forward neural networks discussed above, there are different NN modifications which are capable to model transient phenomena. One example are recurrent neural networks (RNN) which are extensively used in many applications such as speech recognition and machine translation (Graves et al., 2013). The main idea behind this approach is to use the data from the past to predict the current target variable. For instance, in case of VFM, it takes the pressure and temperature measurements from the previous time step in order to estimate the flow at the current time step. In contrast, the feed-forward neural networks typically consider the data from the current time step only, so it performs steady state mapping only. In principle, it is possible to also include the past data into the feed-forward neural network, however, this approach has not been considered in the literature so far. At the same time, the RNN approach has been used in Virtual Flow Metering for transient flow estimation, and it is important to emphasize this in a separate section.

One example of utilizing RNNs for VFM is the work by Andrianov (2018). He used Long-Short Term Memory (LSTM) model which is a type of recurrent neural networks. Using synthetic well test data, he showed the capabilities of the LSTM method not only for estimating but

also forecasting the flowrates in the future time. In addition, he also considered the LSTM model for severe slugging prediction which is a highly dynamic multiphase flow phenomenon which typically occurs in risers. The results showed that the model was able to make accurate predictions of the volumetric flowrate of the periodic slugging flow in the riser.

Another example of RNN VFM system is the work by Loh et al. (2018). They also used an LSTM model for gas rate predictions for two natural gas wells. They trained the algorithm on the data of one well and made predictions on the new data for both wells. The results showed that the model is capable to predict the gas flowrates well in general, however, for the well whose data was not used in training, the predictions sometimes were not accurate. In addition to this analysis, they also combined the LSTM model with ensamble Kalman filter which we will discuss in the next chapter, and showed that adding the method of combining the two approaches allows to obtain more accurate flow estimates for both wells.

Omrani et al. (2018) compared performance of an LSTM neural network with a feed-forward NN and showed that under dynamic conditions such as shut-in and start-up of the well, the LSTM model has a better performance and even able to track changes of liquid-gas ratio during production.

Sun et al. (2018) used an LSTM NN for predicting oil, gas and water flowrates from shale wells. Such an application is very promising because, in general, shale wells have highly transient behavior which can be difficult to capture with feed-forward NNs and other steady state data-driven algorithms. The authors showed that the LSTM model is capable not only to predict the flowrates for the well whose historical data was used for training but also it is possible to predict the flow for a new well using the historical data from neighboring wells.

4.2.3.3. Other data-driven VFM solutions. In addition to the neural networks, some other methods were used to estimate multiphase flowrates from the collected measurements. One of the methods has been developed and applied in actual oil and gas production systems. FieldWare Production Universe (FW PU) is a data-driven VFM software which is used in Shell's fields around the world. The idea for the development of this software came from the Smart Fields initiative which aimed to use smart equipment, technologies and processes to optimize field production in Shell's fields (Bogaert et al., 2004; Poulisse et al., 2006). By 2011, the system had been running on around 60% of Shell's producing fields covering America, Europe, Africa, the Middle and Far East (Cramer and Goh, 2009; Dolle et al., 2007; Gerrard et al., 2007; Goh et al., 2008).

The data required for FW PU data-driven model is collected during Deliberately Disturbed Well Test (DDWT). DDWT is a well test procedure in which a well is routed to a test separator and then an operator deliberately changes the parameters in a stepwise manner, track it with the equipment and measures the single-phase flow at the test separator. By testing the well at various conditions, it is possible to construct a function which describes a well model. The function may have a general form as the following (Poulisse, 2009):

$$q_i(t) = f_i(g_{1i}(t), g_{2i}(t), .. g_{Ni}(t)) \tag{24}$$

where i – well number, $q_i(t)$ – flowrate, g_{Ni} – system parameter (e.g. wellhead pressure).

By performing DDWTs for each well, the well models can be constructed for each well and then combined in the estimation of the total field flowrate as:

$$q(t)_{estimated} \cong \sum_{i=1}^{N} \gamma_i g_i(t) \tag{25}$$

In this expression, γ_i is an unknown weight coefficient which must be iteratively found from the fact that the estimated and monitored (measured) flowrates should be substantially equal (Poulisse, 2009).

In order to apply the FW PU data-driven models for a field start-up phase, multiple runs of physical multiphase flow models can also be used. These pre-generated synthetic production data are then used to create the data-driven models (Poulisse et al., 2006). These models can then be re-trained when actual production data become available.

Apart from the widely used method applied in FW PU, some other data-driven methods have been used for VFM, mostly for research purposes. For instance, Xu et al. (2011) utilized Support Vector Machine approach to predict the flowrates based on the Venturi pressure difference values from the experiments which outperformed the neural network approach.

Zangl et al. (2014) considered linear regression (LR) and random forest (RF) for flowrate estimation, in addition to the backpropagation neural network. All the methods showed a reasonable performance with low average errors. The authors also used the models to perform Monte Carlo analysis in order to test the sensitivity of the model to input parameters. This study showed an advantage of using data-driven models for flowrate predictions as the run time is quick which makes it possible to perform many simulations for a reasonable time period. Bello et al. (2014) also used a linear regression model with a preliminary extraction of the training features using PCA. The resulted hybrid intelligence system produced good oil and gas rate predictions.

Grimstad et al. (2015) applied B-spline surrogate models for the flowrate estimation. In order to obtain the data for the algorithm, they used the pressure drop, choke and inflow performance models from Prosper and then fitted the results with the cubic spline interpolation function. The estimation results were compared to OLGA and showed a good performance.

Bikmukhametov and Jäschke (2019) applied gradient boosting algorithm with regression trees as a VFM system to predict oil flowrates in different field development cases. They considered the cases when VFM is used as a back-up system for a MPFM and as a standalone solution. The algorithm was trained on the data generated by OLGA software. The results showed that the algorithm has a good potential for multiphase flowrate predictions even having relatively small datasets from the well tests and the measurements from the MPFM. In addition, the algorithm can further be combined with neural networks within ensembles to improve the flowrate prediction accuracy.

4.3. Field experience with data-driven VFM systems

In this section, we describe the real operational experience reported in the literature using the data-driven models discussed in the previous section. The number of field applications with data-driven models is lower than with the first principles methods. The main reason for this is the fact that the industry effort over the past 50 years was mostly focused on the development of the first principles models, so that many vendors offer the products based on this approach. However, currently the industry is also trying to utilize the enormous amount of data collected in the fields every day and the research effort in this area has also increased over the past several years as we observed in the previous section.

Regarding the actual applications of data-driven methods in oil and gas production, the FW PU showed a robust and accurate performance for conventional and multizone wells and capable to track the dynamic changes in production systems. The estimates produced by the software can further be used for optimization and forecasting purposes (Cramer et al., 2011; Goh et al., 2008; Poulisse et al., 2006). Law et al. (2018) used FW PU Virtual Flow Meter for chemical injection optimization.

Denney et al. (2013) showed performance of NeuralFlow in a field over nine months period without a need to be re-calibrated. There are also some examples of applying data-driven VFM systems in fields which were developed for a specific field case. Garcia et al. (2010) developed a neural network to estimate the production and injection rates in fields in Brazil using a typical set of pressure, temperature and choke measurements for the network input and obtained the error level

of 4–7%. Olivarez et al. (2012) overcame problems with empirical choke flowrate estimations by developing a neural network solution which improved reliability of the field metering system. Ziegel et al. (2014) used a VFM system based on a neural network to predict oil and gas flowrates in a field with gas coning in the North Sea using the data from well tests. Al-Jasmi et al. (2013) developed a radial basis neural network able to predict the flowrates 30 days ahead with 90% confidence in wells with ESPs.

4.4. Summary of data-driven VFM applications

In Table 2, we give an overview of the discussed applications of data-driven modeling in Virtual Flow Metering systems. The table emphasizes the models features used in the works, the predicted variables, the input data for the training and the respective paper. In addition, we point out the origin of the training and test data and the fact if the sensitivity analysis to the input data was conducted.

5. Application of state estimation for transient modeling in VFM systems

5.1. Introduction

So far, we have discussed the first principles and data-driven modeling methods applied for Virtual Flow Metering. Most of the discussed methods describe steady state solutions meaning that they do not accurately estimate transient flows. In order to estimate flows under transient conditions, the time dependency of the system must be considered. This requires two necessary conditions: (1) dynamic models that accurately describe the transient behavior of the production system that may be based on the first principles or data-driven approach; (2) dynamic formulation of the training/optimization algorithm which considers the past states of the system. As we saw in the description of the first principles VFM systems, requirement (1) is typically satisfied, however, the requirement (2) is not, because typically the data validation and reconciliation algorithm has a steady state formulation. In the data-driven VFM systems, most of the methods do not satisfy both requirements.

One solution to this problem is using state estimation approach together with first principles or data-driven models to estimate the transient flows. In the literature, several application examples of state estimation for Virtual Flow Metering are described, in which the authors use first principles models and data-driven models together with state estimation techniques to estimate the oil and gas flowrates under transient conditions using the available measurement data. In this section, we will describe the main idea behind the most often used state estimation techniques for VFM such as Kalman filter modifications and then consider its applications in Virtual Flow Metering.

5.2. Description of the state estimation techniques applied for dynamic VFM systems

One of the most common state estimation techniques is the Kalman filter (Kalman, 1960). The Kalman filter is an optimal estimator meaning that, under some assumptions, the mean value of the estimation errors sum goes to a minimum value (Singh and Mehra, 2015). Despite the fact that the Kalman filter is extensively used in various applications, it is not widely spread in the petroleum industry. This is because most of the systems in this industry have non-linear behavior which restricts the usage of the Kalman filter. To overcome this, several extensions were developed to apply the Kalman filter concepts to non-linear systems. Some of the most common extensions are extended Kalman filter (EKF) (Jazwinski, 1970), ensemble Kalman filter (EnKF) (Eversen, 2003) and unscented Kalman filter (UKF) (Julier et al., 2000). For estimation of multiphase flowrates, the first two options have been considered.

The Kalman filter and its variants are algorithms that use a dynamic model to propagate estimates of the states together with the variance-covariance matrices in time. While the original Kalman filter was developed for linear systems, the extended Kalman filter uses a linearization of the non-linear model around the current estimate. Given the system with available measurements, the idea behind the state estimator is to predict the state values based on the noisy measurements obtained from the system. To construct the EKF, we need to discretize a state-space model of a non-linear system in time. The states of the system typically include variables which we would like to estimate, for example, in case of VFM, pressure, holdup or flowrates. The EKF will integrate the discretized model over time considering the process noise and the measurements. A good example of the adaptation of the conservation equations in the context of flow estimation to the state space form is described by (Gryzlov et al., 2013).

The Ensemble Kalman filter allows to avoid linearization but generate the estimates of the state vector and the covariance using so-called ensembles. The EnKF is able to solve highly non-linear problems more accurately compared to the EKF, while for problems with small non-linearities their performance is approximately the same. The computational time depends on the order of the system under consideration. For higher order systems, the EnKF is usually the fastest option (Leskens et al., 2008). More discussions about the comparison of the EKF and EnKF can be found in Leskens et al. (2008) and Reichle et al. (2002).

Another estimation technique which has been used for VFM is Moving Horizon Estimation (MHE). This approach is based on formulating an optimization problem to find the states of a dynamic model that best match measurement data during a specified time period (horizon) in the past. When new measurement data become available. The horizon is shifted, such that the oldest data point is discarded and the newest point is included. This procedure is repeated at given sample times. MHE is becoming a popular estimation technique for many industrial applications and a vast amount of literature is available on this method. For a more detailed description about the method, please see Rao et al. (2001).

5.3. Reported research on state estimation methods applied for dynamic VFM systems

Despite the fact that state estimation methods for VFM applications are not widely used in industry, there have been several research efforts in this area. Bloemen et al. (2006) considered the extended Kalman filter to predict the flowrates in gas-lift wells. To estimate the flowrates of a two-phase flow, they assumed that noisy pressure measurements are taken along the wellbore. For the model part, the drift-flux formulation was considered. It was shown that under dynamic conditions caused by the choke opening, the model was able to estimate the gas and liquid flows accurately.

Leskens et al. (2008) considered a three-phase flow in a unilateral horizontal well and applied the EKF for flowrate estimation. It was assumed that five downhole pressure and four temperature sensors were available for the EKF. The wellhead measurements were not considered. The authors showed that without the noise the model worked well while with the noise the method was unable to track the flowrate changes.

To extend the work by Leskens et al. (2008), De Kruif et al. (2008) considered both two and three-phase flows in unilateral and multilateral wells using the EKF. In the two-phase case in the unilateral well, six downhole pressure and temperature measurements were sufficient to estimate the flow accurately. For the three-phase case, downhole data were not enough for good estimations. However, wellhead pressure sensors helped to improve the predictions. Another interesting finding was the fact that using only wellhead data was sufficient to predict the flowrates. However, the model was not able to track the changes of the inflow in time. Instead, the time delay response was observed. This led to the conclusion that the downhole sensors are necessary in order to track flowrate changes accurately. As for the multilateral case, the authors showed that even with the downhole and

Table 2
Summary of data-driven models for VFM applications.

Method	Method features	Predicted flowrate	Data origin	P_{BH}	T_{BH}	P_{WH}	T_{WH}	C_V	Gas lift rate	WC	P_{FL}	Other	Sensitivity to input	Paper
	Conventional NN trained by L-M and NN with ICA/PSO/GA for weights optimization	Oil	Field	✓	✓	✓	✓							Ahmadi et al. (2013)
	NN trained by L-M with early stopping	Oil/Gas	Field	✓		✓	✓	✓					✓	Al-Qutami et al. (2017b)
Feed-forward NN	RBFN with Gaussian radial basis function. Trained by Orthogonal Least Squares	Gas	Field	✓		✓	✓	✓					✓	Al-Qutami et al. (2017c)
	NNE trained by L-M with early stopping and NN with regression tree learners	Oil/gas/water	Field	✓	✓	✓		✓	✓	✓	✓			Al-Qutami et al. (2017a)
	NNE trained by L-M with scaled conjugate gradient and Bayesian regulation. Applied simple and weighted averaging and NN meta-learner for the output layer	Liquid/Gas	Field	✓		✓	✓	✓						Al-Qutami et al. (2018)
	NN for critical choke flow; compared to empirical choke models	Oil/Gas	Field			✓		✓		✓		✓		AlAjmi et al. (2015)
	NN applied to real operation in a field with ESPs	Liquid	Field			✓						✓		Al-Jasmi et al. (2013)
	NN integrated with Fuzzy Logic to select the best performing model	Oil	Field			✓	✓							Alimonti and Falcone (2004)
	NN with Imperialist Competitive Algorithm for weights optimization	Oil	Field	✓	✓	✓	✓							Berneti and Shahbazian (2011)
	NN applied in real field operation	Oil	Field	✓	✓	✓	✓	✓	✓	✓		GOR		Garcia et al. (2010)
	NN trained with L-M	Oil	Field	✓	✓	✓	✓							Hasanvand and Berneti (2015)
	NN trained using ESP data	Oil	Field									✓		Denney et al. (2013)
	NN trained with L-M using simulated and field data and tested for sensitivity to data uncertainty	Oil/Gas	Synthetic/Field	✓	✓	✓	✓	✓			✓	✓	✓	Omrani et al. (2018)
	NN applied in real field operation	Oil	Field	✓	✓	✓	✓	✓		✓	✓	✓		Olivarez et al. (2012)
	NN with PCA for dimensionality reduction	Gas/Water	Experiment									RDP		Shaban and Tavoularis (2014)
	NN with PCA for dimensionality reduction	Gas/Water	Experiment									VDP		Xu et al. (2011)
	NN trained by the gradient descent method on multi-rate well test data	Oil/Water	Field			✓	✓		✓		✓		✓	Zangl et al. (2014)
	NN trained on well test data	Gas/Liquid	Field			✓		✓	✓			✓		Ziegel et al. (2014)
Recurrent NN	LSTM NN to estimate dynamic current and future flowrates	Oil/Gas/Water	Synthetic			✓	✓				✓			Andrianov (2018)
	LSTM NN and LSTM NN with ensemble Kalman filter to predict transient oil flowrate	Gas	Field	✓	✓	✓	✓	✓						Loh et al. (2018)
	LSTM and feed-forward NN trained on steady state and dynamic conditions	Oil/Gas	Synthetic/Field	✓	✓	✓	✓	✓			✓	✓	✓	Omrani et al. (2018)
	LSTM for multiphase flows estimation in unconventional wells	Oil/Gas/Water	Field			✓						✓		Sun et al. (2018)
Model identification with DDWT	Model identification using data from DDWT	Oil/Gas/Water	Field	✓	✓	✓	✓	✓				✓		(Gerrard et al., 2007; Poulisse, 2009) and therein references
B-spline	B-spline surrogate model which approximates simulated data	Liquid	Synthetic	✓	✓	✓	✓	✓						Grimstad et al. (2015)
Gradient Boosting with RT	Gradient boosting algorithm with regression trees as weak learners	Oil	Synthetic	✓	✓	✓	✓	✓						Bikmukhametov and Jäschke (2019)
RTE	Regression trees ensembles. Minimum leaf size or early stopping used for stopping	Oil/Gas/Water	Field	✓	✓	✓		✓	✓	✓	✓			Al-Qutami et al. (2017a)
FL	Automatic selection of the membership function	Oil	Field	✓	✓	✓	✓							Ahmadi et al. (2013)
SVM	SVM models trained to predict gas and water flowrates	Gas/Water	Experiment									VDP		Xu et al. (2011)
LR	Multiple Linear Regression method	Oil/Water	Field			✓	✓		✓		✓		✓	Zangl et al. (2014)
RF	Decision tree approach with 700 nodes	Oil/Water	Field			✓	✓		✓		✓		✓	Zangl et al. (2014)
PCR	Linear regression with Principal Component Analysis	Oil/Gas	Field	✓	✓	✓	✓	✓		✓		GOR		Bello et al. (2014)

wellhead sensors, the model was not good enough to estimate the flow correctly. This is because the model needs correction for the specific branch of the multilateral well at the wellhead which is not possible as the flows from all the branches commingle inside the wellbore.

Lorentzen et al. (2010a) used the ensemble Kalman filter to predict the gas inflow at four different zones in the wellbore. To do this, downhole temperature sensors were used together with the transient drift-flux model. The model showed promising results by estimating the flows accurately. In a similar work, Lorentzen et al. (2010b) considered a well with two branches and used temperature measurements with and without pressure sensor data to estimate the flow by use of the EnKF. They showed that using only temperature sensors can be sufficient to estimate the gas flowrate from a particular well branch.

Gryzlov et al. (2013) utilized the extended Kalman filter for the flowrate estimation problem. Several cases were considered including flowrate and holdup estimation. At first, it was assumed that in each of 50 discretization blocks the pressure measurements were available. Then, the number of sensors were reduced by a factor of three and six. The results showed that by reducing the number of sensors, the estimation error increases. The conclusion was that each inflow point must be equipped with at least two pressure sensors, however, this requires a closer investigation.

Muradov and Davies (2009) applied the extended Kalman filter for zonal rate allocation in synthetic and real multizone wells and compared its performance with optimization techniques. The results showed that even though all the methods were suitable for the application, the EKF was the most suitable for noisy measurement data.

Binder et al. (2015) consider Moving Horizon Estimator for flowrate estimation in a well with an ESP. For the input, bottomhole, downhole and pump pressure sensors were considered together with pump parameters. The method showed an accurate performance and was suggested to be used for industrial applications.

In the works described above, the state estimation methods are applied to the first principles models. However, it can also be applied to the data-driven model if the model is dynamic, for instance, a recurrent neural network. Loh et al. (2018) applied the ensemble Kalman filter together with an LSTM network and compared the performance with a pure LSTM model. The results showed that the ensemble Kalman filter gives an opportunity for the LSTM model to better capture the flow behavior and preform more accurate multiphase flowrate estimation.

In addition to the aforementioned studies, there are several works which do not consider estimation methods for VFM directly but describe models which can be suitable for this purpose. Aarsnes et al. (2016) conducted a review work on multiphase flow models which can be used for estimation algorithms. Some aspects of implementing the Kalman filter variations for drilling applications can be also accounted when constructing a state estimator for VFM purpose. For such examples, please see Aarsnes et al. (2014a, 2014b) and Nikoofard et al. (2017). The state estimation techniques can also be used to estimate the multiphase flow model parameters such as slip and friction coefficients (Lorentzen et al., 2003, 2001).

5.4. Discussion on using state estimation in dynamic VFM systems

State estimation methods can be a promising tool for dynamic estimation of multiphase flowrates in VFM systems. These methods have the following advantages for VFM applications:

- Have a potential to use additional data from the production to improve estimates in a simple manner
- Filter noisy measurements and solve the estimation problem within one algorithm
- Have a potential in accurate flow estimation using MHE and data-driven models that are fast to evaluate
- Can be used to estimate unmeasured variables

However, apart from the positive sides, there are disadvantages which make application of these methods in VFM systems challenging:

- The methods have not been used in the industrial VFM applications, so that operational experience is absent
- It is a complex approach which includes physical and statistical modeling, so the model development cost is high
- Difficult tuning

Taking the aforementioned points into account, we conclude that the state estimation methods are a promising approach for VFM, but the challenges with its construction complexity have to be overcome in order to make these methods applied for VFM more often.

6. Comparison of VFM methods

In the previous sections, we described the VFM methods which have been developed for industrial and academic applications. In this section, we would like to emphasize the advantages and disadvantages of using a particular VFM solution and also compare it with physical multiphase flow meter. Marshall and Thomas (2015) compared VFM in general with MPFM and test separators but did not distinguished the difference between the VFM methods. In this section, we add the comparison between the VFM methods and also specify other additional points of interest. Table 3 shows the methods comparison. In addition to this table, please see Bringedal and Phillips (2006) and Varyan (2016) for more detailed discussions about potential savings and cost reduction using VFM.

7. VFM literature summary

In this section, we give an overview of the available contributions on Virtual Flow Metering. In Table 4, the material summary is structured in such a way that all the relevant papers can be found based on a topic of interest. Here we aim to include all the works which contributed to the VFM development. The works under each sub-section of the table is presented by the published date order.

8. Challenges and opportunities for VFM development

Even though a vast research effort in the development of Virtual Flow Metering systems has been conducted, there are still many opportunities for this technology to improve and become a more reliable source of multiphase flowrates estimates. Based on the revised literature, in this section we propose several possible directions for the research and development of first principles and data-driven VFM systems.

8.1. First principles VFM systems

A further evaluation of the VFM sensitivity to the input parameters is required. As a starting point, one can take the evaluation by Amin (2015), Toskey (2011), Varyan et al. (2015), Tangen et al. (2017) and Lansagan (2012) and address the revealed contradictive points from the studies which we emphasized before. In addition, a systematic evaluation of the accuracy of sub-models under various conditions can be conducted. It can useful to see how separate models perform (e.g. choke and thermal-hydraulic models) with changing GORs and sensor accuracy. This can lead to selecting a correct VFM strategy at different stages of the field life cycle.

Another question is how accurate the models must be in order to construct an accurate VFM system? Can the required accuracy of the models be reduced by robust data validation and reconciliation techniques? We saw that there are several commercial VFM systems available and each has its own accuracy level of the used models. Some systems mostly rely on high fidelity multiphase models (e.g. OLGA and

Table 3
Comparison of VFM methods, MPFM and test separators.

Metering method		Advantages	Disadvantages
Virtual Flow Metering	VFM in general	- Real-time or near-real-time monitoring - Low cost solution - Does not require physical intervention to fix the problem unless most of the sensors fail - May be well integrated with other software to maximize production	- Depends on the sensor accuracy - Requires periodical tuning - Depends on the model accuracy
	First principles VFM	- Uses well-proven and known modeling methods - Operational experience is relatively long - Well suited for steady state or near-steady state situations - Many vendors available - Can be used to model other operational problems such as slugging, erosion, hydrates occurrence - Can be used to estimate unmeasured variables	- Require deep knowledge about the physics which describes the system - Quasi-steady state. Fit parameters in a certain point in time having the previous solution, hence might have a delay to capture dynamic situations - Highly depends on PVT data accuracy - Tuning process is not straightforward - High computational cost compared to data-driven VFM
	Data-driven VFM	- Does not require deep knowledge about the physics which describes the system - When the model is trained, it has low computational cost for flowrate predictions compared to other VFM methods - Easy to update continuously with newly obtained data - Easy to combine different parameters from different parts of the production system without constructing a complex physical model	- Not suitable when limited historical data is available - Most of the methods are steady state. Research on using this VFM approach for dynamic situations is required. - Limited operational experience - Can be applied to data within or near the training data range, otherwise calibration and re-training is required - Advanced feature engineering requires process insights
Physical Flow Metering	MPFM	- Vast operational experience because widely used in the industry - Real-time monitoring - Handles dynamic multiphase flow metering - Many vendors are available	- High cost technology - Requires periodical calibration and accurate PVT data - Exposed to failures, erosion and blockage - Requires expensive physical intervention to fix problems - May produce inaccurate measurements if conditions are out of the operational range
	Test separator	- Accurate flowrate estimation - Can be used as the reference with high confidence - Allows to estimate other important parameters such as fluid and reservoir properties	- No real-time monitoring - Loss of production which leads to high cost of operation - Requires vast experience of operators to make accurate well tests - Performance of other wells may be affected during the well test

K-Spice VFM systems) while the others on the reconciliation techniques (e.g. ValiPerformance). By answering these questions, we could understand what we should focus on in the future VFM development: an accurate tuning and optimization strategy or accurate system models, for instance, tubing and choke models.

Even when the VFM is tuned well, it will be necessary to re-tune the model after some production time. The tuning requires the knowledge about both operational and software features which make the process complicated. As such, an auto-tuning strategy would be a valuable asset in order to make VFM to be a standalone flow metering solution in the fields.

One of the issues influencing the VFM performance is the accuracy of PVT data which has to be continuously updated. This is linked to the tuning strategy discussed above. As such, one could also think of a more robust implementation of the VFM system in terms of the PVT change. If the system becomes less sensitive to the PVT error, this will result in less frequent well testing for model tuning and the tuning in general. One possible way may be measuring total mass flowrate, mixture densities and water cut at wellhead conditions and using it as a tuning parameter.

We saw that state estimation methods can be a promising tool for constructing an accurate dynamic first principles VFM system. The methods may be useful in solving the following problems: flowrate estimation under transient conditions; removing the influence of noise and even drift of measurement data on the VFM estimates; estimation of zonal well inflow and flow from multilateral wells. However, to proceed in incorporating these methods into the first principles VFM systems, the following questions have to be answered first: how to perform a robust tuning of the estimation methods; is the typical well configuration with downhole and wellhead sensors enough for accurate estimation or more sensors are needed; can the models be easily recalibrated for new field conditions. In addition, more investigations using real field data are required. In this way, the potential of utilizing the state estimation methods for the first principles VFM systems will actually be revealed.

In order to proceed in developing accurate transient flow estimation using first principles VFM systems, it can be promising to develop methods for numerical optimization of large-scale complex high-fidelity dynamic models that provide real-time derivatives that can be used by an optimization solver.

8.2. Data-driven VFM systems

Various data-driven models are considered in this work. One of the emerging data-driven models in VFM is based on neural networks which seems to have a big application potential. Despite the fact that the academic results are promising, a lot of work has to be done in order to make NNs to be widely applicable as an industrial VFM solution. In addition to consideration of neural networks applications, other more general research directions are given below.

Performance of data-driven models in general and neural networks in particular is highly dependent on feature engineering. Oil and gas productions systems include many parameters which influence a particular well, so may be potentially used as input features to the neural network. At the same time, finding an optimal set of features as well as hyperparameters of the neural network is a challenging task which is an ongoing research in the field of machine learning. As such, development of the approach which could identify the most informative features and optimal set of neural network hyperparameters at the same time will be a strong contribution towards accurate and robust flowrate estimates from a data-driven VFM model.

So far, only maximum likelihood estimation approach has been used for VFM modeling meaning that only the most likely value of the

Table 4
Summary of VFM manuals and literature contributions.

First principles VFM systems

Commercial VFM systems (description of models and field experience)

OLGA Online:
(Schlumberger Limited., 2014) – description of models used in OLGA Online VFM (manual)
K-Spice:
(Patel et al., 2014) – implementation of K-Spice VFM in Alta field which showed a good performance during the tests
(Kongsberg, 2016) – description of models used in K-Spice VFM system (manual)
(Tangen et al., 2017) – sensitivity analysis of K-Spice VFM system under various conditions with a digital twin approach
(Couput et al., 2017) – summary of Total experience with K-Spice VFM. Emphasized that despite the advantages of the VFM costs, it still needs skilled people to tune and calibrate the software which can be a challenge for operator companies
FlowManager:
(Rasmussen, 2004) – discusses principles and possible applications of VFM as well as field experience with FlowManager
(Holmås and Løvli, 2011) – describes models and numerical schemes used in FlowManager as well as field applications
(Holmås et al., 2013) – discusses applications of FlowManager as a flow assurance system in Ormen Lange and Vega fields in the North Sea and used as a back-up system to the MPFMs
(Varyan et al., 2015) – performed several sensitivities studies with FlowManager and compared performance with MPFMs
(Løvli and Amaya, 2016) – shows six cases of FlowManager VFM applications including gas condensate and oil fields during normal conditions as well as start-up operations.
WMS:
(van der Geest et al., 2000) – describes the models used in WMS and its performance on synthetic data
(van der Geest et al., 2001) – discusses successful WMS applications in Troika field in the Gulf of Mexico
(Melbø et al., 2003) – discusses application of WMS in the North Sea including cases with unreliable sensor information
(ABB, 2004) – application of WMS VFM in Bonga field, Nigeria.
(Bringedal et al., 2006) – application of WMS VFM in Bonga field, Nigeria.
Virtuoso:
(Haldipur, 2011; Haldipur and Metcalf, 2008) – describes models and computational methods used in Virtuoso as well as various field applications
(Parthasarathy and Mai, 2006) – presents Virtuoso applications as a back-up, monitoring and substitute system for MPFMs
ValiPerformance:
(Couput et al., 2008) – discusses examples of the software installation in an onshore field in France and a complex subsea field as a back-up and reduction uncertainty system
(Wising et al., 2009) – discusses the models used in ValiPerformance and its implementation with DVR algorithm
(Couput and Renaud, 2010) – describes an example of the software performance in the Middle East operated by Total with 16 wells with ESPs
(Petukhov et al., 2011) – describes the software models and successful testing in Ceiba oil field in Equatorial Guinea
(Haouche et al., 2012a; 2012b) – describe the software models including ESP with density correction factor as well as field tests and operation
(Couput et al., 2017) – summary of Total experience with ValiPerformance VFM.
Rate&Phase:
(Foot et al., 2006; Heddle et al., 2012) – describe types of software models and its performance on more than 300 production and injection wells
FieldWatch:
(Roxar, 2015) – description of models used in FieldWatch VFM (manual)
Prosper:
(Acuna, 2016; Ma et al., 2016; Omole et al., 2011) – used Prosper as an engine for VFM in real field cases and then combined it with external optimization techniques to estimate the flowrates continuously and optimize field production
(PETEX, 2017) – description of models used in Prosper (manual)
Sensitivity, comparative and economic studies:
(Bringedal and Phillips, 2006) – compares VFM with test separator and MPFM solutions from technological and economic points of view
(Toskey, 2011) – performs comparison of several VFM software based on synthetic data from OLGA which included several case studies with different set of parameters for flowrate estimation. In addition, conducted a survey of vendors about the VFM product features
(Lansagan, 2012) – considers sensitivity study on influence of measurement degradation, input uncertainty and availability on VFM estimates
(Amin, 2015) – describes comparison of several VFM software based on real field data. In addition, performs a sensitivity study of VFM to the input PVT data
(Varyan et al., 2015) – describes a sensitivity study of FlowManager VFM with respect to the input parameters
(Mokhtari and Waltrich, 2016) – compares different wellbore and choke models for VFM
(Varyan, 2016) – discusses potential cost savings using VFM compared to test separators and MPFMs
(Tangen et al., 2017) – sensitivity analysis of K-Spice VFM under various conditions with a digital twin approach
(Bikmukhametov et al., 2018) – describes statistical analysis of effect of sensor degradation and failure as well as heat transfer modeling methods on VFM flowrate estimates

Choke model VFM

(Delarolle et al., 2005; Faluomi et al., 2006) – developed a choke model, validated it with experimental data and CFD analysis and applied the model at field conditions in Italy, North and West Africa and the Gulf of Mexico
(Campos et al., 2010) – used a choke model as a VFM tool in an integrated production model of Urucu field
(Loseto et al., 2010) – used a choke model as a VFM tool in an integrated production model of Don fields
(Ajayi et al., 2012; Allen and Smith, 2012) – used models of downhole inflow control valves to construct a VFM system
(Moreno et al., 2014) – used a choke model as a VFM tool together with an optimization algorithm to optimize field production
(Espinoza et al., 2017; Hussain et al., 2016) – used empirical choke models to estimate the flowrate at field conditions
(Cheng et al., 2018) – combined choke model with thermal-hydraulic and IPR models for creating a VFM system which used in real field application in an offshore field

ESP model VFM

(Camilleri et al., 2016b; 2016c; 2016a; 2015; Camilleri and Zhou, 2011) – consider ESP models with various modifications and field case studies in which ESP first principles models act as Virtual Flow Meters
(Haouche et al., 2012a; 2012b) – describe the software models including ESP with density correction factor as well as field tests and operation

(*continued on next page*)

Table 4 (*continued*)

First principles VFM systems

Commercial VFM systems (description of models and field experience)

Data-driven VFM systems

Industrial applications (neural networks)

NeuraFlow:

(Denney et al., 2013) – describes the performance of NeuraFlow in field conditions

(Baker Huges, 2014) – describes the approach used for NeuraFlow software

Patchwork applications:

(Garcia et al., 2010)– describes a neural network application for production and injection rates estimation in fields of Brazil using a typical set of pressure, temperature and choke opening measurements

(Olivarez et al., 2012) – describes a neural network for production estimation when choke models showed unsatisfying performance

(Al-Jasmi et al., 2013) – used a radial basis neural network to forecast oil production 30 days ahead in wells with ESPs

(Ziegel et al., 2014) – used a neural network as a VFM system to predict oil and gas flowrates in a field in the North Sea

Industrial applications (other methods)

FieldWare Production Universe:

(Bogaert et al., *2004*; *Poulisse* et al., *2006)* – discuss the first ideas of developing a data-driven VFM system as a part of Smart Fields production technologies

(Cramer et al., *2011*; *Cramer and Goh, 2009*; *Dolle* et al., *2007*; *Gerrard* et al., *2007*; *Goh* et al., *2008*; *Law* et al., *2018*; *Poulisse, 2009*; *van Den Berg* et al., *2010)* – describe FieldWare application in many production examples from America, Europe, Africa and the Middle East to estimate the flowrates and optimize production

Research works (neural networks)

Feed-forward neural networks

(Qiu and Toral, 1993) – considers a neural network for oil and gas flowrates estimation using experimental data with pressure transducers

(Berneti and Shahbazian, 2011) – describes application of Imperialist Competitive Algorithm for initial weights optimization in a neural network for estimation of oil production

(Hasanvand and Berneti, 2015) – trained a neural network by Levenberg-Marquardt algorithm for oil rate predictions

(Xu et al., *2011)* – used Principal Component Analysis in order to reduce dimensionality of the feature space from the experiemntal data sets to produce input variables for neural networks

(Ahmadi et al., *2013)* – describes application of various derivative free algorithms for weights optimization of a neural network to make accurate estimates of oil production

(Zangl et al., *2014)* – constructed a neural network to estimate oil and water rates by the use of multi-rate well tests

(Shaban and Tavoularis, 2014) – used Principal Component Analysis in order to extract features from the experiemntal data sets to produce input variables for neural networks

(AlAjmi et al., *2015)* – describes application of a neural network to predict the flow through a choke by including not only pressure and temperature measurements but also WC and a choke model for critical flow

(Al-Qutami et al., *2017a)* – describes ensemble learning by combining neural networks and regression trees to estimate oil production and compares the model performance with homogeneous neural networks

(Al-Qutami et al., *2017b)* – developed a neural network to estimate the flowrates based on real production data as well as performed sensitivity studies of input parameters

(Al-Qutami et al., *2017c)* – used a radial basis neural network for the flowrate estimates as well as performed sensitivity studies of input parameters

(Al-Qutami et al., *2018)* – considers different methods for ensemble learning with neural networks for production estimation

Recurrent neural networks

(Andrianov, 2018) – used LSTM recurrent neural networks on synthetic well test data to estimate and forecast oil production

(Loh et al., *2018)* – compared performance of LSTM NN and LSTM NN combined with ensemble Kalman filter to predict transient oil flowrates

(Omrani et al., *2018)* – compared LSTM with feed-forward NN under transient conditions, performed sensitivity analysis of NN predictions with respect to data uncertainty and proposed a method for back-allocation of well flowrates using total flowrate measurements from a separator

(Sun et al., *2018)* – used LSTM models for predicting oil, gas and water flowrates from unconventional shale production

Research works (other methods)

(Xu et al., *2011)* – describes application of Support Vector Machine for flowrate estimation based on Venturi pressure difference from experiments

(Zangl et al., *2014)* – describes comparison of neural networks with linear regression and random forest methods

(Bello et al., *2014)* – describes a linear regression model with a preliminary extraction of the training features using PCA for flowrate estimation

(Grimstad et al., *2015)* – used B-spline models to approximate models from a commercial simulator which are then used for VFM purposes

(Bikmukhametov and Jäschke, 2019) – used gradient boosting with regression trees to estimate oil flowrates for different field development cases

Application of state estimation methods for VFM

(Bloemen et al., *2006)* – describes application of extended Kalman filter (EKF) for flowrate prediction in gas-lift wells

(Leskens et al., *2008)* – shows application of EKF for three-phase flowrate estimation in a unilateral horizontal well

(De Kruif et al., *2008)* – discusses EKF for two and three-phase flow estimation in unilateral and multilateral wells using different number and placement of measurements

(Muradov and Davies, 2009) – considers EKF for zonal rate allocation in synthetic and real multizone wells and compared its performance with optimization techniques

(Lorentzen et al., *2010a)* – discusses application of EKF to predict the gas inflow at four different zones in the wellbore

(Lorentzen et al., *2010b)* – considers a well with two branches and used temperature measurements with and without pressure sensor data to estimate the flow by use of the ensemble Kalman filter

(Gryzlov et al., *2013)* – considers different cases including flowrate and holdup estimation using EKF

(Binder et al., *2015)* – consider Moving Horizon Estimation for flowrate estimation in a well with an ESP

flowrates is estimated by a data-driven algorithm. However, these estimates will always have uncertainty due to different distributions of training and actual production data, noise in data, errors in reference measurements of flowrates from well tests and sensors, etc. Accurate estimation of these uncertainties in VFM applications may be valuable. It will allow using reconciliation techniques for better flowrate estimates using separator measurements as well as incorporating these uncertainties into daily and long-term production optimization.

Most of the data-driven algorithms described in this paper are able to model steady state systems and might fail to model transient fluid flow accurately. As Andrianov (2018), Loh et al. (2018) and Omrani et al. (2018) showed, there are neural network architectures which are able to capture the dynamic systems behavior. However, it is likely to happen that recurrent neural networks will not always outperform other data-driven methods even under transient conditions. As such, more work should be done in this direction to reveal the full potential of recurrent neural network architectures for making more accurate multiphase flowrate estimations, especially under transient conditions. For instance, identifying the required time frequency of the measurements and strategy for tuning the time window size can be a valuable asset.

As the industry has good knowledge of the first principles models for multiphase flow, it can also be valuable utilize this knowledge for making hybrid solutions together with data-driven models. There are different research directions to investigate. First, ensemble learning with

data-driven and first principles models can be used. Another possibility may be applying physical models for training purposes, for example, in transient or lack of data situations. In addition, creating input features based on the first principles of multiphase flow may help the algorithm to map the input with output variables and produce better predictions.

Only a few works have been done on the ensemble learning of data-driven algorithms for VFM, while it has been well investigated for many other applications. With ensemble learning the model the behavior of the model becomes less explainable, but it may produce better estimates. At the same time, the model explanation may not always be necessary for flow monitoring. The potential of ensemble learning for VFM applications is certainly unrevealed and can be addressed in the future research work in this area.

As Loh et al. (2018) showed, the state estimation methods can be used not only with the first principle models but also with dynamic data-driven models, for instance, an LSTM neural network. Using the state estimation methods in this case can help the data-driven model produce accurate flowrate estimates having even a small training dataset or noisy input data. However, since only one attempt has been made in incorporating the state estimation methods in data-driven models, this research direction has many opportunities for revealing additional advantages of utilizing this approach.

9. Conclusions

Virtual Flow Metering is a promising approach for flowrate estimation due to its low cost, real-time monitoring capabilities and an easy integration with other software solutions. There are different approaches to estimate multiphase flowrates which are used in the industry or are at the research phase. Currently, the first principles approach is the most often used Virtual Flow Metering tool in operation as a standalone solution or as a back-up system for physical multiphase flow meters. Despite an active use of the first principles VFM systems, this approach still has many challenges to solve, such as model and PVT data tuning and handing transient flow behavior using dynamic optimization or state estimation techniques.

Data-driven methods are becoming more and more popular due to an increasing amount of field data and recent advances in development and understanding of data-driven algorithms as well as increase of computational power used for algorithm training. State estimation methods are still not often used in the industry and have mostly academic applications, however, the methods have several strong advantages, for instance, transient flow modeling integrated with noisy measurement data. The main challenge associated with this method is that it typically requires good models and is difficult to tune and these points have to be addressed on the future research. In addition, there is a potential in combining state estimation methods with data-driven models where a detailed physical model is not required, while the advantage of incorporating noisy measurement data still holds.

Independently on the applied VFM approach, systematic model tuning is one of the main reasons why VFM is not the main multiphase flow metering solution. The first reason for this is the fact that obtaining accurate flowrate measurements for tuning is difficult, especially in subsea fields, so it is challenging to establish a robust procedure for VFM tuning. Also, the model tuning itself is a hard task and requires a deep understanding of the models and other underlying principles. As such, developing auto-tuning strategies is an important task which has to be solved by VFM vendors to increase popularity of VFM solutions for multiphase flow metering.

Another problem is estimating uncertainty of VFM predictions and taking it into account to make accurate predictions. Depending on the applied method, this includes uncertainty of models, measurements, PVT data and reference flowrates. Accurate estimating and reducing these uncertainties is an important issue which has to be addressed in the future research for all the VFM methods.

A promising direction for research can be development of a VFM system which uses approaches of first principles and data-driven modeling together and takes advantages of each method. This approach can be called a hybrid VFM system. A hybrid model should be able to adapt to conditions of a particular field such as measurement data availability, stage of the field development, frequency of well tests for model tuning, uncertainty of the measurements, etc. In addition, by combining several VFM methods it will be possible to obtain several estimates of the same quantity which can increase the estimation confidence.

Irrespectively of the method, VFM is one of the steps towards low cost field development solutions which is steadily being integrated in subsea oil and gas fields around the world. The trend of an efficient data use in the industry also supports the concept of VFM. We believe that the future research and pilot tests may strengthen capabilities of VFM methods which will provide more trust for the operators to utilize VFM technology in a reliable and effective manner.

Acknowledgments

This work was carried out as a part of SUBPRO, a Research-based Innovation Centre within Subsea Production and Processing. The authors gratefully acknowledge the financial support from SUBPRO, which is financed by the Research Council of Norway, major industry partners, and NTNU.

References

Aarsnes, U., Flåtten, T., Aamo, O., 2016. Review of two-phase flow models for control and estimation. Annu. Rev. Contr. 42, 50–62. https://doi.org/10.1016/j.arcontrol.2016.06.001.

Aarsnes, U., Meglio, F., Aamo, O., Kaasa, G., 2014a. Fit-for-Purpose modeling for automation of underbalanced drilling operations. In: SPE/IADC Managed Pressure Drilling & Underbalanced Operations Conference & Exhibition, . https://doi.org/10.2118/168955-MS.

Aarsnes, U., Meglio, F., Evje, S., Aamo, O., 2014b. Control-oriented drift-flux modeling of single and two-phase flow for drilling. In: Proceedings of the ASME 2014 Dynamic Systems and Control Conference, . https://doi.org/10.1115/DSCC2014-6121.

ABB, 2004. Well Monitoring System.

Abrahart, R., See, L., Solomatine, D., 2008. Practical Hydroinformatics: Computational Intelligence and Technological Developments in Water Applications. Springer.

Åbro, E., Couput, J., de Leeuw, R., 2017. Joining efforts between operators within multiphase metering technology. In: 35th International North Sea Flow Measurement Workshop.

Acuna, I., 2016. Effective methodology for production metering and allocation using real-time virtual metering in a mature offshore oilfield-study of the greater angostura field. In: SPE Trinidad and Tobago Section Energy Resources Conference, . https://doi.org/10.2118/180887-MS.

Agarwal, R., Li, Y., Ngheim, L., 1990. A regression technique with dynamic-parameter selection for phase behavior matching. SPE Reserv. Eng. 5. https://doi.org/10.2118/16343-PA.

Ahmadi, M., Ebadi, M., Shokrollahi, A., Majidi, S., 2013. Evolving artificial neural network and imperialist competitive algorithm for prediction oil flow rate of the reservoir. Appl. Soft Comput. 1085–1098. https://doi.org/10.1016/j.asoc.2012.10.009.

Ajayi, A., Fasano, T., Okuns, G., 2012. Real time flow estimation using virtual flow measurement techniques: a field application in intelligent well completion. In: Nigeria Annual International Conference and Exhibition, . https://doi.org/10.2118/162948-MS.

Al-Jasmi, A., Goel, H., Nasr, H., Querales, M., Rebeschini, J., Villamizar, M., Carvajal, G., Knabe, S., Rivas, F., Saputelli, L., 2013. Short-term production prediction in real time using intelligent techniques. In: EAGE Annual Conference & Exhibition Incorporating SPE Europec.

Al-Qutami, T., Ibrahim, R., Ismail, I., 2017a. Hybrid neural network and regression tree ensemble pruned by simulated annealing for virtual flow metering application. In: Conference on Signal and Image Processing Applications ICSIPA, . https://doi.org/10.1109/ICSIPA.2017.8120626.

Al-Qutami, T., Ibrahim, R., Ismail, I., Ishak, M., 2018. Virtual multiphase flow metering using diverse neural network ensemble and adaptive simulated annealing. Expert Syst. Appl. 93, 72–85. https://doi.org/10.1016/j.eswa.2017.10.014.

Al-Qutami, T., Ibrahim, R., Ismail, I., Ishak, M., 2017b. Development of soft sensor to estimate multiphase flow rates using neural networks and early stopping. Int. J. Smart Sens. Intell. Syst. 10, 199–222. https://doi.org/10.21307/ijssis-2017-209.

Al-Qutami, T., Ishak, M., Ibtahim, R., Ismail, I., 2017c. Radial basis function network to predict gas flow rate in multiphase flow. In: Proceedings of the 9th International Conference on Machine Learning and Computing, pp. 141–146. https://doi.org/10.1145/3055635.3056638.

Al-Safran, E., Kelkar, M., 2009. Predictions of two-phase critical-flow boundary and mass-flow rate across chokes. SPE Prod. Oper. 24. https://doi.org/10.2118/109243-PA.

AlAjmi, M., Alarifi, S., Mahsoon, A., 2015. Improving multiphase choke performance prediction and well production test validation using artificial intelligence: milestone. In: SPE Digital Energy Conference and Exhibition, . https://doi.org/10.2118/

173394-MS.
AlDabbous, M., Al-Kadem, M., AlMashhad, A., AlSadah, A., Alzahrani, M., 2015. MPFM commissioning optimization: a case study. In: Abu Dhabi International Petroleum Exhibition and Conference, . https://doi.org/10.2118/177900-MS.
Alimonti, C., Falcone, G., 2004. Integration of multiphase and Fuzzy logic in field performance monitoring. SPE Prod. Facil. 19. https://doi.org/10.2118/87629-PA.
Allen, C., Smith, R., 2012. New state of the art asset-optimization data applications for intelligent completions in digital oilfields. In: North Africa Technical Conference and Exhibition, . https://doi.org/10.2118/150848-MS.
Amin, A., 2015. Evaluation of commercially available virtual flow meters (VFM systems). In: Offshore Technology Conference, . https://doi.org/10.4043/25764-MS.
Andrianov, N., 2018. A machine learning approach for virtual flow metering and forecasting. IFAC-Pap. Online 51, 191–196. https://doi.org/10.1016/j.ifacol.2018.06.376.
Ashford, F., 1974. An evaluation of critical multiphase flow performance through wellhead chokes. J. Pet. Eng. 26. https://doi.org/10.2118/4541-PA.
Ausen, H., Stinessen, M., Fonnes, D., Holm, H., 2017. Uncertainty evaluation applied to a model-based Virtual Flow Metering system. In: 18th International Conference on Multiphase Production Technology.
Baker Huges, 2014. NeuraFlow Virtual Flow Meter.
Barnea, D., 1987. A unified model for predicting flow-pattern transitions for the whole range of pipe inclinations. Int. J. Multiph. Flow 13, 1–12. https://doi.org/10.1016/0301-9322(87)90002-4.
Bello, O., Ade-Jacob, S., Yuan, K., 2014. Development of hybrid intelligent system for virtual flow metering in production wells. In: SPE Intelligent Energy Conference & Exhibition, . https://doi.org/10.2118/167880-MS.
Bendiksen, K., Malnes, D., Moe, R., Nuland, S., 1991. The dynamic two-fluid model OLGA: theory and application. SPE Prod. Eng. 6. https://doi.org/10.2118/19451-PA.
Berneti, S., Shahbazian, M., 2011. An imperialist competitive algorithm artificial neural network method to predict oil flow rate of the wells. Int. J. Comput. Appl. 26, 3137–4326. https://doi.org/10.5120/3137-4326.
Bikmukhametov, T., Jäschke, J., 2019. Oil production monitoring using gradient boosting machine learning algorithm. In: 12th on Dynamics and Control of Process Systems Including Biosystems (Accepted Publication).
Bikmukhametov, T., Stanko, M., Jäschke, J., 2018. Statistical analysis of effect of sensor degradation and heat transfer modeling on multiphase flowrate estimates from a virtual flow meter. In: Society of Petroleum Engineers - SPE Asia Pacific Oil and Gas Conference and Exhibition 2018, APOGCE 2018.
Binder, B., Pavlov, A., Johansen, T., 2015. Estimation of flow rate and viscosity in a well with an electric submersible pump using moving horizon estimation. IFAC-Pap. Online 48, 140–146. https://doi.org/10.1016/j.ifacol.2015.08.022.
Bishop, C., 2006. Pattern Recognition and Machine Learning (Information Science and Statistics). Springer-Verlag.
Bloemen, H., Belfroid, S., Sturm, W., Verhelst, F., 2006. Soft sensing for gas-lift wells. SPE J. 11. https://doi.org/10.2118/90370-PA.
Bogaert, P., Yang, W., Meijers, H., Dongen, J., Konopczynski, M., 2004. Improving oil production using smart fields technology in the SF30 satellite oil development offshore Malaysia. In: Offshore Technology Conference, . https://doi.org/10.4043/16162-MS.
Bradley, H. (Ed.), 1987. Petroleum Engineering Handbook. Society of Petroleum Engineers.
Bringedal, B., Morud, S., Hall, N., Momah, B., 2006. Online water-injection optimization and prevention of reservoir damage. In: SPE Annual Technical Conference and Exhibition, . https://doi.org/10.2118/102831-MS.
Bringedal, B., Phillips, A., 2006. Application of virtual flow metering as a back-up or alternative to multiphase flow measuring devices. In: Subsea Controls and Data Acquisition 2006: Controlling the Future Subsea.
Buffa, F., Baliño, J., 2017. Review of multiphase flow models for choke valves. In: IV Journeys in Multiphase Flows.
Câmara, M., Soares, R., Feital, T., Anzai, T., Diehl, F., Thompson, P., Pinto, J., 2017. Numerical aspects of data reconciliation in industrial applications. Processes 5, 1–38. https://doi.org/10.3390/pr5040056.
Camilleri, L., Ei Gindy, M., Rusakov, A., 2016a. Providing accurate ESP flow rate measurement in the absence of a test separator. In: SPE Annual Technical Conference and Exhibition, . https://doi.org/10.2118/181663-MS.
Camilleri, L., Ei Gindy, M., Rusakov, A., 2015. Converting ESP real-time data to flow rate and reservoir information for a remote oil well. In: SPE Middle East Intelligent Oil and Gas Conference and Exhibition, . https://doi.org/10.2118/176780-MS.
Camilleri, L., Gindy, M., Rusakov, A., 2016b. ESP real-time data enables well testing with high frequency, high resolution, and high repeatability in an unconventional well. In: Unconventional Resources Technology Conference San Antonio, . https://doi.org/10.15530/URTEC-2016-2471526.
Camilleri, L., Gindy, M., Rusakov, A., Bosia, F., Salvatore, P., Rizza, G., 2016c. Testing the untestable… delivering flowrate measurements with high accuracy on a remote ESP well. In: Abu Dhabi International Petroleum Exhibition & Conference, https://doi.org/10.2118/183337-MS.
Camilleri, L., Zhou, W., 2011. Obtaining real-time flow rate, water cut, and reservoir diagnostics from ESP gauge data. In: Offshore Europe, pp. 6–8. https://doi.org/10.2118/145542-MS.
Campos, S., Balino, J., Slobodcicov, I., Filho, D., Paz, E., 2014. Orifice plate meter field performance: formulation and validation in multiphase flow conditions. Exp. Therm. Fluid Sci. 58, 93–104. https://doi.org/10.1016/j.expthermflusci.2014.06.018.
Campos, S., Teixeira, A., Vieira, L., Sunjerga, S., 2010. Urucu field integrated production model. In: SPE Intelligent Energy Conference and Exhibition, . https://doi.org/10.2118/128742-MS.
Cheng, B., Li, Q., Wang, J., Wang, Q., 2018. Virtual subsea flow metering technology for gas condensate fields and its application in offshore China. In: Conference on Ocean, Offshore and Arctic Engineering, . https://doi.org/10.1115/OMAE2018-77120.
Cholet, H., 2008. Well Production, Practical Handbook. Technip.
Coats, K., Smart, G., 1986. Application of a regression-based EOS PVT program to laboratory data. SPE Reserv. Eng. https://doi.org/10.2118/11197-PA.
Corneliussen, S., Couput, J., Dahl, E., Dykesteen, E., Frøysa, K., Malde, E., Moestue, H., Moksnes, P., Scheers, L., Tunheim, H., 2005. Handbook of Multiphase Flow Metering. Tekna.
Couput, J., Laiani, N., Richon, V., 2017. Operational experience with virtual flow measurement technology. In: 35th International North Sea Flow Measurement Workshop.
Couput, J., Louis, A., Danquigny, J., Transforming, E., 2008. Transforming E&P data into knowledge : applications of an integration strategy. In: Intelligent Energy Conference and Exhibition, . https://doi.org/10.2118/112517-MS.
Couput, J., Renaud, C., 2010. Field & installation monitoring using in line data validation & reconciliation: application to offshore fields in Middle East and West Africa. In: SPE Intelligent Energy Conference and Exhibition, . https://doi.org/10.2118/128717-MS.
Cramer, R., Goh, K., 2009. Data driven surveillance and optimization for gas, subsea and multizone wells. In: SPE Digital Energy Conference and Exhibition, . https://doi.org/10.2118/122554-MS.
Cramer, R., Griffiths, W., Kinghorn, P., Schotanus, D., Brutz, J., Mueller, K., 2011. Virtual measurement value during start up of major offshore projects. In: International Petroleum Technology Conference, . https://doi.org/10.2523/14518-MS.
Cunningham, P., 2008. Dimension reduction. Mach. Learn. Technol. Multimed. 91–112. https://doi.org/10.1007/978-3-540-75171-7_4.
Da Paz, E., Balino, J., Slobodcicov, I., Filho, D., 2010. Virtual metering system for oil and gas field monitoring based on a differential pressure flowmeter. In: SPE Annual Technical Conference and Exhibition, pp. 1431–1440. https://doi.org/10.2118/133895-MS.
De Kruif, B., Leskens, M., Linden, R., Alberts, G., 2008. Soft-sensing for multilateral wells with down hole pressure and temperature and surface flow measurements. In: Abu Dhabi International Petroleum Exhibition and Conference, . https://doi.org/10.2118/118171-MS.
Delarolle, E., Bonuccelli, M., Antico, L., Faluomi, V., 2005. Virtual metering and flow allocation: models tools and field results. In: Offshore Miditerranean Conference and Exhibition.
Denney, S., Wolfe, B., Zhu, D., 2013. Benefit evaluation of keeping an integrated model during real-time ESP operations. In: SPE Digital Energy Conference, . https://doi.org/10.2118/163704-MS.
Dolle, N., Francois, G., Tendo, F., Overschee, P., 2007. Combining testing-by-difference, geochemical fingerprinting and data-driven models: an integrated solution to production allocation in a long subsea tieback. In: Offshore Europe, . https://doi.org/10.2118/108957-MS.
Escuer, C., Mahieu, C., Sicsic, P., 2018. Dynamic integrity management of flexible pipe through condition performance monitoring. In: OTC Kuala Lumpur, . https://doi.org/10.4043/28347-MS.
Espinoza, R., Uniyal, S., Rivadeneira, I., 2017. Integrated surveillance in cheleken block offshore Turkmenistan using automated steady state and transient models. In: Abu Dhabi International Petroleum Exhibition Conference, . https://doi.org/10.2118/188357-MS.
Eversen, G., 2003. The Ensemble Kalman filter: theoretical formulation and practical implementation. Ocean Dyn. 53, 343–367. https://doi.org/10.1007/s10236-003-0036-9.
Falcone, G., Hewitt, G., Alimonti, C., Harrison, B., 2001. Multiphase flow metering: current trends and future developments. In: SPE Annual Technical Conference and Exhibition, . https://doi.org/10.2118/71474-MS.
Falcone, G., Hewitt, G.F., Alimonti, C., 2009. Multiphase Flow Metering: Principles and Applications. Elsevier.
Faluomi, V., Dellarole, E., Bonuccelli, M., Antico, L., 2006. Virtual metering system for oil and gas fields monitoring: design, implementation and applications. In: 5th North Am. Confernce Multiph. Technol.
Famili, A., Shen, W., Weber, R., Simoudis, E., 1997. Data preprocessing and intelligent data analysis. Intell. Data Anal. 1, 3–23. https://doi.org/10.1016/S1088-467X(98)00007-9.
Foot, J., Webster, M., Vaughan, D., Yusti, C., 2006. ISIS-A real-time information pipeline. In: Intelligent Energy Conference and Exhibition, . https://doi.org/10.2118/99850-MS.
Garcia, A., Almeida, I., Singh, G., Purwar, S., Monteiro, M., Carbone, L., Hedeiro, M., 2010. An implementation of on-line well virtual metering of oil production. In: SPE Energy Conference and Exhibition Utrecht, . https://doi.org/10.2118/127520-MS.
Gerrard, C., Taylor, I., Goh, K., de Boer, F., 2007. Implementing real time production optimization in Shell exploration & production in europe-changing the way we work and run our business. In: Offshore Europe, . https://doi.org/10.2118/108515-MS.
Gilbert, W., 1954. Flowing and gas-lift well performance. Drill. Prod. Pract. 143, 127–157.
Goh, K., Pine, B., Yong, I., Vanoverschee, P., Lauwerys, C., 2008. Production surveillance and optimisation for multizone smart wells with data driven models. In: Intelligent Energy Conference and Exhibition,. Amsterdam, the Netherlands, . https://doi.org/10.2118/112204-MS.
Golan, M., Whitson, C., 1991. Well Performance. Prentice Hall.
Goldszal, A., Monsen, J., Danielson, T., Bansal, K., Yang, Z., Johansen, S., 2007. LedaFlow 1D: simulation results with multiphase gas/condensate and oil/gas field data. In: 13th International Conference on Multiphase Production Technology, BHR-2007-A2.
Goodfellow, I., Bengio, Y., Courville, A., 2016. Deep Learning.
Graves, A., Abdel-rahman, M., Hinton, G., 2013. Speech recognition with deep recurrent neural networks. In: Acoustics, Speech and Signal Processing (Icassp), pp.

6645–6649. https://doi.org/10.1109/ICASSP.2013.6638947.
Grimstad, B., Robertson, P., Foss, B., 2015. Virtual flow metering using B-spline surrogate models. IFAC Pap. Online 48, 292–297. https://doi.org/10.1016/j.ifacol.2015.08.046.
Gryzlov, A., 2011. Model-based estimation of multi-phase flows in horizontal wells. Deltf 5–15 PhD dissertaiton, ISBN: 978-90-6464-455-9.
Gryzlov, A., Schiferli, W., Mudde, R., 2013. Soft-sensor: model based estimation of inflow in horizontal wells using the extended Kalman filter. Flow Meas. Instrum. 34, 91–104. https://doi.org/10.1016/j.flowmeasinst.2013.09.002.
Gunnerud, V., 2011. 2011. On Decomposition and Piecewise Linearization in Petroleum Production Optimization. Norwegian University of Science and Technology.
Haldipur, P., 2011. Virtual Metering.
Haldipur, P., Metcalf, G., 2008. Virtual metering technology field experience examples. In: Offshore Technology COnference, . https://doi.org/10.4043/19525-MS.
Haouche, M., Tessier, A., Deffous, Y., Authier, 2012a. Virtual flow meter pilot: based on data validation and reconciliation approach. In: SPE International Production and Operations Conference & Exhibition, . https://doi.org/10.2118/157283-MS.
Haouche, M., Tessier, A., Deffous, Y., Authier, J., Couput, P., Caulier, R., Vrielynck, B., 2012b. Smart metering: an online application of data validation and reconciliation approach. In: SPE Intelligent Energy International, . https://doi.org/10.2118/149908-MS.
Hasanvand, M., Berneti, S., 2015. Predicting oil flow rate due to multiphase flow meter by using an artificial neural network. Energy sources, Part A recover. Util. Environ. Eff. 37, 840–845. https://doi.org/10.1080/15567036.2011.590865.
Hastie, T., Tibshirani, R., Friedman, J., 2009. The Elements of Statistical Learning. Springer New York Inc.
Heddle, R., Foot, J., Rees, H., 2012. ISIS rate & phase: delivering virtual flow metering for 300 wells in 20 fields. SPE Intell. Energy Int. https://doi.org/10.2118/150153-MS.
Holmås, K., Løvli, A., 2011. FlowManager Dynamic: a mutiphase flow simulator for online surveillance, optimization and prediction of subsea oil and gas production. In: 15th International Conference on Multiphase Production, BHR-2011-F3.
Holmås, K., Lunde, G., Setyadi, G., Angelo, P., Rundrum, G., 2013. Ormen Lange flow assurance system (FAS) - online flow assurance monitoring and advice. In: Offshore Technology Conference, . https://doi.org/10.4043/24297-MS.
Hornik, K., Stinchcombe, M., White, H., 1989. Multilayer feed-forward networks are universal approximators. Neural Netw. 6080, 359–366. https://doi.org/10.1016/0893-6080(89)90020-8.
Hussain, A., Vega, J., Hassane, M., Yusaf, S., Abdaul-Halim, A., 2016. Enhancing smart completion capabilities by integration with digital oil field real time monitoring system in a green field of ADMA-OPCO. In: Abu Dhabi International Petroleum Exhibition & Conference, . https://doi.org/10.2118/183240-MS.
Idso, E., Sperle, I., Aasheim, R., Wold, M., 2014. Automatic subsea deduction well testing for increased accuracy and reduced test time. In: Abu Dhabi International Petroleum Exhibition and Conference, . https://doi.org/10.2118/171840-MS.
Jazwinski, A., 1970. Stochastic Processes and Filtering Theory. Academic Press.
Joshi, N., Joshi, B., 2007. Multiphase measurements and sampling–operating experience. In: SPE Annual Technical Conference and Exhibition, . https://doi.org/10.2118/108626-MS.
Julier, S., Uhlamann, J., Durrant-Whyte, H., 2000. A new method for the nonlinear transformation of means and covariances in filters and estimators. IEEE Trans. Autom. Control 45, 477–482. https://doi.org/10.1109/9.847726.
Kalman, R., 1960. A new approach to linear filtering and prediction problems. J. Basic Eng. 82. https://doi.org/10.1115/1.3662552.
Kongsberg, 2016. LedaFlow Engineering Manual.
Lansagan, R., 2012. A study on the impact of instrument measurement uncertainty, degradation, availability and reservoir and fluid properties uncertainty on calculated rates of virtual metering systems. In: 30th International North Sea Flow Measurement Workshop.
Law, H., Phua, P., Briers, J., Kong, J., 2018. Extending virtual metering to provide real time exception based analytics for optimizing well management and chemical injection. In: Offshore Technology Conference Asia, . https://doi.org/10.4043/28503-MS.
Lea, J., Bearden, J., 1999. On and offshore problems and solutions. In: SPE Mid-continent Operations Symposium, . https://doi.org/10.2118/52159-MS.
Leskens, M., Smeulers, J., Gryzlov, A., 2008. Downhole multiphase metering in wells by means of soft-sensing. In: SPE Intelligent Energy Conference and Exhibition, . https://doi.org/10.2118/112046-MS.
Lew, A., Mauch, H., 2006. Dynamic Programming: A Computational Tool. Springer.
Lockhart, R.W., Martinelli, R.C., 1949. Proposed correlation of data for isothermal two-phase, two-component flow in pipes. Chem. Eng. Prog. 45, 39–48.
Loh, K., Omrani, P., van der Linden, R., 2018. Deep learning and data assimilation for real-time production prediction in natural gas wells. arXiv Prepr. arXiv:1802.05141.
Lorentzen, R., Fjelde, K., Frøyen, J., Lage, A., Nævdal, G., 2001. Underbalanced and low-head drilling operations: real time interpretation of measured data and operational support. In: SPE Annual Technical Conference and Exhibition, . https://doi.org/10.2118/71384-MS.
Lorentzen, R., Nævdal, G., Lage, A., 2003. Tuning of parameters in a two-phase flow model using an ensemble Kalman filter. Int. J. Multiph. Flow 29, 1283–1309. https://doi.org/10.1016/S0301-9322(03)00088-0.
Lorentzen, R., Nævdal, G., Saevareid, O., 2010a. Soft multiphase flow metering for accurate production allocation. In: SPE Russian Oil and Gas Technical Conference Exhibition, . https://doi.org/10.2118/136026-MS.
Lorentzen, R., Sævareid, O., Nævdal, G., 2010b. Rate allocation: combining transient well flow modeling and data assimilation. In: SPE Annual Technical Conference and Exhibition, . https://doi.org/10.2118/135073-MS.
Loseto, M., Bagci, A., Gilbert, R., Chacon-Fonseca, J., 2010. Virtual flowrate metering in subsea producers & injectors enables integrated field & reservoir management: don development case study. In: SPE Intelligent Energy Conference and Exhibition, . https://doi.org/10.2118/128678-MS.
Løvli, A., Amaya, C., 2016. A virtual flow metering system throughout life of field. In: Upstream Production Measurement Forum.
Ma, X., Borden, Z., Porto, P., Burch, D., Huang, N., Benkendorfer, P., Bouquet, L., Xu, P., Swanberg, C., Hoefer, L., Barber, D., Ryan, T., 2016. Real-time production surveillance and optimization at a mature subsea asset. In: SPE Intelligent Energy International Conference and Exhibition, . https://doi.org/10.2118/181103-MS.
Marshall, C., Thomas, A., 2015. Maximizing economic recovery - a review of well test procedures in the North Sea. In: 33rd International North Sea Flow Measurement Workshop.
Melbø, H., Morud, S., Bringedal, B., van der Geest, R., Stenersen, K., 2003. Software that enables flow metering of well rates with long tiebacks and with limited or inaccurate instrumentation. In: Offshore Technology Conference, . https://doi.org/10.4043/15363-MS.
Mokhtari, K., Waltrich, P., 2016. Performance evaluation of multiphase flow models applied to virtual flow metering. In: 11th International Conference on Engineering Sciences, . https://doi.org/10.2495/AFM160091.
Moreno, G., Garriz, A., Badessich, M., Bottesi, G., 2014. Production data integration for virtual flow metering. In: SPE Annual Technical Conference and Exhibition, . https://doi.org/10.2118/170838-MS.
Morra, G., Naeem, D., Alwant, A., Sridhar, S., Hussein, A., 2014. New approach for in-line production testing for mature oil fields using clamp-on SONAR flow metering system. In: SPE Latin America and Caribbean Petroleum Engineering, . https://doi.org/10.2118/169257-MS.
Muradov, K., Davies, D., 2009. Zonal rate allocation in intelligent wells. In: EUROPEC/EAGE Conference and Exhibition, . https://doi.org/10.2118/121055-MS.
Mursaliyev, A., 2018. Implementation of virtual flow metering concept in Kashagan field. In: SPE Annual Caspian Technical Conference and Exhibition, Astana, Kazakhstan. https://doi.org/10.2118/192592-MS.
Nikoofard, A., Aarsnes, U., Johansen, T., 2017. State and parameter estimation of a drift-flux model for underbalanced drilling operations. IEEE Trans. Control Syst. Technol. 25, 2000–2009. https://doi.org/10.1109/TCST.2016.2638683.
Nydal, O., 2012. Dynamic models in multiphase flow. Energy Fuel. 26, 4117–4123. https://doi.org/10.1021/ef300282c.
Olivarez, G., Quintero, C., Gimenez, E., 2012. Production monitoring using artificial intelligence. In: SPE Intelligent Energy International, . https://doi.org/10.2118/149594-MS.
Omole, O., Saputelli, L., Lissanon, J., Nnaji, O., Gozalez, F., Wachel, G., Haldjipieris, P., 2011. Real-time production optimization in the okume complex field, offshore Equatorial Guinea. In: SPE Digital Energy Conference and Exhibition, . https://doi.org/10.2118/144195-MS.
Omrani, S., Dobrovoschi, I., Belfroid, S., Kronberger, P., Munoz, E., 2018. Improving the accuracy of virtual flow metering and back-allocation through machine learning. In: Abu Dhabi International Petroleum Exhibition & Conference, . https://doi.org/10.2118/192819-MS.
Parthasarathy, P., Mai, M., 2006. Bridging the gap between design world and online, real-time, dynamic simulation world. Offshore technology conference. In: Offshore Technology Conference, . https://doi.org/10.4043/27232-MS.
Patel, P., Odden, H., Djoric, B., Garner, R.D., Vea, H., 2014. Model based multiphase metering and production allocation. In: Offshore Technology Conference, . https://doi.org/10.4043/25457-MS.
Pedersen, K., Thomassen, P., Fredenslund, A., 1988. On the dangers of tuning equation of state parameters. Chem. Eng. Sci. https://doi.org/10.1016/0009-2509(88)85039-5.
Peng, D., Robinson, D., 1976. A new-constant equation of state. Ind. Eng. Chem. 15. https://doi.org/10.1021/i160057a011.
Perkins, T., 1993. Critical and subcritical flow of multiphase mixtures through chokes. SPE Drill 8 Complet.. https://doi.org/10.2118/20633-PA.
PETEX, 2017. User Manual.
Petukhov, A., Saputelli, L., Hermann, J., Traxler, A., Boles, K., Nnaji, O., Venugopal, D., 2011. Virtual metering system Application in the Ceiba field, offshore Equatorial Guinea. In: SPE Digital Energy Conference and Exhibition, . https://doi.org/10.2118/144197-MS.
Pinguet, B., Haddad, N., Birkett, G., 2005. fluid properties on the main path for multi-phase meters and wet gas meter accuracy: an analytical approach. In: 4th South East Asia Hydrocarbon Flow Measurement Workshop.
Poulisse, H., 2009. No Title. US20070295501A1.
Poulisse, H., van Overschee, P., Briers, J., Moncur, C., Goh, K., 2006. Continuous well production flow monitoring and surveillance. In: SPE Intelligent Energy Conference and Exhibition, . https://doi.org/10.2118/99963-MS.
Prechelt, L., 2012. Neural Networks: Tricks of the Trade. Springer, pp. 53–67.
Qiu, J., Toral, H., 1993. Three-phase flow-rate measurement by pressure transducers. SPE Annual Technical Conference and Exhibition. . https://doi.org/10.2118/26567-MS.
Rao, C., Rawlings, J., Lee, J., 2001. Constrained linear state estimation—a moving horizon approach. Automatica 37, 1619–1628. https://doi.org/10.1016/S0005-1098(01)00115-7.
Rashid, K., Bailey, W., Couët, B., 2012. A survey of methods for gas-lift optimization. Model. Simul. Eng. 2012. https://doi.org/10.1155/2012/516807.
Rasmussen, Å., 2004. Field Applications of Model-Based Multiphase Flow. North Sea Flow Measurement Workshop.
Rastoin, S., Schmidt, Z., Doty, D., 1997. A review of multiphase flow through chokes. J. Energy Resour. Technol. 119, 1–10. https://doi.org/10.1115/1.2794216.
Redlich, O., Kwong, J., 1949. On the thermodynamics of solutions; an equation of state; fugacities of gaseous solutions. Chem. Rev. 44, 233–244.
Reichle, R., Walker, J., Koster, R., Houser, P., 2002. Extended versus ensemble kalman filtering for land data assimilation. J. Hydrometeorol. 3, 728–740. https://doi.org/

10.1175/1525-7541(2002)003<0728:EVEKFF>2.0.CO;2.
Retnanto, A., Weimer, B., Kontha, N., Triongko, H., Azim, A., Kyaw, H., 2001. Production optimization using multiphase well testing: a case study from East Kalimantan, Indonesia. In: SPE Annual Technical Conference and Exhibition, . https://doi.org/10.2118/71556-MS.
Roxar, 2015. METTE User Manual.
Sachdeva, R., Schmidt, Z., Brill, J., Blais, R., 1986. Two-phase flow through chokes. In: SPE Annual Technical Conference and Exhibition, . https://doi.org/10.2118/15657-MS.
Sampath, J., Selmer-Olsen, S., Solbakken, T., Schüller, R., 2006. Critical and sub-critical oil/gas/water mass flow rate experiments and predictions for chokes. SPE Prod. Oper. 21. https://doi.org/10.2118/88813-PA.
Schlumberger Limited, 2014. OLGA User Manual.
Schüller, R., Solbakken, T., Selmer-Olsen, S., 2003. Evaluation of multiphase flow rate models for chokes under subcritical oil/gas/water flow conditions. SPE Prod. Facil. 18. https://doi.org/10.2118/84961-PA.
Selmer-Olsen, S., 1995. Subsea chokes as multiphase flowmeters:production control at troll olje. In: Proc. Of the BHR Group 7th Intl.Conference on Multiphase Production. Cannes, France.
Shaban, H., Tavoularis, S., 2014. Measurement of gas and liquid flow rates in two-phase pipe flows by the application of machine learning techniques to differential pressure signals. Int. J. Multiph. Flow 67, 106–117. https://doi.org/10.1016/j.ijmultiphaseflow.2014.08.012.
Shippen, M., Bailey, W.J., 2012. Steady state multiphase flow - past, present, and future, with a perspective on flow assurance. Energy Fuels 4145–4157. https://doi.org/10.1021/ef300301s.
Singh, Y., Mehra, R., 2015. Relative study of measurement noise covariance R and process noise covariance Q of the kalman filter in estimation. J. Electr. Electron. Eng. 10, 112–116. https://doi.org/10.9790/1676-1061112116.
Soave, G., 1972. Equilibrium constants from a modified redlich-kwong equation of state. Chem. Eng. Sci. 27. https://doi.org/10.1016/0009-2509(72)80096-4.
Solomatine, D., See, L., Abrahart, R., 2009. Data-driven modeling: concepts, approaches and experiences. pp Springer. Pract. Hydroinf. 17–30. https://doi.org/10.1007/978-3-540-79881-1_2.
Stanley, G., 1982. Online data reconciliation for process control. In: AICHE Annual Meeting.
Sun, J., Ma, X., Kazi, M., 2018. Comparison of decline curve analysis DCA with recursive neural networks RNN for production forecast of multiple wells. In: SPE Western Regional Meeting, . https://doi.org/10.2118/190104-MS.
Tangen, S., Nilsen, R., Holmås, K., 2017. Virtual flow meter - sensitivity analysis. In: 35th North Sea Flow Measurement Workshop.
Thorn, R., Johansen, G., Hjertaker, B., 2013. Three-phase flow measurement in the petroleum industry. Meas. Sci. Technol. 233–957. https://doi.org/10.1088/0957-0233/24/1/012003.
Toskey, E., 2011. RPSEA Evaluation of Flow Modeling Final Report. (Houston, TX).
van Den Berg, F., Goh, K., van Donkelaar, E., Parchewsky, R., 2010. Remote monitoring and production optimisation in Shell. In: SPE Russian Oil and Gas Conference and Exhibition, . https://doi.org/10.2118/136384-MS.
van der Geest, R., Broman, W., Johnson, T., Fleming, R.H., Allen, J., 2001. Reliability through data reconciliation. In: Offshore Technology Conference, . https://doi.org/10.4043/13000-MS.
van der Geest, R., Morud, S., Zaostrovski, A., 2000. Oil well Allocation: the ultimate interpolation problem. IFAC Proc. 3, 437–442. https://doi.org/10.1016/S1474-6670(17)38579-8.
Van der Waals, J., 1870. Continuity of the gaseous and liquid state of matter. Nature 2.
Varyan, R., 2016. Cost saving of implementing virtual flow metering at various fields and engineering phases - a case study. In: Offshore Technology Conference Asia, . https://doi.org/10.4043/26637-MS.
Varyan, R., Haug, R., Fonnes, D., 2015. Investigation on the suitability of virtual flow metering system as an alternative to the conventional physical flow meter. In: SPE/IATMI Asia Pacific Oil & Gas Conference and Exhibition, . https://doi.org/10.2118/176432-MS.
Vogel, J., 1968. Inflow performance relationships for solution-gas drive wells. J. Pet. Technol. 243, 83–92.
Waltrich, P., Barbosa, J., 2011. Performance of vertical transient two-phase flow models applied to liquid loading in gas wells. In: SPE Annual Technical Conference and Exhibition, . https://doi.org/10.2118/147128-MS.
Whitson, C., Torp, S., 1983. Evaluating constant volume depletion data. J. Pet. Technol. 35. https://doi.org/10.2118/10067-PA.
Whitson, C.H., Brule, M.R., 2000. Phase Behavior, SPE Monograph.
Wising, U., Kalitventzeff, P., Campan, J., Vrielynck, B., 2009. Improving operations through increased accuracy of production data. In: SPE Offshore Europe, . https://doi.org/10.2118/124766-MS.
Xu, L., Zhou, W., Li, X., Tang, S., 2011. Wet gas metering using a revised Venturi meter and soft-computing approximation techniques. IEEE Trans. Instrum. Meas. 60, 947–956. https://doi.org/10.1109/TIM.2010.204593.
Zangl, G., Hermann, R., Schweiger, C., 2014. Comparison of methods for stochastic multiphase flow rate estimation. In: SPE Annual Technical Conference and Exhibition, . https://doi.org/10.2118/170866-MS.
Zhang, H., Wang, Q., Sarica, C., Brill, J., 2003. Unified model for gas-liquid pipe flow via slug dynamics—Part 1: model development. J. Energy Resour. Technol. 125, 266–273. https://doi.org/10.1115/1.1615246.
Zhang, X., Speranza, A., Mustafa, M., Sreeton, R., 2017. Improving reliability of multiphase flow metering with thermodynamic models and correct configuration. In: AIChE 2017.
Ziegel, E., Shirzadi, S., Wang, S., Bailey, R., Griffiths, P., Ghuwakewala, K., Johnson, D., 2014. A data-driven approach to modeling and optimization for a North Sea asset using real-time data. In: SPE Intelligent Energy Conference and Exhibition, . https://doi.org/10.2118/167850-MS.
Zuber, N., Findlay, J., 1965. Average volumetric concentration in two-phase flow systems. J. Heat Transf. 87, 453–468. doi10111513689137. https://doi.org/10.1115/1.3689137.

Abbreviations

ANN: Artificial Neural Network
BOM: Black Oil Model
CAPEX: Capital Expenditure
DDWT: Deliberately Disturbed Well Test
DVR: Data Validation and Reconciliation
EKF: Extended Kalman Filter
EnKF: Ensemble Kalman Filter
EoS: Equation of State
ESP: Electric Submersible Pump
FL: Fuzzy Logic
FW PU: FieldWare Production Universe
GOR: Gas-Oil Ratio
GA: Generic Algorithm
ICA: Imperialist Competitive Algorithm
IPR: Inflow Performance Relationship
L-M: Levenberg-Marquardt
LR: Linear Regression
LSTM: Long-Short Term Memory
MHE: Moving Horizon Estimation
MPFM: Multiphase Flow Meter
MSE: Mean Squared Error
NN: Neural Network
NNE: Neural Network Ensemble
OPEX: Operating Expenditure
PCA: Principle Component Analysis
PCR: Principle Component Regression
PR: Peng-Robinson
PSO: Particle Swarm Optimization
PVT: Pressure Volume Temperature
RBFN: Radial Basis Function Network
RDP: Rotameter Pressure Drop
RF: Random Forest
RK: Redlich-Kwong
RNN: Recurrent Neural Network
RT: Regression Tree
RTE: Regression Tree Ensemble
SA: Simulated Annealing
SQP: Sequential Quadratic Programming
SRK: Soave-Redlich-Kwong
SVM: Support Vector Machine
UKF: unscented Kalman filter
VDP: Venturi Pressure Drop
VFM: Virtual Flow Meter/Virtual Flow Metering
WC: Water Cut
WMS: Well Monitoring System

Nomenclature

A_1: cross-sectional area upstream the choke, m^2
A_2: cross-sectional area at the choke throat, m^2
B_f: linear Forchheimer equation constant
C_0: profile parameter
C_b: backpressure equation constant
C_D: choke discharge coefficient
C_f: quadratic Forchheimer equation constant
C_{op}: choke opening
D: pipe diameter, m
e: specific heat exchange with the environment, m^2/s^2
E_k: total energy, m^2/s^2
f_{fric}: friction factor
F_{ki}: interphase friction, $kg/(m^2 \cdot s^2)$
F_{kw}: wall friction term, $kg/(m^2 \cdot s^2)$
F_{tot}: total wall friction, $kg/(m^2 \cdot s^2)$
g: gravitational constant, m/s^2
g_i: system parameter
h: fluid specific enthalpy, m^2/s^2
h_k: k-phase specific enthalpy, m^2/s^2
i: index of the training example/well number
k_k: effective phase thermal conductivity, $kg \cdot m/(s^3 \cdot K)$
$\dot{m}$: mass flow rate, kg/s
n: power constant
N: ensemble/training dataset size
O_k: additional momentum exchange terms, $kg/(m^2 \cdot s^2)$
O_{tot}: total source term, $kg/(m^2 \cdot s^2)$
p: system pressure, Pa
P_B: bubble point pressure, Pa

P_{BH}: bottomhole pressure, Pa
P_{FL}: flowline pressure, Pa
P_R: reservoir pressure, Pa
P_{WHCU}: wellhead upstream choke pressure, Pa
P_{WHCD}: wellhead downstream choke pressure, Pa
PI: productivity index, Pa·s/ m^3
$q_{estimated}$: estimated volumetric flowrate, m^3/s
q_i: volumetric flowrate of i-well, m^3/s
q_g: gas volumetric flowrate, m^3/s
q_o: oil volumetric flowrate, m^3/s
$q_{o,\max}$: maximum oil volumetric flowrate, m^3/s
Q_{ext}: additional net external heat transfer sources, kg/(s^3·K)
Q_{ki}: interfacial heat transfer rate of k-phase with other fields, kg/(s^3·K)
Q_{kw}: phase transfer rate at pipe wall, kg/(s^3·K)
s_i: unmeasured variable
$s_{\max}$: minimum unmeasured value constraint
$s_{\min}$: minimum unmeasured value constraint
t: time, s
T: system temperature, K
T_{BH}: bottomhole temperature, K
T_k: k-phase temperature, K
T_{WHCU}: wellhead upstream choke temperature, K
T_{WHCD}: wellhead downstream choke temperature, K
u_d: drift velocity, m/s
u_g: gas velocity, m/s
u_k: k-phase velocity, m/s
u_m: mixture velocity, m/s
U: total heat source term, kg/(m·s^2)
U_{tot}: total source term including wall heat transfer, mass transfer and sources, $kg^2/(s^2 \cdot m^4)$
w: specific work done on the system, m^2/s^2
w_t: measurement noise
x: pipe axial coordinate, m
$y_{meas\ i}$: measured value
$y_{predicted\ i}$: predicted value
$y_{\min}$: minimum measured value constraint
$y_{\max}$: maximum measured value constraint
α_k: k-phase volume fraction
γ_i: weight coefficient
Δp: pressure drop across the choke/electric submersible pump, Pa
θ: pipe/wellbore inclination angle
ρ: fluid density, kg/m^3
ρ_k: k-phase density, kg/m^3
ρ_m: mixture density, kg/m^3
σ_i: measurement uncertainty
Ψ: mass transfer source, kg/(m^3·s)
ξ: pump speed, rpm

2.1 Discussion on fluid properties influence in multiphase flow estimation problems

Despite the fact that we have tried to deliver a thorough overview on Virtual Flow Metering in Paper I, there is one important point that has not been sufficiently discussed in the paper but rather briefly mentioned. This point concerns the influence of phase properties (also referred as PVT properties) accuracy on estimation results of multiphase flowrates using Virtual Flow Meters and its comparison with physical multiphase flow meters (MPFMs). In this section, we would like to discuss this topic in more detail because it will also appear in the rest of the PhD thesis.

As we mentioned in Section 3.3.1.4 of the paper, both VFMs and MPFMs rely on fluid properties when computing the phase flowrates and converting it from local to standard conditions, and we have seen such discussions both in the literature and in personal discussions with petroleum engineers who use multiphase flow estimation methods in daily work. However, what we miss to discuss is the way how these properties are used in VFMs and MPFMs, and the possible differences and inaccuracies that fluid characterization uncertainties might introduce to the flow estimation problem.

2.1.1 Multiphase flow meter estimation approach

First, let us consider the general framework of MPFMs that is used for flowrate computing, because it has not been sufficiently described in Paper I. Multiphase flow meters typically consist of two major parts: devices that measure gas, oil and water fractions and devices that compute phase velocities. The gas, oil and water fractions can be measured by various methods such as gamma-rays attenuation and electrical impedance (Thorn et al. (2012)). The phase velocities might not be necessarily measured but instead computed from results of other measurements and the relationships that link the velocities and the measured variables. One of the most frequently used approaches is using Venturi meters that measure the pressure difference between upstream and Venturi throat locations (Falcone (2009)). From the pressure difference, the phase velocities are computed that are used to compute phase volumetric flowrates.

To better understand the entire computation procedure, let us setup the main equations that are used within multiphase flow meters based on a Venturi meter example. First, inlet pressure P, temperature T and pressure drop between the inlet and the Venturi throat ΔP are measured. Then, gas, oil and water fractions (α_g, α_o and α_w respectively) are measured by densitometers using, for example, the gamma-rays attenuation method.

In the next step, PVT model is used to determine gas, oil and water densities (ρ_g, ρ_o and ρ_w respectively), that are computed at the inlet pressure (P) and temperature (T) conditions. As discussed in Paper I, the PVT model can be represented as a Black Oil model or a compositional model, depending on the information and data available for production engineers. Ideally, these models are tuned to separator well tests as often as possible. When untuned, the uncertainty into the flowrate computation enters at this stage.

Having computed the phase densities and the phase volume fractions, liquid density can be computed based on the volumetric basis as the following:

$$\rho_l = \frac{\alpha_o \rho_o + \alpha_w \rho_w}{\alpha_l} \tag{2.1}$$

where ρ_l denotes the liquid density and α_l - the liquid volume fraction (α_l = α_o + α_w).

The next thing to be done is to determine the phase velocities. As we consider a Venturi meter example, the phase velocities and consequently the volumetric flowrates are computed from the mixture mass flowrate m_{mix} that can be calculated using the following equation:

$$m_{mix} = C \frac{\pi}{4} \frac{\beta^2 D^2}{\sqrt{1-\beta^4}} \sqrt{2 \rho_{mix} \Delta P} \tag{2.2}$$

where C denotes the tuning coefficient, β - the ratio between the throat diameter d_{th} and the pipe diameter upstream of the Venturi D computed as $\frac{d_{th}}{D}$, ρ_{mix} - the mixture density.

The only variable that is missed in Eq. 2.2 is the mixture density. If we would have a homogeneous flow, we could compute the mixture density directly based on the known phase densities and volume fractions. However, the assumption about homogeneity of multiphase flow is usually strong for Venturi meters, even if a homogenizer device is installed at upstream of the meter. In most cases, we have slip in the flow, meaning that the gas phase moves faster than the liquid phase. The slip ratio S is defined as follows:

$$S = \frac{U_g}{U_l} \tag{2.3}$$

where U_g denotes the gas phase velocity and U_l denotes the liquid phase velocity.

To take into account the slip effect in the mixture density, we first need to determine the gas quality (or gas mass fraction) x_g assuming that the slip is present in the flow. The gas quality relation can be derived from Eq. 2.3, and the resulting form is as follows:

$$x_g = \frac{\rho_g \alpha_g S}{\rho_g \alpha_g S + \rho_l \alpha_l} \tag{2.4}$$

Assuming that we can compute the gas quality that considers the slip effect, the mixture density can be computed as follows:

$$\frac{1}{\rho_{mix}} = \frac{1 - x_g}{\rho_l} + \frac{x_g}{\rho_g} \tag{2.5}$$

The problem now is that we have two unknown variables x_g and S that must be determined to close the system of equations. One of the most common approaches to deal with this situation is to use a void (gas) fraction correlation that links the gas volume fraction (we measure that), the gas quality and the fluid densities (Thorn et al. (2012)). As an example, we write the Chisholm correlation (Chisholm (1985)), but other correlations can be used too. The Chisholm correlation has the following form:

$$\alpha_{g\,Ch} = \left[1 + \left(\frac{\rho_l}{\rho_{mix}}\right)^{0.5} \left(\frac{1 - x_g}{x_g}\right) \left(\frac{\rho_g}{\rho_l}\right)\right]^{-1} \tag{2.6}$$

Combining Eq. 2.5 and Eq. 2.6 and stating that $\alpha_{g\,Ch} = \alpha_g$, we can determine the gas quality value x_g and ρ_{mix}. Then, using the computed values and the pressure drop measurement in Venturi (ΔP) , we can compute the mixture mass flowrate using Eq. 2.2.

Having computed the mixture mass flowrate and the gas quality, we then can determine the gas and liquid mass flowrates respectively as follows:

$$m_g = x_g m_{mix} \tag{2.7}$$

$$m_l = (1 - x_g) m_{mix} \tag{2.8}$$

Then, the gas, oil and water volumetric flowrates can be computed as:

$$q_g = \frac{m_g}{\rho_g} \tag{2.9}$$

$$q_o = \alpha_o \frac{m_l}{\rho_l} \tag{2.10}$$

$$q_w = \alpha_w \frac{m_l}{\rho_l} \tag{2.11}$$

The described above calculation procedure will be further used to evaluate sensitivity of multiphase flow meters accuracy with respect to fluid properties. Looking at the equations above, it is very hard to derive an analytical expression for a volumetric flowrate with respect to only fluid properties and the pressure difference across the meter. For instance, when trying to solve the Chisholm's correlation for x_g and eliminating the mixture density, we end up with:

$$\alpha_{g\,Ch} = \left[1 + \left(\frac{\left(1 - x_g + x_g \frac{\rho_l}{\rho_g}\right)\left(1 - x_g^2\right)}{x_g^2}\right)^{0.5} \left(\frac{\rho_g}{\rho_l}\right)\right]^{-1} \tag{2.12}$$

Further "simplifications" obviously do not make the relationship easier, as such we will evaluate a magnitude of the fluid properties influence based on simulation results.

2.1.2 Virtual Flow Metering estimation approach

In Paper I, we described the most common approaches and equations that are used in Virtual Flow Metering to estimate multiphase flow rates. To evaluate sensitivity of VFM accuracy with respect to fluid properties, we will use a well tubing model only. The main reason for this is the fact that choke models that are used for VFM are generally similar the model of a Venturi meter and have the form of Eq. 2.2. The main difference is that in MPFM the phase fractions are measured while in the choke model-based VFMs they are computed. In the tubing model, however, the fluid properties are used in each control volume when solving a system of non-linear equations, so that the influence of fluid properties are harder to evaluate without the problem simulations.

To estimate the fluid properties sensitivity, we use a steady state drift-flux model whose details are described in Paper V of this thesis. In terms of fluid properties, the model considers the Black Oil formulation and mass transfer of gas from the oil phase to the gas phase. Mass balance equations are written for gas and liquid phases while the momentum balance is written for a flow with mixture properties.

As for deriving an analytical dependency of the flowrates with respect to fluid properties, this is also a non-trivial problem. This is because, despite the fact that the mass and momentum balances seem to depend on the fluid densities linearly, the relations that compute friction factors, the phase fractions and the slip effect are highly non-linear. The details of the gas fraction correlation with slip used in the model can be found in Bhagwat and Ghajar (2014). The friction correlation can be found in Eq. 20 in Paper V.

2.1.3 Evaluation procedure

Evaluation of density influence on flowrate estimates.

As an example, for both metering approaches, we will consider the potential effect of wrong density computation by a PVT model. This choice is made because, in the equations provided in the sections above and in Paper I and V, we see that it is the major parameter that influences the flowrate estimates. For a tubing-based Virtual Flow Meter that uses the Black Oil model, it is also highly dependent on the Black Oil properties such as solution gas-oil ratio (R_s) and formation volume factors (B_o, B_g and B_w), and less dependent on phase viscosities.

In practice, if a PVT model is not well-tuned to the actual properties of the produced fluid, errors will exist in the Black Oil properties as well as in densities and viscosities. It is potentially possible to perform a thorough evaluation of MPFM/VFM accuracy on all the properties. We will, however, consider a different approach. First, we will assume that the local phase densities ($\rho_{g,o,w}$) are computed with the reference to the densities at standard conditions as follows:

$$\rho_{g,o,w} = \frac{\rho_{\bar{g},\bar{o},\bar{w}}}{B_{g,o,w}} \tag{2.13}$$

where $\rho_{\bar{g},\bar{o},\bar{w}}$ denotes gas, oil and water densities respectively at standard conditions, $B_{g,o,w}$ - the formation volume factors of gas, oil and water respectively.

In this way, by assuming that the PVT model is biased by, for instance, 10%, we can introduce the same error to both MPFMs and VFMs, such that in MPFMs the densities will be wrong locally at the Venturi inlet, while for the tubing-based VFM, the densities will be biased for each control volume computations. This allows a more systematic comparison between the two flowrate estimation methods. Also, in order to avoid additional estimation error for the tubing-based VFM, we will **not** introduce error into the Black Oil properties. As such, we assume that the bias in the PVT model mostly affects the accuracy of the density values. To compute the flowrate errors with respect to the true values, we use Mean Absolute Percentage Error (MAPE) with the following form:

$$MAPE = \frac{1}{N}\sum_{n=1}^{N}\left|\frac{q_{true} - q_{est}}{q_{true}}\right| \tag{2.14}$$

where N denotes the number of sample points, q_{true} - the true phase flowrate and q_{est} - the estimated phase flowrate.

Notes on influence of Black Oil properties on flowrate converting. It is important to note that it is a common practice in the oil and gas industry to report the flowrates at standard conditions. However, when computing the flowrates using the aforementioned methods, we refer to the local flowrates. As such, if the Black Oil properties are biased, there will be inevitable errors when converting the local flowrates to standard conditions. The dependency is, however, easy to evaluate because it is linear. For instance, when computing the gas flowrate at standard conditions from the rate at local conditions, the following relation is typically used:

$$q_{\bar{g}} = \frac{q_g}{B_g} + \frac{q_o R_s}{B_o} \tag{2.15}$$

where $q_{\bar{g}}$ denotes the gas flowrate at standard conditions, q_g - the gas flowrate at local conditions, q_g - the oil rate at local conditions , R_s - the solution gas-oil ratio, B_g and B_o - the gas and oil formation volume factors respectively.

As such, the Black Oil properties are critical when reporting the flowrates at standard conditions and the flowrate estimation error will be as large as the error in the properties. Also notice that the principle in converting the rates form local to standard conditions is the same for both MPFMs and VFMs, as such we will not make such a comparative evaluation.

Multiphase flow meter conditions. To compute the sensitivity of a multiphase flow meter on a bias in density values, we introduce a uniformly distributed error of $\pm\mathbf{10\%}$ into the standard density values. This procedure will be the same for a Virtual Flow Meter. As such, when converting to local conditions, the magnitude of the error will hold. Then, for each sample of the biased densities, the local gas, oil and water flowrates are computed using Eq. 2.1-2.11. We perform 2500 simulations using the samples from density distributions. We also assume that we have measurements of the phase fractions α_g, α_o and α_w and keep the water-oil ratio constant. All the required parameters that are used for estimation are listed in Table 2.1.

Virtual Flow Meter conditions. As discussed, we use the steady state drift-flux model for a tubing-based first principles VFM. For the tubing configuration, we

Parameter/Variable	Value
Density error	10%
Upstream diameter (D)	0.3 m
Throat diameter (d_{th})	0.15 m
Venturi pressure drop (ΔP)	1 bar
Wellhead pressure (P_{WH})	20 bar
Wellhead temperature (T_{WH})	20°C
Measured gas volume fraction (α_g)	0.6
Measured oil volume fraction (α_o)	0.17
Measured water volume fraction (α_w)	0.23
Water cut (WC)	0.3
Gas density at standard conditions ($\rho_{\bar{g}}$)	0.8 $\frac{kg}{m^3}$
Oil density at standard conditions ($\rho_{\bar{o}}$)	750 $\frac{kg}{m^3}$
Water density at standard conditions ($\rho_{\bar{w}}$)	1000 $\frac{kg}{m^3}$

Table 2.1: Venturi geometry, measured parameters and standard fluid properties used for MPFM flowrate estimation

consider a vertical pipe with the height of 1000 m and the diameter of 0.2 m. The phase densities at standard conditions are the same as in Table 2.1. To tune the VFM to the data, we use the bottomhole volumetric flowrates as the manipulated variables. We assume that we have measured and fixed pressure boundary and temperature boundary conditions at the wellhead as well as the temperature at the bottomhole. Also, we assume that we have a pressure measurement at the bottomhole, and this pressure value is used in the objective function, such that we minimize the difference between the measured and the computed (VFM-estimated) pressure by an optimization solver. The pressure and temperature conditions are:

- Wellhead pressure (P_{WH}) - 20 bar (fixed boundary condition)
- Wellhead temperature (T_{WH}) - 20°C (fixed boundary condition)
- Bottomhole temperature (T_{BH}) - 70°C (fixed boundary condition)
- Bottomhole pressure (P_{BH}) - 100 bar (fixed reference measurement for tuning)

2.1.4 Estimation results

Before comparing the simulation results, we would like to emphasize that matching the absolute values of the flowrate estimates between MPFM and VFM is not

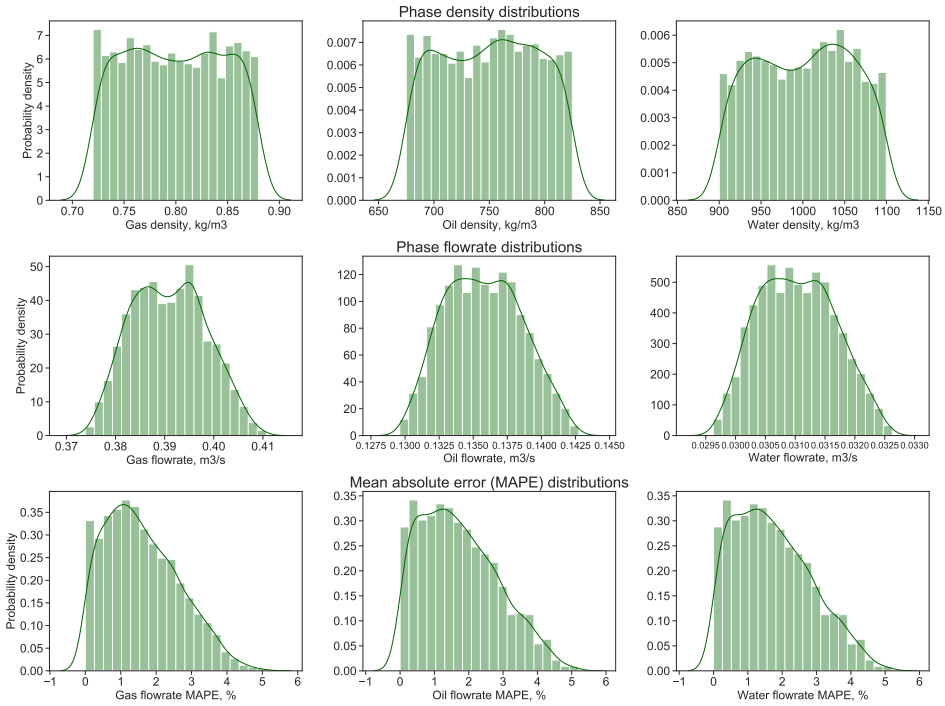

Figure 2.1: Sensitivity estimation results for a Venturi MPFM assuming $\pm 10\%$ error in densities

the goal of the simulations. The main idea is to compare the error for each estimation method relative to unbiased (true) flowrates. As such, some deviations between the values obtained with a MPFM and a VFM can exists, because it is a bit hard to find the exact values of pressure difference, Venturi dimensions and tubing geometry such that the phase flowrate values match perfectly, even using the same PVT model. However, we have tried to achieve similar flowrate values and the results are comparable.

First, consider the estimation results for a MPFM. Figure 2.1 shows the obtained distributions of flowrates and MAPEs for the uniformly distributed phase densities with the error of $\pm 10\%$. We see that due to a high non-linearity of the relations, the resulting flowrate distribution is non-uniformly distributed. The MAPE distributions are right-skewed because it computes absolute error values. The obtained mean MAPE errors are:

- Mean MAPE for gas flowrate: 1.60%

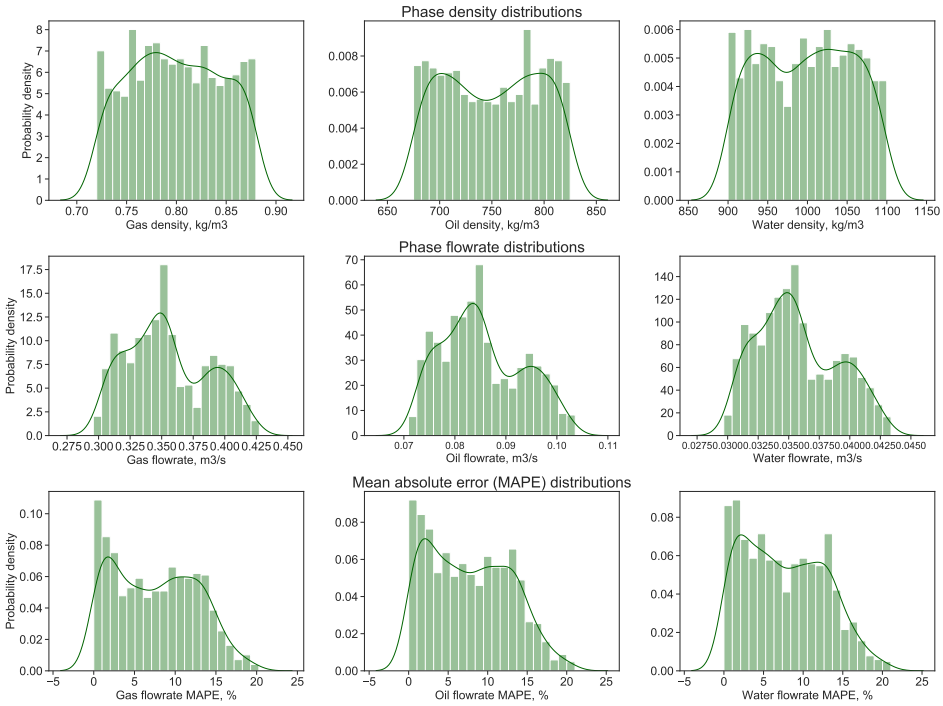

Figure 2.2: Sensitivity estimation results for a tubing model-based VFM assuming $\pm 10\%$ error in densities

- Mean MAPE for oil flowrate: 1.73%
- Mean MAPE for water flowrate: 1.73%

We see that despite the MAPE error might reach up to 5%, the mean error is smaller by a factor of 6 with respect to the error in phase densities. The median error values are around 1.5%. The values of the errors can be slightly different for different phase fractions, but additional simulations showed that the mean MAPEs are within 2%. As such, the simulations show that multiphase flow meters are not very sensitive to a relatively high errors in PVT-computed densities. However, we have to notice that in these simulations we assume that the phase fractions are perfectly measured. This is done intentionally because we want to evaluate the PVT-related inaccuracies. In a real scenario, imperfect phase fraction measurements will lead to higher flowrate estimation errors. Also, no noise is considered in pressure and temperature measurements that can also influence the accuracy of the computed phase densities. On the other hand, if we assume that the noise level is included

in the 10% error that we used for simulations, then we might not need additional evaluation.

Now, we consider the estimation results from a Virtual Flow Meter shown in Figure 2.2. From the figure we see that the MAPE values are larger than the ones obtained for the MPFM. The mean MAPE values are:

- Mean MAPE for gas flowrate: 7.18%
- Mean MAPE for oil flowrate: 7.83%
- Mean MAPE for water flowrate: 7.72%

The error in the flowrate values can be different for different conditions, however, we can generally conclude that PVT-related errors for a physics-based Virtual Flow Meter are larger and more critical than for a multiphase flow meter. We believe that it is caused by the fact that the distributions of the phase volume fractions along the well are dependent on the accuracy of phase densities. A small deviation in phase densities can cause deviations in phase volume fraction that, overall, can lead to a noticeably different pressure distribution along the well. This, in turn, results in an error of a Virtual Flow Meter which minimizes the error between the computed and the measured pressure drop along the well. In a multiphase flow meter, however, the fractions are typically measured, as such, the phase densities do not influence the accuracy of the phase volume fractions, at least directly. Please note, that we did not assume errors in viscosity values that can also introduce additional errors. As such, before applying a VFM to a flow estimation system in an oil and gas field, it is very important to take care of the PVT-model accuracy, especially if multiphase flow meters are not installed in the field.

References

Bhagwat, S.M., Ghajar, A.J., 2014. A flow pattern independent drift flux model based void fraction correlation for a wide range of gas–liquid two phase flow. International Journal of Multiphase Flow 59, 186–205.

Chisholm, D., 1985. Two-phase flow in heat exchangers and pipelines. Heat transfer engineering 6, 48–57.

Falcone, G., 2009. Multiphase flow metering principles. Developments in petroleum science 54, 33–45.

Thorn, R., Johansen, G.A., Hjertaker, B.T., 2012. Three-phase flow measurement in the petroleum industry. Measurement Science and Technology 24, 012003.

Chapter 3

Machine Learning Applications to Multiphase Flow Estimation Including Hybrid Approaches (Paper II and III)

This chapter consists of two papers. Paper II describes application of gradient boosting algorithm for the task of estimation of multiphase flow rates. Paper III describes in detail how to combine various machine learning algorithms with process engineering physics to accurately estimate produced multiphase flowrates. A short overview of each paper is given at the beginning of each paper's section.

3.1 Oil Production Monitoring Using Gradient Boosting Machine Learning Algorithm (Paper II)

Paper II describes application of gradient boosting algorithm for the task of estimation of multiphase flow rates using readily available measurements in the field such as pressure, temperature and choke opening. The main motivation for this paper was the fact that in most of the previously published work on the topic of multiphase flowrate estimation, neural networks have been used. As such, the authors wanted to check capabilities of another powerful algorithm for this task which is, in general, able to make accurate predictions for non-linear regression tasks. Various case studies have been considered including different validation schemes and dataset sizes to fully investigate the algorithms capabilities. Another motivation was to see if it is potentially possible to substitute a multiphase flow meter by a machine learning model using test separator flow measurements for tuning. The results of such simulations are compared to the cases where a Virtual Flow Meter is used as a back-up system to a multiphase flow meter.

Bikmukhametov, T., and Jäschke, J. (2019). Oil Production Monitoring using Gradient Boosting Machine Learning Algorithm. IFAC-PapersOnLine, Volume 52(1), 514-519, doi.org/10.1016/j.ifacol.2019.06.114

Available online at www.sciencedirect.com

ScienceDirect

IFAC PapersOnLine 52-1 (2019) 514–519

IFAC Papers Online CONFERENCE PAPER ARCHIVE

Oil Production Monitoring using Gradient Boosting Machine Learning Algorithm ⋆

Timur Bikmukhametov * **Johannes Jäschke** *

* *Dept. of Chemical Engineering, Norwegian University of Science and Technology (NTNU), NO-7491 Trondheim, (e-mail: timur.bikmukhametov@ntnu.no, johannes.jaschke@ntnu.no)*

Abstract: Data-driven solutions for multiphase flowrate estimation in oil and gas production systems are among the alternatives to first principles virtual flow metering systems and hardware flow metering installations. Some of the most popular data-driven methods in this area are based on artificial neural networks which have been proven to be good virtual flow metering tools. However, neural networks are known to be sensitive to the scaling of input data, difficult to tune and provide a black-box solution with occasionally unexplainable behavior under certain conditions. As an alternative, in this paper, we explore capabilities of the Gradient Boosting algorithm in predicting oil flowrates using available field measurements. To do this, we use an efficient implementation of the algorithm named XGBoost. In contrast to neural networks, this algorithm is insensible to data scaling, can be more intuitive in tuning as well as it provides an opportunity to analyze feature influence which is embedded in algorithm learning. We show that the algorithm provides accurate flowrate predictions under various conditions and can be used as a back-up as well as a standalone multiphase flow metering solution.

Keywords: Virtual flow metering, machine learning, production monitoring, gradient boosting, soft sensing.

1. INTRODUCTION

Accurate measurements of oil, gas and water flowrates are a critical part in production optimization, reservoir management and flow assurance of petroleum production systems (Falcone et al. (2001)). A traditional method for measuring these flowrates is well testing which can be conducted by re-routing a well stream into a test separator, or by changing wellhead choke opening and tracking the change of the rates at an inlet separator. Another alternative are multiphase flow meters (MPFMs) which allow to avoid separating the multiphase flow streams while measuring the flowrates from single wells or a cluster of wells in real time. Despite this advantage, MPFMs are expensive and can be a subject to degradation and costly repair (Patel et al. (2014)).

Another possible way to estimate the multiphase flowrates is to combine field measurements such as pressure and temperature with first principles mathematical models which accurately represent specific system parts or the system as a whole. Some measurements are used as inputs to the model (as model boundary conditions) together with tuning variables such as flowrate or choke discharge coefficient. The remaining measurement values are estimated by the models. The differences between the estimated and actual measurement values are minimized by an optimization solver. This approach is called Virtual Flow Metering (VFM) and can be used as a back-up to MPFMs as well as a standalone metering solution.

As an alternative to the first principles models, one can use a data-driven approach in order to estimate the flowrates. In this case, the specifics of the production system such as geometry of the well tubing or choke are not considered and only field measurements are used to identify the system model. The advantage of using these models is a low computational cost and relative simplicity in comparison to the first principles VFM methods that typically solve complex PDE conservation equation systems. These facts are especially of advantage if one does not have full access to the first principles model equations, for instance, in a commercial multiphase flow solver. In this case, computing gradients for optimization is computationally very expensive, while the data-driven models can provide the gradients at a much lower cost. This allows a well-trained data-driven model to predict the flowrates in real time with a sampling time of seconds, while VFM based on first principles models may have a significant time delay due to solving the embedded non-linear optimization problem.

The most popular data-driven approach in VFM is based on feed-forward neural networks (NNs) with various modifications of structures and weights optimization, see Berneti and Shahbazian (2011) and AL-Qutami et al. (2018) with therein references. Despite the reasonable accuracy of NNs, there are some disadvantages associated with them. First, it is difficult to establish good rules for NN architecture construction, such that creating a successful structure of the NN requires strong user experience and can be time consuming. Also, the accuracy of NNs is

⋆ The authors gratefully acknowledge the financial support from the center for research-based innovation SUBPRO, which is financed by the Research Council of Norway, major industry partners, and NTNU.

10.1016/j.ifacol.2019.06.114

dependent on the scale of the input features and target variables, such that NNs require data normalization (Sola and Sevilla, 1997). This is especially the case in VFM since the scale of the features varies widely. Also, the resulting NN is used as a black-box model and sometimes it is difficult to understand the reason behind its behavior. Hyperparameters tuning to avoid model overfitting is also often a challenge in NNs training.

Gradient Boosting (GB) is another efficient method for solving non-linear classification and regression problems. Here we construct an ensemble of weak learners (simple algorithms) into a strong learner which is used to solve a particular problem (Friedman (2001)). One of the most popular modifications of GB is applying regression trees as weak learners which is called Tree Gradient Boosting. Among various implementations of Tree Gradient Boosting, eXtreme Gradient Boosting (*XGBoost*) by Chen and Guestrin (2016) is a popular algorithm for solving machine learning problems. In this work, we apply this algorithm implementation. In contrast to NNs, GB does not require scaling of the features which makes it more convenient for VFM applications. In addition, despite many hyperparameters, the tuning process of GB can be considered more intuitive and flexible compared to NN's tuning. For instance, increasing the number of trees by one allows a careful model adjustment while increasing the number of nodes in NNs by one may lead to a large change of the model performance and possible overfitting, especially in small datasets. Another advantage of GB is the feature importance analysis which can be performed directly in algorithm training without additional manipulations which gives an opportunity to better understand the algorithm behavior and get additional insights of the system parameters.

In this paper, we analyze capabilities of XGBoost in predicting oil flowrates from a subsea well under realistic conditions. We show how the algorithm can be used in different field development strategies as a back-up system for a multiphase flow meter or a standalone solution using the information from well tests. In addition, we analyze the performance of K-Fold and early stopping cross-validation schemes together with a tuning procedure for selecting an accurate set of XGBoost hyperparameters for VFM applications. The implementation of the algorithm for this paper can be found on `https://github.com/NRT23`.

2. XGBOOST ALGORITHM

In this section, we give an overview of basic principles of Gradient Boosting and its implementation in XGBoost algorithm based on the paper by Chen and Guestrin (2016).

Consider a dataset $\mathcal{D} = \{(x_i, y_i)\}$ $(i = 1...n,\ x_i \in \mathbb{R}^m,\ y_i \in \mathbb{R})$, meaning that we have m features for each of n observation examples which correspond to the target variable y. A tree ensemble prediction for a given observation i is produced as a sum of predictions from K additive functions

$$\hat{y}_i = \phi(x_i) = \sum_{k=1}^{K} f_k(x_i) \tag{1}$$

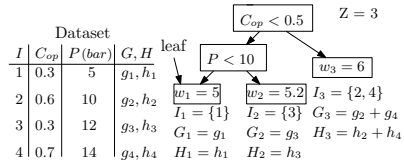

I	C_{op}	$P(bar)$	G, H
1	0.3	5	g_1, h_1
2	0.6	10	g_2, h_2
3	0.3	12	g_3, h_3
4	0.7	14	g_4, h_4

Fig. 1. Example of a regression tree in XGBoost for VFM

where f_k is a regression tree predicting the value $f_k(x_i)$ for the *i-th* example. By training an ensemble of regression trees, we want to minimize the objective function with loss terms (l) and regularization terms (Ω)

$$L(\phi) = \sum_i l(y_i, \hat{y}_i) + \sum_k \Omega(f_k) \tag{2}$$

with

$$\Omega(f) = \gamma Z + \frac{1}{2}\lambda \left\| w \right\|^2, \tag{3}$$

where γ and λ are hyperparameters to penalize the model complexity defined by the number of leaves Z and leaf weight values w. The loss term (l) can be expressed in a form of the user's interest, for instance, as the mean squared error for regression problems.

The objective in (2) is minimized in an iterative manner by adding a regression tree at each iteration. This leads us to the following objective function at *t-th* iteration

$$L^t = \sum_{i=1}^{n} l(y_i, \hat{y_i}^{t-1} + f_t(x_i)) + \Omega(f_t) \tag{4}$$

Applying a second order Taylor expansion and removing the terms independent of f_t, it can be shown that the following approximation of (4) can be obtained (Chen and Guestrin, 2016)

$$\tilde{L}^t = \sum_{i=1}^{n} [g_i f_t(x_i) + \frac{1}{2} h_i f_t^2(x_i)] + \Omega(f_t) \tag{5}$$

where g_i and h_i are the first and second order derivatives of $l(y_i, \hat{y_i}^{(t-1)})$ w.r.t. $\hat{y_i}^{(t-1)}$. Defining I_j as a group of observations in the *j-th* leaf in a particular tree structure and taking into account that the tree produces the same weights score for the observations in one leaf, we can compute the optimal leaf weights w_j^* and the corresponding optimal value of the objective approximation $\tilde{L}^t$ (Chen and Guestrin, 2016)

$$w_j^* = \frac{\sum_{i \in I_j} g_i}{\sum_{i \in I_j} h_i + \lambda} \tag{6}$$

$$\tilde{L}^t(q) = -\frac{1}{2} \sum_{j=1}^{T} \frac{(\sum_{i \in I_j} g_i)^2}{\sum_{i \in I_j} h_i + \lambda} + \gamma Z \tag{7}$$

where q denotes a particular tree structure. Equation (7) is used as an evaluation criteria to find an optimal split of the tree. The tree is grown greedily to avoid enumerating all possible structures q meaning that the algorithm starts splitting from a single leaf and adds branches according to (7). Fig. 1 shows a simple example of an XGBoost regression tree with the algorithm notations and measurement data of pressure and choke opening used in VFM. To get a better understanding of the splitting procedure, consider I_L and I_R to be the left and right groups of observations after the tree node split. Having

this information, we can calculate a loss reduction caused by the split

$$L_{split} = \frac{1}{2}\left[\frac{\left(\sum_{i\in I_L} g_i\right)^2}{\sum_{i\in I_L} h_i + \lambda} + \frac{\left(\sum_{i\in I_R} g_i\right)^2}{\sum_{i\in I_R} h_i + \lambda} - \frac{\left(\sum_{i\in I} g_i\right)^2}{\sum_{i\in I} h_i + \lambda}\right] - \gamma \quad (8)$$

The loss reduction (8) is used to evaluate each possible split by linear scanning of sorted values for each feature in each node. The best split is the one which gives the *maximum* value of the loss reduction. When the splitting is finished, the leaf values are assigned according to (6).

For a more detailed explanation of XGBoost algorithm derivation and its additional features such as shrinking tree outputs the interested reader is referred to the original paper by Chen and Guestrin (2016).

3. PRODUCTION SYSTEM MODELING

We consider a simple subsea production system which consists of an oil well, a flowline, a riser and an inlet separator with a constant pressure, see Fig. 2. The parameters of the system are shown in Table 1. The well is equipped with a multiphase flow meter (MPFM), choke, pressure (P) and temperature (T) sensors which are installed at the bottomhole, upstream and downstream of the choke. In addition, information about the choke opening (C_{op}) is available. The system performance is simulated in OLGA which is one of the leading simulation tools for multiphase flow transport in oil and gas production systems (Bendiksen et al. (1991)). To manipulate the choke opening and inflow sources as well as collect simulation results, we use MATLAB together with an OPC (Open Platform Communication) server.

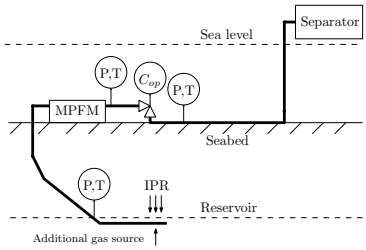

Fig. 2. Schematic representation of the production system

To model the reservoir inflow, we use the Inflow Performance Relationship (IPR) formulated by Vogel's equation (Vogel et al. (1968)). To mimic the reservoir depletion effect, we introduce a *linear reservoir pressure decline* with respect to the production time. The IPR does not consider transient effects in the near-wellbore region. Therefore, to simulate dynamic effects related to the change of the bottomhole pressure caused by the choke position change, occasional gas breakthroughs from injection wells and other possible disturbances such as production wells interaction, we include an additional gas source which has a periodic form represented by the following relationship

$$\dot{m}_{Source} = \dot{m}_{max} \cdot C_{op} \cdot \left[1 + a \cdot sin\left(\frac{\pi \cdot s}{T_{source}}\right)\right] \quad (9)$$

Table 1. System and simulation parameters

Parameter	Value	Parameter	Value
True vertical depth	2010 m	$\dot{m}_{\max}$	0.35 kg/s
Measured depth	3110 m	T_{MPFM}	72
Flowline length	1000 m	T_{Source}	144
Riser length	100 m	a	0.5

where $\dot{m}_{max}$ denotes the maximum mass gas source value, C_{op} - the choke opening, s - the time step, a and T_{source} - the amplitude and the period of the sin function respectively. In this relationship, we assume that the disturbance gas flow is proportional to the choke opening, such that when the choke is closed the effect vanishes. At the same time, by introducing a periodic function, we mimic dynamic reservoir responses and possible disturbances on the well without introducing random behavior. This trick together with the reservoir pressure decline is done in order to mimic a realistic system behavior, and to challenge the VFM to predict the varying flowrates. Otherwise, a steady state behavior of the IPR would produce a specific flowrate value to a specific choke position which makes the case unrealistic as well as simplifies the training and predicting process for the machine learning algorithm. A more advanced approach could be to couple OLGA with a reservoir simulator which would describe the reservoir response in a more precise way. This will be considered in future work.

To calculate the multiphase flowrate meter predictions, we assume that 100% flowrate measurements by the MPFM are within ±5% accuracy with respect to the true value and model the predictions by the following relationship

$$Q_{MPFM} = Q_{True}\left[1 + 0.05 \cdot sin\left(\frac{\pi \cdot s}{T_{MPFM}}\right)\right] \quad (10)$$

where T_{MPFM} denotes the period of the sin function. The periodic function with a large period value allows to model the measurement error with a certain accuracy and at the same time avoid unrealistic random fluctuations under stable flow conditions which we would obtain by introducing simply a random measurement error.

4. CASE STUDIES

We perform several case studies which represent different situations of oil production monitoring and for each case consider two different cross-validation schemes: K-Fold and early stopping. As the flowrate prediction from an oil reservoir is time dependent, it can be considered as a time series problem. In this case, the K-fold cross-validation should be applied in a nested manner (Fig. 3, left) which is different from the traditional K-fold cross-validation approach. First, the available data is divided into training and test datasets. The training set is again divided in K-folds. No shuffling is involved in the splitting process. Then the model is trained on (1, 2, .., K-1) folds combined (starting from fold 1 only) and validated on (2, 3, .., K)th fold. The obtained errors on K-1 test folds are averaged to make conclusions about the model accuracy and generalization. In this manner, the algorithm is not trained on the future data and tested on the past data as would happen in non-nested cross-validation. Finally, the algorithm is re-trained on the entire training data and tested on the test dataset to evaluate the model gener-

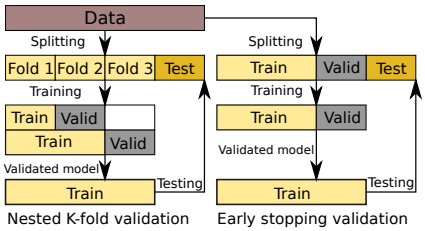

Fig. 3. Schematic representation of validation schemes

alization. In early stopping (Fig. 3, right), the available data set is divided into 3 subsets: training, validation and test. The algorithm is trained on the training set while the error is also monitored on the validation set. The training is stopped when the error on the validation set stops decreasing after adding a specified number of new trees. The performance of the obtained model is checked using the test dataset.

In this work, the test datasets are selected to be 15% of the available training data for both K-Fold and early stopping. In early stopping, another 15% of the data is dedicated for the validation dataset. For K-fold validation the number of folds is 5.

The data are generated using the production system architecture shown in Fig. 2. The performance of the system is simulated for a period of 2 years. The obtained production profile without the well tests performance is shown in Fig. 4 (top). The period is divided into 4 quarters 180 days each. At the beginning of each quarter, a well test is conducted to obtain reliable information about the well performance. We collect the measurements every 8 hours during the normal production time and every 30 mins during the well tests. The following measurements are collected for the algorithm training and predicting the flowrates in the future time period:

- Pressure and temperature at the bottomhole, upstream and downstream of the choke
- Choke opening and oil flowrates from the MPFM or well tests

We analyze 3 case studies which have several sub-cases each. For 2 case studies we also compare the performance of K-Fold and early stopping cross-validation approaches. Each case considers a separate field development strategy, so we analyze the performance of GB VFM for various situations of production operation. The detailed description of each case study is discussed below.

4.1 Case 1 - MPFM data

In this case, we assume that we do not have information from the well tests and use the flowrate measurements from the MPFM only. This case is possible when well testing is expensive and rarely performed. For this case, we perform 3 cases studies by extending the training datasets as the production time evolves. For instance, in the first study (Case 1.1) we assume that the data from the first half a year is available for training (Q_1 in Fig. 4) and we would like to predict the flowrates for Q_2. As the time evolves and we obtain more training data, in Case 1.2 we use the data from Q_1 and Q_2 for training

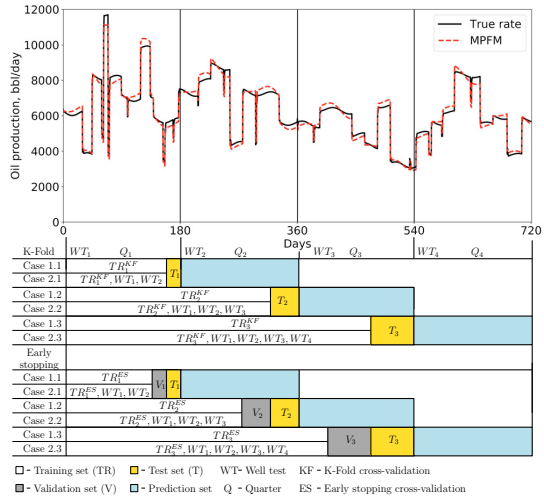

Fig. 4. Production profile with data splitting schemes

and testing the model and perform predictions on Q_3. This procedure is done for K-Fold and early stopping approaches. Fig. 4 (bottom) visualizes the dataset splitting for training, validation, testing and predicting for each case and each cross-validation method.

4.2 Case 2 - MPFM and well test data

In this case, we combine the well tests and MPFM data for training. Well tests can be conducted even if MPFMs are installed in order to calibrate these devices as well as update information about reservoir properties and the well performance. Similarly to Case 1, we extend the training datasets as the time evolves. The well testing procedure is explained in more details in Case 3 description. As in Case 1, we conduct the studies for K-Fold and early stopping cross-validation. Fig. 4 shows the dataset splits for training, validation, testing and predicting for the sub-cases of Case 2.

4.3 Case 3 - Well test data

In this case, we assume that the MPFM is not installed at the wellhead and training data is available only from the well tests. This situation can happen when MPFMs are not economically or operationally feasible to install because of high cost or flow assurance challenges and instead well tests are performed to track the production rates. To generate data for GB VFM, we propose well testing with step-wise changes of the choke opening over the possible operating range. In this case, we assume the choke opening to be within the range of 0.05 and 0.7 and we perform the well test with a choke opening increment of 0.05. Also, we perform a few additional tests around the expected well operating point. In this case, we expect the operating point to be within the range of 0.10 and 0.4 and perform several additional step changes over this range. More information on the well testing procedure including visualization can be found under `https://github.com/NRT23`.

The problem in this situation is the fact that the amount of data is limited, so that obtaining a validation and test

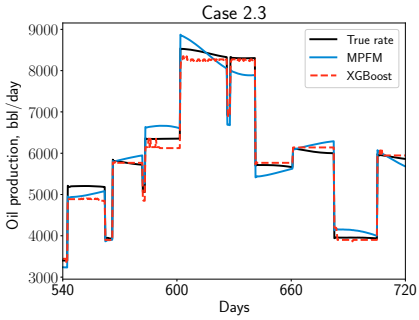

Fig. 5. Comparison of GB VFM and MPFM predictions

datasets for model evaluation and overfitting control is difficult. Even K-Fold cross-validation may not help in this case, since there are only a few measurements for each point of the gradually changing choke opening. In this work, we assume that there is no available data for model testing and train the model until the training dataset is well fitted. Table 2 shows the matrix of the datasets usage in Case 3.

Table 2. Matrix of datasets for Case 3

Case	Train	Validation	Test	Prediction
Case 3.1	WT_1	-	-	Q_1
Case 3.2	WT_1, WT_2	-	-	Q_2
Case 3.3	WT_1, WT_2, WT_3	-	-	Q_3
Case 3.4	WT_1, WT_2 WT_3, WT_4	-	-	Q_4

4.4 XGBoost application and tuning

In this work, we use Python implementation of XGBoost. To select hyperparameters, we use random search approach. To explore a large subspace of the hyperparameters, we perform 10 random searches 10 iterations each for both K-Fold and early stopping in each sub-case study.

5. RESULTS AND DISCUSSION

In this section, we analyze the simulation results for each simulation case separately and afterwards make general remarks about the performance of XGBoost for Virtual Flow Metering. To evaluate the performance on the predicting datasets, we use Mean Absolute Percentage Error (MAPE) which shows the average absolute percentage deviation of the predictions from the true value

$$MAPE = \frac{1}{m}\sum_{i=1}^{m}\left|\frac{y_i - \hat{y}_i}{y_i}\right| \cdot 100 \qquad (11)$$

To compare the XGBoost performance for Case 1 and Case 2, we also calculate MAPE between the multiphase flow meter measurements and the true rate.

Table 3 summarizes the simulations results from all the cases. For the sub-cases of Case 1, we see that with the increase of the dataset size, the performance of both validation methods improves, however, for the early stopping cases this improvement is negligible. Another observation is that early stopping outperforms K-folds in Case 1.1 and Case 1.2 while in Case 1.3 K-Fold method outperforms

Table 3. MAPE of GB VFM and MPFM

Method	MAPE					
	Case 1.1		Case 1.2		Case 1.3	
GB VFM[1]	KF[2]	ES[3]	KF	ES	KF	ES
	6.49%	5.21%	6.50%	5.17%	4.88%	5.11%
	Case 2.1		Case 2.2		Case 2.3	
GB VFM	KF	ES	KF	ES	KF	ES
	2.08%	2.09%	3.39%	3.68%	2.02%	2.13%
	Case 1.1/2.1		Case 1.2/2.2		Case 1.3/2.3	
MPFM[4]	3.15%		3.09%		3.14%	
	Case 3.1	Case 3.2		Case 3.3	Case 3.4	
GB VFM	5.85%	3.29%		3.26%	3.88%	

[1] - Gradient Boosting Virtual Flow Meter
[2] - K-Fold cross-validation
[3] - Early stopping cross-validation
[4] - Multiphase Flow Meter

early stopping. The reason for this can be the fact that K-fold validation is performed in a nested manner, so that in the first two cases the model is constructed in a relatively small datasets, especially when the number of training folds is small. However, in Case 1.3 the data becomes large enough even in 1 fold to construct a model which well represents the data. However, one should notice that this situation might not always be the case. For instance, if the validation dataset was very different from the prediction one, early stopping would potentially show less accurate performance than K-Fold method in all the cases.

Another important observation from Table 3 is the fact in all the sub-cases of Case 2 the error is lower both for K-Fold and early stopping than in the corresponding sub-cases of Case 1. This shows that adding the information from the well tests helps to improve flowrate predictions with GB VFM. Another observation for Case 2 is that K-Fold outperforms early stopping in each sub-case. This shows that for the data with higher variability added by the well tests, K-Fold cross-validation can be a more robust way of the algorithm training. Potentially, the performance of early stopping in cases with well testing data can be improved by a better selection of the data splitting strategy. For instance, a part of the well test dataset can be included into the validation set while in our work we used well test data in the training dataset only.

Overall, we observe that the MAPE from GB VFM is comparable with the error from the MPFM, especially in Case 1.3 and Case 2. An example of the flowrate predictions by GB VFM is shown in Fig. 5. The figure shows that during some production time the constant piecewise approximations by the regression trees is good enough and have values closer to the true rate than the simulated MPFM rate predictions while in some parts constant piecewise predictions can be relatively inaccurate. Potentially, the performance of GB VFM can be further improved by applying linear function approximations instead of constant piecewise ones which may have a better ability to interpolate the flowrate predictions.

Another interesting observation from Table 3 is that a very small error is achieved in Case 2.1 even though this case does not have the largest training dataset. The reason for this is the fact that the choke opening values in Q_2 (prediction dataset for Case 2.1) coincidentally matched the values considered during the well tests multiple times. Since the flowrate estimates from the well tests does not

include the MPFM uncertainty, the resulted error is even lower than the error from the MPFM. This result is promising meaning that by performing a well-planned well testing around the expected operating point can lead to very accurate flowrate predictions by GB VFM.

As for the sub-cases of Case 3, we see the tendency of the error decline as the training set increases. An additional sub-case (Case 3.1) in Case 3 was included to see if we can use well tests from the beginning of the field operation for VFM purposes without a need of MPFM installation. As we can see from Table 3 the error in Case 3.1 is relatively large in comparison with the MPFM while with the new data obtained the error becomes comparable. Thus, potentially the combination of the well testing performed in a step-wise choke opening manner with GB VFM can be used as a standalone solution. However, at the initial production phase the accuracy can be low. One solution for this problem can be performing longer and more rigorous well tests for the initial stage with reducing well test complexity as the time evolves.

Even though we observed that the errors in Case 3 are comparable with MPFM, one should notice that the training was done without validation and test datasets, so that even well a fitted algorithm produced good results. In a real case, the well tests measurements may not have such a good accuracy as in the considered case and may have more noise both in variables (pressure and temperature measurements) and flowrate measurements, so that an overfitted model will most likely give worse predictions than the presented ones. In this case, obtaining more data from well testing and using it as a validation/test datasets can be a solution to control model overfitting.

In addition to the performance analysis, it is worth to emphasize limitations and possible challenges of GB VFM implementations in real systems. First of all, in this work we assumed that the measurements are free of noise. In reality, the measurements will always contain random and possibly drift errors which would make the implementation of the algorithm more challenging. In addition, the used constant piecewise regression trees have limited capabilities in extrapolating the target variable which can be important in real systems when new data goes outside the range of training data. This problem can be addressed by implementing linear regression trees as weak learners in GB.

6. CONCLUSIONS AND FUTURE WORK

In this work, the XGBoost implementation of Gradient Boosting algorithm was used to predict oil flowrates from a simple subsea production system under various field development strategies. The algorithm showed a performance comparable with a hardware multiphase flow meter and has a potential to be used as a back-up as well as a standalone solution for Virtual Flow Metering even provided with a small training dataset. Depending on the available dataset size and variability, K-Fold or early stopping cross-validation strategies can be used to obtain a good algorithm performance. Random search strategy of the algorithm selection combined with a careful parameter tuning produces good results of the flowrate predictions. The simulation results showed that by combining GB algorithm with the flowrate measurements from well testing over a wide operating range of the well, it is possible to make accurate flowrate predictions starting from an early production stage. The future work can address improvements of GB application for VFM by using linear regression tree models as weak learners. as well as challenges associated with the uncertainty of the flowrate measurements and limited data availability from the well tests.

Apart from improving the algorithm using more advanced learners, the future work may also address utilizing GB together with artificial neural networks within ensemble learning to make even better predictions. However, one should be careful when implementing this approach because it inevitably leads to a less explainable model. In addition, adding pressure and temperature data from other parts of production systems may also boost the performance. Potentially, installing more sensors for gathering algorithm training data and conducting rigorous well tests as proposed in this work can be less costly than investing into experiments for tuning first principle models or installing expensive hardware devices such as multiphase flow meters. This question should be addressed by companies when developing flowrate monitoring systems in existing and especially new fields.

REFERENCES

AL-Qutami, T.A., Ibrahim, R., Ismail, I., and Ishak, M.A. (2018). Virtual multiphase flow metering using diverse neural network ensemble and adaptive simulated annealing. *Expert Systems with Applications*, 93, 72–85.

Bendiksen, K.H., Maines, D., Moe, R., Nuland, S., et al. (1991). The dynamic two-fluid model olga: Theory and application. *SPE production engineering*, 6(02), 171–180.

Berneti, S.M. and Shahbazian, M. (2011). An imperialist competitive algorithm artificial neural network method to predict oil flow rate of the wells. *International journal of computer applications*, 26(10), 47–50.

Chen, T. and Guestrin, C. (2016). Xgboost: A scalable tree boosting system. In *Proceedings of the 22nd acm sigkdd international conference on knowledge discovery and data mining*, 785–794. ACM.

Falcone, G., Hewitt, G., Alimonti, C., Harrison, B., et al. (2001). Multiphase flow metering: current trends and future developments. In *SPE annual technical conference and exhibition*. Society of Petroleum Engineers.

Friedman, J.H. (2001). Greedy function approximation: a gradient boosting machine. *Annals of statistics*, 1189–1232.

Patel, P., Odden, H., Djoric, B., Garner, R.D., Vea, H.K., et al. (2014). Model based multiphase metering and production allocation. In *Offshore Technology Conference-Asia*. Offshore Technology Conference.

Sola, J. and Sevilla, J. (1997). Importance of input data normalization for the application of neural networks to complex industrial problems. *IEEE Transactions on Nuclear Science*, 44(3), 1464–1468.

Vogel, J. et al. (1968). Inflow performance relationships for solution-gas drive wells. *Journal of petroleum technology*, 20(01), 83–92.

3.2 Discussion of Paper II - Oil Production Monitoring Using Gradient Boosting Machine Learning Algorithm

Due to the page limitations of the publication, it was not possible to discuss all the details and motivation of the assumptions used in the paper, so this section is intended to make additional clarifications and discussions for Paper II.

3.2.1 Remarks on production system setup

First of all, it is important to discuss the process of data generating. All the data used in this paper is synthetic meaning that it is generated using a commercial multiphase flow simulator. The well setup and profile used in these simulations are taken from a real well example with a three-phase fluid with GOR of 153 Sm^3/Sm^3 and WC of 0.3 (30 %). Despite the fact that the three-phase flow is considered, only oil production monitoring case is discussed. The main reason is that in this paper, we are more interested in understanding the capabilities of Gradient Boosting in performing the Virtual Flow Metering task in general and difference scenarios of its possible usage rather than expanding this task to all three phases. Another reason is the page limitation of the paper. However, it would have been interesting to see the performance of the algorithm for the gas and water phases.

As pointed out in the paper, during the well tests the noise is not introduced into the flow measurements and this fact can be addressed in future work. The reason for choosing these conditions is the fact that typically well tests are considered to be more accurate that the estimates produced by a multiphase flow meter and, in fact, used to calibrate these devices. Since we artificially introduced an error into the estimates generated by a multiphase flow meter, we decided not to include a measurement error into well tests in order to reflect the fact that the results from well tests are more accurate and can be confidently used for model tuning. If we have had real data for the analysis, this would not have been an assumption, but due to the artificial nature of the data, such an assumption is made. In addition, we would like to point out that we do not assume any PVT-related errors for both the multiphase flow meter and the Virtual Flow Meter.

3.2.2 Remarks on manipulated and independent variables and their time scales

Despite the fact that the example of the well setup is close to real, the production scenarios are synthetic and generated to test different cases that can be met when operating an oil and gas field. There are several manipulated and independent variables that are used in these simulations. The first and the main variable is the

choke opening that is responsible for all high flow changes during the production period. Changes of the choke opening initially influence the short time scale flow behavior such as sudden local flow fluctuations, change of the pressures across the choke, the downhole pressure and, as the result, the pressure fluctuations along the well tubing. In a slightly longer time scale, the choke opening defines magnitude of the flowrate value which will be achieved when the system reaches steady state conditions.

Secondly, the gas inflow source at the downhole is introduced. This is an "artificial" independent variable meaning that it is not available to production engineers in real field operation. This variable is introduced with the aim to simulate a potential slow dynamic reservoir response to the changes of the production choke settings, that is why it is assumed that the amount of the injected gas flow disturbance is proportional to the choke opening value. As shown in Eq. 9 in the paper, the form of the source is periodic. Such a form is an assumption and in a real field operation scenario it may not necessarily be the case. However, this assumption simplifies the simulation process and also make it more consistent and reproducible. It is also important to point out that even if the choke position is constant, such a form of the disturbance imitates a slowly changing dynamic response of the reservoir and/or often existing mutual wells' interaction behavior that has a longer time scale than the short time scale transients caused by the choke position changes. There can be, of course, other possibilities to simulate the middle/long time scale response of the reservoir and the reader can approach this problem with another more realistic case. The best possibility to do so can be to link OLGA's well simulations with OLGA-ROCX which is OLGA's module that can be used to simulate the near-wellbore reservoir behavior together with the multiphase flow physics occurring in the well tubing.

The last independent variable is the reservoir pressure that is assumed to have a linear decline trend over the production period to simulate the reservoir depletion phenomenon. In addition to mimicking a more realistic production situation, it is also introduced into the simulations to create a slow time dependency in the production setup. In real case scenarios, other slow production changes might occur over time, for instance, fluid properties changes, however, it is not considered in this work.

3.2.3 Time scales of the phenomena considered for machine learning model training and testing

Having the manipulated and independent variables discussed in detail, we can notice that they are responsible for different time scale phenomena occurring in the system. In this work, even though the simulations were performed in the transient

mode in OLGA, they are done in such a way that the short time scale transient phenomena are not captured in the training, validation and test data. This is because when the new manipulated/independent variables' values (choke position and downhole gas source) are introduced into the system, the data are not gathered until the system reaches steady state conditions in terms of the short time scale behavior. In this case, the steady state conditions are defined when, after the changes of the manipulated variables, the system states such as flowrate, pressures and temperatures stop changing over time. As such, no averaging is involved in the sampling process. Despite the fact that the level of the choke position change can be different between the points in time, it is observed that the system reaches steady state at maximum of 10 min after the changes in variables, so that the sample point is taken at least in 10 min since the changes are introduced. As such, the different levels of the choke position are introduced to better test interpolation capabilities of the Gradient Boosting algorithm in estimating the oil flowrate. The choke openings are constructed nearly under random value assumption in the range of [0.1-0.4] when performing simulations for the production scenarios. The choke openings used in this work are in the range of [0.05-0.7] when simulating well tests.

As the result of excluding the short time scale transient phenomena, the dynamic processes that are considered in the simulations and included for evaluation of the machine learning model are the slow dynamic responses introduced through the downhole gas disturbance and the linear reservoir pressure decline.

As such, all the manipulated/independent variables used in the simulations in Paper II are related to different time scales of the system. A potential influence of these time scales on the model performance and its existence in the training, validation and test sets is discussed in the next section.

3.2.4 Time dependency and its potential influence on Virtual Flow Metering model accuracy

As discussed above, even though the short time scale phenomena are not included in the model training, because the gas disturbance has the time-periodic form and the reservoir pressure has a linear decline, it introduces the time dependency into sensor measurements and the flowrate with respect to the longer time scale. This can be very well seen in Figure 3.1, where the oil rate during the production is depicted together with the rates obtained during the well tests, while in the paper the tests rates are excluded from the figure. First, we can notice the generally decreasing trend over the production period. But secondly and more importantly, we observe that for the same choke openings applied during the well tests, the computed rates are different, that again emphasizes the slow time dependency in

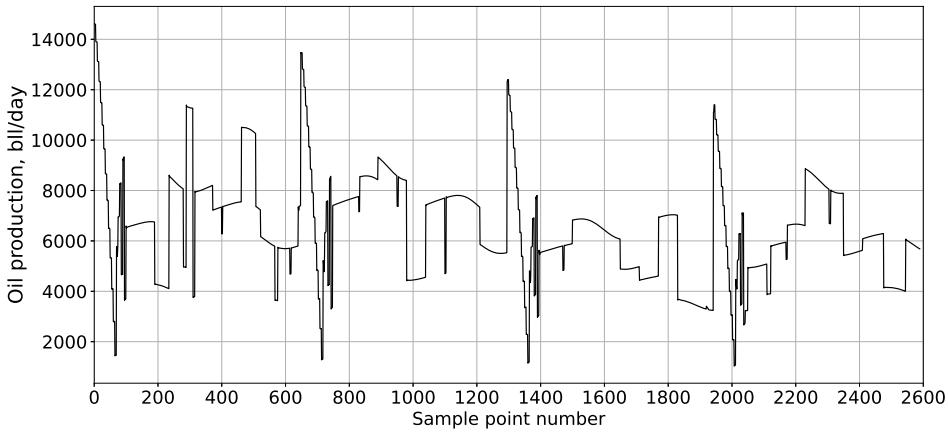

Figure 3.1: Well production with well tests

the data.

Despite the fact that in most cases Gradient Boosting is considered as an algorithm that is trained for independent data points without taking the time dependency into account, it is in general possible to include the past data into algorithm. This can be done by simply introducing the time-lag features, such that the algorithm sees what happened before the current time step. In this paper, however, such an approach is not considered and only the current measurements are taken into account. It could potentially be beneficial consider the past measurements, but, most likely, the performance would improve only slightly, especially for the cases with a small training set, because the changes in the production behavior would be rather small. Moreover, when increasing the dataset size, the slowly changing dynamic behavior of the system becomes included into the training data, such that the algorithm becomes more and more capable to capture this trend. For this reason, the nested cross-validation is introduced in the paper in order to prevent the algorithm from better capturing this trends when knowing the future training data.

For an additional discussion on how including data from the future in a time-dependent problem might lead to wrongly estimated model capabilities, let us consider the following example which is simple and intuitive but is still illustrative. In this example, we will not even select hyperparameters based on cross-validation, but use the same linear regression algorithm for all the validation schemes. We will then observe how the error varies between the validation sets and how it is different from the test set.

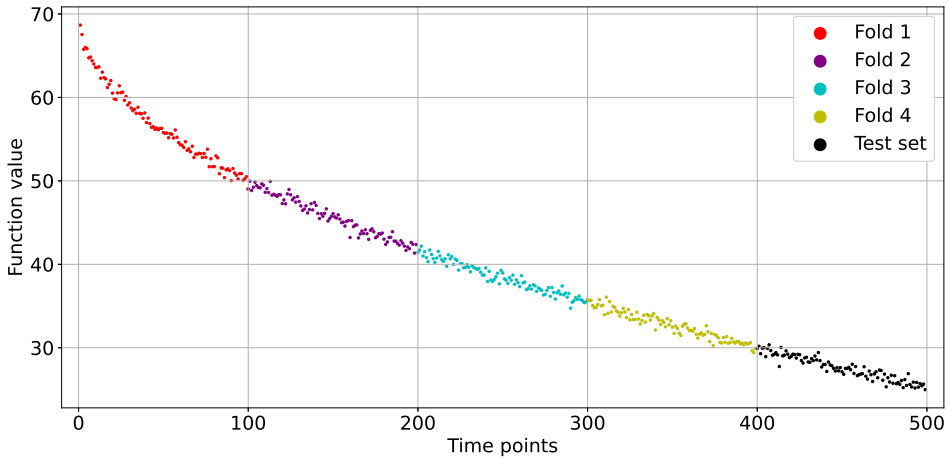

Figure 3.2: Non-linear time dependent data used for testing cross-validation schemes

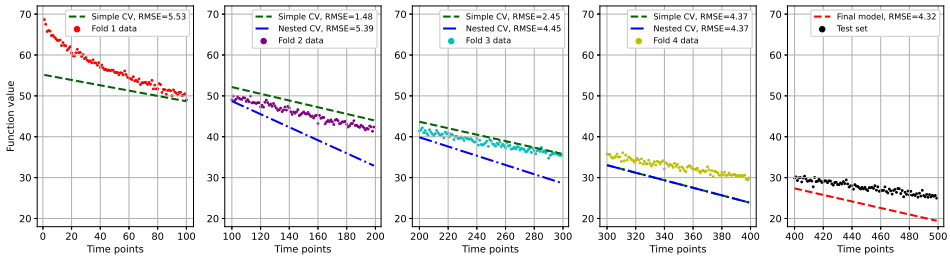

Figure 3.3: Predictions of the linear model with simple and nested cross-validation schemes

Let us assume that the data follows a decreasing non-linear behavior which becomes more and more linear with time, and has some random noise with zero mean and a small variance, as shown in Figure 3.2. In the figure, the data follows the function of the form $f(t) = 70 - 2\sqrt{t}$ with a white noise around it. Note that the function value at a certain time step is dependent on this time step value and not dependent on the previous time step values, so that we can say that the data points are independent on each other, as in the case with steady state flow in a well. To check potential differences between simple (conventional) and nested cross-validation schemes, we fit a linear model to this data and validate it using these two strategies. To do it, the data of 500 time points is spitted into 4 validation folds of 100 points each and 1 test set that also consists of 100 points. When the model is checked on the validation sets, it is re-trained based on the entire training

set and tested on the test set.

Within the simple cross-validation scheme, one fold is assumed to be the validation set and the rest three folds are used for training. As such, the following training-validation sets are considered:

- Training: Fold 1, 2, 3 | Validation: Fold 4;
- Training: Fold 1, 2, 4 | Validation: Fold 3;
- Training: Fold 1, 3, 4 | Validation: Fold 2;
- Training: Fold 2, 3, 4 | Validation: Fold 1;

Within the nested cross-validation scheme, only subsequent folds can be used for validation, and for each validation step one fold is appended to the previously used set. As such, the following training-validation sets are considered:

- Training: Fold 1 | Validation: Fold 2;
- Training: Fold 1, 2 | Validation: Fold 3;
- Training: Fold 1, 2, 3 | Validation: Fold 4;

In Figure 3.3, the regression results of the linear model for each fold and test set using two cross-validation schemes are shown. For Fold 1, the nested-validated model is not used because there is no prior fold to be trained on. For Fold 4, both models produce the same result because they are trained on the same folds (1, 2 and 3). From the results we see that the nested model continuously improves the prediction (RMSE decreases) when more and more training data is used, and the validation RMSE on Fold 4 is very close to the RMSE on the test set. The mean RMSE of the nested model is 4.73 which is close to the RMSE on the test set which is 4.32. Also, it is very logical that the error on the test data set is smaller than the mean error on the validation sets because the number of data points is small and the trend of the data is well-predicted. This leads to the fact that when the model is trained on the entire training set, its predictive capabilities should increase. As such, we conclude that by applying the nested cross-validation scheme on a slowly time-dependent dataset, we can generally make a representative assessment of the model performance.

When considering the results using the conventional cross-validation scheme, we see that by introducing the "future" data into the training, for instance, Folds 3 and

4 when validated on Fold 2, we definitely overestimate the model performance such that the estimated error is low (RMSE=1.48). This obviously happens because for the model it becomes much easier to interpolate the results between the prior fold (Fold 1) and subsequent folds (Folds 3 and 4). As such, it leads to the misleading results about the overall model performance because the mean RMSE for the simple cross-validation scheme is 3.46, which, in this case, is contradictive because with the presented data the predictive capabilities of the model should increase when more and more data come due to a near-linear origin.

It is also important to note that when new data come, we will not have access to the "future" data for this new data set, as such we will not be able to perform interpolation for such a time dependent case. This additionally confirms the point of using nested cross-validation scheme for the time dependent problem. The results from this example ca be easily related to higher dimensional space and non-linear models, such as the one considered in the paper.

Coming back to the Virtual Flow Metering problem, it is in general true that multiphase flow production depends on time, both in short and long time scales. In the case considered in the paper, it is a long time scale while in real operation it can be both scales. As such, to contribute to the correct treatment of the problem using machine learning approaches in future research in this topic, we suggested using the nested cross-validation scheme to avoid misleading results that can be produced by a biased model, as shown in the example above.

3.3 Combining Machine Learning and Process Engineering Physics Towards Enhanced Accuracy and Explainability of Data-Driven Models (Paper III)

Paper III describes applications of hybrid (physics combined with machine learning) approaches applied to multiphase flowrate estimation case study where a Virtual Flow Meter used as a back-up system to a multiphase flow meter. In this paper, the authors consider different methods for combining machine learning and physics of process engineering systems and show how these approaches make the simulations outcomes more accurate and explainable compared to purely data-driven modeling approaches. The main motivation behind this paper was the fact that in the vast majority of previous studies of using machine learning techniques for multiphase flowrate estimation purposes, prior knowledge about physical behavior of the system was avoided. As such, the authors wanted to investigate the potential of using combined approaches based on real oil well data.

Bikmukhametov, T., and Jäschke, J. (2020). Combining Machine Learning and Process Engineering Physics Towards Enhanced Accuracy and Explainability of Data-Driven Models. Computers and Chemical Engineering, Volume 138, 10683, doi.org/10.1016/j.compchemeng.2020.106834

Computers and Chemical Engineering 138 (2020) 106834

Contents lists available at ScienceDirect

Computers and Chemical Engineering

journal homepage: www.elsevier.com/locate/compchemeng

Combining machine learning and process engineering physics towards enhanced accuracy and explainability of data-driven models☆

Timur Bikmukhametov*, Johannes Jäschke

Dept. of Chemical Engineering, Norwegian University of Science and Technology (NTNU), Trondheim NO-7491, Norway

ARTICLE INFO

Article history:
Received 20 December 2019
Revised 21 March 2020
Accepted 25 March 2020
Available online 19 April 2020

Keywords:
Machine learning
Explainable machine learning
Hybrid modeling
First principles modeling
Process engineering
Virtual flow metering

ABSTRACT

Machine learning models are often considered as black-box solutions which is one of the main reasons why they are still not widely used in operation of process engineering systems. One approach to overcome this problem is to combine machine learning with first principles models of a process engineering system. In this work, we investigate different methods of combining machine learning with first principles and test them on a case study of multiphase flowrate estimation in a petroleum production system. However, the methods can be applied to any process engineering system. The results show that by adding physics-based models to machine learning, it is possible not only to improve the performance of the purely black-box machine learning models, but also to make them more transparent and interpretable. We also propose a step-by-step procedure for selecting a method for combining physics and machine learning depending on the process engineering system conditions.

1. Introduction

Over the past several years, machine learning risen popularity due to advances in the development of deep neural networks and computational power of hardware which allows training of such networks with millions of parameters. Major advances of machine learning applications and research are mainly related to computer vision and natural language processing, and, in some cases, the performance of the developed algorithms reaches or even exceeds the human performance (Liu et al., 2019). The success of deep learning also attracted attention of the process industry towards various machine learning models (Qin and Chiang, 2019; Shang and You, 2019) where historically models are constructed based on the first principles of physics resulting in mass, momentum and energy balances written for a system under consideration. These models are usually "transparent" meaning that the change of the model input leads to the expected change of model output because the relations between the input and output are written explicitly. However, the construction cost of these models may be high, especially if the process system is large and has a complex non-linear behavior. Also, deep understanding of the system is required to create an accurate model with a correct physical behavior. In addition, these models are often required to be tuned to the process under consideration to make accurate predictions of the estimated variable (Matzopoulos, 2011).

In contrast to first principles models, machine learning models in process engineering systems estimate variables directly from data by exploiting the ability of finding complex patterns without providing an explicit form of it. This makes machine learning models easier to construct in comparison to first principles models. However, in addition to data requirements, a major drawback of these models is their black-box nature, and making machine learning algorithms transparent is currently an active field of research (Roscher et al., 2019). In the recent review of opportunities of machine learning for process data analytics, Qin and Chiang (2019) emphasized that in order to make machine learning algorithms widely applicable for process systems, we need to incorporate first principles knowledge into machine learning algorithms, consider uncertainties and produce interpretable solutions.

In this paper, we address the issue of explainability of machine learning models through combining them with first principles models. In addition, we show how combining machine learning models with first principles can improve their accuracy. To demonstrate the performance of the proposed methods, we use a

☆ The authors gratefully acknowledge the financial support from the center for research-based innovation SUBPRO, which is financed by the Research Council of Norway, major industry partners, and NTNU. Particularly, the authors acknowledge Equinor for providing field data for this study as well as its employees Audun Faanes, Tor Kjelby and Torstein Kristoffersen for assisting with getting the data quickly.

* Corresponding author.
E-mail addresses: timur.bikmukhametov@ntu.no (T. Bikmukhametov), johannes.jaschke@ntnu.no (J. Jäschke).

https://doi.org/10.1016/j.compchemeng.2020.106834

multiphase flow estimation problem in oil and gas production systems. This case is well-suited for this purpose because multiphase flow is a complex phenomenon which is usually modeled as using first principles but can also be approached using machine learning models for some applications. In the literature, most attempts for combining first principles and machine learning models for process engineering systems in general, and oil and gas applications in particular, lead to estimation of first principles models parameters using machine learning algorithms. The history of such methods is relatively long. For instance, Psichogios and Ungar (1992) used a neural network to estimate unmeasured cell growth rate in a bioreactor process back in 90/s. For the oil and gas applications, a similar approach has been applied many times to estimate properties of an oil reservoir and multiphase flows in pipes such as permeability, porosity, rock type, reservoir fluid properties and liquid hold-up (Ahmadi and Chen, 2018; Anifowose et al., 2017; Klyuchnikov et al., 2019; Onwuchekwa et al., 2018; Kanin et al., 2019).

In this work, we do not use machine learning for estimation of first principles model parameters. Instead, we propose several other approaches to combine machine learning algorithms and first principles models. These approaches are much less investigated in the literature and there is a need to address this important issue. One example of such an approach, where, in addition to parameter estimation using a machine learning model, an approach of parallel combination of first principles models and machine learning model for a industrial hydrocracking unit was discussed by Bhutani et al. (2006). In this work, however, we enhance this approach proposing its several formulations and testing them at different system behavior and provide guidelines on which selecting the proper formulation depending on the system conditions.

As such, the main contributions of this paper are the following:

1. We propose new and enhance some of the previously reported methods of combining first principles and machine learning models and discuss advantages and disadvantages of each method (Section 2). In addition, we propose heuristic step-by-step guidelines on selecting a method for combining physics and machine learning for specific system conditions and desired accuracy (Section 6).
2. We investigate how physics-aware machine learning algorithms improve accuracy and explainability over pure data-driven estimation approaches via qualitative modeling of physical phenomena and model-agnostic feature analysis. In our case study, the analysis also shows how physics-aware machine learning models become able to reveal complex pattern behavior of the system, for instance, transient multiphase flow behavior in wells, gas condensation and release of gas from a hydrocarbon mixture (Section 5). However, we do not create a formal mathematical framework to get fully explainable machine learning models. Instead, via case study we make one step towards more transparent machine learning models by combining formal interpretability approach, machine learning and physics via a complex case study.
3. We show how consistent tuning using Bayesian optimization techniques contributes to consistent comparison of structurally different combinations of first principles and machine learning models (Sections 2.3.1 and 5).

In general, the problem of creating fully explainable machine learning is difficult, because it requires a rigorous definition of explainability, which is an ill-defined problem, because what is obvious to one person may be difficult to understand to another. Therefore, we adopt an engineering approach here in this paper, where we present different approaches for combining machine learning and simplified first principles models, and then analyze the results in terms of accuracy and feature influence. This feature importance is then analyzed and interpreted with physical systems understanding. In our case, the feature importance analysis give us new insights into the system, that are not obvious when setting up the model, as discussed in Section 5.1.2.

We believe that the results in this paper are a contribution towards the overall goal of better machine learning models. The overview of modelling approaches and the heuristic guidelines can be useful for practitioners. At the same time, it can be valuable for the research community to further test and develop methods and analyze the approaches.

The case study used in this work considers oil and gas production from a well which is a part of a petroleum production system. A typical petroleum production system consists of several main parts: a reservoir, production wells, flowlines, a processing facility, injection wells and transportation pipelines (Fig. 1). In the majority of cases, oil and gas is extracted from a reservoir in a form of a mixture and not as a single phase fluid. Often, in addition to oil and gas, formation water is present as another mixture phase. This mixture goes through production wells and flowlines to a processing facility where the phases are separated and processed. Then, water can be re-injected into the reservoir to enhance oil recovery or disposed to the environment if sufficiently cleaned. A part of the gas may also be re-injected and the remaining gas is transported together with oil for either further processing or usage as raw substances (Falcone et al., 2001). In case of an offshore platform, oil is typically transported by tankers.

Having good estimates of the produced volume of each phase (oil, gas and water) for each well allows to efficiently perform production optimization and reservoir management (Falcone et al., 2001). For instance, the reservoir model can be updated, so that water and gas re-injection strategies can be adjusted to increase overall oil production. In addition, insights about flow assurance issues can be obtained such as hydrate formation, erosion and (severe) slugging (Falcone et al., 2001; Patel et al., 2014).

A simple method to obtain the multiphase flowrates is to use test separators at the processing facility, shown in Fig. 1, by performing well testing. Here, single phase flowrates are estimated using a separator and flow meters at the separator outlets. By changing openings of a production choke of the well of interest and recording the changes of the total phase flowrate at the separator outlet, it becomes possible to estimate the rates of the well (Idso et al., 2014). This method typically produces quite accurate estimates of the flow. However, it has high operational expenses due to the production loss during the tests and requires high expertise from operating engineers. As such, such tests cannot be performed very often and usually the rates between the test are assumed to be constant which is generally not the case in practice. In addition, manipulating the production choke can often affect operation of surrounding wells which can lead to the drift of the operating points of these wells (Idso et al., 2014).

An alternative estimation method is the use of multiphase flow meters (MPFM) - hardware installations capable of estimating the flow in real time without separating the phases (Falcone et al., 2009). However, despite the ability to estimate the flow in real time, these devices are expensive and exposed to failure which introduces costly interventions, especially in offshore and subsea fields. In addition, MPFMs need to be re-calibrated by well testing from time to time due to changes of fluid properties (Falcone et al., 2001; Patel et al., 2014).

Another alternative is to create a mathematical model of the production system and estimate the flowrates by combining this model and readily available field measurements such as pressure, temperature and choke opening. This approach is called Virtual Flow Metering (VFM) and shown as a flow metering alternative in Fig. 1. A Virtual Flow Meter can work as a standalone metering solution or as a back-up system for a multiphase flow

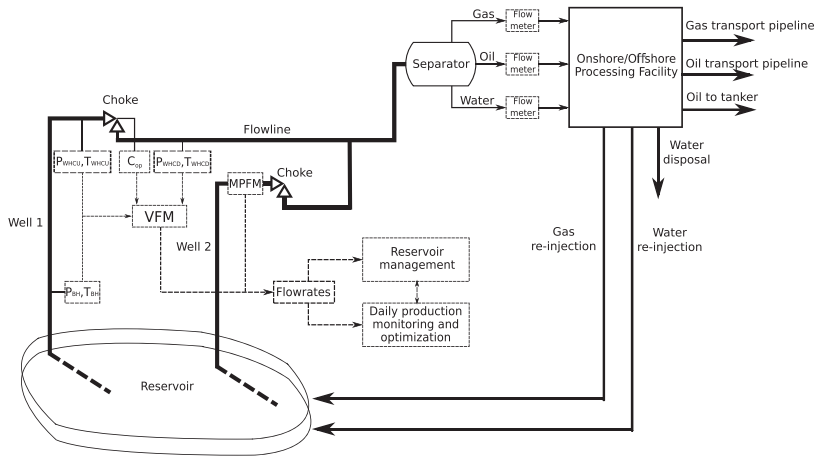

Fig. 1. Schematic representation of a typical production system with a multiphase flow meter (MPFM) and a Virtual Flow Meter (VFM) together with available measurements and typical production and processing stages. In the measurements, P denotes the pressure, T- the temperature, BH - bottomhole, WHCU - wellhead choke upstream, WHCD - wellhead choke downstream, C_{op} - the choke opening.

Table 1
Recent research work on machine learning applications for Virtual Flow Metering.

Applied algorithm	Short Summary	Reference
MLP neural network	Estimated liquid and gas rates using a neural networkensemble trained with scaled conjugate gradient and Bayesianregulation. Explored usage of meta-learners for the output layer.	AL-Qutami et al. (2018)
	Estimated gas rate with Gaussian radial basis function neuralnetwork to speed-up learning keeping good accuracy.	AL-Qutami et al. (2017)
	Estimated gas and liquid rates using multi-rate welltest data. Compared neural network with random forest.	Zangl et al. (2014)
LSTM	Estimated dynamic oil, gas and water rates for productionand severe slugging cases based on synthetic data. UsedLSTM to forecast the rates into the future.	Andrianov (2018)
	Compared LSTM with MLP neural network at steady state anddynamic conditions and showed advantages of using LSTM.	Shoeibi Omrani et al. (2018)
	Used LSTM as a model in the Kalman filter to correct biasprediction of a vanilla LSTM.	Loh et al. (2018)
	Used LSTM for multiphase flowrate estimation of transientunconventional wells data.	Sun et al. (2018)
Gradient boosting	Used gradient boosting to create a VFM as a back-up system fora MPFM. Showed how to combine the algorithm with welltest to replace MPFM. Performed sensitivity studies withrespect to the dataset size and validation methods.	Bikmukhametov and Jäschke (2019b)

meter (Lunde et al., 2013). There are two main alternatives for VFM modeling: first principles models and machine learning models (Bikmukhametov and Jäschke, 2019a). In case of first principles models, the mathematical model is constructed using laws of physics which describe the production system such as mass, momentum and energy conservation equations of the multiphase flow mixture though pipes and production choke valves. This approach requires deep domain knowledge, and the accurate models are often difficult to construct and solve numerically. In addition, due to the embedded optimization problem for parameter tuning, first principles VFM systems can perform very slowly for large production systems. However, such models are transparent and provide good overview of the processes in the production systems and the results can further be used to describe system behavior at different conditions.

In case of a machine learning model, as discussed above, deep understanding of the system behavior is not required and often the flow is estimated directly from data with no or little pre-processing. Different algorithms have been applied for machine learning Virtual Flow Metering including feed-forward neural network, gradient boosting and Long-Short-Term-Memory (LSTM) neural network. The most recent and relevant publications are summarized in Table 1. A comprehensive summary of the available literature and aspects of first principles and machine learning VFM systems is provided by Bikmukhametov and Jäschke (2019a).

Despite a reasonable accuracy of machine learning in VFM reported by the authors listed in Table 1, machine learning VFM systems, as other data-driven process engineering systems, typically provide a black-box solution which is hard to interpret. In fact, in all the mentioned works in Table 1, the authors introduce raw measurements directly into machine learning algorithms without implementing knowledge of multiphase flow physics. This is one of the main reasons why machine learning VFM systems are still rarely used in practice (Bikmukhametov and Jäschke, 2019a). To overcome this problem, we will investigate how different combinations of machine learning algorithms with first principles may improve accuracy and explainability of data-driven Virtual Flow Metering models.

This paper is organized as follows. In Section 2, we start with descriptions of the proposed methods, continue with machine learning algorithms description and the procedure for its tuning. In Section 3, we describe the system which is modeled by the methods investigated in this work as well as show how exactly these methods are adopted to Virtual Flow Metering. In Section 4, we describe case studies selected for investigation. In Section 5, we discuss the obtained results using the proposed methods. In Section 6, we summarize the most important points from Section 5 and propose a step-by-step procedure for selecting a method to combine first principles and machine learning depending on different conditions. Finally, in Section 7, we make conclusions from our work.

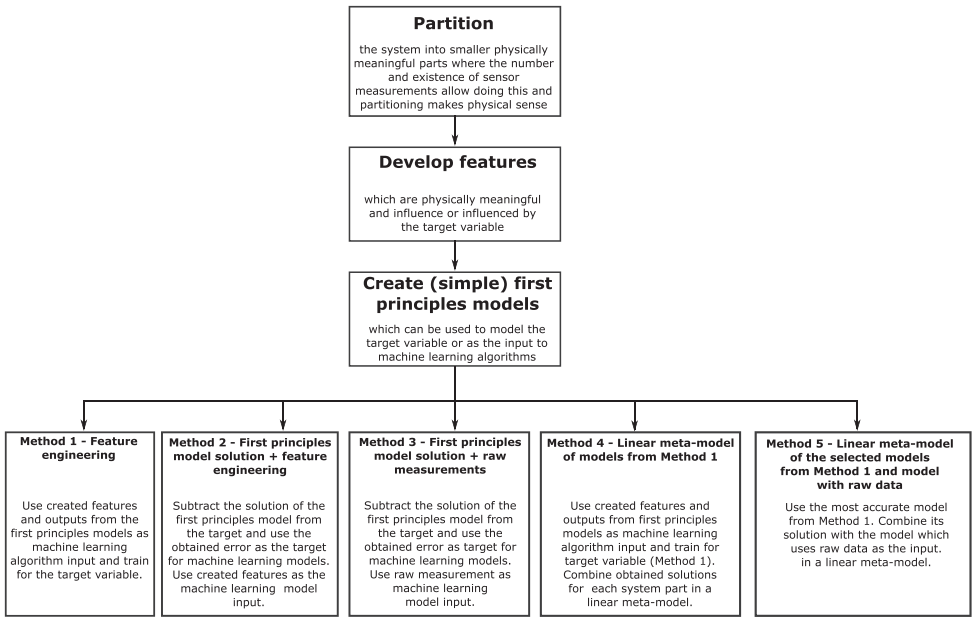

Fig. 2. Overview of the proposed combinations of first principles and machine learning models and main steps of their development for any process engineering system.

2. Methods

In this section, we describe the proposed methods for combining machine learning with first principles models and the machine learning algorithms which are used to implement the methods. We also discuss which parameters of the algorithms are tuned as well as the tuning procedure which is implemented using Bayesian Optimization approach.

2.1. Proposed methods for combining first principles and machine learning

2.1.1. Introduction to the proposed methods

Up to now, in machine learning Virtual Flow Metering solutions reported in the literature, the measurements of pressures and temperatures available in the system have been used directly as input features without advanced transformations (Zangl et al., 2014; AL-Qutami et al., 2017; 2018). Apart from that, in some cases, complex structures have been used in order to create a model, for instance, simulated annealing combined with different types of learners within one algorithm (AL-Qutami et al., 2018). This makes the results from the obtained model even more unexplainable than a plain neural network.

To contribute to the improved explainability and accuracy of machine learning models for process engineering systems in general and petroleum production systems in particular, we propose and test several different methods. The short summary of the methods is shown in Fig. 2.

First, we propose to partition a big system under consideration into small physically meaningful parts. In this context, it means that the part may represent a part of the system, process or equipment whose parameters influence the target variable. Please note, that this action makes sense when it is viable physically and the number and existence of sensors allow doing this. Then, physically meaningful features should be developed which may include combinations of the original raw measurements alone or with external data which can be generated based on the process knowledge. In addition, simple first principles models may be constructed which are able to estimate the target variable at least qualitatively. In this work we do not assume that the first principles models can be build easily for the system under consideration. In many cases it is difficult or impossible to do due to the complexity. However, we do assume that the first principles models can be simplified to the level of abstraction which is enough for the machine learning model to understand the qualitative behavior of the system, when combined with the simplified first principles model. Then, the obtained features and models are used in several proposed methods. In Section 2.1.2, we describe each method in more detail, but in general, all of proposed methods give an opportunity to evaluate each model separately, which makes it easier to interpret the simulation result and the model behavior. In addition to the explainability advantages, it helps to create more accurate solutions than using raw data directly. This is because the main task for a machine learning model is to reveal how to combine the given features using the model parameters, for instance, weights of a neural network, to accurately estimate the target. However, if we directly introduce the way how original raw measurements should be combined based on known physics of a process, we reduce the feature space and possibly create features which contain more information about the target variable. Below, we provide the description of each method.

2.1.2. Detailed description of the proposed methods

Method 1 - Feature engineering. Feature engineering is a well-known method for constricting machine learning models, so, in this work, we propose the guidelines on how this method may be applied to get accurate and explainable results in physical process systems. The proposed approach includes creating physically meaningful features instead of using raw measurements directly. By physically meaningful features we mean combinations of the original raw measurements alone or with external data which can be generated based on the process knowledge. Preferably, the designed features should be well-interpretable, self-explanatory and related to a particular system part. At the same time, the fea-

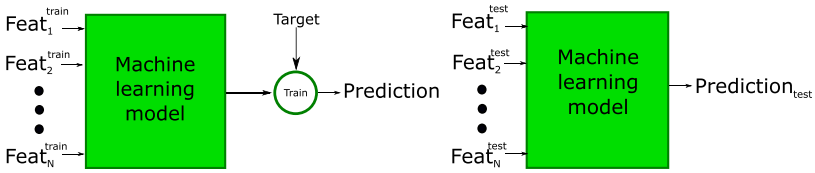

(a) Training phase of Method 1 (b) Test phase of Method 1

Fig. 3. Training and test procedures for Method 1 - feature engineering.

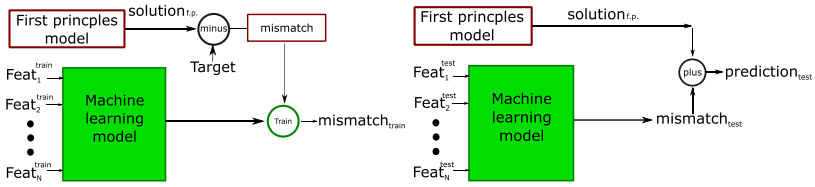

(a) Training phase of Method 2 (b) Test phase of Method 2

Fig. 4. Training and test procedures for Method 2 - first principles model solutions and feature engineering.

tures should not necessarily be complex, but must contain some information about the target variable. The form and parameters included in the features will be case dependent and rely on expert domain knowledge. The general schematic representation of the training and test phases for feature engineering method is shown in Fig. 3.

Physically meaningful features may be further divided into simple features and complex first principles features. Simple features are the ones which are linear or non-linear combinations of the raw measurements. The complex first principles features may be, for instance, features represented as a solution of the equation which aims to model the target variable using the raw measurements and external data extracted using the process knowledge. In Section 3.3, we provide examples of features of the oil and gas production system.

Method 2 - First principles model solutions and feature engineering. In this method, we use solutions from the developed first principles models for each part of the process system. The obtained solutions are then subtracted from the true value of the target variable, such that we obtain the mismatch between the developed model and the actual value of the target. Then, this error is used as a target variable for a machine learning model. In this method, we again use created features as the input to the machine learning model to train the model to cover the mismatch.

The hypothesis here is that the obtained solution from the first principles model does not explain the system behavior, so that the created features are still well-correlated with the target variable (mismatch). As a result, by using them as the input machine learning features, we aim to learn the residual pattern of the system behavior. Fig. 4 summarizes the details of Method 2.

Method 3 - First principles model solution and raw measurements. This method is similar to Method 2. The major difference is that we use raw measurements from the system as the input to the machine learning models with the aim to explain the mismatch between the first principles model solution and the true target value.

The hypothesis in this method is that the obtained mismatch between the first principles model solution and the target does not contain the information which can be described by simple or complex first engineered features. For instance, it can be the case when some hidden patterns/disturbances exist in the system and is not covered by the proposed physical relationships implemented. If so, this method might work better than Method 2, in which we use the first principles features as the input to the algorithm aiming to cover the mismatch. Fig. 5 shows the details of Method 3.

Method 4 - Linear meta-model of models with created features. In this method, we combine solutions from models created in Method 1 using a linear meta-model. The idea here is to give a weight to the prediction from each model of a particular system part, for instance, choke and tubing, and then sum the weighted predictions to get the final outcome. The weights for each submodel are tuned using linear regression techniques, such that the weighted sum of the sub-models accurately describe the system.

The hypothesis here is that at certain conditions a particular model can produce better results than another model. If so, the output from this model multiplied by the associated weight will have a closer value to the target than another model. By combining the solutions from several models, we can take the advantage each model and obtain the solution which is more accurate then the solution from a single model. The schematic representation of the training and test phases for Method 4 is shown in Fig. 6.

Method 5 - Linear meta-model of the selected model with created features and model with raw data. In this method, we combine the solution of any of the models obtained using Method 1, i.e. the model with the created features, with the model which uses the raw data as features.

The hypothesis here is that even by obtaining the best model using the created features, there is still some unrevealed data structure which cannot be described by the model while the raw data model can do it, at least partially. As such, the combined solution will be more accurate than both the best feature engineered model and the model with raw input data. Fig. 7 shows the details of Method 5.

In some cases, one may argue that one specific model will be more accurate and another model will make the overall prediction worse. However, we do not give these weights just by assigning them, they are learned from the data which means, on average, the predictions from such a model will most likely be better on the new test set. This idea is similar to a normal linear regression case. For a particular point in space one value of weight can be better because then the line will go exactly thorough one particular point. However, this mostly likely not be beneficial for other points. As such, the proposed method is simply linear regression, but instead of features, we are giving model values, which on av-

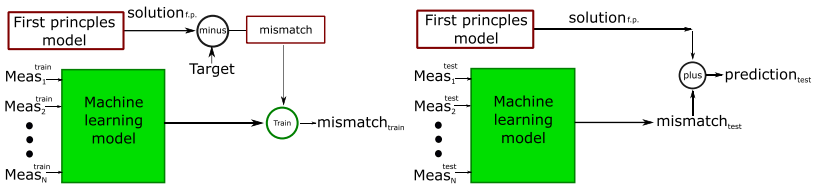

(a) Training phase of Method 3 (b) Test phase of Method 3

Fig. 5. Training and test procedures for Method 3 - first principles model solutions and raw measurements.

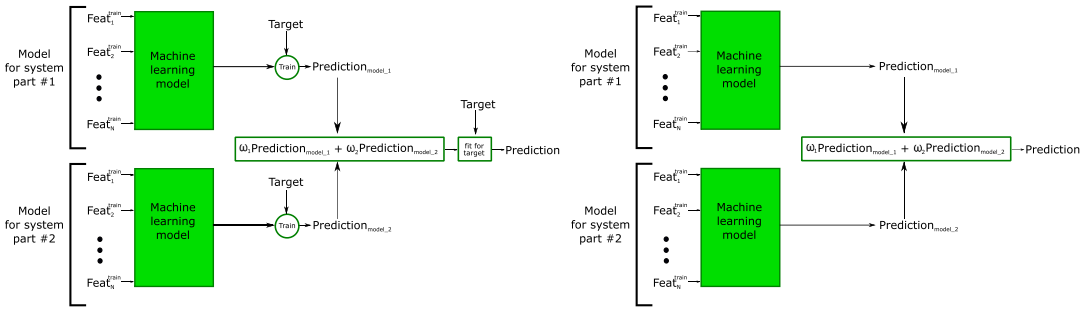

(a) Training phase of Method 4 (b) Test phase of Method 4

Fig. 6. Training and test procedures for Method 4 - linear meta-model of models with created features.

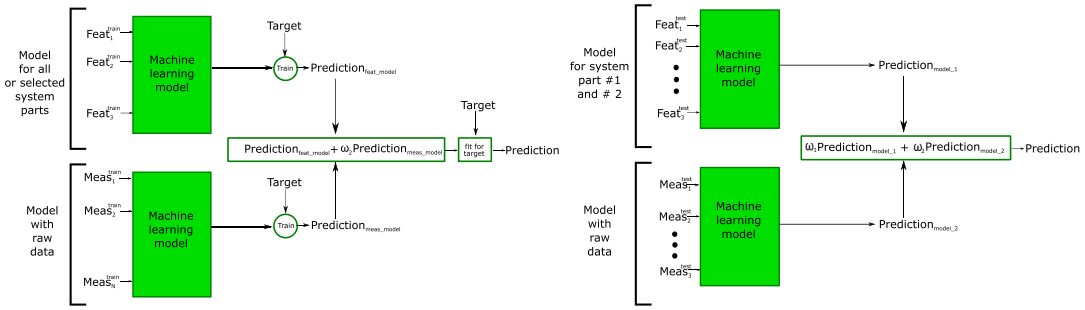

(a) Training phase of Method 5 (b) Test phase of Method 5

Fig. 7. Training and test procedures for Method 5 - linear meta-model of the selected model with created features and model with raw data.

erage will produce more accurate predictions on the test set. In an ideal case, one would want to have adaptive weights which know that for this particular point it needs to use this particular model is better and we just need to choose that model. However, this is another direction of research and will not be covered in our paper.

2.2. Applied machine learning algorithms

In this section, we provide a brief overview of the machine learning algorithms used in this paper, namely Gradient boosting, Multilayer Perceptron and Long-Short Term Memory Neural Networks. More specifically, we describe the selected hyperparameters and its tuning and the role in the model training and predictive capabilities.

2.2.1. Gradient boosting and tuned parameters

The first algorithm used for machine learning VFM in this work is gradient boosting with regression trees implemented in XGBoost package (Chen and Guestrin, 2016). Gradient boosting is based on sequential construction of shallow regression trees which form an ensemble and perform the final value estimate as a sum of the trees' predictions (Friedman, 2001). In XGBoost implementation, the algorithm minimizes the following objective function in an iterative manner adding a regression tree at each iteration:

$$J = \sum_{i=1}^{N} (y_i - [\hat{y}_i^{(t-1)} + f_t(x_i)])^2 + \Omega(f_t) \tag{1}$$

with

$$\Omega(f_t) = \gamma Z + \frac{1}{2}\lambda_{GB}\|w\|_2^2 \tag{2}$$

where y_i denotes the true value of the $i-th$ example, $i-$ the index of a training example, $t-$ the number of the currently constructed regression tree, $N-$ the number of examples in the training set, $\hat{y}_i^{(t-1)}-$ the sum of the $t-1$ trees, f_t- the prediction of the current tree on the $i-th$ example, $\Omega(f_t)-$ the regularization term, $\gamma-$ the penalty term for the model complexity expressed as the number of leaves Z, $\lambda_{GB}-$ the penalty term of the weight values w.

Table 2
Hyperparameter space and other parameters used for machine learning algorithms training.

Algorithm	Hyperparameter	Range (oil rate)	Range (gas rate)	Other parameters/concepts	Approach
Gradient boosting	maximum tree depth	[3:12]	[3:9]	Splitting algorithm	Greedy linear search
	regularization λ	[0.001:0.1]	[0.0001:0.1]	Maximum number of trees	200
	regularization γ	[0.001:0.1]	[0.0001:0.1]	Framework	XGBoost
	minimum child weight	[1:3]	[1:4]		
MLP neural network	learning rate	[0.0001:0.001]	[0.0001:0.001]	Activation function	ReLU
	regularization	[0.00005:0.005]	[0.00005:0.05]	Optimization algorithm	Adam
	number of layers	[1:5]	[1:5]	Maximum number of epochs	1000
	number of nodes	[5:25]	[10:30]	Framework	Tensorflow
LSTM	learning rate	[0.0001:0.01]	[0.0001:0.01]	Activation function	tanh
	window size	[1:15]	[1:15]	Optimization algorithm	Adam
	dropout rate	[0.05:0.2]	[0.05:0.2]	Maximum number of epochs	3
	number of LSTM units	[10:40]	[10:40]	Framework	Keras
	number of LSTM layers	[1:3]	[1:3]		

The algorithm minimizes the difference between the sum of all the previous predictions and the true value by adding a new tree. To manipulate the training of gradient boosting, we tune the maximum depth of regression trees which is responsible for the complexity of the function which algorithm is able to approximate. In addition, we tune regularizing coefficients γ and λ_{GB} to prevent overfitting as well as the "minimum child weight" parameter which identifies the minimum number of instances required in each node to become a split. The larger the "minimum child weight", the more conservative the algorithm becomes (Chen and Guestrin, 2016). By adjusting these parameters, we try to find a good trade-off between the bias and variance of the model and strengthen generalizing capabilities on unseen data. Table 2 summarizes the hyperparameters and its ranges used for tuning.

2.2.2. MLP Neural network and tuned parameters

Feed-forward (Multilayer Perceptron (MLP)) neural networks are one of the most popular types of artificial neural networks in machine learning (Goodfellow et al., 2016). They are constructed using neurons which are interconnected with weights and stacked in layers. The weights are used in order to fit the algorithm to the data which is typically done via backpropagation algorithm and gradient-based optimization method (Rumelhart et al., 1988) which usually minimizes the following objective function:

$$J = \frac{1}{N}\sum_{i=1}^{N}(\hat{y}_i - y_i)^2 \tag{3}$$

where i denotes the index of a training example, $N-$ the number of training examples in the training set, $\hat{y}_i-$ the estimated value of the $i-th$ example, y_i- the true value of the $i-th$ example.

A feed-forward neural network is a universal approximator (Hornik et al., 1989) which means that it can approximate any function given sufficient structural complexity. To approximate nonlinear functions, neural networks use an activation function in each neuron. Among other alternatives, ReLU activation function is a popular choice for feed-forward neural network regression (Agarap, 2018) because it does not suffer from exploding and vanishing gradients, so we also use it in this work. Despite the advantage of strong approximating abilities, a neural network can easily overfit the training data which will create high variance on unseen data. As such, often the objective function in Eq. 3 is adjusted with a regularization term:

$$J = \frac{1}{N}\sum_{i=1}^{N}(\hat{y}_i - y_i)^2 + \lambda_{NN}\|w\|_2^2 \tag{4}$$

where λ_{NN} denotes the regularization coefficient, $\|w\|_2^2-$ the l_2-norm of neural network weights.

In this work, we use the objective function as shown in Eq. (4) and consider the regularization coefficient λ_{NN} as a hyperparameter to be tuned. As in the case with gradient boosting, by tuning the regularization coefficient, we aim at finding a good trade-off between the bias and variance of the model and avoid overfitting to the data noise.

To minimize the cost function J in Eq. (4), we use the "Adam" gradient based optimization algorithm (Kingma and Ba, 2014). Despite the fact that the learning rate is proposed to be adaptive in Kingma and Ba (2014), in this work, we use it as a tuning hyperparameter to find a good initial guess of the learning rate for the algorithms. In addition, we also try to find the best architecture of the network, so we also tune the number of layers and neurons simultaneously with the learning rate and regularization coefficient. Table 2 summarizes hyperparameters of neural networks and its ranges used for tuning.

2.2.3. LSTM Neural network and tuned parameters

Long-Short-Term-Memory is a special type of recurrent artificial neural networks which is designed for sequential type of data such as speech and text (Hochreiter and Schmidhuber, 1997). In terms of regression for Virtual Flow Metering, the sequence of data is a series of measurements in time. So, by using an LSTM for modeling of the time dependent target, we use past measurements of pressure and temperature in order to predict the flow at the current time step. As such, one of the goals in using LSTM in this study is to evaluate how the sliding window approach which considers the past data can help in improving the current time step estimates. In previous works on using LSTM for VFM, this important parameter has not been investigated (Loh et al., 2018; Sun et al., 2018).

There are different possible configurations of LSTM such as many(inputs)-to-many(outputs), many-to-one or one-to-many. In this work, we use many-to-one configuration, such that several input units (measurements back in time) are used in order to estimate the oil and gas flowrates respectively, at the current time step. As such, one of the hyperparameters of the network is the time window that is the number of time steps in the past which are used for the current estimate. The number of time steps is then equal to the number of cells in a LSTM layer.

An LSTM neural network may consist of several layers, which is also the case for this work, and the layers have many-to-many connections. We tune the number of LSTM layers because it directly influences the possible complexity of the function which the network is able to approximate.

Greff et al. (2016) showed that, in addition to the number of layers and cells in the LSTM layer, it is also important to tune the learning rate in LSTM networks to achieve good performance, so we include it as a tuning hyperparameter. To regular-

ize LSTM and prevent overfitting, in the extensive LSTM tuning by Greff et al. (2016) it was proposed to use input noise instead of using ridge regularization as we do in the feed-forward (MLP) neural network case (Eq. 4). However, to experiment with more tuning parameters and regularization techniques, we use dropout (Cheng et al., 2017) on the weights which connect the last LSTM layer and one dense layer which computes the final estimates of the flowrate. The range of the LSTM hyperparameters and other parameters are shown in Table 2.

2.3. Hyperparameter tuning and comparison procedure of case studies

To be successfully applied to any data, machine learning algorithms have to be well tuned. By this, we mean that a good algorithm architecture has to be selected as well as the values of these hyperparameters have to be tuned accurately. This is typically one of the most difficult and critical parts of machine learning modeling. We need to find a good "bias-variance trade-off" (Hastie et al., 2005) meaning that the model that has small bias and variance on the training set must have comparable bias and variance on the test set, so it has good generalizing capabilities.

In general, it can be difficult to compare different algorithms in a fair manner, because it is possible to give one algorithm (or method) an advantage by making a more accurate tuning than for another one if desired. In our case, in addition to have 3 algorithms to compare, we also have 12 cases for each algorithm (Section 4). To produce accurate and trustworthy results, we developed a pipeline for training and evaluation the methods which is designed not to give an advantage to any case or algorithm. This pipeline uses Bayesian optimization for algorithms tuning as a core and searches the hyperparameters over the same space for all the cases for the same machine learning algorithm. In the next sections, we present the main concept behind Bayesian optimization and the developed tuning pipeline.

2.3.1. Bayesian optimization

Bayesian optimization is a suitable concept for optimizing a function which is computationally expensive to evaluate (Frazier, 2018). Typically, this function does not have an analytical expression and can be a black-box which gives output values for a given input. The idea behind Bayesian optimization is to create a surrogate model of the objective function with corresponding uncertainties using Gaussian Processes regression. Gaussian Processes is a Bayesian machine learning method that is why this optimization approach is called Bayesian. Using this approach, the algorithm decides where to evaluate the function next, given the observed objective function values and corresponding uncertainties (Frazier, 2018). This problem is known as the "exploration-exploitation" trade-off (Berger-Tal et al., 2014).

To describe Bayesian optimization in more detail, let us define the function to be optimized as $f(x)$. Here, $x \in \mathbb{R}^d$ is the function input where d is the dimension of the input space. In case of hyperparameter optimization for a machine learning algorithm, $f(x)$ can be an error function on a validation set and d is the number of hyperparameters, for instance, $d = 2$ if we tune the learning rate and regularization coefficient. Let us further assume that we have already evaluated the objective function at $x_{1:n}$, where n is the number of evaluated points. Our goal is to find such x^*, so that it gives the maximum (in case of hyperparameter optimization - minimum) of the function at x given $x_{1:n}$, i.e.:

$$x^* = arg\max_x(-f(x|x_{1:n})) \tag{5}$$

By solving Eq. (5), we find the set of hyperparameters which minimizes the error on the validation set. However, the only way to evaluate $f(x)$ is to give input x to the black-box function and obtain output, so that we cannot simply evaluate gradients for finding descent direction of the function.

To solve this problem, we use the concept of Gaussian Processes regression. First, we specify a normal prior distribution (typically with zero mean) over the entire parameter space $\mathbb{R}^{N \times d}$, such that:

$$f(x_{1:N}) \sim \mathcal{N}(0, K(x_{1:N}, x_{1:N})) \tag{6}$$

where $K(x_{1:N}, x_{1:N})$ denotes the covariance between the points $x_{1:N}$ and $N-$ the number of parameter values.

Then, given the observed values $f(x_{1:n})$, we compute the mean and variance of the posterior distribution of the function $f(x)$ using the following expression for Gaussian Processes regression (Rasmussen and Williams, 2017):

$$\mu_n(x) = K(x, x_{1:n})K(x_{1:n}, x_{1:n})^{-1} f(x_{1:n}) \tag{7}$$

$$\sigma_n(x)^2 = K(x, x) - K(x, x_{1:n})K(x_{1:n}, x_{1:n})^{-1}K(x_{1:n}, x) \tag{8}$$

If at this point we were required to provide the best set of hyperparameters, we would say that this is x^* which gives $f_n^* = max(f(x_{1:n}))$. However, if we are allowed to take one more sample anywhere in the hyperparameter space, we can check if we can find a better set. After the new sample, the highest value of the function can be $f(x)$ in case $f(x) \geq f_n^*$ or it is going to be still f_n^*. As such, the possible improvement of the function is $f(x) - f_n^*$. Therefore, we want to make a new evaluation at x which produces the largest improvement. However, the challenge is that we do not know the value $f(x)$ until we take a sample of it. In this case, the solution is the fact that we can take the *expected value of this improvement* (Frazier, 2018):

$$EI_n(x) = E_n[f(x) - f_n^*] \tag{9}$$

where $EI_n(x)$ denotes the expectation of the posterior distribution given the values of $f(x_{1:n})$.

Finally, we take a new sample where $EI_n(x)$:

$$x_{n+1} = arg\max_x EI_n(x) \tag{10}$$

The sampling stops when the specified number of sampling steps is reached. This optimizing strategy (acquisition function) is called Expected Improvement and this is what we use in this work to find an optimal set of hyperparameters for the machine learning algorithms. Further details about how to compute the closed form of the acquisition function in Eq. (9) are provided by Frazier (2018).

2.3.2. Tuning pipeline

To tune the algorithms, first, we need to split the data into training, validation and test parts. Since we have time dependency in the data, we perform k-fold cross-validation with mixed folds. Since we perform an extensive hyperparameter optimization search for many cases, we cannot use nested k-fold cross-validation because it is computationally too costly. As such, we split the data into 60% for training, 25% for validation and 15% for test sets and use only one set to validate the algorithms.

Another challenge is to choose how to perform fine tuning of epochs and trees together with other hyperparameters. The procedure we propose is to fix a certain number of epochs/trees which corresponds to a relatively deep training. Then, for this fixed number, we select hyperparameters using Bayesian optimization based on the validation set error. Then, using the obtained set of hyperparameters for each algorithm, we perform fine tuning of the number of epochs/trees using early stopping by monitoring the error on the validation set. The same hyperparameter space is used for all the cases within one algorithm.

Having the algorithm ready, we re-train it on the combined training and validation sets by taking advantage of all the data

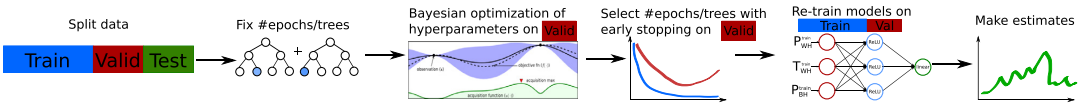

Fig. 8. Proposed pipeline for algorithms tuning and case comparison.

available for training and finally evaluate it on the test set. A summary of the proposed tuning pipeline is shown in Fig. 8. Table 2 shows hyperparameters and their range used in the tuning pipeline.

Note that the procedure above is designed such that we:

- Do not give any preference to any particular case and any particular algorithm;
- Select a good set of hyperparameters via extensive Bayesian optimization search;
- Avoid overfitting via early stopping and regularization;
- Allow another possibility for overfitting control by changing the hyperparameter space boundaries.

2.4. Feature analysis methods

Machine learning algorithms are often treated as black-box solutions which are hard to interpret. In this work, we investigate if features which are based on physics principles can contribute to a better understanding of machine learning models behavior.

There are several methods which can be used to interpret machine learning models. A good review of these methods is provided by Molnar et al. (2018). For non-linear models, the methods can be divided into model-specific and model-agnostic methods. For instance, tree-based algorithms such as gradient boosting and random forest have embedded model-specific methods which evaluate feature importance based on the selected criteria (Chen and Guestrin, 2016; Genuer et al., 2010). However, sometimes, different criteria produce different feature importance for the same algorithm, which can make results confusing.

As we compare different algorithms in this work and also aim to avoid misleading conclusions within each algorithm, we use model-agnostic approach for evaluation of feature importance. This means that such methods are applicable to any machine learning model and use the same principles independently of the algorithm under evaluation. This will allow us to compare different algorithm using the same principles, so the conclusions can be well generalized. We use the feature importance and partial dependence plots implemented in Skater Python library (Kramer et al., 2018). In this package, feature importance evaluation is based on the theoretic information criterion which estimates the entropy of the prediction change supplied by a perturbation of a feature. The partial dependence plots are adopted from Hastie et al. (2005), and describe the global influence of a particular feature given that other features are kept constant. As such, both methods are global interpretation methods, so that they analyze the influence of features over the entire dataset, rather than explaining the local behavior as, for instance, LIME method does (Ribeiro et al., 2016). We use global interpretation because, in this work, we are interested in the overall relationships between the features and the targets. However, local interpretations may also be useful for Virtual Flow Metering, for instance, when the flow pattern is changed and we are interested in the analysis of the conditions at which it happens. We keep these local investigations for future work.

We applied the methods discussed above to gradient boosting and feed-forward neural networks, but have not applied to the LSTM networks due to its dependency on a particular feature in time. Such analysis has not been implemented yet neither in the package nor by us, so we also keep this analysis for future work too.

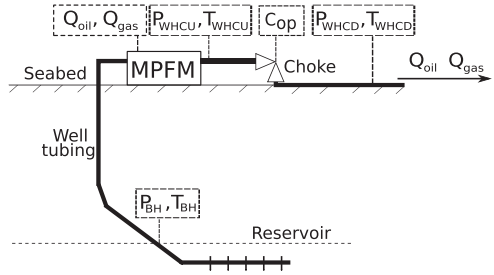

Fig. 9. Schematic representation of the investigated system with available measurements.

3. Description of the system and data

3.1. System and data

3.1.1. Overview

To test the proposed approaches, we use field data from one of the subsea fields on the Norwegian Continental Shelf. The system and the available measurements are shown in Fig. 9. For the input to the algorithms, the following data is available:

- Pressure and temperature at the bottomhole of the well (P_{BH}, T_{BH});
- Pressure and temperature upstream of the choke (P_{WHCU}, T_{WHCU});
- Pressure and temperature downstream of the choke (P_{WHCD}, T_{WHCD});
- Choke opening (C_{op});
- Well tubing length (L_{tubing});
- Well tubing diameter (D_{tubing});
- Fluid composition.

In this system, a multiphase flowmeter (MPFM) is installed at the wellhead which measures oil and gas flowrates, Q_{oil} and Q_{gas} respectively. The measurements of pressures, temperatures, choke opening and flowrates are available at every minute. The length and diameter of the tubing are fixed by the system design and do not change during operation. The data available for training is the historic production for 210 days and shown in Fig. 10. As we see in Fig. 10, the system has a very unstable behavior during the entire production time. The flowrates of oil and gas fluctuate a lot which makes difficult it for a machine learning algorithm to estimate it accurately.

We will construct machine learning algorithms based on the flowrate measurements from the meter, so that the machine learning model will work as a back-up system. If the multiphase flowmeter fails or starts producing unrealistic results, the VFM solution will infer the current flowrates. As such, the target variables for training are (Fig. 10):

- Oil flowrate (Q_{oil});
- Gas flowrate (Q_{gas}).

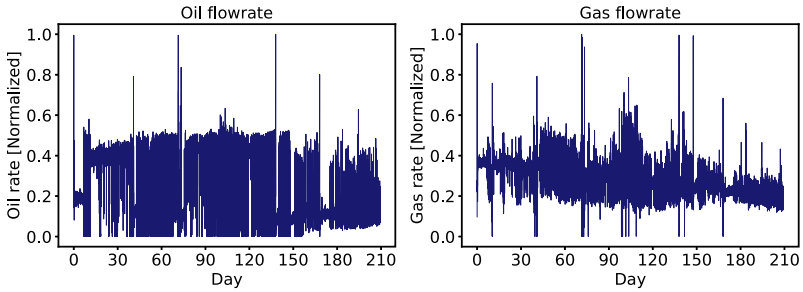

Fig. 10. Normalized oil and gas flowrates from the subsea well under consideration.

In oil and gas production operation, the fluid composition is not always available. In the dataset used in this work, the fluid composition is given, however, this information is assumed to be very unreliable, because it comes from measurements that were taken a long time ago, and the composition may have changed over time. As such, the fluid properties estimated using this composition can be misleading and give a noticeable estimation error. Therefore, we would like to avoid using estimates of fluid properties such as density or viscosity as much as we can in the first principles models, while maintaining the qualitative physical behavior of the created models.

In practice, there may be a possibility to re-estimate the fluid properties given a new Gas-Oil-Ratio (GOR) by performing a new well test, however, this information is not available in our setting. However, it is useful and interesting to investigate predictive capabilities of physics-aware machine learning algorithms under these realistic conditions.

3.2. Applied first principles models

In this section, we introduce the first principles models which are used in combinations with machine learning algorithms using the proposed methods discussed in Section 2.1. To create a combined Virtual Flow Metering systems with machine learning and physics of the multiphase flow in petroleum systems, we propose to use two first principles models: Bernoulli model for choke and No-Pressure-Wave drift flux model for tubing.

3.2.1. Choke model

The Bernoulli equation is often used to describe single phase flow in hydraulic systems and it is the basis for the simplest model used to describe fluid flow over a choke. The equation describes the fluid momentum between two points:

$$P_1 - P_2 = \frac{\rho}{2}(U_2^2 - U_1^2) \tag{11}$$

where P_1 denotes the pressure at point 1, P_2 - the pressure at point 2, ρ - the fluid density, U_1 - the fluid velocity at point 1, U_2 - the fluid velocity at point 2.

Typically, a choke is modeled as a sudden contraction which is called choke throat. In this case, Eq. (11) is applied between the point before the throat (point 1) and at the throat (point 2). Considering the fact that the volumetric flowrate $Q = A \cdot U$, we obtain:

$$Q = C_d A_2 \sqrt{\frac{2(P_1 - P_2)}{\rho\left(1 - \left(\frac{A_2}{A_1}\right)^2\right)}} \tag{12}$$

where C_d denotes the discharge coefficient, A_1– the pipe cross sectional area before the choke, A_2–the area of the choke throat.

The discharge coefficient C_d is typically a function of the choke opening C_{op}, and used to tune the model to the data at hand. Because measuring pressure at the choke throat is difficult, pressure measurement after (downstream) the choke is often considered as P_2. As such, according to the introduced notation in Figs. 1 and 9, $P_1 = P_{WHCU}$ and $P_2 = P_{WHCD}$.

Eq. (12) is valid for single phase flow. To apply this to a multiphase flow case, the single phase flowrate is usually multiplied by a two-phase multiplier, for instance, the Chisholm multiplier (Chisholm, 1983) which depends on the fluid properties at measured conditions. Because the fluid properties may change over time, and a two-phase multiplier as well as mixture density may be inaccurate in this case, we will not introduce two-phase multiplier into the choke model and will use the model outputs as computed below.

In addition, the mixture density ρ_{mix} must be introduced instead of single phase density ρ. The ratio A_2/A_1 can be considered as the choke opening (C_{op}) because A_1 is the constant area of the pipe and A_2 is changing depending on how open the choke is. As the discharge coefficient C_d is a function of the choke opening which form we do not necessarily know, we simplify it by assuming a linear relationship. Considering this, we obtain a simple expression for the mixture volumetric flowrate across the choke Q_{mix}^{choke} which is used in this work:

$$Q_{mix}^{choke} = C_{op} A_2 \sqrt{\frac{2(P_{WHCU} - P_{WHCD})}{\rho_{mix}\left(1 - C_{op}^2\right)}} \tag{13}$$

Finally, by multiplying Q_{mix}^{choke} with volumetric fraction of a fluid phase (for instance, oil), we can obtain the phase volumetric flowrate. The remarks on how the volumetric fractions are found are discussed in Section 3.2.3.

3.2.2. Tubing model

For the tubing model, we use a "No-Pressure-Wave" form of the drift flux multiphase flow model (Masella et al., 1998) which is described by the following equation:

$$\frac{dP}{dl} = \frac{\xi_{mix}\rho_{mix}U_{mix}^2}{2D_{tubing}} + \rho_{mix} g \sin(\beta) \tag{14}$$

where P denotes the fluid pressure, l– the pipe axial coordinate, ξ_{mix}– the friction factor coefficient, U_{mix}– the mixture velocity, D_{pipe}– the tubing diameter, ρ_{mix}– the mixture density, g– the

gravitational acceleration constant, $\beta-$ the inclination angle of the pipe.

This equation is a simplification of the transient drift flux model (Masella et al., 1998). Here, it is assumed that the flow is at steady state and that the effect of acoustic waves is negligible for the considered time scale. We can solve this equation given the pressures at the bottomhole and the wellhead and the fluid properties for the mixture. The same as for the choke model, the fluid properties can be the bottleneck for accurate predictions of the flow due to it is potential inaccuracy. Moreover, the friction coefficient is also dependent on them. As such, to avoid additional source of inaccuracy, we keep the friction coefficient constant.

Typically, Eq. (14) is solved numerically together with the mass balances for each phase in each discretization mesh point along the pipe axial coordinate. In this work, we test simplified first principles modeling approaches and want to use machine learning to take care of the model inaccuracies. As such, by averaging the fluid properties and the geometry over the pipe axial direction and integrating Eq. (14), the solution for the multiphase mixture in tubing becomes:

$$Q_{mix}^{tubing} = \sqrt{\frac{(P_{BH} - P_{WH} - \bar{\rho}_{mix} g H)\pi^2 D_{tubing}^5}{8\xi_{mix} L_{tubing} \bar{\rho}_{mix}}} \tag{15}$$

with

$$\bar{\rho}_{mix} = \frac{\rho_{mix@WH} + \rho_{mix@BH}}{2} \tag{16}$$

where P_{BH} and P_{WH} denote bottomhole and wellhead pressure respectively, $\rho_{mix@WH}$ and $\rho_{mix@BH}-$ the mixture density at the wellhead and bottomhole conditions respectively, $H-$ the height (elevation) of the tubing, $L_{tubing}-$ the tubing length, $\xi_{mix}-$ the friction factor coefficient, $\beta-$ the inclination angle of the tubing.

3.2.3. Remarks on fluid properties computation for first principles models

We see that even the simplest process models require accurate measurements and fluid properties data to compute the flowrate accurately. As discussed, in our case, the fluid properties can be relatively inaccurate because the composition is provided at the beginning of production when the system was installed, while the production data is at the late stage. This is exactly the place where machine learning can enter and solve the problem with less effort. As we still need some approximations of the fluid properties, we use the given (uncertain) fluid composition and Soave-Redlich-Kwong (SRK) Equation of State (EoS) (Soave, 1972) implemented in a commercial thermodynamic package. To obtain the phase volumetric fractions and densities, we use simple flashing. We iterate over the pressure and temperature condition range met in the problem, save the results in look-up tables and then interpolate the properties for any given pressures and temperatures at any time step. This approach is commonly used in first principles simulators of multiphase flow.

3.3. Adaptation of methods for combining machine learning and first principles for VFM

In this section, we discuss how the developed first principles models and features are used within the methods proposed in Section 2.1. The overall summary of the used features for the input in each method and case study can be found in Table 3 in Section 4.

Please note, that all the developed models in this work use a single output, such that we estimate only one target variable each time. As such, we constructed separate models for oil and gas rates. From our experience, making separate models for oil and gas (i.e. for different outputs) produces better results and allows much more flexible tuning. On the other hand, neural networks also allow multiple output regression without any single problem. As for gradient boosting, in this case, two separate algorithms are always needed.

3.3.1. Adaptation of method 1 - feature engineering

As discussed, we partition the system into the tubing and choke parts and create the following features:

- Pressure drop over the choke ($\Delta P_{choke} = P_{WHCU} - P_{WHCD}$);
- Pressure drop over the tubing ($\Delta P_{tubing} = P_{BH} - P_{WHCU}$);
- Temperature drop over the choke ($\Delta T_{choke} = T_{WHCU} - T_{WHCD}$);
- Temperature drop over the tubing ($\Delta T_{tubing} = T_{BH} - T_{WHCU}$).

Despite being simple, these features have direct relationships with the target variables - the oil and gas flowrates. This is because in any process system, pressure difference is the main driving force for the flow to go from one point to another. As such, pressure drop over the well tubing and choke can be a good indicator of the flow magnitude. At the same time, the flow magnitude and disturbances is what define the temperature drop over the tubing and choke. In terms of explainability, these features make more sense than raw pressure and temperature measurements which can be hard to interpret with respect to the change of the target variable (flowrate).

As we propose in Fig. 2, we can also use outputs from the created first principles models as input features to machine learning models. As such, we use the following additional features:

- Choke mixture volumetric flow (Q_{mix}^{choke}) (Eq. (13));
- Tubing mixture volumetric flow (Q_{mix}^{tubing}) (Eq. (15)).

The reason why we use mixture volumetric flow and not the separate oil and gas volumetric flows is the fact that we know that the fluid properties are inaccurate in our case, so we want to avoid using them as much as possible. At the same time, the mixture flow can be sufficient to give the machine learning algorithms additional insights about the qualitative behavior of the multiphase flow and improve prediction accuracy. Fig. 11 summarizes the adaptation of training and testing procedures shown in Fig. 3 for Virtual Flow Metering.

3.3.2. Adaptation of method 2 - first principles model solutions and feature engineering

In this method, we use solutions of Eqs. (12) and Eq. (15) transformed to the phase volumetric flowrates via multiplying it by the phase volumetric fractions pre-computed in a thermodynamic package. The obtained solutions are then subtracted from the true phase rate, such that we obtain the mismatch between the developed model and the actual flow measurements from the field. Then, this error is used as a target variable for a machine learning model. The procedure of training and testing the algorithms for Method 2 shown in Fig. 4 is adapted for Virtual Flow Metering in Fig. 12.

3.3.3. Adaptation of method 3 - first principles model solution and raw measurements

As discussed before, Method 3 is similar to Method 2, while the main difference is that raw measurements are used as the input to the machine learning models with the aim to cover the mismatch between the first principles model solution and the target. When adapting this method to the Virtual Flow Metering example, pressure and temperature measurements along the systems are used as the input features to the machine learning models. Fig. 13 illustrates the adaptation of the method to Virtual Flow Metering.

Table 3
Summary of the considered case studies.

Case study	ML algorithm input	First principles model solution	Training target
Case 1	P_{BH}, T_{BH}, P_{WHCU}, T_{WHCU}, P_{WHCD}, T_{WHCD}	not used	Q_{phase}^{true}
Case 2.1	ΔP_{choke}, ΔT_{choke}, Q_{mix}^{choke}	not used	Q_{phase}^{true}
Case 2.2	ΔP_{choke}, ΔT_{choke} Q_{mix}^{choke}	Choke model $Q_{phase}^{choke} = Q_{mix}^{choke}\alpha_{phase@WH}$	$mismatch = Q_{phase}^{true} - Q_{phase}^{choke}$
Case 2.3	P_{BH}, T_{BH}, P_{WHCU}, T_{WHCU}, P_{WHCD}, T_{WHCD}	Choke model $Q_{phase}^{choke} = Q_{mix}^{choke}\alpha_{phase@WH}$	$mismatch = Q_{phase}^{true} - Q_{phase}^{choke}$
Case 3.1	ΔP_{tubing}, ΔT_{tubing}, Q_{mix}^{tubing}	not used	Q_{phase}^{true}
Case 3.2	ΔP_{tubing}, ΔT_{tubing} Q_{mix}^{tubing}	Tubing model $Q_{phase}^{tubing} = Q_{mix}^{tubing}\alpha_{phase@WH}$	$mismatch = Q_{phase}^{true} - Q_{phase}^{tubing}$
Case 3.3	P_{BH}, T_{BH}, P_{WHCU}, T_{WHCU}, P_{WHCD}, T_{WHCD}	Tubing model $Q_{phase}^{tubing} = Q_{mix}^{tubing}\alpha_{phase@WH}$	$mismatch = Q_{phase}^{true} - Q_{phase}^{tubing}$
Case 4.1	ΔP_{choke}, ΔT_{choke}, Q_{mix}^{choke} ΔP_{tubing}, ΔT_{tubing}, Q_{mix}^{tubing}	not used not used	Q_{phase}^{true}
Case 4.2	ΔP_{choke}, ΔT_{choke}, Q_{mix}^{choke} ΔP_{tubing}, ΔT_{tubing}, Q_{mix}^{tubing}	Choke and tubing model $\tilde{Q}_{phase}^{choke/tubing} = (Q_{ophase}^{choke} + Q_{phase}^{tubing})/2$	$mismatch = Q_{phase}^{true} - \tilde{Q}_{phase}^{choke/tubing}$
Case 4.3	P_{BH}, T_{BH}, P_{WHCU}, T_{WHCU}, P_{WHCD}, T_{WHCD}	Choke and tubing model $\tilde{Q}_{phase}^{choke/tubing} = (Q_{phase}^{choke} + Q_{phase}^{tubing})/2$	$mismatch = Q_{phase}^{true} - \tilde{Q}_{phase}^{choke/tubing}$
Case 5	Q_{phase}^{choke}, Q_{phase}^{tubing}	not used	Q_{phase}^{true}
Case 6	Q_{phase}^{choke} or Q_{phase}^{tubing} or $Q_{phase}^{choke/tubing}$ and $Q_{phase}^{Case\,1}$	not used	Q_{phase}^{true}

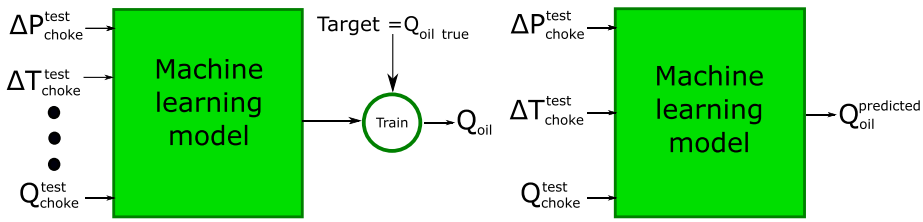

(a) Training phase of Method 1 in VFM systems (b) Test phase of Method 1 in VFM systems

Fig. 11. Method 1 (feature engineering) adapted for Virtual Flow Metering.

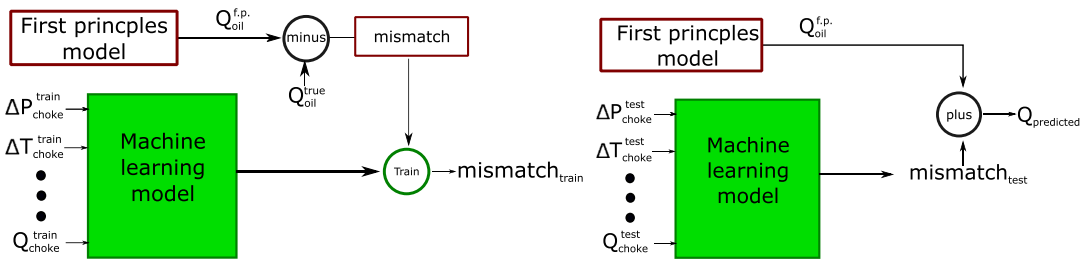

(a) Training phase of Method 2 (b) Test phase of Method 2

Fig. 12. Method 2 (first principles model (choke and tubing) solutions and feature engineering) adapted for Virtual Flow Metering.

3.3.4. Adaptation of method 4 - linear meta-model of models with created features

In this method, we combine solutions from models created in Method 1 for the choke and tubing system parts and then sum the weighted predictions to get the final outcome. Fig. 14 shows the adaptation of the method to Virtual Flow Metering.

3.3.5. Adaptation of method 5 - Linear meta-model of the selected model with created features and model with raw data

In this model, any of the models (choke or tubing or choke and tubing) with created features can be used together with the model which uses raw measurements as the input. In this work, we use the model with both choke and tubing features. Fig. 15 shows how the method is applied for Virtual Flow Metering systems.

4. Case studies

This section provides an overview of the considered case studies. The summary of the selected case studies, input features, used first principles models and training targets is shown in Table 3.

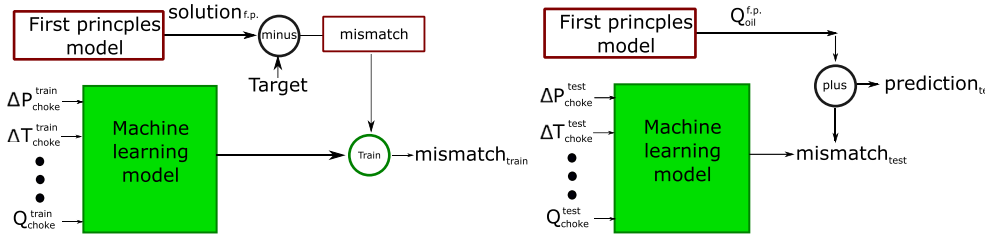

(a) Training phase of Method 3 (b) Test phase of Method 3

Fig. 13. Method 3 (first principles model (choke and tubing) solution and raw measurements) adapted for Virtual Flow Metering.

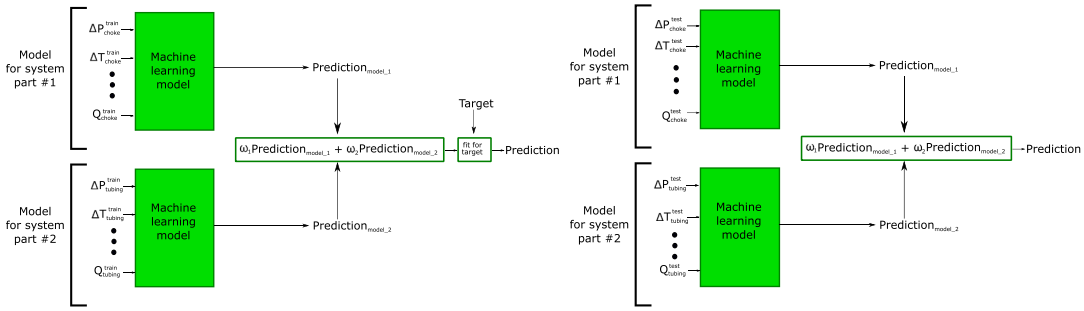

(a) Training phase of Method 4 (b) Test phase of Method 4

Fig. 14. Training and test procedures Method 4 - linear meta-model of models with created features.

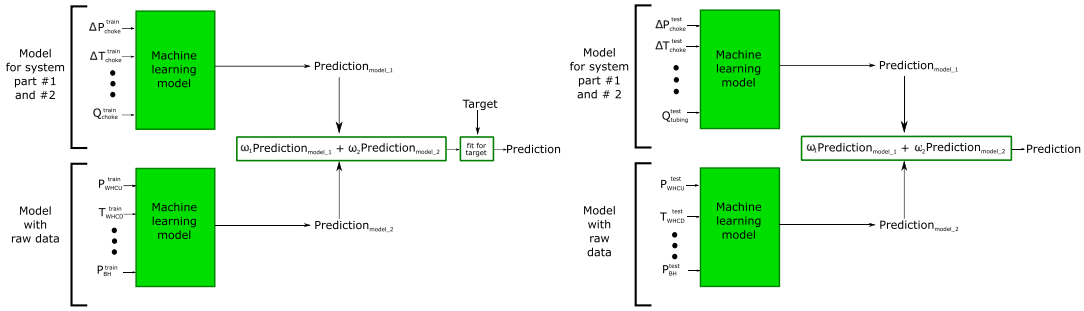

(a) Training phase of Method 5 (b) Test phase of Method 5

Fig. 15. Training and test procedures Method 5 - Linear meta-model of the selected model with created features and model with raw data.

Case 1 is the base case which is used for comparison with all the other cases. In this case study, raw measurements are used as the input to the machine learning algorithms without any transformation. This is the approach which has been used in the data-driven Virtual Flow Meters in the literature so far and often used in estimation of parameters in process engineering systems using machine learning. This base case will be compared with the proposed approaches of combining machine learning with first principles models.

Case 2 considers methods 1, 2 and 3 applied to the production choke. More specifically, **Case 2.1** considers using Method 1 (feature engineering) applied for the choke, so that the inputs to the machine learning algorithms are ΔP_{choke}, ΔT_{choke} and Q_{mix}^{choke}. This case will show if the measurements related to the choke only can describe the flow accurately.

In **Case 2.2**, Method 2 (first principles model solution + feature engineering) is used such that the solution of the choke model for $Q_{oil/gas}$ is obtained and the mismatch between the solution and the true value is covered using an algorithm with choke features ΔP_{choke}, ΔT_{choke} and Q_{mix}^{choke} as inputs.

In **Case 2.3**, Method 3 (first principles model solutions + raw measurements) is used and raw measurements are used for the algorithm which is trained to cover the mismatch. Table 3 summarizes the used combinations for the cases.

Case 3 is similar to Case 2, but it considers methods 1, 2 and 3 applied to the production tubing. As such, **Cases 3.1, 3.2** and **3.3** are conceptually identical to Cases 2.1, 2.2 and 2.3, but instead of choke, tubing first principles model and features are used (Table 3).

Case 3 considers method 1, 2 and 3 applied to choke and tubing combined. More specifically, **Case 4.1** considers all the features for choke and tubing combined as the inputs to the machine learning model, so it again follows Method 1.

In **Case 4.2**, to use Method 2 we used averaged solution from the choke and tubing models for Q_{oil} and then cover the mismatch using both tubing and choke features.

In Case 4.3, we cover the mismatch by using the raw measurements as features. Again, the discussed case studies are summarized in Table 3.

Case 5 considers Method 4 - using a linear meta-model for the algorithms which are based on the engineered features. We consider this case only for the choke (Case 2.1) and tubing models (Case 3.1) combination. This is because this is the simplest yet effective way to combine all the available models and measurements.

Case 6 considers Method 5 - using a linear meta model which combines the selected model with engineered features (we selected the model from Case 4.1) with the model from Case 1 which uses the raw data as the input.

Remarks on other possible case studies. It is possible to create a meta-model over the other cases, and even a meta-model on top of other two meta-models which combine, for instance, first principles models solution and mismatches. However, it will introduce additional unexplanability of the models as well as it leads to a tricky implementation without necessarily providing a better accuracy.

5. Results and discussion

In this section, we describe the estimation results for gradient boosting, MLP neural networks and LSTM and feature analysis for gradient boosting and MLP neural networks. First, we thoroughly describe the estimation results from gradient boosting including the estimation accuracy and transparency of the data-driven models which is developed through combining first principles and machine learning models. After that, we discuss the results of neural networks and LSTM mostly focusing on the differences between the results of these algorithms and gradient boosting to avoid repetition of similar conclusions. We also discuss the differences between static algorithms (MLP neural network and gradient boosting) and dynamic algorithm (LSTM). Please note, that we do not provide a feature analysis of LSTM neural networks, because the current version of the feature analysis tool (Skater) does not provide such capabilities due to its dependency on a particular feature in time. Nevertheless, we decided to include the estimation results of the LSTM, because they provide insights about the importance of considering past time steps data in estimating the current time target value. As such, it provides the basis for conclusions on the conditions at which dynamic methods should be preferred over the static ones.

5.1. Analysis of gradient boosting results

5.1.1. Overview of flowrate estimation results

In this section, we analyze the results of oil and gas flowrate estimation using gradient boosting based models. While the original time resolution of the data is 1 minute, for better visualization, the estimation results are averaged over the period of 5 minutes. This allows to see if the algorithm is able to capture the general multiphase flow trends rather than occasional flowrate spikes which are not essential to capture. The results for oil and gas flow estimation using gradient boosting based models are shown in Fig. 16.

When to use feature engineering (Method 1) and when to use first principles-based models (Method 2 and 3)?

The first observation in Fig. 16 is that in some cases, feature engineering methods outperform other methods while in other they do not. As feature engineering method is the simplest one in terms of construction cost, it is useful to know under which conditions it can be effectively applied which will allow to avoid constructing more complex combinations of first principles and machine learning models.

First, consider the oil rate estimation case (Fig. 16a) and compare the feature engineering-based methods with other proposed methods. The accuracy of these models in comparison with the base case is discussed in the next sections.

We see that the cases with engineered features (Case 2.1, 3.1 and 4.1) generally outperform all the other models using the proposed methods (Case 2.2 and 2.3, Case 3.2 and 3.3, Case 4.2 and 4.3 respectively) except the meta-model approaches. However, in the gas flow estimation (Fig. 16b), when the first principles models are combined with the raw measurements (Case 2.3, 3.3 and 4.3), such models generally perform equally good or better than the feature engineering models.

The major difference between the oil and gas flowrates is the complexity of the system behavior. From the test set representation in Fig. 16 as well as from the entire dataset in Fig. 10, we see that the oil rate behavior is much more unstable and does not have the same trend in the train and test sets, while the gas rate has much smaller fluctuations and the trend is observable. As such, we see that when the system behavior is relatively complex (in this case - oil rate behavior) and the constructed first principles models are relatively simple as in this work, it is better to use feature engineering methods as a simple yet accurate solution. This is because for a complex system behavior, simple first principles models may not be accurate enough to accurately represent it. At the same time, well-engineered features may be well-correlated with the target variable (in this case - the oil flowrate), such that the model produces accurate results.

When the system behavior has a moderate complexity, (in this case - gas rate behavior), so that even simple first principles models are accurate enough, its combination with the raw data may be a good choice as it can be seen in Fig. 16 (Case 2.3, 3.3 and 4.3).

As for the Method 2, when the first principles models are used together with the simple and complex first principles features, it does not improve the performance as we see from Fig. 16 (Case 2.2, 3.2 and 4.2) for both oil and gas rates. The reason for this may be the fact that the features are better correlated with the original target variable and not the mismatch, while the first principles models solution may also not be very accurate, which in total deteriorates the performance, as we see in Fig. 16 (Case 2.2, 3.2 and 4.2), especially for the oil rate estimation.

Influence of first principles models accuracy on estimation accuracy and on capturing physical effects The next important discussion is related to the one in the section above with a particular focus on the influence of the accuracy of the first principles models on the estimation accuracy.

Comparing the choke-based (Case 2.1, 2.2 and 2.3) and tubing-based (3.1, 3.2 and 3.3) machine learning models, we see that the proposed first principle choke model is not a solid basis to accurately represent the oil rate behavior, such that it has a lower accuracy than the base case (Case 1) with just raw measurement input data. However, the choke-based machine learning models show a moderate accuracy for the gas estimation case and Case 2.3 even outperform the model in Case 1.

At the same time, the first principles tubing model and related features are relatively accurate to represent the flow well. Even though the model may not be able to account for high oil flowrate fluctuations, the general flow behavior is accurately represented and all the constructed tubing-based machine learning models outperform the model from Case 1.

As such, we conclude that in order to be applied alone for oil rate estimation within machine learning VFM, the proposed first principles choke model must be improved for this specific case. One possibility to do that is to change the model type which resolves the flow more accurately and accounts for more complex physics such as gas slip, as suggested by Schuller et al. (2006), who found that by introducing the slip relationship, a choke model typically produces more accurate estimates. Another possibility is to perform some pre-tuning of the model using simple linear regres-

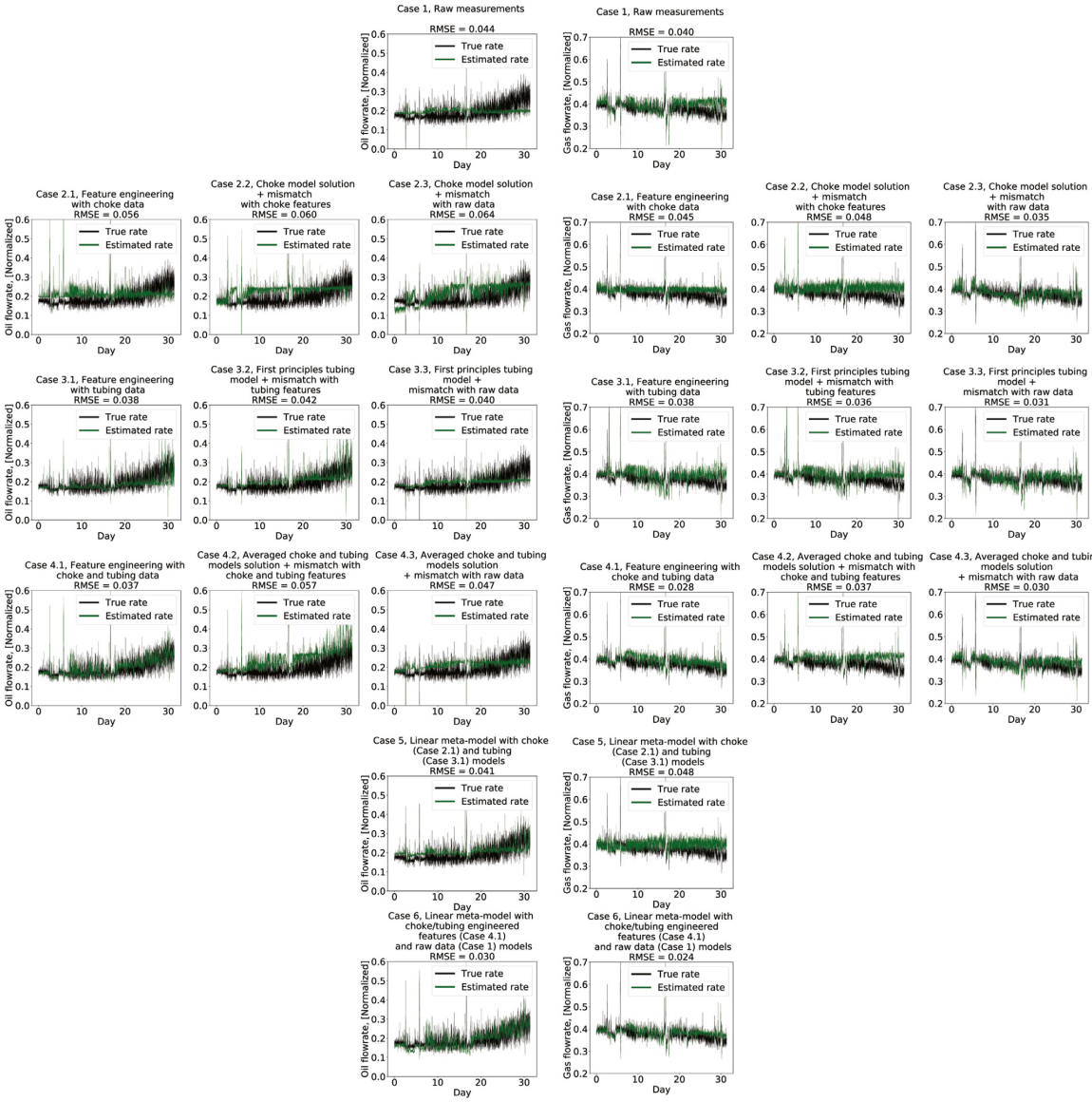

(a) Predicted oil flowrates

(b) Predicted gas flowrates

Fig. 16. Oil and gas rates estimation by gradient boosting based models. The results are averaged over 5 minutes period, i.e. one point - 5 minute averaged rate.

sion techniques and then use the model as the basis for the combinations with machine learning algorithms as proposed in this work.

Despite the fact that the first principles tubing model shows a reasonable accuracy, it can also be further improved. For instance, the model can be solved numerically for a small number of mesh points along the tubing and only then combined with machine learning, so that the model will provide a more accurate solution than the one presented here. We keep these investigations for future work.

It is worth noting that despite the choke model alone is not accurate enough, it can still be used to further improve the accuracy of the tubing model results. We can see that Case 4.1 for both oil and gas rates produces one of the most accurate results, if not considering the meta-models from Case 6. This is likely because the choke and tubing models in this case can be better at estimating different flow conditions. In fact, we see that for the oil rate predictions, the choke model based algorithms (Case 2) follow a more transient behavior of the system, such that we see predictions of flowrate fluctuations with some occasional spikes which try to capture even higher fluctuations, but often overestimating them. This is different from the cases with the tubing model based machine learning models (Case 3), where we see a more smooth flow. This behavior is physically meaningful because the choke model is a lo-

cal (static) model which means that any flow disturbance across the choke will suddenly be reflected in the change of pressures and temperatures taken at the inlet and outlet of the system. On the other hand, if a flow disturbance occurs at the bottomhole of the well, this will be reflected at the bottomhole measurements first and only after some time reach the wellhead measurements. For the gas flow cases, the behavior of both models is relatively similar due to low flow fluctuations.

Improved model generalization One of the potential advantages in including physics information into machine learning models can potentially be improved model generalizability. This is the ability of the model perform well on the unseen data. In physical and process engineering systems, this can be exemplified if the machine learning model is able to describe system under conditions, which have been barely seen in the training set. In our case, the model generalization is seen to be improved significantly for several cases. indeed, in Case 4.1, we see that by combining the first principles models as features, we are able to capture the rising oil rate trend at the end of the estimation period as well as the decreasing gas rate trend, while when using the pure data-driven models (Case 1), it is not possible. As such, by combining the models, we can achieve improved machine learning model generalization and the overall improvement of the results. This strengthens the fact that the combined approach of physics-based machine learning modelling may be able to significantly improve machine learning model generalization, especially compared to a pure data-driven approach.

Meta-models performance

The next important discussion concerns the meta-models performance. While the meta-models have the highest construction cost, they may not necessarily have the highest accuracy. For instance, we see that the accuracy of Case 6 for both oil and gas rates is the highest among the cases, while Case 5 meta-models are not as accurate. The reason for this is the accuracy of the sub-models used in the meta-models. Since the accuracy of the model with choke-based features (Cases 2.1) is not high, it deteriorates the results of the meta-model. As such, we conclude that it is better to combine the models using engineered features within one algorithm (such as in Case 4.1), than in a meta-model (Case 5), if the performance of separate models is not accurate. However, if the models are accurate enough, the joint meta-model can further improve the performance, such as in Case 6.

Also, we conclude that when using the raw data models within a meta-model, we can improve the performance of the physics-based machine learning models and, at the same time, keep the overall model explainable because the weight of the raw data model in the meta-model shows its contribution to the overall solution. As such, we are able to see which part of the process is resolved by the physics-aware algorithms and which part is still unresolved and covered using the raw data algorithm. A detailed analysis is shown in Section 5.1.2.

Advantages of comparing different physics-aware machine learning models using the proposed approach

The observed results in the sections above emphasize one of the most important conclusions from this work: by analyzing and comparing the simulation results using the proposed approaches with physically meaningful features, separating the system into sub-parts and creating first principles models for each system part, it becomes possible to better understand the physical behavior of the system, make conclusions about the drawbacks of the applied models and propose solutions to create more accurate approaches. This is not the case when raw measurements are used directly. In that case, even if the solution is accurate, it is hard or impossible to comprehend if the solution is physically meaningful or not and propose future improvements.

In Table 4, we suggest possible cases which can be met by conducting *simultaneous* model analysis using Method 1 (feature engineering), Method 2 (first principles model solution + feature engineering) and Method 3 (first principles model solution + raw data). Here, we propose possible solutions to the problems which can arise during such analysis, so that the table can be used as an initial reference when the proposed methods applied to any process engineering system. For instance, if we see that feature engineering method produces low accuracy, while the combinations of the first principles models with raw data has high accuracy and adding features to such model reduces the accuracy (the first raw in the table), it is evident that in this case the features are poorly designed. As such, to further improve the accuracy, the features should be re-designed.

Of course, other situations may occur during the analysis which are not shown in Table 4, for instance, the accuracy of two methods are identically high or low, but using the logic in the table, it will be easy to comprehend the solution for any case.

5.1.2. Feature analysis

Apart from the potential of improving the accuracy of the models, first principles-based algorithms allow to check if the model follows the expected physical behavior. Also, it can help to reveal some additional patterns in the data. To explore these opportunities, we perform a feature analysis of the constructed models. Fig. 17 shows the feature importance while Fig. 18 shows the partial dependence plots for oil and gas rate (or oil and gas rate mismatch) prediction models based on the gradient boosting algorithm. As the values are standardized in model training and testing, they are removed from the partial dependencies plots because they do not add any value, while removing them allows a better visualization. The plots are used to identify the qualitative behavior of the models. It is also worth noting that the partial dependence plots are not produced for Case 5 and Case 6, because in these cases the meta-models are considered, so that the partial dependence plots will be identical to the plots of the meta-model sub-models and the importance of sub-models is shown in Fig. 17.

Poor features identification

The first interesting observation is that in the oil rate estimation case, the choke flow constructed feature has high importance when used in the separate choke model cases (Case 2.1 and 2.2), while when used with all the other features in Case 4.1, the feature has low importance. At the same time, the tubing mixture volume flow feature has high importance in both Case 3.1 and 4.1. From this observation, we conclude that the choke mixture flow feature is not representative enough to describe the flow behavior. This conclusion is supported by the rate estimation results shown in Fig. 16a where we see that the accuracy of Case 2.1 and 2.2 is low. We observe that by relying on the choke mixture flow feature, the algorithm makes poor flow estimates. At the same time, the tubing mixture flow feature is better designed and this is again confirmed by the results from Fig. 16a where the tubing based models are relatively accurate. When all the features are combined (Case 4.1 and 4.2), the gradient boosting algorithm is capable to distinguish good features (tubing model related), make the full use of relatively poor features (choke model related) and improve the estimates.

Transparency of meta-models

As for the importance of the meta-models features, Fig. 17 shows the absolute values of the meta-model weights. We see that the meta-models rely on the more accurate models (tubing and tubing/choke) which is what we would like to have. We see that in the gas estimation case, the meta-model gives higher weights to the raw data model than in the oil case. This coincides with what we saw in the rate estimation section, where adding the raw data model to the first principles model improved gas rate estimation accuracy (Case 2.3, 3.3 and 4.3) while in the

Table 4
Analysis of methods for combining first principles with machine learning and proposed problem solutions.

Accuracy				
Feature engineering	First principlesmodel solution+ mismatch withfeature engineering	First principlesmodel solution+ mismatch withraw data	Conclusion	Solution
low	average	high	Accurate first principles model,but features are poorly designed(too simple) to describe the system.	Re-design featuressuch that they describethe target more accurately
low	high	average	Accurate first principles model,features are somewhat correlated withmismatch but generally poorly designed	Re-design existing features makingthem more complex andaccurate than the created ones
average	low	high	Inaccurate first principles modeland features, raw data betterdescribe the system behavior	Entirely revise the modeland engineered features
average	high	low	Inaccurate first principles modelbut well designed features	Revise the model to furtherimprove accuracy of the solution
high	low	average	Inaccurate first principles modeland features are not correlated withthe mismatch	Revise the model, make itmore complex such that it betterdescribes the system behavior
high	average	low	Inaccurate first principles modelbut well-designed features	Revise the model, make it morecomplex such that it betterdescribes the system behavior

oil rate estimation, this does not improve the performance as significantly. As such, we can say that the constructed models which are based on the physics-based features (Case 4.1) are better in explaining the given dataset than the raw measurement models (Case 1), especially for estimation of the oil rate, because of its better performance and higher weight values in the meta-models. At the same time, there is still a potential in improving the created model accuracy which should increase importance of the physics-based machine learning model even further when combined in a linear meta-model with the raw measurement model.

From the estimation and feature importance observations regarding the meta-models, we conclude that, in addition to the improved estimation accuracy by using the linear meta-model structures, we can also evaluate the potential of improving the physics-based machine learning models itself. For instance, in Case 5-type meta-models, these improvements consider separate models for each system part, i.e. we can check if, for instance, by introducing the slip relation into the choke model, the importance of the choke model in the meta-model increases or decreases and compare with the obtained estimation results. More importantly, the same can be said for the physics-based machine learning model of the entire system used in Case 6. That is, by creating different (more complex or less complex) physics-aware models and comparing their contribution in the meta-model with the raw data models, we can check if the new proposed model reduces the influence of the raw data based model. The higher the influence of the model, the better the model is, because in such a case, the new constructed model will better explain the data and reveal the patterns which were previously unrevealed by a simpler model. Again, it is expected that the model with the higher importance will have higher estimation accuracy.

Insights about physical behavior of the system

In addition to the better explainability of the machine learning algorithms, we can get extract insights about the fluid behavior in the system using the constructed feature importance and partial dependencies plots.

Temperature drop effect. Consider the partial dependence plots for Case 3.1 for both oil and gas predictions. We see that for the tubing case, the larger the temperature drop is, the higher oil flowrate is. This is the opposite to the gas case, where we see that with the rise of the temperature drop, the gas rate decreases. Such model behavior well corresponds to the thermodynamic behavior of a hydrocarbon mixture. That is, with the decrease of temperature of the mixture, more hydrocarbon mass starts being condensed from the gas phase and accumulated in the liquid phase. By considering that the reservoir temperature is relatively constant, the decrease of the temperature of the fluid will be mainly caused by the heat transfer along the well tubing. As such, more hydrocarbon will be observed in the liquid phase if the temperature drop along the tubing rises. Such behavior is more difficult to see for Case 4.1 because the algorithms rely less on the temperature drop feature, so that such partial dependence is less identifiable.

Explanation of complex multiphase flow behavior. Another observation for the tubing model is that with the increase of the mixture flow feature value, we see the increase of the gas rate and the decrease of the oil rate. As such, the model tells us that the increase of the mixture volumetric flowrate from the well will mainly correspond to the increase of the gas production and decrease of the oil production. This is exactly the behavior of most wells at the late production stage, when we see the increase of the gas and/or water production and decrease of the oil production. The model captures this relation from the training set.

At the same time, for the choke model in Case 2.1, we see that the increase of the constructed feature of the mixture flow and pressure drop corresponds to the increase of rates with some occasional non-linear fluctuations caused by the flow irregularities and non-smooth solutions produced by gradient boosting algorithm. For the oil rate, however, this dependence is more difficult to see because of the low importance for the algorithm when estimating the flow, as we observed in Fig. 17a. Such behavior gives us further insights about the system. In our case, the choke opening is almost always constant, so the increase of the pressure drop over the choke will correspond to the increase of the flowrate. As the mixture flowrate feature is also proportionally dependent on the pressure drop, it is positively correlated with the rates. The reason why the choke model behaves differently from the tubing model in terms of the increase/decrease of the phase rate when increasing the choke mixture rate is that the flowrate measurements are taking at the end of the tubing and before the choke (Fig. 9), as such the degassing/liquid accumulation effects are considered in the tubing model through the fluid density change, while in the choke model such effect is not considered.

Another observation is that the pressure related features such as pressure drop across the choke and tubing is generally more important for the gas estimation than for the oil estimation. This results is physically meaningful because the gas behavior is much

(a) Feature importance for oil estimation algorithms (b) Feature importance for gas estimation algorithms

Fig. 17. Feature importance analysis for gradient boosting based estimation algorithms.

more affected by the pressure changes due to its high compressibility.

As such, through the provided analysis we see that it is possible to answer two questions: "Can we trust the model?" and "Can we get the new insights about the system?". More specifically, when we observe that the model is able to describe even a simple system behavior in a correct way, the trust in the model increases. In addition, after getting deeper insights about the model behavior thorough the analysis, we can dig into a more complex physics, for instance, which we did not think of before the analysis, e.g., the local degassing effects of the multiphase flow in case of our work.

Advantages of using the proposed feature analysis

Generally, we can say that, in addition to the evaluation of the algorithms transparency, the evaluation of the feature importance

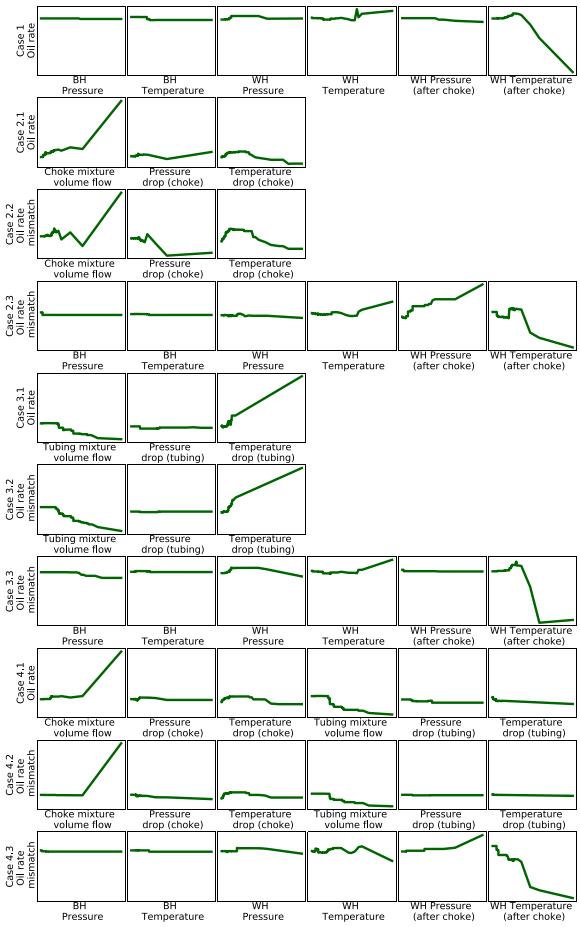

(a) Partial dependence plots (oil predictions)

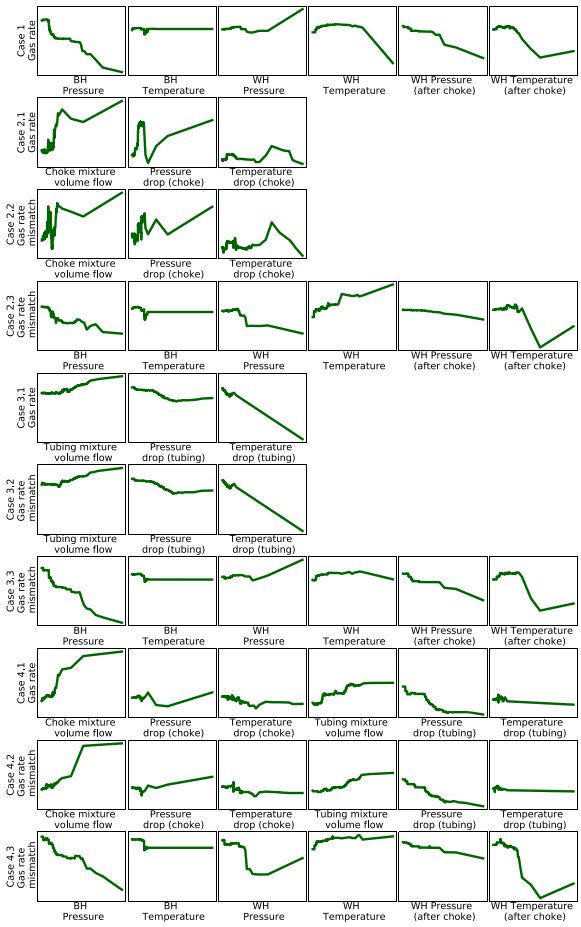

(b) Partial dependence plots (gas predictions)

Fig. 18. Partial dependence plots for gradient boosting based models. The plots show the qualitative relationship between the features and the target variable. Occasional spikes are associated with flow irregularities and non-smooth solutions provided by the gradient boosting algorithm.

and partial dependencies shows possible directions for improving the estimation capabilities of each particular model. This means that by taking the discussed evaluation into account, we can distinguish which features and models behave non-physically, so that we can identify the bottlenecks and try to improve the models and features such that they better correspond to the expected physical behavior of the system. As a result, improvements of the estimation accuracy can be expected.

All the discussed observations would be hard or impossible to recover from the plots related to Case 1 only. An importance of a particular measurement can tell us much less than a physically interpretable feature as well as a comparative study of combinations of the first principles with machine learning algorithms. However, analysis of raw measurements can still be useful to conduct even for the model which uses raw measurements in order to see which measurements can be totally irrelevant and not included into the first principles features and models. For instance, in this case, this is the choke opening measurement in Case 1. This can be especially useful for modeling and analyzing of large scale systems.

5.2. Analysis of neural network results

5.2.1. Flowrate estimation results

Results overview and similarities between MLP neural network and gradient boosting results Fig. 19 shows the estimation results of the oil and gas flowrates using MLP neural networks. Generally, we see that the behavior of the models corresponds to the results obtained using the gradient boosting based models, such that most of the trends observed in the gradient boosting case, can also be observed here. For instance, we see that the combinations of choke and tubing features are able to improve the performance and to reconstruct the rising oil rate trend and decreasing gas rate trend at the end of the estimation period (Case 4.1). Apart from that, adding the raw data to the choke and tubing models in the gas estimation case boosts the performance (Case 2.3, 3.3 and 4.3). The same as with gradient boosting, the meta-model from Case 6 achieves the highest performance for both oil and gas rates. We will not go into detail about the neural networks behavior in cases where it is similar to the gradient boosting behavior, because these trends are well discussed in sections related to the gradient boosting results.

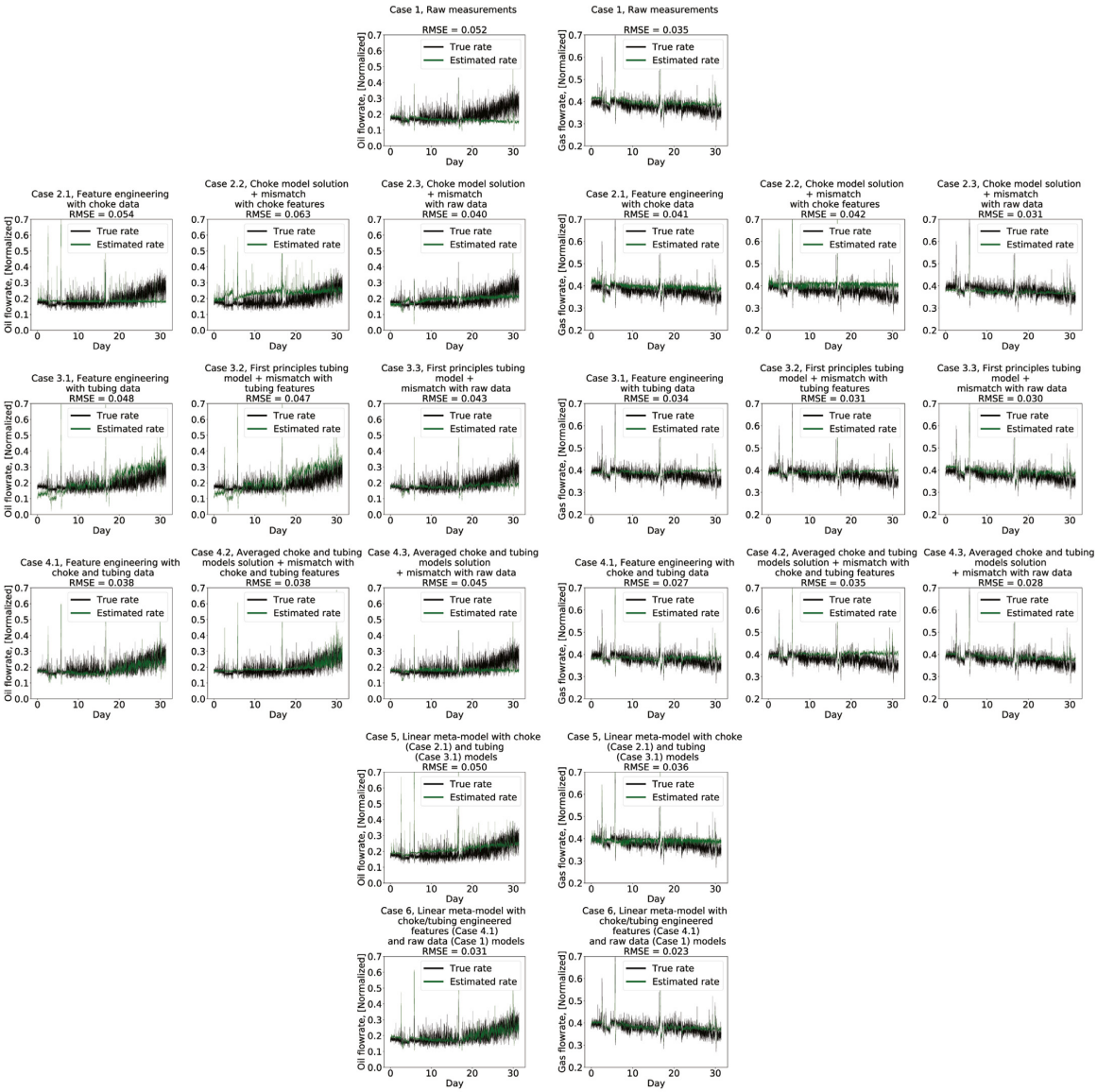

(a) Predicted oil flowrates (b) Predicted gas flowrates

Fig. 19. Oil and gas rates estimation by MLP neural network based models. The results are averaged over 5 minutes period, i.e. one point - 5 minute averaged rate.

Instead, we will focus on the differences between gradient boosting and neural networks. To compare the results between two algorithms closer, Tables 5 and 6 show the comparative summary of the estimation results.

Differences between MLP neural network and gradient boosting results

The first difference between the results is that the neural networks are not able to use the tubing model and related features (Case 3.1, 3.2 and 3.3) as efficiently as gradient boosting providing less accurate results closer to the base case (Case 1) accuracy, while still more accurate. The reason for this may be the fact that, as will be shown in Section 5.2.2, the neural networks rely very much on the "Tubing mixture volume flow" feature and almost do not consider "Tubing pressure drop" and "Tubing temperature drop" features. However, the "Tubing mixture volume flow" alone may be too simple to accurately describe the flow. At the same time, gradient boosting based models do consider pressure and temperature drop features (Fig. 17a) which is likely why it helps the algorithm to better estimate the flowrates.

We also see that for the gas estimation cases, in each case the MLP neural networks outperform gradient boosting, which is not the same for the oil estimation. The exact reason for such behavior is unclear, but one explanation for such behavior may be that neural networks in general and MLP neural networks in particu-

(a) Feature importance for neural network (oil prediction) (b) Feature importance for neural network (gas prediction)

Fig. 20. Feature importance analysis for MLP neural network.

lar may be better at regression of more smooth values and system behavior (in this case - gas flow) because neural networks are typically better than gradient boosting in interpolation tasks. This is because gradient boosting with regression trees produces piecewise constant predictions while neural networks produce smooth interpolation approximations. This hypothesis will also be checked and discussed later for LSTM neural networks.

5.2.2. Feature analysis

Feature analysis overview and similarities between MLP neural network and gradient boosting results

Fig. 20 shows the feature analysis of the MLP neural networks based models. We see that for most of the cases with physics-based features, the feature importances are similar between the neural networks and gradient boosting. Some minor differences

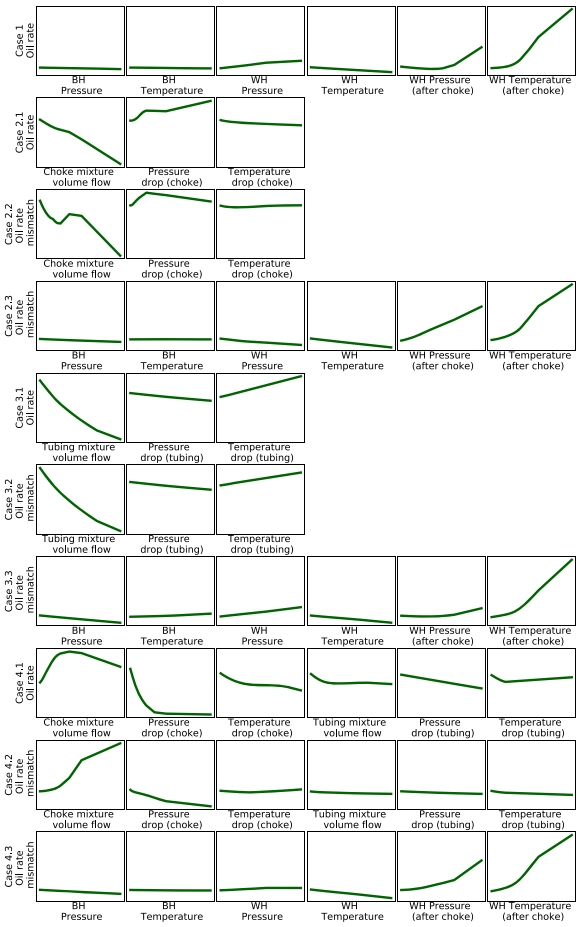

(a) Partial dependence plots (oil predictions)

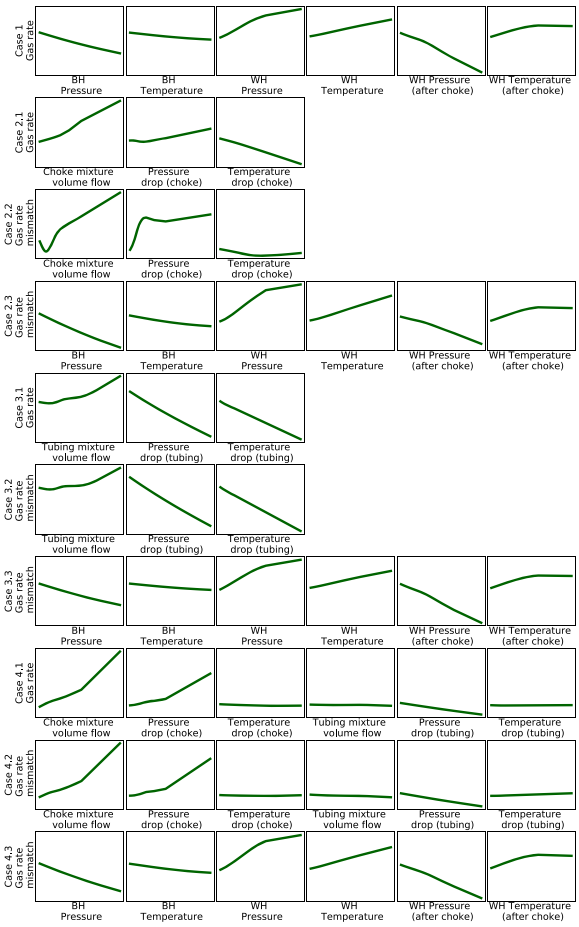

(b) Partial dependence plots (gas predictions)

Fig. 21. Partial dependence plots for MLP neural network based models. The plots show the qualitative relationship between the features and the target variable. The plots do not have non-convex spikes as in the gradient boosting case due to smooth solutions provided by neural networks.

exist, but they are caused by differences in the algorithms nature. What is more important is that the partial dependencies plots shown in Fig. 21 produce similar trends in most of the cases between neural networks and gradient boosting, except the fact that the plots produced by neural networks are more smooth. As such, we see that the algorithms interpret the physical behavior of the system in a similar way. This emphasizes that the consistent approach for machine learning modeling with first principles proposed in this work allows to produce consistent results and reveal the main structure of the data. It also emphasizes the fact that using a model-agnostic approach for feature evaluation can be more suitable and insightful than model-specific ones and gives the opportunity to better evaluate the validity of the produced estimates.

Differences between MLP neural network and gradient boosting feature analysis results

The major difference between MLP neural networks and gradient boosting partial dependencies plots is that the neural networks estimate the decrease of the oil flow when the choke mixture flow increases when used in Case 2.1 and 2.2. This is different from what gradient boosting suggests and what we would expect based on the physical understanding of the system. At the same time, when all the features are used together (Case 4.1 and 4.2), the neural networks give a more similar behavior to the gradient boosting which we found to be physically meaningful. The reason why the neural network gives this unreasonable evaluation of the choke mixture flow feature when used in the choke model alone is hard to explain and kept for future investigations. Despite some small differences, we can still see the big advantage of using physics-based features in terms of improved and consistent explainability of different models and algorithms, when compared to the raw data models.

5.3. Analysis of LSTM results

5.3.1. Flowrate estimation results

As discussed, for the LSTM neural network, only the estimation results are analyzed while the feature importance analysis is not conducted because the LSTM dependence on time step features which is not implemented in the Skater library used for the analysis. Despite the absence of feature importance analysis, we decided to include these results because it allows to analyze the depen-

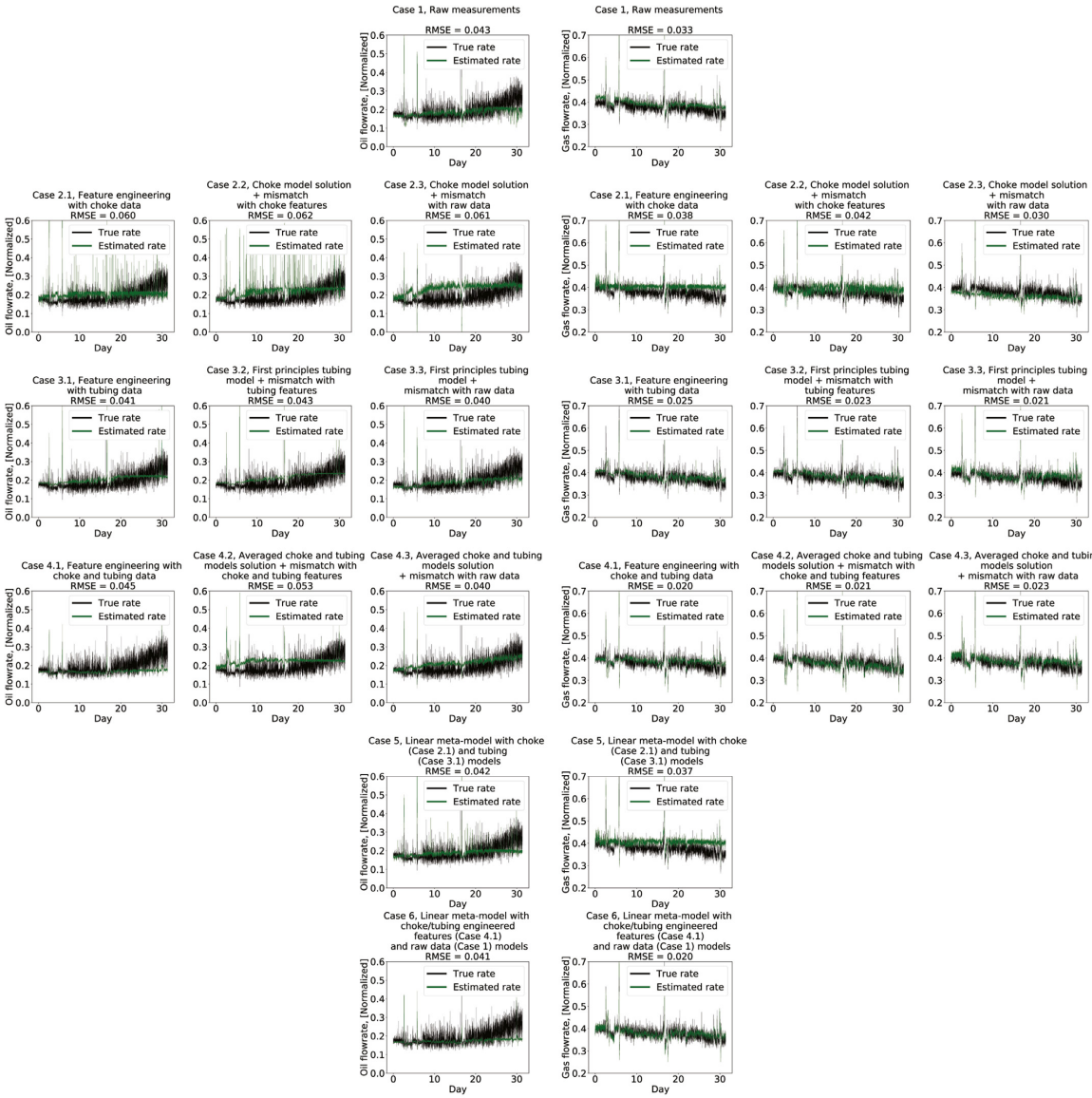

(a) Predicted oil flowrates (b) Predicted gas flowrates

Fig. 22. Oil and gas rates estimation by LSTM neural network. The results are averaged over 5 minutes period, i.e. one point - 5 minute averaged rate.

dence of the results accuracy at the current time step on the data from the past time steps and compare it with the static approach used in MLP neural networks and gradient boosting.

Results overview and similarities between LSTM and gradient boosting/MLP neural network results

Fig. 22 shows the simulation results for the oil and gas flowrate estimation using LSTM neural networks. From the results we see some of the trends observed for gradient boosting and MLP neural networks can also be observed here. For instance, for the oil flowrate estimation, the pure choke-based machine learning models (Case 2.1, 2.2 and 2.3) do not perform well while try to capture dynamic behavior of the system which is represented by flowrate spike estimates. Also, similar to MLP neural networks and gradient boosting, the tubing-based machine learning models (Case 3.1, 3.2 and 3.3) capture a more steady state behavior of the system producing smooth oil flow estimation results. We also see that, similar to MLP neural networks, LSTM neural networks produce better results for gas rate estimation case, while in oil rate estimation cases gradient boosting is generally more accurate. This fact confirms the hypothesis, made for MLP neural networks previously, that the reason for such behavior is that neural network are generally better at predicting smooth regression trends due to their high interpola-

tion capabilities. However, trends with high fluctuations may be, in some cases, better described by piecewise constant approximations by gradient boosting.

Differences between LSTM and gradient boosting/MLP neural network results

The first difference between the algorithms to notice is that even when combining choke and tubing features in the oil case (Case 4.1), the rising trend at the end of the estimation period is not captured. So, we can see that, despite the LSTM network uses the previous measurements to predict the flow at the current time step, it does not necessarily help to produce an accurate estimate. In fact, we observed that the MLP neural network and gradient boosting, being totally different algorithms but both taking only the current time step measurements, were able to estimate the increasing flowrate trend accurately. The LSTM, however, in Case 4.1, takes 15 past time step measurements to make a prediction. As such, we conclude that it is not always a good idea to take the past measurements into account in order to predict the target variable value at the current time step. For instance, in case of the oil flowrate, the flow behavior is irregular which makes it difficult for the LSTM network to accurately reconstruct the time dependent flow pattern.

For the gas case, however, the LSTM generally performs much better than gradient boosting and MLP neural networks. We see that the gas flow behavior is much more stable, so that it is easier for the LSTM to reconstruct the time dependent pattern of the flow. The average time window chosen by the LSTM networks among the cases for the gas rate estimation via Bayesian optimization is 10, however, the exact value is case dependent.

When should we use LSTM in estimation of process system variables?

Summarizing all the results on LSTM and comparing it with static models of MLP neural networks and gradient boosting, we can conclude that using LSTM may be beneficial when the trend of the target variable is relatively smooth, but more importantly, assumed to have a time dependent pattern. In this work, the gas flowrate follows such a trend. This can be seen not only on the estimation result of the test data set show in Fig. 22b, but also in Fig. 10 where the entire gas flowrate trend is shown. In fact, in Fig. 10 we see that despite the fluctuating behavior, the gas flowrate has a systematic decreasing trend in time. The oil flowrate, however, has many irregular ups and downs, such that it is nearly impossible for a machine learning algorithm to reconstruct such a behavior. Therefore, when an LSTM is used to estimate it, the algorithm may try to learn the trend in time which simply does not exist which leads to high estimation error.

6. Results summary

In this section, we summarize the results of 72 cases which consider 12 different case studies of combining machine learning with first principles using 3 different machine learning algorithms. First, using Fig. 23, we describe how the reader can choose a suitable method for combining first principles models with machine learning depending on the process system under consideration by following a step-by-step approach. In Table 5, we summarize and average the RMSE for each algorithm and each flowrate. Such comparison is intended to shown which algorithm was the most accurate on average over the case studies conducted in this work for different system behaviors (oil and gas rates). Table 6 shows the average error over the algorithms (MLP neural network, gradient boosting, LSTM) for each first principles model as well as the averaged meta-model results to give more insights about the accuracy of the proposed methods. Then, we discuss the overall applicability of each method and its potential improvements.

How to choose the best method for your system?

In this work, we extensively tested several methods which vary by their accuracy, construction cost and applicability to different system conditions. In Fig. 23, we summarize the procedure of how all the proposed methods can be most effectively used when applied to modeling of a new process engineering system. By following these guidelines, the reader will hopefully be able to quickly choose the method which satisfies the desired accuracy and the amount of time available for model construction. Below in this section, we summarize the results which we observed in this work and which became the basis for creating Fig. 23 with the proposed selection guidelines.

Most accurate algorithms for oil and gas flowrates

From Table 5, we see that, among the algorithms, in the oil case, MLP neural network performs best on average (mean RMSE=0.0458), while gradient boosting shows slightly worse mean RMSE and LSTM performs relatively poorly. However, for the gas flowrate, the mean RMSE of LSTM is much lower than for MLP neural network and gradient boosting. As such, we confirm so-called "No Free Lunch" theorem (Wolpert et al., 1997) which states that there is no single algorithm which fits best for all cases. In this particular case, since the oil flowrate fluctuations are highly irregular, the time dependent pattern which LSTM is trying to find may not exist, so that the learning of the non-existing pattern deteriorates the results. As such, the algorithms which use only one time step measurements (MLP neural network and gradient boosting) outperform LSTM and perform almost equally well. At the same time, when the flow fluctuations have a more regular behavior and may have a time dependent pattern as in the gas rate case, LSTM is able to fit the data much better by taking advantage of the previous time step data.

Superior accuracy of meta-models and applicability of feature engineering

From Table 6 we see that in the meta-model which combines the model with all the created features for choke and tubing with the raw data model (Method 5) outperforms all the other methods which results in the best averaged performance (RMSE=0.0340 and 0.0233). If choosing between the methods which do not consider meta-modeling, feature engineering (Method 1) shows the best performance (italic values). From this we conclude that if the goal of modeling is to achieve the highest performance, the linear meta-models which combines most of the available information is a good choice. Such models are slightly more difficult to construct, but they still maintain the interpretable behavior and generally improve the performance. Otherwise, the feature engineering method is another possibility which is slightly easier to construct that the meta-models, less accurate but still shows a good performance.

Applicability and future improvements of Methods 2 and 3 - combinations of first principles model solutions and machine learning models

As for the other methods of combining first principles and machine learning (Method 2 and 3), in this case, they performed less accurately than other discussed methods. However, this does not mean that we should not consider them to apply for other cases. For instance, as we observed for the gas estimation case, the combination of the first principles models with raw data (Case 2.3, 3.3 and 4.3) produced accurate performance. However, in the oil rate estimation case which has irregular behavior, the proposed models appear to be too simple to describe the system behavior accurately. As such, to be successfully applied, the models would need to be improved prior to modeling.

One possibility to do this is to pre-solve the models numerically for a small number of mesh points while maintaining the computational efficiency, so that the solution may not be very accurate, but still much better than one averaged over the entire system. An-

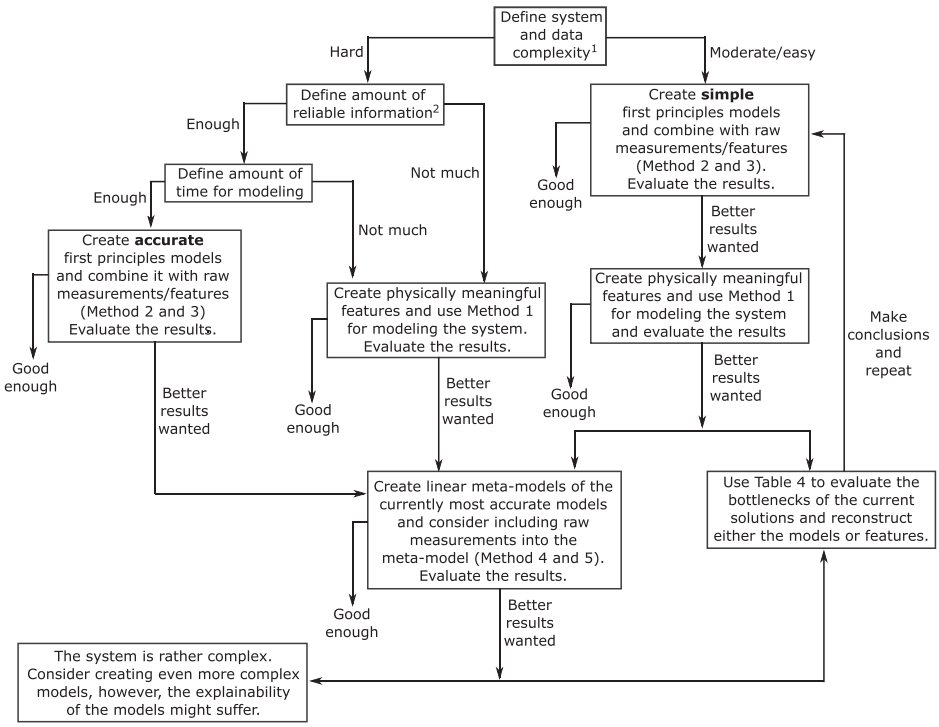

1 - The system complexity does not have a specific metric and should be defined by a domain knowledge expert. It may include the size of the system, complexity of the physical phenomenon, lack of physical understanding and first principles models for parts of the system, potential hidden patterns in the phenomenon, target variable behavior such as trend and distribution, etc.

2 - Amount of reliable information is case dependent and does not have a specific metric. It depends on the amount of noise in the data, outliers, number of measurements which are correlated with with the target variable, number of measurements which can be used to create first principles models, amount of data which can be obtained externally based on the process knowledge, etc.

Fig. 23. Summary of the method selection for process system modeling by combining first principles and machine learning models.

Table 5
RMSE summary for the conducted case studies. Underlined values - lowest error within the algorithm for each flowrate, bold values - lowest error for each flowrate within all algorithms, italic bold values - lowest mean error for each flowrate for all cases.

Case	Oil rate			Gas rate		
	XGBoost	MLP NN	LSTM	XGBoost	MLP NN	LSTM
Case 1	0.044	0.052	0.043	0.040	0.035	0.033
Case 2.1	0.056	0.054	0.060	0.045	0.041	0.038
Case 2.2	0.060	0.063	0.062	0.048	0.042	0.042
Case 2.3	0.064	0.040	0.061	0.035	0.031	0.030
Case 3.1	0.038	0.048	0.041	0.038	0.034	0.025
Case 3.2	0.042	0.047	0.043	0.036	0.031	0.023
Case 3.3	0.040	0.043	0.040	0.031	0.030	0.021
Case 4.1	0.037	0.038	0.045	0.028	0.027	0.020
Case 4.2	0.057	0.038	0.053	0.037	0.035	0.021
Case 4.3	0.047	0.045	0.040	0.030	0.028	0.023
Case 5	0.041	0.050	0.042	0.048	0.036	0.037
Case 6	**0.030**	0.031	0.041	0.024	0.023	**0.020**
Mean error	0.0463	***0.0458***	0.0476	0.0367	0.0328	***0.0278***

other possibility is to slightly pre-tune the model to the data, for instance, using a linear model, and then use in combination with machine learning. Finally, the complexity of the models can be increased, so that the model become able to better resolve the system behavior, for instance, in this case, this can be a slip model for the choke equation. However, still computational efficiency should be considered, so that the models should not become very complex. All these proposed improvements will lead to the fact that the solutions from the first principles model will be more accurate, as such the mismatch between the actual target value and the solution will be lower and easier to be covered by a machine learning algorithm.

Table 6
Summary of RMSE averaged over the algorithms for each method and each flowrate, e.g. choke oil RMSE of 0.0566 = (0.056 + 0.054 + 0.060)/3. Underlined values - the lowest error within each method for each flowrate, italic values - the lowest error among the methods *excluding* meta-models, bold values - lowest error for each flowrate among all methods.

Model	Method											
	Base method Raw data measurements as features		Method 1 Feature engineering		Method 2 First principles model solution + feature engineering		Method 3 First principles model solution + raw data model		Method 4 Linear meta-model of models with created features (Case 2 and 3)		Method 5 Linear meta-model of selected model with created features and raw data model (Case 4 and base case)	
	Oil	Gas	Oil	Gas	Oil	Gas	Oil	Gas	Oil	Gas	Oil	Gas
Choke (Case 2)	-	-	0.0566	0.0413	0.0616	0.0440	0.0550	0.0320	0.0443	0.0403	-	-
Tubing (Case 3)	-	-	0.0423	0.0323	<u>0.0440</u>	<u>0.0300</u>	<u>0.0410</u>	0.0273				
Choke and tubing (Case 4)	-	-	*<u>0.0400</u>*	*<u>0.0250</u>*	0.0467	0.0310	0.0440	<u>0.0270</u>	-	-	**0.0340**	**0.0223**
Raw data (base case)	0.0463	0.0360	-	-	-	-	-	-				

7. Conclusions

In this paper, we propose and analyze several methods for combining first principles models with machine learning applied to multiphase flowrate estimation problem in petroleum production systems. For the machine learning algorithms, MLP and LSTM neural networks and gradient boosting were chosen. The proposed methods for combining first principles with machine learning were applied to all the aforementioned algorithms. The algorithms were systematically tuned via a pipeline which is based on the Bayesian optimization approach which ensures fair and accurate model tuning and comparison.

We found that by introducing first principles models into machine learning algorithms, it becomes possible to improve the estimation performance if compared to approaches when raw measurement data is used directly, as it has been done for the considered problem in many other works reported in the literature. We found that for the irregular system behavior, it is better to use static models such as MLP neural networks or gradient boosting and not take past measurements into account. On the other hand, when the system behavior is less complex and has a time-dependent pattern, LSTM neural networks which consider the past measurements show the superior performance.

We discovered that linear meta-models which combine physics-aware machine learning algorithms with raw measurement models show the most accurate performance while maintaining good interpretability. Feature engineering method can also be a good choice to incorporate first principles into machine learning because it has lower development cost than linear meta-models while maintains a reasonable performance. The methods which combine first principles models solution with machine learning showed less accurate performance for complex system behavior than the meta-models and feature engineering approach, while in less complex system they were accurate enough. As such, to be applied for complex systems, the first principles models should be relatively accurate, such that they produce a reasonable solution and small mismatch between its solution and the true target value which can further be covered by machine learning algorithms.

Another important finding is that by introducing physics-based features into machine learning algorithms, it is possible to create much more interpretable models than models which use raw data directly. We showed that by using model-agnostic feature importance evaluation methods and revealing partial dependences between the features and the target, it is possible not only to ensure that the obtained machine learning model behaves physically feasible, but also reveal additional insights about the complex system behavior, hidden patterns, physical phenomena and identify possible directions for the model improvements.

Overall, we conclude that to successfully apply machine learning to complex process engineering systems in general and Virtual Flow Metering in particular, we need to incorporate first principles approaches into machine learning algorithms. This approach creates more accurate and, more importantly, more transparent data-driven solutions which will develop more trust to these systems among the operating professionals and will further contribute to a more efficient and reliable systems operation.

Declaration of Competing Interest

The authors declare that they have no known competing financial interests or personal relationships that could have appeared to influence the work reported in this paper.

Supplementary material

Supplementary material associated with this article can be found, in the online version, at doi:10.1016/j.compchemeng.2020.106834

CRediT authorship contribution statement

Timur Bikmukhametov: Writing - original draft, Writing - review & editing, Conceptualization, Methodology, Software, Formal analysis, Investigation. **Johannes Jäschke:** Writing - original draft, Supervision, Conceptualization.

References

Agarap, A.F., 2018. Deep learning using rectified linear units (relu). arXiv:1803.08375.
Ahmadi, M.A., Chen, Z., 2018. Comparison of machine learning methods for estimating permeability and porosity of oil reservoirs via petro-physical logs. Petroleum.
AL-Qutami, T.A., Ibrahim, R., Ismail, I., Ishak, M.A., 2017. Radial basis function network to predict gas flow rate in multiphase flow. In: Proceedings of the 9th International Conference on Machine Learning and Computing. ACM, pp. 141–146.
AL-Qutami, T.A., Ibrahim, R., Ismail, I., Ishak, M.A., 2018. Virtual multiphase flow metering using diverse neural network ensemble and adaptive simulated annealing. Expert Syst. Appl. 93, 72–85.
Andrianov, N., 2018. A machine learning approach for virtual flow metering and forecasting. IFAC-PapersOnLine 51 (8), 191–196.
Anifowose, F.A., Labadin, J., Abdulraheem, A., 2017. Hybrid intelligent systems in petroleum reservoir characterization and modeling: the journey so far and the challenges ahead. J. Pet. Explor. Prod. Technol. 7 (1), 251–263.
Berger-Tal, O., Nathan, J., Meron, E., Saltz, D., 2014. The exploration-exploitation dilemma: a multidisciplinary framework. PLoS ONE 9 (4), e95693.
Bhutani, N., Rangaiah, G., Ray, A., 2006. First-principles, data-based, and hybrid modeling and optimization of an industrial hydrocracking unit. Ind. Eng. Chem. Res. 45 (23), 7807–7816.
Bikmukhametov, T., Jäschke, J., 2019. First principles and machine learning virtual flow metering: a literature review. J. Petrol. Sci. Eng. 106487.
Bikmukhametov, T., Jäschke, J., 2019. Oil production monitoring using gradient boosting machine learning algorithm. IFAC-PapersOnLine 52 (1), 514–519.

Chen, T., Guestrin, C., 2016. Xgboost: A scalable tree boosting system. In: Proceedings of the 22nd ACM Sigkdd International Conference on Knowledge Discovery and data Mining. ACM, pp. 785–794.
Cheng, G., Peddinti, V., Povey, D., Manohar, V., Khudanpur, S., Yan, Y., 2017. An exploration of dropout with lstms.. In: Interspeech, pp. 1586–1590.
Chisholm, D., 1983. Two-phase flow in pipelines and heat exchangers. G. Godwin in association with Institution of Chemical Engineers.
Falcone, G., Hewitt, G., Alimonti, C., 2009. Multiphase flow metering: Principles and applications, 54. Elsevier.
Falcone, G., Hewitt, G., Alimonti, C., Harrison, B., et al., 2001. Multiphase flow metering: current trends and future developments. In: SPE Annual Technical Conference and Exhibition. Society of Petroleum Engineers.
Frazier, P.I., 2018. A tutorial on bayesian optimization arXiv:1807.02811.
Friedman, J.H., 2001. Greedy function approximation: a gradient boosting machine. Ann. Stat. 1189–1232.
Genuer, R., Poggi, J.-M., Tuleau-Malot, C., 2010. Variable selection using random forests. Pattern Recognit. Lett. 31 (14), 2225–2236.
Goodfellow, I., Bengio, Y., Courville, A., 2016. Deep Learning. MIT Press. http://www.deeplearningbook.org.
Greff, K., Srivastava, R.K., Koutník, J., Steunebrink, B.R., Schmidhuber, J., 2016. Lstm: a search space odyssey. IEEE Trans. Neural Netw. Learn. Syst. 28 (10), 2222–2232.
Hastie, T., Tibshirani, R., Friedman, J., Franklin, J., 2005. The elements of statistical learning: data mining, inference and prediction. Math. Intell. 27 (2), 83–85.
Hochreiter, S., Schmidhuber, J., 1997. Long short-term memory. Neural Comput. 9 (8), 1735–1780.
Hornik, K., Stinchcombe, M., White, H., 1989. Multilayer feedforward networks are universal approximators. Neural Netw. 2 (5), 359–366.
Idso, E.S., Sperle, I.L., Aasheim, R., Wold, M.S., et al., 2014. Automatic subsea deduction well testing for increased accuracy and reduced test time. In: Abu Dhabi International Petroleum Exhibition and Conference. Society of Petroleum Engineers.
Kanin, E., Osiptsov, A., Vainshtein, A., Burnaev, E., 2019. A predictive model for steady-state multiphase pipe flow: machine learning on lab data. J. Petrol. Sci. Eng. 180, 727–746.
Kingma, D. P., Ba, J., 2014. Adam: A method for stochastic optimization arXiv:1412.6980.
Klyuchnikov, N., Zaytsev, A., Gruzdev, A., Ovchinnikov, G., Antipova, K., Ismailova, L., Muravleva, E., Burnaev, E., Semenikhin, A., Cherepanov, A., et al., 2019. Data–driven model for the identification of the rock type at a drilling bit. J. Petrol. Sci. Eng. 178, 506–516.
Kramer, A., Choudhary, P., et al., 2018. Skater: Python library for model interpretation/explanations. https://github.com/oracle/Skater.
Liu, X., Faes, L., Kale, A.U., Wagner, S.K., Fu, D.J., Bruynseels, A., Mahendiran, T., Moraes, G., Shamdas, M., Kern, C., et al., 2019. A comparison of deep learning performance against health-care professionals in detecting diseases from medical imaging: a systematic review and meta-analysis. Lancet Digit. Health 1 (6), e271–e297.
Loh, K., Omrani, P. S., van der Linden, R., 2018. Deep learning and data assimilation for real-time production prediction in natural gas wells arXiv:1802.05141.
Lunde, G.G., Rudrum, G., Angelo, P., Holmas, K., Setyadi, G.R., et al., 2013. Ormen lange flow assurance system (fas)-online flow assurance monitoring and advice. In: OTC Brasil. Offshore Technology Conference.
Masella, J., Tran, Q., Ferre, D., Pauchon, C., 1998. Transient simulation of two-phase flows in pipes. Int. J. Multiphase Flow 24 (5), 739–755.
Matzopoulos, M., 2011. Dynamic process modeling: combining models and experimental data to solve industrial problems. Process Syst. Eng. 7, 1–33.
Molnar, C., Casalicchio, G., Bischl, B., 2018. Iml: an r package for interpretable machine learning.. J. Open Sour. Softw. 3 (26), 786.
Onwuchekwa, C., et al., 2018. Application of machine learning ideas to reservoir fluid properties estimation. In: SPE Nigeria Annual International Conference and Exhibition. Society of Petroleum Engineers.
Patel, P., Odden, H., Djoric, B., Garner, R.D., Vea, H.K., et al., 2014. Model based multiphase metering and production allocation. In: Offshore Technology Conference-Asia. Offshore Technology Conference.
Psichogios, D.C., Ungar, L.H., 1992. A hybrid neural network-first principles approach to process modeling. AIChE J. 38 (10), 1499–1511.
Qin, S.J., Chiang, L.H., 2019. Advances and opportunities in machine learning for process data analytics. Comput. Chemi. Eng. 126, 465–473.
Rasmussen, C.E., Williams, C., 2017. Gaussian processes for machine learning. 2006. Cited on 95.
Ribeiro, M.T., Singh, S., Guestrin, C., 2016. Why should i trust you?: Explaining the predictions of any classifier. In: Proceedings of the 22nd ACM SIGKDD international conference on knowledge discovery and data mining. ACM, pp. 1135–1144.
Roscher, R., Bohn, B., Duarte, M. F., Garcke, J., 2019. Explainable machine learning for scientific insights and discoveries arXiv:1905.08883.
Rumelhart, D.E., Hinton, G.E., Williams, R.J., et al., 1988. Learning representations by back-propagating errors. Cognit. Model. 5 (3), 1.
Schuller, R.B., Munaweera, S.J., Selmer-Olsen, S., Solbakken, T., et al., 2006. Critical and sub-critical oil/gas/water mass flow rate experiments and predictions for chokes. SPE Prod. Oper. 21 (03), 372–380.
Shang, C., You, F., 2019. Data analytics and machine learning for smart process manufacturing: recent advances and perspectives in the big data era. Engineering.
Shoeibi Omrani, P., Dobrovolschi, I., Belfroid, S., Kronberger, P., Munoz, E., et al., 2018. Improving the accuracy of virtual flow metering and back-allocation through machine learning. In: Abu Dhabi International Petroleum Exhibition & Conference. Society of Petroleum Engineers.
Soave, G., 1972. Equilibrium constants from a modified redlich-kwong equation of state. Chem. Eng. Sci. 27 (6), 1197–1203.
Sun, J., Ma, X., Kazi, M., et al., 2018. Comparison of decline curve analysis dca with recursive neural networks rnn for production forecast of multiple wells. SPE Western Regional Meeting. Society of Petroleum Engineers.
Wolpert, D.H., Macready, W.G., et al., 1997. No free lunch theorems for optimization. IEEE Trans. Evol. Comput. 1 (1), 67–82.
Zangl, G., Hermann, R., Schweiger, C., et al., 2014. Comparison of methods for stochastic multiphase flow rate estimation. In: SPE Annual Technical Conference and Exhibition. Society of Petroleum Engineers.

3.4 Discussion of Paper III - Combining Machine Learning and Process Engineering Physics Towards Enhanced Accuracy and Explainability of Data-Driven Models

In Paper III, we considered a multiphase flow estimation problem as an application example of the proposed framework of combining machine learning with process engineering physics. At the same time, as emphasized in the introduction of the paper, the main focus and contributions aimed to be delivered are the general framework of hybrid modelling as well as an attempt to show how this approach can make data-driven models more transparent. As such, deeper details of the considered system are not thoroughly discussed. However, it is also possible that features of the system and its behavior can be of interest for petroleum engineering domain experts, so that it is important to discuss these features in more detail, so this section is intended for this discussion.

3.4.1 Flow conditions discussion

As pointed out in Section 3.1 of the paper, all the data used for model training are $real$, meaning that it was provided by one of the operators of an oil and gas field on the Norwegian Continental Shelf. Since the data was not generated artificially using a multiphase flow simulator, the exact conditions of the well production behavior can only roughly be estimated, purely based on the provided data without additional insights on the transient phenomena development along the well tubing or the production choke. For instance, it is hard to determine if the considered flowrates represent gravity or friction dominated flow conditions.

To deeper understand the challenges of the considered problem, we first analyze dynamic conditions and its time scale for training, validation and test sets. To do this, we use the steady state detection algorithm proposed by Dalheim and Steen (2020). The idea behind the algorithm is that any process signal can be modeled as a linear trend function within a specified time window and has the following form:

$$z_t = b_0 + b_1 t + a_t \tag{3.1}$$

where z_t denotes the signal value, b_0 - the intercept of the linear trend, b_1 - the trend slope, t - the time instance, a_t - the white noise.

In the method, the intercept and the slope are computed over the specified time window and then the standard deviations of the noise and the slope are determined. Then, the null hypothesis stating that the process signal is stationary about the time window intercept b_0 is tested against the two-tailed value of the Student's statistic. Within the algorithm, we assume that steady state is achieved when 90% of the

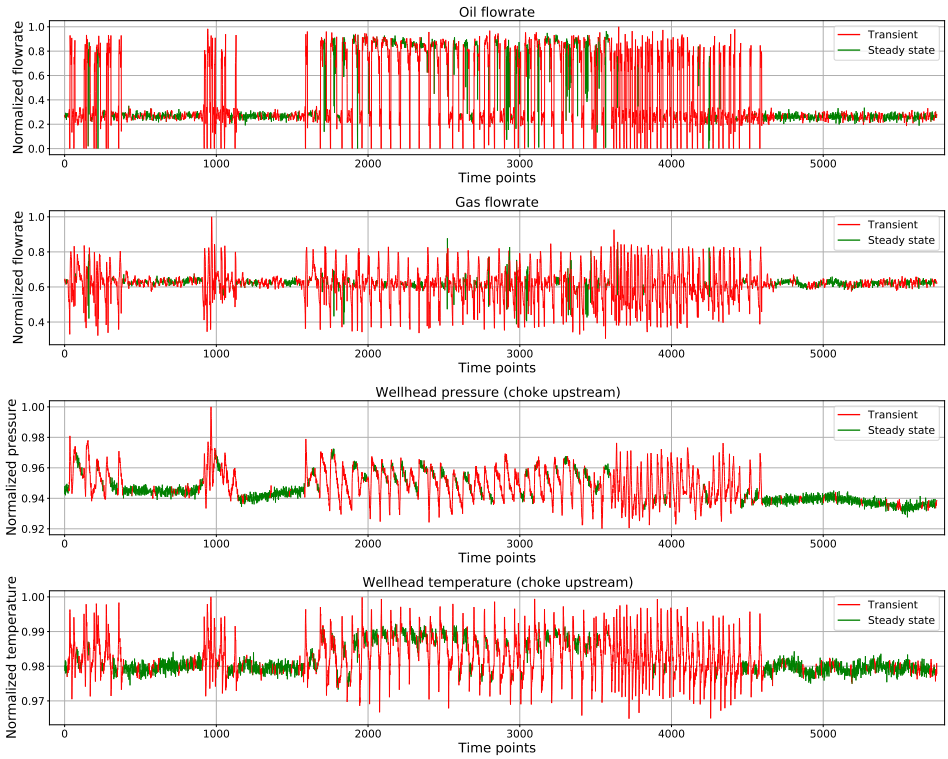

Figure 3.4: Assessment of the used steady state detection algorithm using a 10 min time window

points inside the time window is steady. Using this assumption, each point is evaluated n times (equal to the window size) due to the sliding window approach. Then, the number of times when each point is evaluated to be at steady state is counted. Finally, again assuming that 90% of out n times the point is evaluated to be at steady state, we assign the condition (steady state or transient) that is determined for the particular point. As stated in Dalheim and Steen (2020), the percentage at which the point should be considered to be at steady or transient states highly depends on the application. In this case, several thresholds have been tested for different time window lengths and 90% appeared to be a reasonable value.

To exemplify the ability of this method to identify steady state regions of the flowrates, pressure and temperature signals of the considered multiphase flow problem using the assumed thresholds, a time segment of four days is selected within the training set of the data. The window length of 10 points (10 minutes)

	Window length (min)				
Dataset	5	10	15	30	60
Training	0%	55.4%	77.1%	91.6%	95.1%
Validation	0%	47.9%	73.1%	92.9%	96.9%
Test	0%	64.3%	91.9%	99.1%	99.6%
Whole dataset	0%	54.7%	79.2%	93.8%	96.8%

Table 3.1: Fraction of steady state conditions for the oil flowrate relative to the considered dataset size and different window lengths

is selected for this initial assessment. Figure 3.4 shows the obtained results for oil and gas flowrates as well as wellhead pressure and temperature measurements.

In the figure, we see that in most of the cases the steady state and transient regions are very similar along the time axis for all the evaluated parameters. What is also essential is the fact that the transient regions that can be assessed visually are also evaluated as dynamic by the steady state detection algorithm. The steady state regions are also reasonably well determined. Moreover, we see that between the highly transient regions, steady state regions are also detected. This can be well seen, for instance, in the range of 2000-3000 time points. This observation additionally proves that the used algorithm with the made assumptions is adequate in identifying the states of the system, because it does not overlook potentially steady state conditions inside generally dynamic conditions. In some cases, potentially transient regions are treated as steady state, but the general behavior of the algorithm is considered as satisfactory.

To investigate the behavior of the system along the entire dataset, this algorithm is applied for the oil and gas flowrates as an example within the whole dataset and training, validation and test set separately. We compute the fraction of steady state conditions for each case using different window lengths. The simulations results for the oil flowrate are shown in Table 3.1

From the table, we can make several observations. First, we see that the test set has larger steady state fractions for all window lengths if compared to the training and validation sets. Secondly, at the window length of 30 min, for all the cases the steady state fraction reaches 90% and higher which means that it can be said that generally the system can be considered to be at steady state within the time scale of 30 min. However, even at 15 min the fraction is almost 80% (and almost 92% for the test case) which is also high and one can assume that the system is close to steady state within the time scale of 15 min. Finally, we see that within the time window of 5 min, none of the datasets reaches steady state conditions.

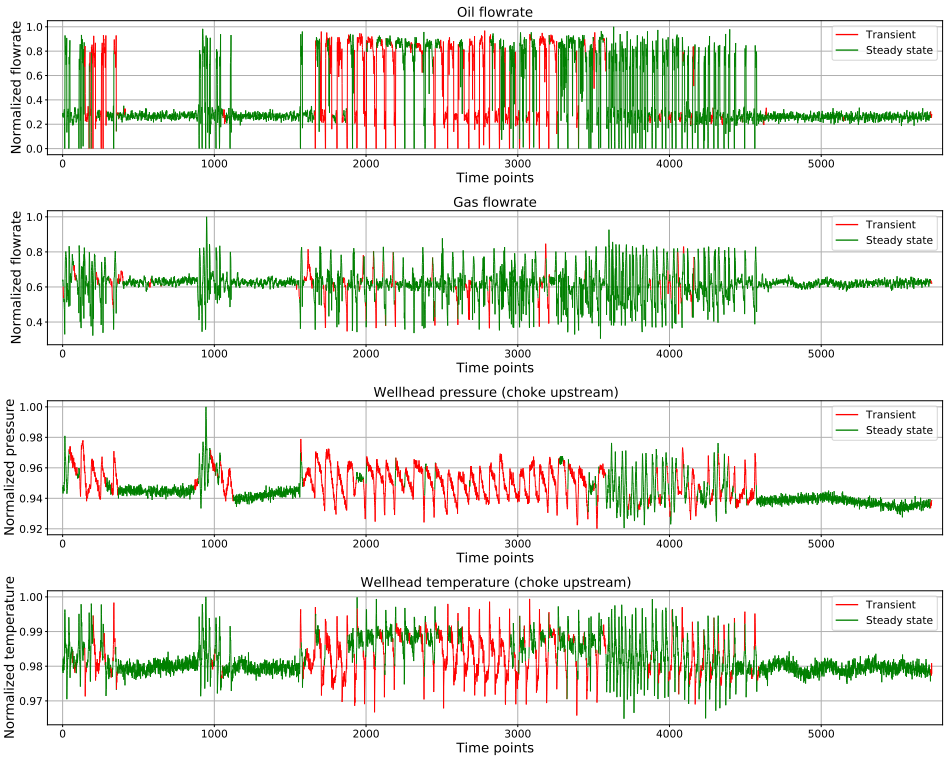

Figure 3.5: Assessment of the used steady state detection algorithm for 30 min time window

	Window length (min)				
Dataset	5	10	15	30	60
Training	0%	43.8%	61.6%	91.1%	91.5%
Validation	0%	37.9%	59.5%	91.5%	92.9%
Test	0%	63.9%	83.3%	94.4%	96.4%
Whole dataset	0%	46.3%	66.1%	92.1%	93.2%

Table 3.2: Fraction of steady state conditions for the gas flowrate relative to the considered dataset size and different window lengths

Table 3.2 shows the same simulation results but for the gas flowrate. Within the table we observe similar trends and the magnitude of values if compared to the oil flowrate results. However, we see that the steady state fractions for the gas flowrate are generally lower than for the oil flowrate for the same window lengths.

Overall, based on the visual assessment and the simulations results shown in Table 3.1 and 3.2, we can conclude that the adequate timescale to describe the dynamics of the system is somewhere in the range between 10 and 20 min, and 15 min can be considered as a good average value. A smaller time scale, for instance, 5 min, resulted in the fact that no steady state presents in the data, while in Figure 3.4 we can clearly identify steady state regions which are similar for the flow, pressure and temperature measurements. At the same time, the larger time scales overestimate the fraction of steady state conditions. This conclusion is made based on the assessment of the same data range as in Figure 3.4 but for the time scale of 30 min. The results of the simulations are shown in Figure 3.5. In the figure we see that some of the regions which are clearly unsteady are treated as steady, for instance, around the 1000^{th} time point and between the 3000^{th} and 4000^{th} time points.

3.4.2 Additional discussion on simulation results by hybrid machine learning algorithms

Provided the new analysis of the flow conditions above, we would like to additionally discuss some of the obtained simulation results to dig deeper into the abilities of hybrid machine learning algorithms in estimating process engineering parameters. However, before this, it is important to mention the information about the fluid and system characteristics that are not well-described in the paper. Despite the fact that we considered only oil and gas flowrates for the flow estimation problem, the water phase is also present in the multiphase flow. Based on the information on the estimated flow by the multiphase flow meters, it has been determined that the average value of the local water cut (WC) at the multiphase flowrate conditions is 0.55 with standard deviation of 0.16. The Gas-Oil ratio (GOR) at standard conditions is not known, but the average local gas volume fraction is 0.29 with standard deviation of 0.05. Another point that is not well-mentioned in the paper but that most likely has an impact on the result is the choke level information. The mean value of the choke opening is 0.62 and during most of the operation time the choke position is constant while the pressure drop over the choke can significantly fluctuate around the mean value of 6.53 bar and the standard deviation of 3.1 bar.

Influence of flow conditions on choke model-based algorithms. As discussed in the paper, the choke model-based models for all the cases and machine learning algorithms perform worse when compared to the tubing-based models and combined models with tubing and choke features together. One of the discussed points why this can be the case was the fact that we used a simple choke model which does not take into account more complex effects such as gas slip. Considering the fact that the mean gas volume fraction is relatively high as discussed above, the can

indeed affect the performance of the model. However, this assumption was not tested in the paper and was left for future work. In the additional analysis, we have checked this assumption and found that by introducing the slip effect through the Chisholm slip model (Chisholm (1985)), no noticeable improvement is observed and the feature of the mixture mass flow through the choke with and without slip for the oil rate target has the Spearman correlation of 0.16 and the Pearson correlation of 0.12. The difference between the models with and without the slip effect in the correlation values was in the order of 0.001 which is negligible. As such, it is not expected to have better predictive capabilities. Also, the correlation values themselves are small which additionally proves the obtained results with low accuracy of choke-based models.

However, the main reason why the choke model does not work well is the fact that the oil rate has very small correlation values of 0.02 relative to the pressure drop over the choke and the liquid rate (oil + water) has the correlation values about 0.3 which is still not high. This, in turn, results in low correlation for the mixture mass rate feature discussed above. In addition, we observed that the pressure across the choke fluctuates quite significantly while the choke opening is constant. All these facts result in a low accuracy of the choke-based machine learning models.

Influence of flow conditions on steady vs transient machine learning models. As we discussed in the paper, for the oil rate, gradient boosting and feed-forward neural networks showed a better predictive performance when compared to the LSTM-based models while for the gas rate, LSTM neural networks were better. Our visual assessment of the level of instabilities and dynamic conditions mentioned in the paper was wrong because it seemed that the oil rate fluctuations are larger and more frequent. However, as we see in Table 3.1 and 3.2, the gas rate has smaller fractions of steady state conditions along the dataset, and the difference is noticeable for the window lengths that are concluded to be representable (10-15 min).

At the same time, the newly obtained results for the steady state detection algorithm additionally prove the simulation results presented in the paper, meaning that the LSTM neural networks should perform better in simulating a dynamic system environment, since it is expected to track the influence of the past state on the current state. Also, as mentioned in the paper, the window sizes selected by the Bayesian Optimization algorithm were, in general, between 10 and 15 steps (minutes) which seems reasonable based on the results obtained by the steady state detection algorithm that also estimates the descriptive time scale of the system within a similar range.

In addition to the time scale of the multiphase phenomena, we can also assess the

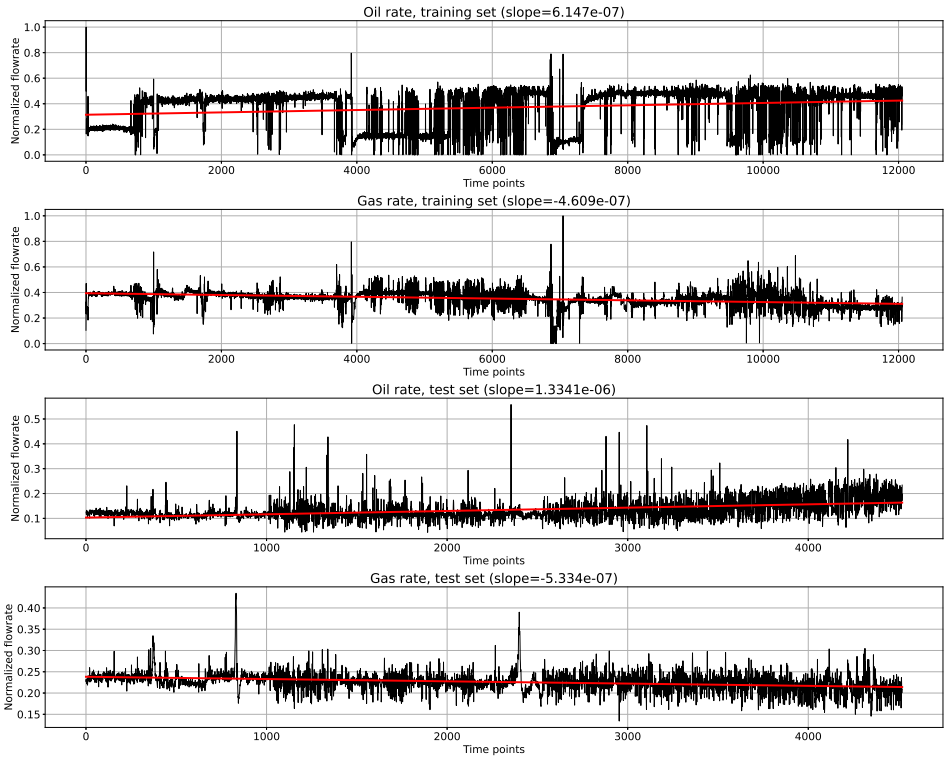

Figure 3.6: Linear slopes of the oil and gas rates on the training and test sets

long time dependency for the training and test ranges of the dataset for both target variables. In the paper, we did not consider such an analysis closely. In Figure 3.6, we plot every 15^{th} value for the training set and every 10^{th} value for the test set of the variables and the linear regression line that represents the time declining trend. The downsampling is made for visualization purposes.

From the figure we see that the slope for the gas rate for both training and tests are very similar (around 15% difference), while the long-term time trend of the oil rate differs by more than 50%. Moreover, when de-trending the long-term time flowrate dependency (i.e. subtracting the linearly regressed value from the data), the distributions of the data for the gas rate are similar for the training and test sets, while for the oil rate they are very different. The distributions are shown in Figure 3.7. We see that none of the modes observed in the training set for the oil rate is close to the mean/median observed in the test set. This means that if the linear trend is well-captured by a machine learning model in the training for the gas rate, it is relatively easy to make accurate regression on the test set, which

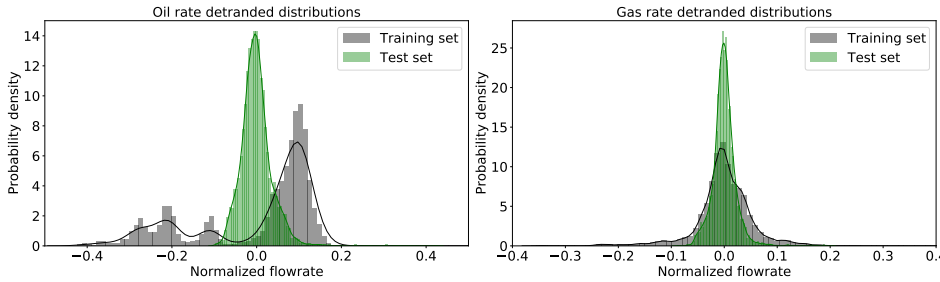

Figure 3.7: Distributions of the flowrate data when the linear time trend is removed

is not the same for the oil rate. Since LSTM takes into account not only short, but the long-term phenomena as well, it is capable to reconstruct the trend in the test set for the gas rate well using choke and tubing models alone, as it can be seen in Fig. 22 in the paper. The static algorithms, however, are not accurate in such trend representing. As for the oil rate, all the algorithms have difficulties in reconstructing the trends using only choke and tubing models alone, until more complex models are made.

As such, we conclude that the results obtained in the paper are consistent with what we observe when we digging deeper into different timescales of the system behavior. We see that the window length selected by the Bayesian Optimization is similar to the time scale of the system obtained through the evaluation of the data by the steady state detection algorithm. We also revealed additional confirmations why LSTM performed well for gas rate prediction and found out that this machine learning algorithm is powerful in capturing short and long time scale phenomena of process engineering systems provided that the system behavior is consistent in time.

3.4.3 Discussion on PVT properties and its influence on the flowrate estimates

As we discussed in the paper, the fluid composition was given to perform estimation. However, the accuracy of this composition was under doubts, as such the computed phase properties that are used for the first principles models that are combined with machine learning algorithms are not expected to be accurate. On the other hard, as we discussed in Section 2.1 of this thesis, multiphase flow meter estimates also depend on accuracy of the PVT data. As such, it can be argued that we fit our hybrid machine learning models to potentially wrong flowrates produced by the multiphase flow meter.

In principle, this is a valid argument, however, there are several reasons on why we try to avoid using the provided fluid composition. First of all, since the data considered for estimation in Paper III are real, the provider of the data was not completely sure that the given PVT data is the one used for computing the volumetric flowrates by the multiphase flow meter. It was said that this fluid composition can be considered as a reasonable one, but there is no assurance that this exact composition has been used for multiphase flow estimation by the MPFM, and also the composition was taken long time ago. This is why we claimed that the PVT properties that are computed using the given composition can be inaccurate.

Another interesting point is that, as we found out in Section 2.1 of this thesis, the influence of errors in PVT properties can be more severe for Virtual Flow Meters than for MPFMs. This analysis has been conducted after the paper was published, but now it can be considered as an additional argument for avoiding the usage of erroneous fluid properties for hybrid VFM models. Of course, in our approach in Paper III, we consider a totally different VFM system if compared to the one used in Section 2.1, and the conclusions obtained in the discussion in Section 2.1 cannot be directly related to the models in Paper III. On the other hand, if we consider the models in Eq. 13 and 15 of Paper III, the results are proportional to $\sqrt{rho_{mix}}$. This can lead to roughly 3% error, if assume that the densities are biased by 10%, as we did in Section 2.1. If we would have multiplied it by a wrongly computed phase fraction, we could introduced an additional error. Again, this analysis has not been done in the paper, but can be considered as an additional argument for avoiding an extensive use of potentially wrong PVT data for hybrid VFM systems.

The last but not the least, in the paper, we tried to consider a general framework of hybrid machine learning modeling. This means that the Virtual Flow Metering has been taken as an example for testing the proposed framework out. As such, the example of uncertain PVT properties was also inspired by the fact that in many process engineering systems the properties of the processed medium might not be fully available. We are aware that such assumptions might seem slightly artificial for the provided example of VFM since the target variable can also be influenced by wrong fluid properties. However, if assuming that the flowrates are measured relatively accurately, we proved that by using the models that reflect the general behavior of the system and avoiding unnecessary errors, it is possible to obtain good estimation results in process engineering systems suing hybrid machine learning models.

References

Chisholm, D., 1985. Two-phase flow in heat exchangers and pipelines. Heat transfer engineering 6, 48–57.

Dalheim, Ø.Ø., Steen, S., 2020. A computationally efficient method for identification of steady state in time series data from ship monitoring. Journal of Ocean Engineering and Science .

Chapter 4

Estimation of Uncertainties of First Principles Multiphase Flow Models Using Sensitivities and Bayesian Machine Learning

This chapter consists of two papers. Paper IV describes the sensitivity analysis of a first principles-based Virtual Flow Meter with respect to the measurement noise, drift and simplicity of heat transfer modeling of a well tubing. Paper V describes applications of Bayesian Machine Learning for tuning first principles models based on a case study of a three-phase pipe flow model.

4.1 Statistical Analysis of Effect of Sensor Degradation and Heat Transfer Modeling on Multiphase Flowrate Estimates from a Virtual Flow Meter (Paper IV)

Paper IV describes the sensitivity analysis of a first principles-based Virtual Flow Meter with respect to the measurement noise, drift and simplicity of heat transfer modeling of a well tubing. It exemplifies the importance of model re-calibration and the need for measurement drift handling in multiphase flowrate estimation systems. The main motivation for this paper was to see how the first principles-based Virtual Flow Metering systems react to the uncertainties in measurements such as noise and drift as it is usually present in real field applications, but such analysis has not been conducted before. In addition, it was interesting to see which kind of simplifications are possible to make for the first principles Virtual Flow Metering systems in terms of heat transfer modeling because the rigorous approach requires a lot of effort and simplifications of this process are desirable.

Bikmukhametov, T., Stanko, M., and Jäschke, J. (2018). Statistical Analysis of Effect of Sensor Degradation and Heat Transfer Modeling on Multiphase Flowrate Estimates from a Virtual Flow Meter. SPE Asia Pacific Oil and Gas Conference and Exhibition. Society of Petroleum Engineers, doi.org/10.2118/191962-MS

Society of Petroleum Engineers

SPE-191962-MS

Statistical Analysis of Effect of Sensor Degradation and Heat Transfer Modeling on Multiphase Flowrate Estimates from a Virtual Flow Meter

Timur Bikmukhametov, Milan Stanko, and Johannes Jäschke, Norwegian University of Science and Technology

This paper was prepared for presentation at the SPE Asia Pacific Oil & Gas Conference and Exhibition held in Brisbane, Australia, 23–25 October 2018.

Abstract

Accurate flowrate measurements in petroleum production systems are important for optimization, fiscal metering, and production allocation. Sometimes, Virtual Flow Meters (VFMs) are used for this purpose instead of physical meters to reduce cost. These systems estimate the flowrates using a computational model that represents accurately the production system of interest. Since VFM systems mostly rely on pressure and temperature measurements, it is important to understand how accuracy and degradation of sensors influence the VFM flowrate estimates.

In this work, a VFM system for a subsea oil well was created using a transient multiphase model built in a commercial software and controlled from an external computational routine. A statistical analysis of VFM simulation results was performed to quantify the effect of pressure sensors degradation on the VFM flowrate estimates. In addition, the effect of temperature matching and a segmented approach to represent the well heat transfer were evaluated.

The analysis showed that the sensor degradation effect should be considered in VFM systems carefully, especially if a high estimation accuracy is required. Measurement drift was found to be the most critical factor of the sensor degradation but high measurement noise can also cause considerable errors of the flowrate estimates. In addition, it was found that a complex representation of the wellbore heat transfer is not required to obtain accurate flowrate predictions and simplified models can be used instead.

Introduction

In oil and gas production, continuous information about oil, gas and water flowrates from each well is important for production optimization, rate allocation and reservoir management (Falcone et al. 2001). In offshore field developments, it is often the case that the field has shared licenses so that accurate estimates of the produced volume of hydrocarbons are essential to determine partner share. This case also holds for smaller subsea fields which are tied-in with the existing infrastructures.

In addition to the conventional approach of flowrate estimation using well test separators, physical multiphase flow meters (MPFM) are used for this purpose (Falcone et al. 2009). The advantage of the multiphase flow meters is the fact that they can measure flowrates without separating the oil, gas and water streams first as it is typically performed in test separators. By mounting them inline on the wellhead, there

is no need to re-route well production to perform the testing, thus, measurements can be often obtained in real-time. On the other hand, these devices are expensive and exposed to failures and degradation which requires costly interventions for repair or replacement of the meters (Patel et al. 2014).

Another alternative is Virtual Flow Metering. This technology uses measurements from sensors (typically pressure and temperature) together with a numerical model of the system to estimate flowrates. Depending on the extension and type of the model, it usually requires some information about physical parameters of the system (e.g. pipe size, fluid properties, thermodynamic behavior and choke opening) as presented by Holmås and Løvli (2011) and Melbø et al. (2003). By combining all this information, it is possible to estimate the flowrates of oil, gas and water by modeling specific parts of the production system such as wellbore, choke, near-well region or using a combination of these models (Haldipur and Metcalf 2008). The discrepancies between the estimated and reference parameters can be minimized using an optimization algorithm (Holmås and Løvli 2011).

Since Virtual Flow Meters rely on sensor readings for real-time flowrate estimation, it is important to understand the influence of the sensors accuracy on the flowrate predictions. In general, sensors in oil and gas wells are exposed to harsh conditions such as high pressure and temperature, sand erosion and scaling. This is particularly true for downhole sensors. Such conditions cause mechanical degradation which increases the measurement noise and drift. (Kikani et al. 1997). As such, one of the questions addressed in this paper is how the sensor degradation impacts the VFM flowrate estimates. A somewhat similar question was addressed by Tangen et al. (2017) and Lansangan (2012). In both cases, the authors introduced an error to the measurements and estimated the VFM accuracy. However, in the analysis only extreme values were considerd, i.e. only the maximum deviations of the flowrates were calculated for specific values of the measurement errors.

In this paper, in addition to the extreme values, we estimate the entire probabilistic distribution of the flowrates and compare the distribution parameters under various measurement errors to estimate the trend. To do this, we performed multiple simulations under random measurement errors and evaluated the results using statistical methods. The results of this analysis can contribute to a deeper understanding by VFM customers about the effect of the measurement error on the flowrate estimates, such that they can evaluate when this effect is important and should be considered during the field operation.

Another aspect which can influence the precision of the flowrate estimates is the fidelity of the applied models. For example, in a VFM system we can assume that the heat transfer coefficient is constant along the wellbore and then use it as a tuning parameter to fit a specific temperature at the wellhead. However, in reality the heat transfer coefficient varies along the wellbore due to the mechanical structure of the well. In this paper, we consider both constant and varying heat transfer coefficients for the heat transfer VFM part to study the difference between the approaches. The results from this study can contribute to optimization of VFM tuning strategies in terms of accuracy and computational time.

Well architecture and fluid properties

In this study, we consider a subsea oil well. The well consists of a conductor, surface, intermediate and production casings, liner and tubing. Fig. 1 shows the well profile and the mechanical structure, fluid properties and formation parameters. For the heat transfer modeling study, the well is divided into 5 sections based on the number of layers in a particular section. The walls of the tubing pipes with thickness ω_j are shown in black color, cement is represented in grey and mud in yellow. All radial distances from the well center line are shown as R_j.

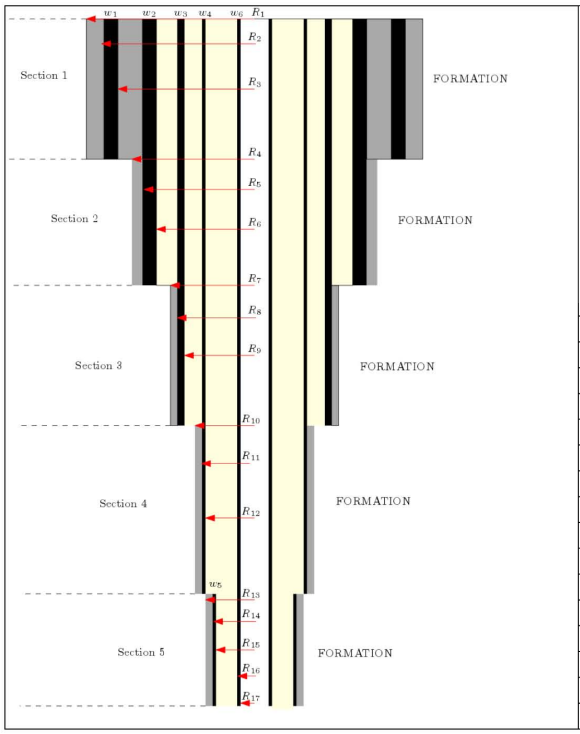

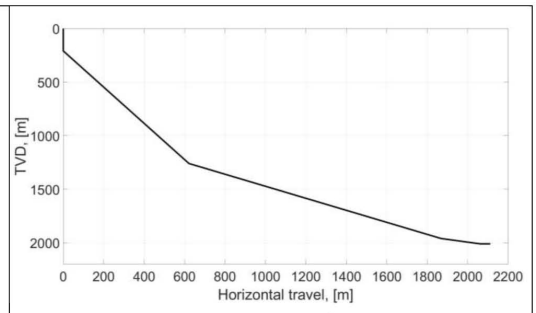

Parameter	Value
GOR, Sm^3/Sm^3	153.7
WC, %	30
Total well length, m	3110
Tubing inner diameter, m	0.0622
Bottomhole pressure, bar	160
Wellhead pressure, bar	40
Bottomhole temperature, ^{0} C	70
Wellhead temperature, ^{0} C	57
Reservoir temperature, ^{0} C	70
Seabed temperature, ^{0} C	8
Formation heat conductivity, W/m.K	1.5912
Wall heat conductivity, W/m.K	45.2573
Cement heat conductivity, W/m.K	0.98
Mud heat conductivity, W/m.K	0.6054
Formation heat diffusivity, m^2/h	0.003716

Figure 1—Well architecture, fluid properties and system parameters

The model employed in the VFM scheme considers only the flow in the tubing, so that we do not include choke simulations. As such, we utilize the following measurements:

- Bottomhole pressure (P_{wf})
- Bottomhole temperature (T_{wf})
- Wellhead pressure (P_{wh})
- Wellhead temperature (T_{wh})

One of the most common fluid characterization software package was used to generate fluid properties based on a given composition using an equation of state. The bottomhole temperature is assumed to be equal to the reservoir temperature. The geothermal gradient is linearly interpolated from the reservoir to the seabed conditions.

VFM system

The VFM system employed consists of two parts: a model of the physical system and an optimization algorithm. The model is built in such a way that some of the parameters that are measured are an output, and the flowrate is an input, thus the optimization solver is employed to obtain the flowrate that minimizes the difference between measured and predicted values. To link the multiphase solver and the optimizer, we use an OPC server. The main goal of this tool is to read signals from one software and transfer it to another one. A schematic representation of the constructed VFM tool is shown in Fig. 2 on the left.

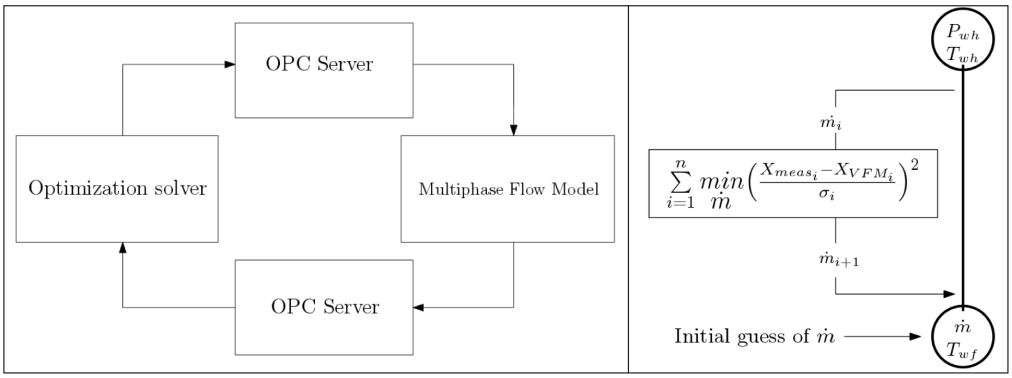

Figure 2—Schematic representation of the VFM system (left) and computational procedure (right). (To start the computational procedure, we introduce an initial guess of the flowrate to the multiphase flow solver which computes the associated wellhead temperature and bottomhole pressure. Then, these values go to the optimization solver which computes the finite difference gradients and iteratively changes the flowrate value until the minimum of the cost function is reached.)

In the multiphase flow solver, for given pressures and temperatures we run transient multiphase flow simulations until they reach a steady state. In the optimization routine, we use the interior-point numerical optimization algorithm to find a flowrate that minimizes an objective function of the following form:

$$\sum_i \left(\frac{X_{meas\,i} - X_{VFM\,i}}{\sigma_i} \right)^2 \tag{1}$$

where $X_{meas\,i}$ denotes measured value, $X_{VFM\,i}$- the predicted value, σ_i – the measurement uncertainty, i – the measurement index.

The computational procedure is shown in Fig. 2 on the right. To initiate the procedure, we introduce an initial guess in the mass source node. Then, the optimization solver iteratively computes finite difference gradients and adjusts the flowrate until the cost converges to a minimum.

Methodology and case studies

Sensor degradation study

Problem description and simulation procedure. Sensor degradation can result in an error growth and possible sensor failure. Two typical measurement error types are noise and drift. In this work, we evaluate quantitatively the effects these errors have on the estimation of flowrates when using a VFM scheme. This was performed explicitly by randomly varying the measurement values within a pre-defined error band. In addition, we study the effect of the sensors failure. As such, we consider the following case studies:

- Case 1: Effect of noise increase in pressure and temperature sensors
- Case 2: Effect of sensor drift in pressure and temperature sensors
- Case 3: Effect of the temperature sensors failure

The problem in all the cases is the fact that we never know the exact value of the measured quantity. Due to noise, the measurement can have any value within the sensor accuracy. Thus, to evaluate the potential spread of VFM flowrate estimates due to the measurement error, we evaluate the random combinations of pressure and temperature measurement values within specified accuracy. Since each simulation takes a considerable computational time due to the optimization routine, we cannot run a very large number of

simulations. Therefore, it is decided to run 200 simulations for each sub-case (which are discussed in details in the next section) and evaluate the flowrates' probability distributions using a statistical analysis.

Fig.3 shows the simulation procedure for the sensor degradation study. To generate a good initial guess of the flowrate estimate, first, we compute the maximum and minimum possible values of pressures and temperatures. These values are computed from the sensor accuracy range. For instance, if the actual pressure value is 100 bar and the noise error is 1%, the minimum pressure value is 99 bar and the maximum value is 101 bar. These values are used to estimate the maximum and minimum possible flowrates which are averaged for the initial guess to the optimization algorithm. Starting from the initial guess, the system iteratively finds the mass flowrate which makes the difference between the VFM predictions and the wellhead temperature and bottomhole pressure to reach a minimum. The mass flowrate is used for tuning instead of the volumetric flowrates due to the limitations in the commercial multiphase flow simulator employed.

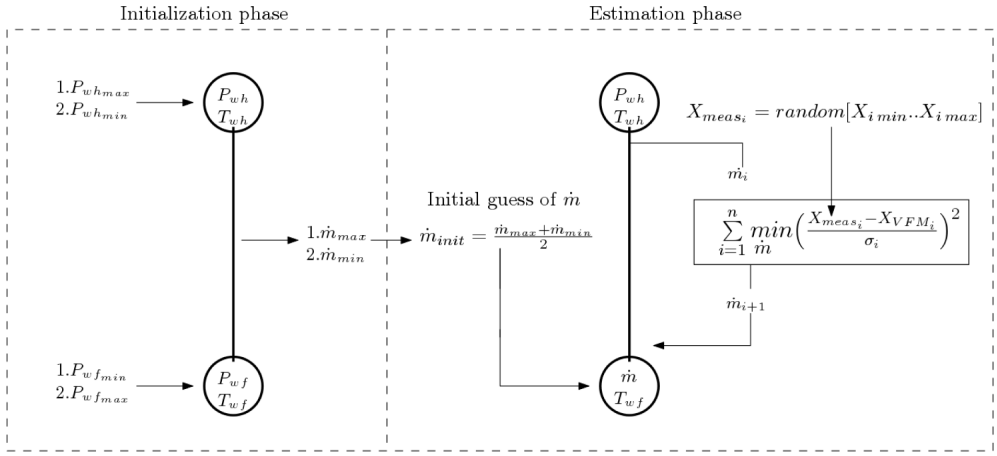

Figure 3—Simulation procedure for the sensor degradation study (In the initialization phase, we compute the maximum and minimum measurement values from the accuracy range which are used to estimate maximum and minimum possible flowrates. These flowrates are averaged to generate a good initial guess of the flowrate for the estimation phase. In the estimation phase, the flowrate is iteratively adjusted by the optimizer until the cost function reaches the minimum.)

Case 1 (Effect of measurement noise). To study the effect of noise on the VFM estimates, we consider three cases:

- Case 1.1: 0.5% noise error – base case
- Case 1.2: 1% noise error
- Case 1.3: 1.5% noise error

The value of the error (0.5%, 1% or 1.5%) represents the maximum possible error in the measurements. For instance, if the actual pressure value is 100 bar and the noise error is 1%, the possible measurement readings are within the interval of 99-101 bar. The noise error values depend on the sensors quality and particular operation conditions, as such the selected values are chosen without any direct reference. The main goal is to quantify the effect of the magnitude of the signal variation band on the flowrate predictions and estimate the associated trend. Also, we do not consider noise filtering because even the filtered signal will have the deviation error which can increase due to the degradation.

Case 1.1 is considered as the base case meaning that the sensors are newly installed and not affected by the degradation. It is worth to mention that this case will be used in other case studies as a base line for

comparison. The degradation effect is modeled in Cases 1.2 and 1.3. Fig. 4 shows an example of the signal under the modeled noise error. The error is randomly introduced to pressure and temperature measurements at the wellhead and bottomhole at the same time.

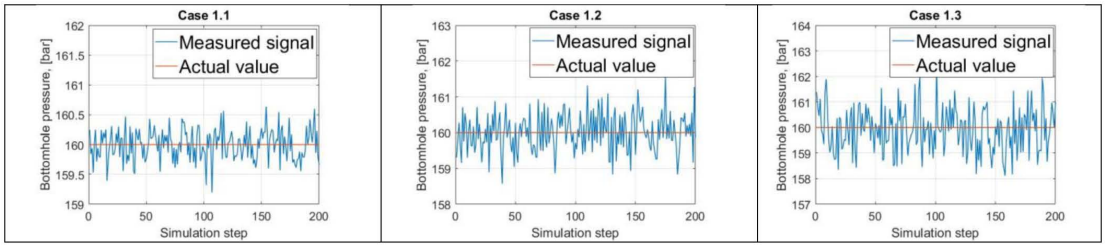

Figure 4—Example of the signal under the measurement error for Cases 1.x

Case 2 (Effect of measurement drift). To model the effect of sensor drift, we consider the following cases:

- Case 2.1: 0.5% drift with 0.5% noise error
- Case 2.2: 1% drift with 0.5% noise error
- Case 2.3: 1.5% drift with 0.5% noise error

All the cases are compared with the Case 1.1 which considers the newly installed equipment. Fig. 5 shows an example of the signal under the modeled drift error. The value of the drift (0.5%, 1% or 1.5%) represents the relative difference of the sensor value to the actual measurement value. For instance, if the actual pressure value is 100 bar and the drift error is 1%, the drifted measurement is 101 bar. In practice, the sensors may have a drift of 0.5 bar/year at certain well conditions. As such, the considered drift values are representable and the outcome of the study shows the possible error of flowrate estimation in case the sensors are not calibrated. Due to the noise, the final value of measurement will be within the range of 100.5-101.5 bar. The error is randomly introduced to pressure and temperature measurements at the wellhead and bottomhole at the same time. Please note that we considered only the drift which increased the measurement values and did not consider decreased values.

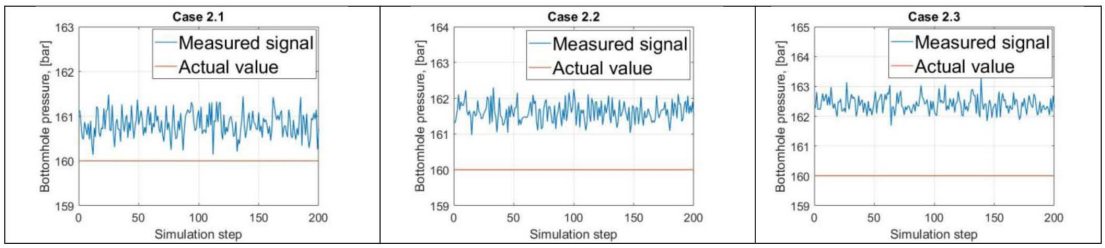

Figure 5—Example of the signal under the measurement error for Cases 2.x

Case 3 (Effect of temperature sensors failure). In this case, we study the effect of the temperature sensors failure, both at the bottomhole and the wellhead. We assume that at some point of the production time the temperature sensors are degraded down to the state when the information from the sensors are unreliable or no longer available. This is a difficult case from the operational point of view because it can be challenging to identify that the sensor shows unreliable information. We do not consider the identification methods and leave it for experienced operators. What we would like to consider is the effect of the broken sensor on the VFM estimates.

When compositional model is used in the VFM system, we need to use temperature to compute the multiphase flow. In case of the sensor failure, one solution can be using the last reliable value of the temperature for the VFM system. In this case, two situations are possible:

- Case 3.1: The temperature sensors fail and the actual temperature does not change
- Case 3.2: The temperature sensors fail and the actual temperature changes

As we consider the cases when the information from the temperature sensors is absent or unreliable, we exclude it from the cost function and use the last reliable value of the temperature in the inflow mass source. As such, the cost function includes only the values of the measured bottomhole pressure. In Case 3.2, we assume that the actual temperature drops by 5 °C, however, the VFM does not capture this because the correct temperature measurement is not available. To quantify the effect of the sensors failure, we compare these cases with Case 1.1 (no degradation).

Heat transfer modeling study

Theory and case study description. In VFM systems, in addition to the flowrate, matching the temperature measurements in the well can be achieved by adjusting the heat transfer coefficient. The overall heat transfer coefficient U is a constant between the thermal flux and the temperature difference of two mediums which can be expressed as:

$$U = \frac{Q}{A\left(T_f - T_{amb}\right)} \tag{2}$$

where Q denotes the heat flux, A – the heat transfer area, T_f – fluid temperature, T_{amb} – ambient (formation) temperature.

Considering the well structure in Fig.1, the heat transfer between the formation and the multiphase flow for each well section can be written as:

$$Q_j = 2\pi R_{inner} L_{\sec} h_{inner}\left(T_f - T_w\right) + \sum_{i=1}^{n} \frac{2\pi R_{inner} L_{\sec} K_j \left(T_{outer\ j} - T_{inner\ j}\right)}{\ln \frac{R_{outer\ j}}{R_{inner\ j}}} + \frac{2\pi L_{\sec} K_{form}\left(T_{cem} - T_{amb}\right)}{T_{D_{\sec}}} \tag{3}$$

where R_{inner} denotes the inner tubing radius, $R_{inner\,j}$ – the inner radius of the *j-th* layer, $R_{outer\,j}$ – the outer radius of the *j-th* layer, h_{inner} – the convective heat transfer coefficient, T_w – the wall temperature, K_j – the thermal conductivity of the *j-th* layer, L_{sec} – the section length, T_{cem} – the cement temperature, K_{form} – the formation thermal conductivity, T_{Dsec} – the dimensionless temperature of the section.

The terms in Eq.3 respectively represent the following heat transfer mechanisms:

- Convective heat transfer between the fluid and the tubing wall
- Heat conduction between the walls and mud (completion fluid)/cement
- Heat conduction between the outer casing wall and the formation

By substituting the left hand side of Eq.3 by Eq.2 taking into account the well mechanical structure of each section from Fig.1 and solving it with respect to U, the following equations for can be obtained:

$$\frac{1}{U_1} = \frac{1}{h_{inner}} + \frac{R_{17}}{K_{mud}}\left[\ln\left(\frac{R_{12}}{R_{16}}\right) + \ln\left(\frac{R_9}{R_{11}}\right) + \ln\left(\frac{R_6}{R_8}\right)\right] + \frac{R_{17}}{K_w}\left[\ln\left(\frac{R_{16}}{R_{17}}\right) + \ln\left(\frac{R_{11}}{R_{12}}\right) + \ln\left(\frac{R_8}{R_9}\right) + \ln\left(\frac{R_5}{R_6}\right) + \ln\left(\frac{R_2}{R_3}\right)\right] + \frac{R_{17}}{K_{cem}}\left[\ln\left(\frac{R_3}{R_5}\right) + \ln\left(\frac{R_1}{R_2}\right)\right] + \frac{T_{D1} R_{17}}{K_{form}} \tag{4}$$

$$\frac{1}{U_2} = \frac{1}{h_{inner}} + \frac{R_{17}}{K_{mud}}\left[\ln\left(\frac{R_{12}}{R_{16}}\right) + \ln\left(\frac{R_9}{R_{11}}\right) + \ln\left(\frac{R_6}{R_8}\right)\right] + \frac{R_{17}}{K_w}\left[\ln\left(\frac{R_{16}}{R_{17}}\right) + \ln\left(\frac{R_{11}}{R_{12}}\right) + \ln\left(\frac{R_8}{R_9}\right) + \ln\left(\frac{R_5}{R_6}\right)\right] + \frac{R_{17}}{K_{cem}}\left[\ln\left(\frac{R_4}{R_5}\right)\right] + \frac{T_{D4} R_{17}}{K_{form}} \tag{5}$$

$$\frac{1}{U_3}=\frac{1}{h_{inner}}+\frac{R_{17}}{K_{mud}}\left[\ln\left(\frac{R_{12}}{R_{16}}\right)+\ln\left(\frac{R_9}{R_{11}}\right)\right]+\frac{R_{17}}{K_w}\left[\ln\left(\frac{R_{16}}{R_{17}}\right)+\ln\left(\frac{R_{11}}{R_{12}}\right)+\ln\left(\frac{R_8}{R_9}\right)\right]+\frac{R_{17}}{K_{cem}}\left[\ln\left(\frac{R_7}{R_8}\right)\right]+\frac{T_{D7}R_{17}}{K_{form}} \tag{6}$$

$$\frac{1}{U_4}=\frac{1}{h_{inner}}+\frac{R_{17}}{K_{mud}}\left[\ln\left(\frac{R_{12}}{R_{16}}\right)\right]+\frac{R_{17}}{K_w}\left[\ln\left(\frac{R_{16}}{R_{17}}\right)+\ln\left(\frac{R_{11}}{R_{12}}\right)\right]+\frac{R_{17}}{K_{cem}}\left[\ln\left(\frac{R_{10}}{R_{11}}\right)\right]+\frac{T_{D10}R_{17}}{K_{form}} \tag{7}$$

$$\frac{1}{U_5}=\frac{1}{h_{inner}}+\frac{R_{17}}{K_{mud}}\left[\ln\left(\frac{R_{15}}{R_{16}}\right)\right]+\frac{R_{17}}{K_w}\left[\ln\left(\frac{R_{16}}{R_{17}}\right)+\ln\left(\frac{R_{14}}{R_{15}}\right)\right]+\frac{R_{17}}{K_{cem}}\left[\ln\left(\frac{R_{13}}{R_{14}}\right)\right]+\frac{T_{D13}R_{17}}{K_{form}} \tag{8}$$

where K_{cem} denotes the thermal conductivity of the cement, K_{mud} – the thermal conductivity of the mud.

In VFM systems, the heat transfer coefficients are often used as one of the parameters to match a specific temperature, e.g. at the wellhead. A reasonable strategy can be computing initial estimates for the heat transfer coefficients using the equations above and then tune it until a satisfactory agreement between the measured and predicted temperature values is reached. This is the first method used in this study.

On the other hand, it is interesting to see if it is possible to achieve the same accuracy as in the previous case without a rigorous representation of the heat transfer. For instance, it might be assumed that the heat transfer coefficient is constant along the wellbore. In this way, only one coefficient value is tuned in VFM to reach the specific temperature. This is the second method used in this study.

As such, we consider two cases:

- Case 4.1: Tuning with multiple heat transfer coefficients
- Case 4.2: Tuning with one heat transfer coefficient

Simulation procedure. As in the sensor degradation case, we randomly choose the pressure and temperature measurement values within a specified sensor accuracy (0.5% noise error) and perform 200 simulations to compute flowrates probability distributions.

To compute the initial estimates of the heat transfer coefficients for each section in Case 4.1, we use Eqs.4-8. First, we compute the heat conduction between the outer layer and formation for each section using the last terms in Eqs.4-8. For calculating the dimensionless temperature T_D, the correlation by Hasan and Kabir (2012) is used:

$$T_D=\ln\left[e^{-0.2t_D}+(1.5-0.3719\cdot e^{-t_D})\sqrt{t_D}\right] \tag{9}$$

$$t_D=\frac{a\cdot t}{R_{outer\ i}^2} \tag{10}$$

where t_D denotes the dimensional producing time, a – the formation heat diffusivity, t – producing time.

For the producing time t, we chose 100 days assuming that this is sufficient for the heat transfer between the fluid and the formation to reach a steady state.

Secondly, we calculate the heat conduction between the casing walls and cement/mud. In each section, the number of layers of the well structure varies which makes these values different from one section to another.

An order of magnitude analysis showed that the inner convection heat transfer between the multiphase flow and the tubing has a little contribution to the heat transfer between the flow and formation. Therefore, we do not include it into the final simulation procedure.

One important thing to mention is the fact that we keep the ratio between the heat transfer coefficients constant when tuning the VFM and use it as constraints in the optimization procedure. This is because we would like to achieve the original pattern of the heat transfer distribution along the wellbore. Otherwise, there might be the case that the algorithm changes one coefficient more than the others, so that the actual heat flux distribution will be changed to something less realistic.

The summary of the simulation procedure is shown in Fig. 6. In the initialization phase, the computed values of the heat transfer coefficients from Eqs.4-8 used as an initial guess and tuned until a specific wellhead temperature is matched. Then, the tuned coefficient values are used as an initial guess for the simulation phase and further adjusted together with the mass source to fit specific pressure and temperature values. The same procedure is used for the single heat transfer coefficient case except the fact that the initial coefficient value is guessed rather than preliminary computed. The computational procedure for the single heat transfer coefficient case is shown in Fig.7.

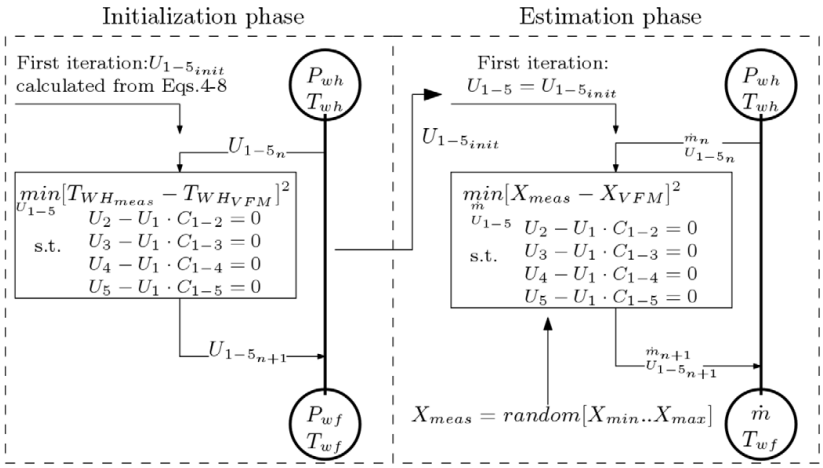

Figure 6—Schematic simulation procedure for Case 4.1 (multiple heat transfer coefficient tuning) (In the initialization phase, we compute the initial values of the heat transfer coefficients using Eqs.4-8 and then iteratively adjust these values until a good match of the wellhead temperature is reached. The obtained values are used as a good initial guess for the estimation phase where the heat transfer coefficients are tuned together with the mass flowrate to reach pressure and temperature values at the wellhead and bottomhole. The ratios between the heat transfer coefficients are kept constant and specified as constraints in the optimization problem.)

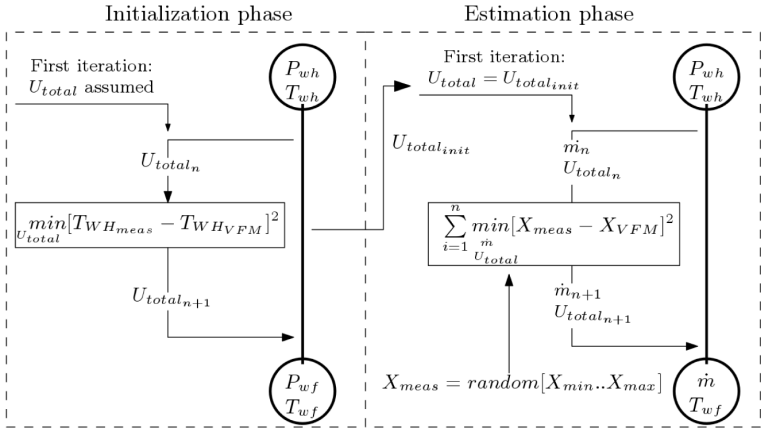

Figure 7—Schematic simulation procedure for Case 4.2 (single heat transfer coefficient tuning) (In the initialization phase, we make an assumption of the heat transfer coefficient and then iteratively adjust this value using the optimizer until a good match of the wellhead temperature is reached. The obtained value is used as a good initial guess for the estimation phase where the heat transfer coefficient is tuned together with the mass flowrate to reach pressure and temperature values at the wellhead and bottomhole.)

Statistical analysis

To analyze the simulations results, we perform a statistical analysis of the resulting flowrate distributions taken from 200 simulations of each case. We use the following procedure:

1. Test data normality.
2. Compute appropriate parameters for statistical and practical significance evaluation (mean/median, standard deviation (variance)/interquartile range).
3. Perform hypothesis testing to test the statistical significance of the results.
4. Evaluate the practical significance of the results.

In step 1, we test the data normality to select the appropriate strategy to compare the data samples. For this purpose, we perform a visual analysis using Q-Q plots and use D'Agostino test to check the normality formally. The Q-Q plot is a graphical method for checking the data normality by plotting quantiles of two distributions in which one distribution is normal. D'Agostino test is a formal statistical test of the data normality which was developed for sample sizes larger than 50 (D'Agostino 1971). In this study, we consider the significance level to be 0.05 which is a common assumption in staistical analysis.

In step 2, when the normality test is completed, we compute the parameters for statistical and practical significance evaluation of the samples. If the data is normally distributed, we select mean and variance for statistical significance evaluation and mean and standard deviation for practical significance evaluation. This is because the standard deviation has the units of the variable evaluated, so that it is easier to interpret the results for practical purposes. If the data is non-normal, we compute median and interquartile range be these parameters can be more representative than mean and standard deviation for this type of data.

In step 3, we perform hypothesis tests to check the statistical difference between the simulated cases. These tests provide an opportunity to check if the differences between the statistical properties of the data samples can be generalized over the populations from which these samples are taken. If the data is normally distributed, we choose 1-sample t-test on paired data differences. The reason for selecting 1-sample test instead of 2-samples test is because the samples are dependent. Indeed, initially we consider a system without the degradation effect and then we consider the same system under the degradation. To compare the variances, Bartlett's test is used (Snedecor and Cochran 1989). If the data is non-normal, we compare the medians using 1-sample sign test on paired differences and variances using Levene's test (Levene 1960).

Finally, in step 4, if we find that the difference between the parameters is statistically significant, we evaluate the practical significance of the obtained results. The evaluation of the practical significance will depend on the case under consideration. In general, we will compare differences of the means or standard deviations (or medians and interquartile ranges) as fractions of the mean estimate as well as the absolute differences values. Fig. 8 summarizes the used statistical analysis.

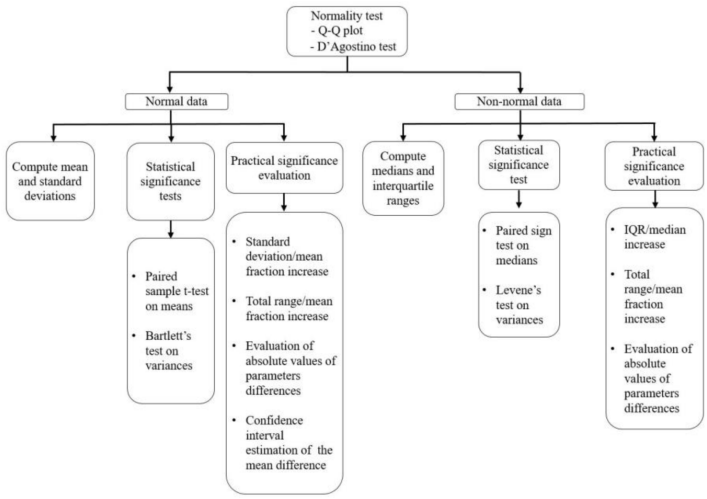

Figure 8—Schematic representation of the statistical analysis

Results

Sensor degradation

Case 1. First, we analyze the case with the increased noise effect due to sensor degradation. Fig. 9 shows the obtained oil and gas flowrate distributions.

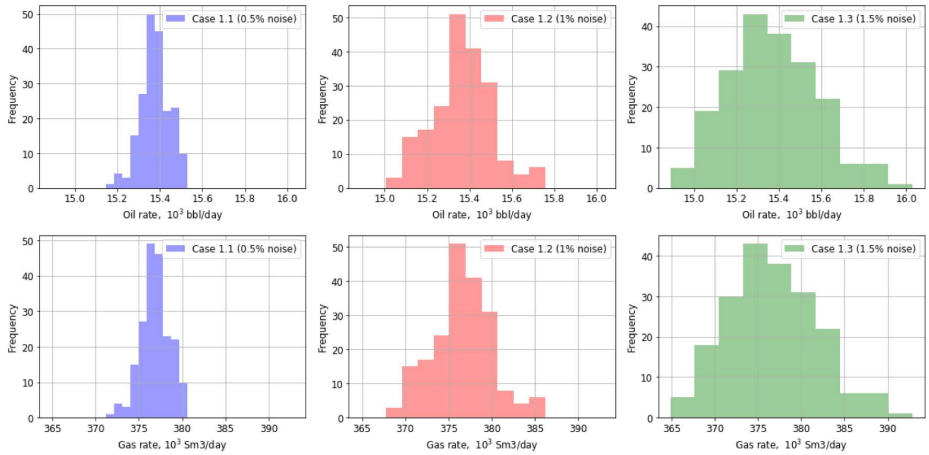

Figure 9—Histograms of VFM flowrate predictions for Cases 1.x

From the figure we see that the respective oil and gas flowrates are represented by the same distribution. This is expected because the volumetric flowrates are computed from the same mass flowrate source by means of a linear transformation. From the figure we can also notice that data are not precisely normal even though the input signals have white noise. The reason for this is the fact that the system is non-linear which can make the output signals to have a different distribution. However, the data might still be considered as normal and must be checked for normality to make valid conclusions. Also, the initial visual analysis

shows that the increase of the noise make the distribution more spread, i.e. increases the data variability. This result was expected. However, the main goal is to quantify this data variability growth and generalize the conclusions for the populations from which the samples are taken.

To perform further analysis, we check the data normality. Fig. 10 shows the visual and formal analysis represented by the Q-Q plots with corresponding p-values from the D'Agostino tests.

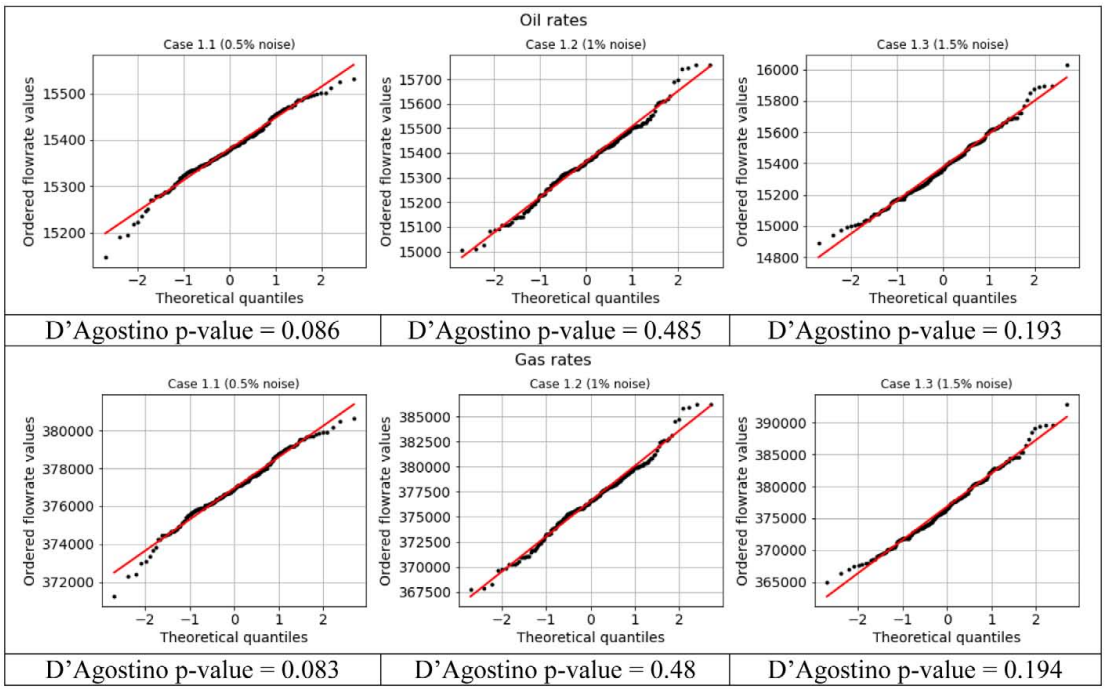

Figure 10—Normality testing of datasets from Cases 1.x

From the Q-Q plots we see that the majority of the data points follow the normal distribution pattern (red line) except a few points. This confirms the visual observations from Fig. 9 that the data is close to normal. By checking the normality formally by D'Agostino test, we cannot reject the null hypothesis that the data is normal at the significance level of 0.05 which is in agreement with the visual analysis.

Since we conclude that the data can be considered as normal, we choose means and standard deviations as measures for the central distribution value and data variability respectively. We also consider the total variation of the flowrate estimates to compare the resulting distributions. Table 1 shows the values of these data.

Table 1—Main statistical parameters of the simulation results of Cases 1.x

	Oil rates		
	Case 1.1	Case 1.2	Case 1.3
Mean, bbl/day	15380.02	15364.14	15374.91
Standard deviation, bbl/day	66.94	130.54	211.32
Total range, bbl/day	384.33	729.40	1141.18
	Gas rates		
	Case 1.1	Case 1.2	Case 1.3
Mean, Sm3/day	376940.80	376517.49	376814.36
Standard deviation, Sm3/day	1640.14	3201.04	5182.83
Total range, bbl/day	9418.93	17903.42	27990.72

From the table we see that the estimates of the means are similar while the variation of the standard deviations is much larger. Now we need to test if these differences are statistically significant. Table 2 shows the differences of means, standard deviations and total ranges between the cases as well as the results from the hypothesis tests on the means and variances equalities.

Table 2—Hypothesis testing and comparison of statistical parameters of Cases 1.x

Parameter/Hypothesis	Case1.1 and Case 1.2	Case 1.1 and Case 1.3
Oil rates		
Sample means difference, bbl/day	15.87	5.1
t-test p-value (H_0: $mean_1$=$mean_2$)	0.16	0.75
Standard deviation difference, bbl/day	75.53	144.39
Total range difference, bbl/day	365.5	756.84
Bartlett's test p-value (H_0: var_1 = var_2)	$2.15 \cdot 10^{-24}$	$1.36 \cdot 10^{-49}$
Gas rates		
Sample means difference, Sm3/day	389.64	126.44
t-test p-value (H_0: $mean_1$=$mean_2$)	0.16	0.75
Standard deviation difference, Sm3/day	1853.55	3542.7
Total range difference, Sm3/day	8991.06	18571.78
Bartlett's test p-value (H_0: var_1 = var_2)	$1.93 \cdot 10^{-24}$	$1.17 \cdot 10^{-49}$

From the table we can make several conclusions. First, we see that based on this study we cannot reject the null hypothesis about the means equalities at the significance level of 0.05. Thus, we conclude that there is no statistically significant difference between the population means which, in turn, tells that the population means can be considered as equal. This seems to be in agreement with the practical significance of the results. The difference in the means varies from 5.1 to 15.87 bbl/day which in practice can be neglected. Therefore, for practical purposes, we can say that if the sensor degradation affects the noise level only, the means of the flowrates estimates are not affected significantly. We see an opposite situation for the data variability. Comparing the statistical significance of the variance differences (Bartlett's test), we see that the null hypothesis is strongly rejected, which means that the populations variances are certainly different.

To estimate the practical significance of variance differences, we compare the absolute and relative values of the standard deviations and total ranges. The relative values are scaled with respect to the means. Fig.11 and Table 2 show that the increase of the measurement error by 0.5% causes the increase of the standard deviation and the total range by approximately 76 bbl/day and 366 bbl/day respectively. These values can be considered as significant. However, as Fig. 11 shows, these values correspond approximately to 0.5% and 2.5% of the mean flowrate value respectively. In certain VFM applications this error might be neglected, however, if the desired accuracy of the flowrate estimation is high, the increase of the measurement noise can cause problems in meeting the aimed accuracy specification. Moreover, the considered measurement error is relatively small, so that for larger measurement variations the associated error can be noticeable. As such, we conclude that the found standard deviation difference is practically significant if the desired accuracy of VFM is high or the noise error is relatively large but can be neglected in other situations. This is because the obtained absolute values are small when scaled with respect to the mean value estimate. The same conclusions can be drawn for the gas rates because we observed that its distribution pattern is the same as for the oil rates.

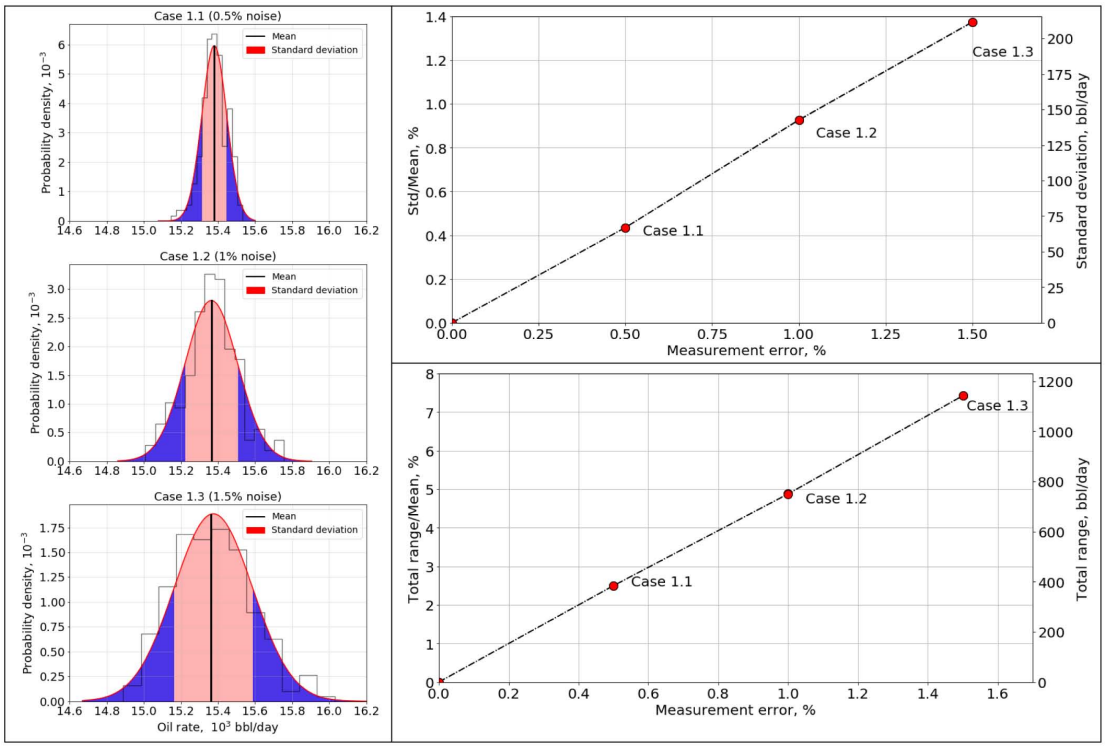

Figure 11—Comparison of standard deviations and total ranges for Cases 1.x
(The left part of the figure visualizes the increase of the data variability depending on the increase of the noise level. The figures on the right quantify this data variability increase. We can see that even though the increase of the standard deviation and total range is relatively big from Case 1.1 to Case 1.2 and Case 1.3, these values may be neglected in many practical applications since they are small fractions of the mean flowrate estimate unless the noise level becomes relatively large.)

Case 2. As the next step, we analyze the effect of measurement drift on the flowrate estimates from the VFM. Fig. 12 shows the oil and gas flowrate distributions. As in the previous case, the respective oil and gas flow rates are represented by the same distribution. As expected, we see a similar data variability between the cases but the migration of the mean value. This is because the noise level is kept the same for all the cases while the mean measurement value is different. Now the task is to evaluate the mean differences from statistical and practical points of view.

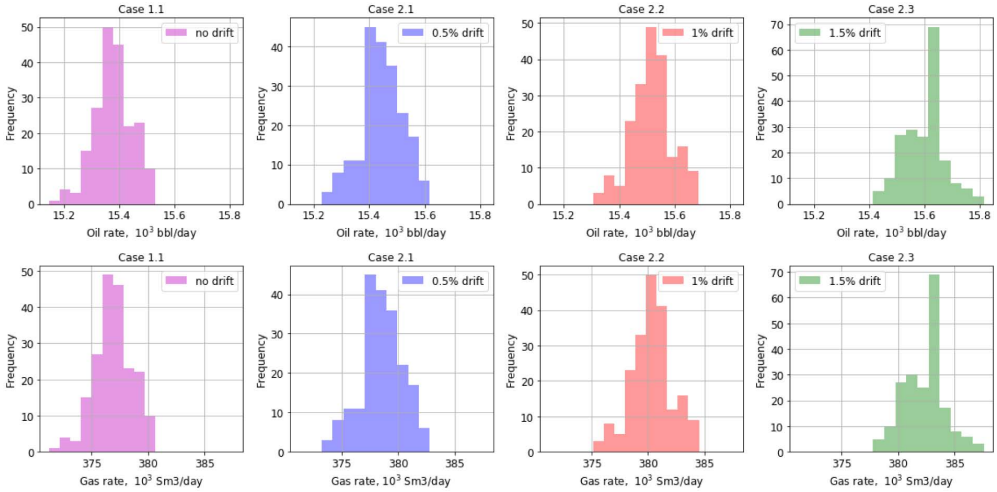

Figure 12—Histograms of VFM flowrate predictions for Cases 2.x and Case 1.1

First, we check the datasets normality. Fig. 13 shows the visual and formal analysis represented by the Q-Q plots with corresponding p-values from the D'Agostino tests. As in the previous case, we see that the majority of the data points follow the normal distribution pattern (red line) except a few points. This suggests that the data is close to normal. By checking the normality formally with D'Agostino test, we cannot reject the null hypothesis that the data is normal at the significance level of 0.05 and assume that the data can be treated as normal.

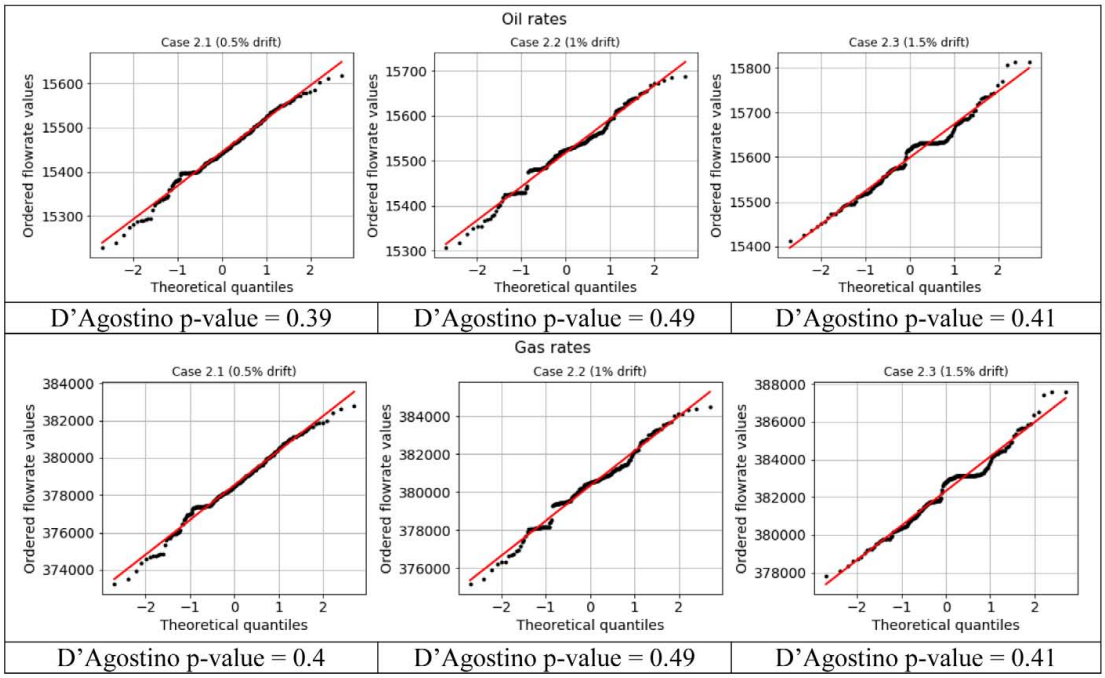

Figure 13—Normality testing of datasets from Cases 2.x

The next step is to compute the means, standard deviations and total ranges of the estimates. Table 3 shows the values of these parameters. From the table we see that the computed standard deviations are similar while the means vary considerably. This is in agreement with what we observed in Fig.12. Table 4 shows the differences of means, standard deviations and total ranges between the cases as well as the results from the hypothesis tests on the means and variances equalities.

Table 3—Main statistical parameters of the simulation results of Cases 2.x

	Oil rates		
	Case 2.1	Case 2.2	Case 2.3
Mean, bbl/day	15444.1	15517.55	15598.33
Standard deviation, bbl/day	75.31	74.54	74.58
Total range, bbl/day	390.39	380.52	399.66
	Gas rates		
	Case 2.1	Case 2.2	Case 2.3
Mean, Sm3/day	378520.31	380331.15	382320.24
Standard deviation, Sm3/day	1846.54	1827.3	1837.02
Total range, bbl/day	9569.27	9331.26	9791.52

Table 4—Hypothesis testing and comparison of statistical parameters in Cases 2.x

Parameter/Hypothesis	Case1.1 and Case 2.1	Case 1.1 and Case 2.2	Case 1.1 and Case 2.3
		Oil rates	
Sample means difference, bbl/day	64.06	137.54	218.34
95% confidence interval of the means difference, bbl/day	[52.4 – 75.74]	[126.68 – 148.4]	[203.89 – 232.74]
t-test p-value (H_0: $mean_1$=$mean_2$)	$8.81 \cdot 10^{-22}$	$3.10 \cdot 10^{-63}$	$2.15 \cdot 10^{-75}$
Standard deviation difference, bbl/day	8.37	7.61	7.65
Total range difference, bbl/day	6.05	3.82	15.33
Bartlett's test p-value (H_0: var_1 = var_2)	0.097	0.13	0.13
		Gas rates	
Sample means difference, Sm3/day	1579.51	3390.35	5379.44
95% confidence interval of the means difference, bbl/day	[1293.63 – 1865.39]	[3124.13 – 3656.56]	[5025.57 – 5733.27]
t-test p-value (H_0: $mean_1$=$mean_2$)	$5.58 \cdot 10^{-22}$	$1.30 \cdot 10^{-63}$	$9.69 \cdot 10^{-76}$
Standard deviation difference, Sm3/day	206.41	187.16	189.19
Total range difference, Sm3/day	150.33	87.68	372.58
Bartlett's test p-value (H_0: var_1 = var_2)	0.095	0.128	0.124

From the table we see that the hypothesis of the equal mean values is strongly rejected, thus we conclude that the population means are certainly different. As for the variances, the hypothesis of its equalities cannot be rejected which means that the variances of the populations are not statistically different at the significance level of 0.05. As such, from the analysis we see that only the means are affected by the measurement drift and the next objective is to estimate the practical importance of the means differences. Fig.14 shows the comparison of the means differences relative to the mean of Case 1.1.

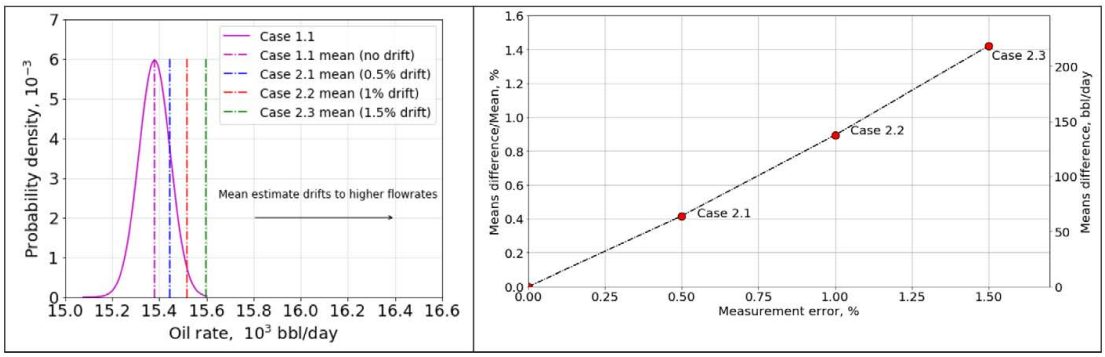

Figure 14—Comparison of the means from Cases 2.x with the mean from Case 1.1 (The left figure visualizes the drift of the mean estimates depending on the drift measurement error. The right figure quantifies the differences in mean estimates depending on the drift error.)

From the figure we see almost a linear relationship between the relative error of the means and the measurement error which is similar to what we previously observed for the standard deviations comparison. More specifically, the increase of the measurement error by 0.5% causes approximately 0.5% increase of the bias of the mean relative to the mean value. However, the error of the means is more critical than the error in standard deviations. This is because the probability of having a significant error of the flowrate estimates increases considerably. It can be seen in Fig.15 where the green shaded area shows the range of the flowrates from Case 1.1 (no degradation) which can be covered by the VFM under the degradation effect. In the left figure, we see that the entire range of the flowrates of Case 1.1 is almost within the standard deviations of Case 1.3. On the other hand, only 50% of the Case 1.1 flowrates is within 50% predictions from Case 2.3. Thus, we conclude that the sensor drift causes more serious flowrate estimation errors and should be carefully considered in VFM systems.

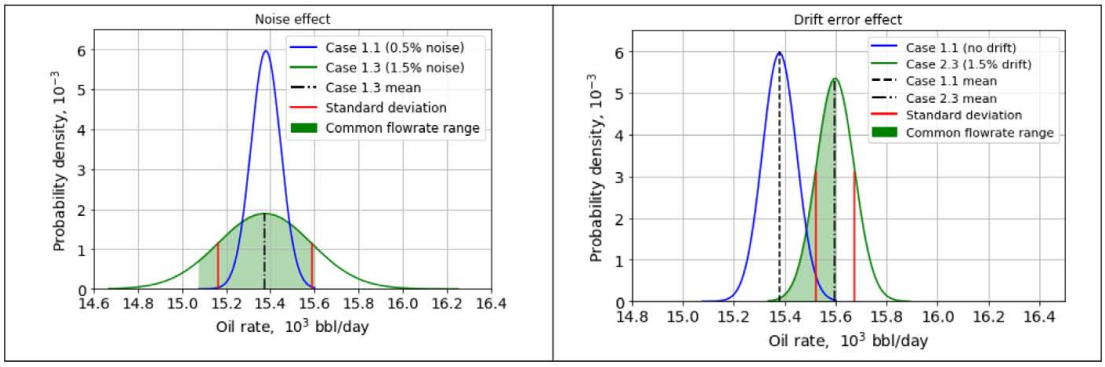

Figure 15—Comparison of the noise and drift degradation effects (The left figure shows that 1.5% noise error introduces the high spread of the flowrate estimations, however, the entire flowrate range of the case with no degradation is almost within the standard deviation of the case with high noise error. The right figure shows that the drift error causes significant estimation error because only 50% of the no drift case can be covered by 50% of the outcomes from the case with 1.5% drift error.)

Case 3. In this section, we compare the cases with a detected temperature sensor failure with Case 1.1 (no degradation effect). Fig.16 shows the comparison of the flowrate distributions of these cases. From the figure we see that the absence of the temperature measurements almost does not change the flowrate distribution.

However, if the actual flow temperature value changes and the VFM does not take it into account, the mean of the flowrate distribution changes considerably.

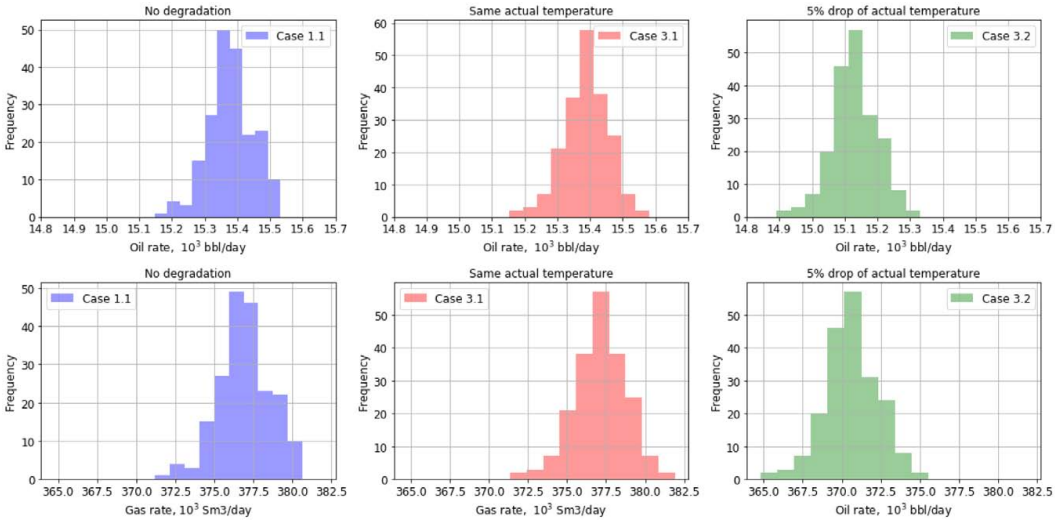

Figure 16—Comparison of flowrate distributions for Cases 3.x and Case 1.1

To quantify this change, again, first, we test the data normality. Fig. 17 shows the visual and formal analysis represented by the Q-Q plots with corresponding p-values from the D'Agostino tests. Similarly to the previous cases, the analysis shows that the data can be considered as normal.

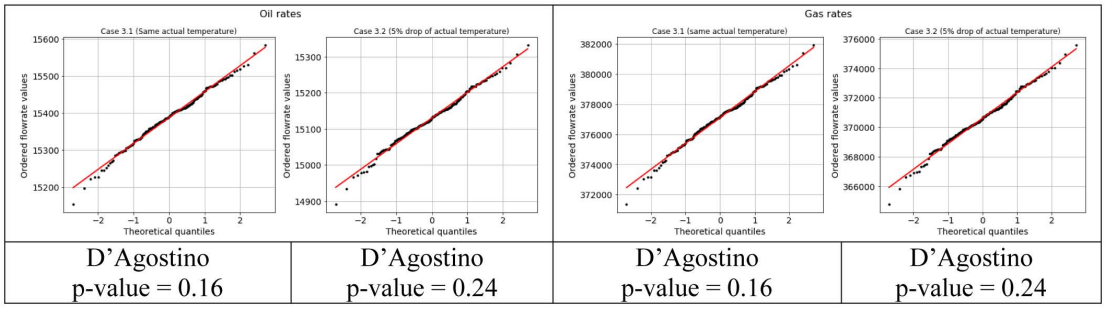

Figure 17—Normality testing of datasets from Cases 3.x

The next step is to compute the means, standard deviations and total ranges of the estimates. Table 5 shows the values of these parameters.

Table 5—Main statistical parameters of the simulation results of Cases 3.x

	Oil rates	
	Case 3.1	Case 3.2
Mean, bbl/day	15386.91	15129.72
Standard deviation, bbl/day	69.6	70.46
Total range, bbl/day	429.37	440.0
	Gas rates	
	Case 3.1	Case 3.2
Mean, Sm3/day	377109.6	370621.84
Standard deviation, Sm3/day	1707.24	1727.53
Total range, bbl/day	10537	10786.84

From the table we see that the computed standard deviations are similar to the ones in Case 1.1. On the other hand, the mean value of Case 3.2 varies considerably from Case 1.1 and Case 3.1. Table 6 shows the differences of means and standard deviations and its statistical significance as well as the total ranges differences.

Table 6—Hypothesis testing and comparison of statistical parameters in Cases 3.x

Parameter/Hypothesis	Case1.1 and Case 3.1	Case 1.1 and Case 3.2
	Oil rates	
Sample means difference, bbl/day	6.9	260.3
t-test p-value (H_0: $mean_1$=$mean_2$)	0.2	$3.01 \cdot 10^{-88}$
Standard deviation difference, bbl/day	2.67	3.53
Total range difference, bbl/day	45.04	55.67
Bartlett's test p-value (H_0: var_1 = var_2)	0.58	0.47
	Gas rates	
Sample means difference, Sm3/day	168.8	6318.95
t-test p-value (H_0: $mean_1$=$mean_2$)	0.2	$1.8 \cdot 10^{-90}$
Standard deviation difference, Sm3/day	206.41	187.16
Total range difference, Sm3/day	1118.13	1367.9
Bartlett's test p-value (H_0: var_1 = var_2)	0.57	0.46

From the table we see that for Case 3.1 the hypothesis of equal population means cannot be rejected while for Case 3.2 it is strongly rejected. At the same time, for both cases the hypothesis about the population variances equalities cannot be rejected. This shows that only the means difference between Case 3.2 and Case 1.1 is statistically significant.

For practical applications, the importance of this difference depends on the desired accuracy of the VFM system. As before, we evaluate the practical significance as a fraction of the mean estimate. In this particular case, the temperature drop of 5 °C causes the mean estimate error 260.3 bbl/day which is 1.7% relative to the mean value. This is a relatively high value and for many practical cases the consequences of such an error can be critical. Since the VFM might have other factors which cause errors (e.g. noise and drift in pressure sensors), the absence of the correct temperature value can play a crucial role. Overall, we conclude that if the actual fluid temperature changes and the VFM system does not capture this change, it can result in relatively high errors of the flowrate estimations. This fact should be taken into account if there is a probability of the reservoir temperature change in a particular field development case (e.g. water breakthrough) or a transient heating up of the well.

Heat transfer study

As in the sensor degradation study, we plot the flowrate distributions for the initial visual analysis of the simulation results. Fig. 18 shows the oil and gas flowrate distributions.

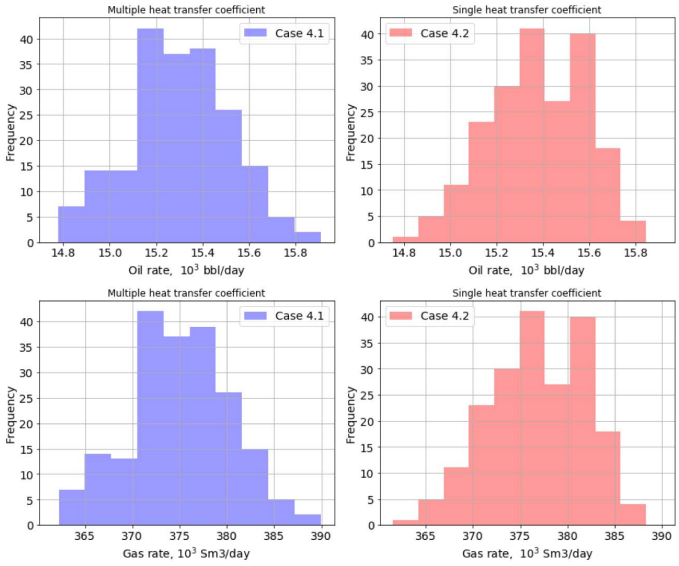

Figure 18—Histograms of VFM flowrate predictions for Cases 4.x

We see that the flowrate distributions in both cases are relatively similar with some occasional differences in frequency values and may follow the normal distribution pattern. Fig.19 confirms this observation. As in all the previous cases, except for a few points, the data samples are on the red line which represents the normal distribution. The normality assumption is also supported by D'Agostino test. Even though the flowrate distributions are relatively similar, we quantify the possible differences and evaluate if this difference is practically important for VFM systems.

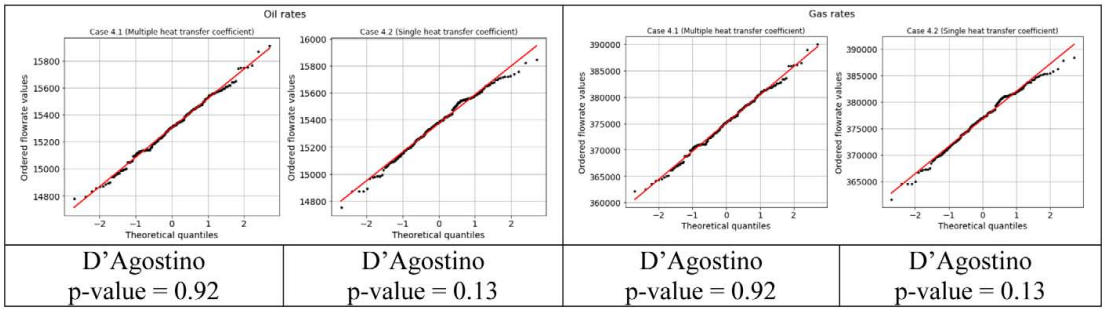

Figure 19—Normality testing of datasets from Cases 4.x

Table 7 shows the statistical parameters and hypothesis tests of Case 4.1 and Case 4.2. From the table we see that the difference between the standard deviations is small and can be considered as statistically insignificant. On the other hand, we can reject the hypothesis about the population means equality at the significance level of 0.05. Thus, this difference is considered as statistically significant. However, we can see that this difference is only 0.45% of the mean value and can be considered as practically insignificant. In the sensor degradation case (Case 2), we observed that the increase of the 0.5% drift measurement error introduced approximately 0.5% growth of the error of the mean estimate and we concluded that this difference was practically important. However, in that case we clearly observed the trend between the

measurement drift and the estimates. In this case, there error caused by a different tuning strategy most likely will not significantly exceed the error of 0.45% which was computed for this particular case. The deviation may slightly change because of different initial guesses of the heat transfer coefficient values, however, there is not a clear evidence that this difference will increase considerably. Moreover, we observed that the difference of variances even statistically insignificant which also strengthens the point the applied tuning strategies practically give the same result.

Table 7—Main statistical parameters and hypothesis tests of the simulation results of Cases 4.x

Oil rates		
	Case 4.1	Case 4.2
Mean, bbl/day	15303.34	15373.77
Sample means difference, bbl/day	70.43	
t-test p-value (H_0: $mean_1$=$mean_2$)	$4.44 \cdot 10^{-5}$	
Standard deviation, bbl/day	216.14	210.96
Standard deviation difference, bbl/day	5.18	
Total range, bbl/day	1131.13	1091.33
Total range difference, bbl/day	39.8	
Bartlett's test p-value (H_0: var_1 = var_2)	0.73	
Gas rates		
	Case 4.1	Case 4.2
Mean, Sm3/day	376917.40	375060.34
Sample mean difference, Sm3/day	1718.79	
t-test p-value (H_0: $mean_1$=$mean_2$)	$4.47 \cdot 10^{-5}$	
Standard deviation, Sm3/day	5297.55	5172.29
Standard deviation difference, Sm3/day	125.26	
Total range, Sm3/day	27715.52	26752.47
Total range difference, Sm3/day	963.05	
Bartlett's test p-value (H_0: var_1 = var_2)	0.74	

Since we found that the strategies produce very similar results in terms of accuracy, we conclude that the approach with only one tuning heat transfer coefficient is more efficient for practical applications. This is because this approach significantly reduces the computational time for tuning and estimation. In this particular case, the computational time was reduced by a factor of 3. Moreover, computing good initial guesses of the heat transfer coefficients using the physics behind can also take the time. In contrast, initializing a good initial guess of one heat transfer coefficient value is relatively easy and requires only one additional simulation. Therefore, we conclude that the tuning strategy with one heat transfer coefficient along the wellbore is accurate enough and suits better for practical applications than the strategy with multiple heat transfer coefficient values.

Conclusions

In this paper, we constructed a Virtual Flow Meter using a multiphase pipe model and an optimization routine from commercial packages and considered two case studies: the effect of the sensor degradation and two different tuning strategies on the VFM estimates. The sensor degradation effect was modeled as the measurement noise increase, measurement drift and sensors failure. As for the tuning strategies, the use of one versus multiple heat transfer coefficients along the tubing was compared. In addition, we applied a method for a statistical analysis approach of case sensitivity studies which evaluates the distribution of the possible outcomes rather than only critical values for specific boundary conditions.

From the sensor degradation study we found that the noise increase introduces the increase of the flowrate estimates variances and observed close to a linear trend between the noise error and growth of the standard deviation. The quantification of the estimation error growth showed that if the measurement noise becomes relatively large, the associated error should be taken into account. However, if the required VFM accuracy is not high, this error can be neglected in practical applications. On the other hand, the measurement drift can

cause more serious estimation deviations since there is almost a linear dependency of the mean estimation value change and the drift measurement error. Thus, it is advisable either to calibrate the sensors (which is hard in practice) or validate the relationship of the VFM predictions and the sensor readings. This can be done by well tests or any other reliable flowrate measurements and preferably carried out more often than a severe sensor drift occurs.

As for the temperature sensor failure, it can be disregarded in case the actual flow temperature does not change. On the other hand, if the actual temperature changes and it is not captured by the VFM, the flowrate predictions can deviate from the correct predictions considerably. This fact should be taken into account if there is a probability of reservoir temperature change.

The case study on different tuning strategies showed that it is not necessary to use a complicated mechanical representation of the well and associated heat transfer coefficients to predict the flowrates accurately. The assumption about the constant heat transfer coefficient along the wellbore gives almost identical results, but can reduce the simulation time substantially. Thus, for practical applications the tuning of a constant heat transfer coefficient along the wellbore is a solid approach.

Acknowledgement

This work was carried out as a part of SUBPRO, a Research-based Innovation Centre within Subsea Production and Processing. The authors gratefully acknowledge the financial support from SUBPRO, which is financed by the Research Council of Norway, major industry partners, and NTNU.

References

D'Agostino, R. 1971. "An omnibus test of normality for moderate and large size samples." *Biometrika* **58** (2): 341.

Falcone, G., Hewitt,G. F. and Alimonti.C. 2009. Multiphase Flow Metering: Principles and Applications. Amsterdam: Elsevier.

Falcone, G., Hewitt,G.F. Alimonti,C. and Harrison.B. 2001. "Multiphase Flow Metering: Current Trends and Future Developments." SPR 71474.

Haldipur, P., and Metcalf.G. 2008. "Virtual Metering Technology Field Experience Examples." OTC. Houston, Texas.

Hasan, A.R., and Kabir.C.S. 2012. "Wellbore heat-transfer modeling and applications." *Journal of Petroleum Science and Engineering* **86-87**: 127–136. 10.1016/j.petrol.2012.03.021.

Holmås, K., and Løvli.A. 2011. "FlowManager Dynamic: A multiphase flow simulator for online surveillance, optimization and prediction of subsea oil and gas production." 15th International Conference on Multiphase Production. Cannes, France.

Kikani, J., Fair,P.S. and Hite.R.H. 1997. "Pitfalls in Pressure Gauge Performance." *SPE Formation Evaluation* **12** (04). 10.2118/30613-PA.

Lansangan, R. 2012. "A Study on the Impact of Instrument Measurement Uncertainty, Degradation, Availability and Reservoir and Fluid Properties Uncertainty on Calculated Rates of Virtual Metering Systems." 30th International North Sea Flow Measurement Workshop.

Melbø, H., Morud,S. Bringedal,B. van der Geest,R. and Stenersen.K. 2003. "Software That Enables Flow Metering of Well Rates With Long Tiebacks and With Limited or Inaccurate Instrumentation." *Offshore Technology Conference*.

Patel, P., Odden,H. Djoric,B. Garner,R. D. and Vea.H.K. 2014. "Model Based Multiphase Metering and Production Allocation." *Offshore Technology Conference*, OTC-25457-MS.

Snedecor, G., and Cochran.W. 1989. Statistical Methods. Iowa State University Press.

Tangen, S., Nilsen,R. and Holmås.K. 2017. "Virtual Flow Meter - Sensitivity Analysis." 35th North Sea Flow Measurement Workshop 2017. Tønsberg, Norway.

4.2 Discussion of Paper IV - Statistical Analysis of Effect of Sensor Degradation and Heat Transfer Modeling on Multiphase Flowrate Estimates from a Virtual Flow Meter

In Paper IV, we considered a multiphase flow estimation problem subject to sensor degradation and heat transfer modeling simplifications. Despite aiming a thorough discussion on influence of the aforementioned factors on the accuracy of multiphase flow estimates, there are several points that we would like to additionally emphasize and elaborate to make better supported conclusions.

Considered flow conditions. First, we would like to point out that the presented results are achieved for a steady state flow. Despite we run a transient multiphase flow simulator, the gradients computed by the optimization solver are taken when the system is at steady state. This means that when the solver sends a new suggested value of the manipulated variable (the mixture mass flowrate), the simulation is run with this value until no change in pressures and temperatures is detected for both bottomhole and wellhead. The main reason for such a simulating procedure is the fact that it makes easier for the optimization solver to find a local minimum, because, if perturbing a transient flow, the values of the gradients for the same value of the manipulated variable within the transient period will be most likely different which means that the minimum is hardly likely to be found. One potential solution to this problem is to perform dynamic optimization by using, for instance, Moving Horizon Estimation (MHE) approach. However, in general, MHE is relatively expensive in terms of computing cost even if a mathematical model is available together with analytical expressions of the gradients. In our case, however, we use the simulator as a black-box model, as such, the gradients are computed by finite differences, and also the computational time of the model itself is relatively long. As such, the overall computational cost makes dynamic optimization to be an infeasible solution.

We also would like to emphasize that the results shown in the paper are made for artificially generated data, so no data from a real field are used in the simulations. As such, the noise and drift errors are assumed to represent a real sensor behavior, but the values of the errors and the estimated flowrates are not taken from any real field production data. The goal of the simulations is to test a "what-if" case meaning that, if we have noise and drift of a discussed magnitude, what will be the influence on the estimation accuracy.

Additional sensitivity studies for GOR and WC. Despite the fact that we only presented the results for oil and gas phases, the simulations have actually been performed for a three-phase flow. As we state in Figure 1 of the paper, the water

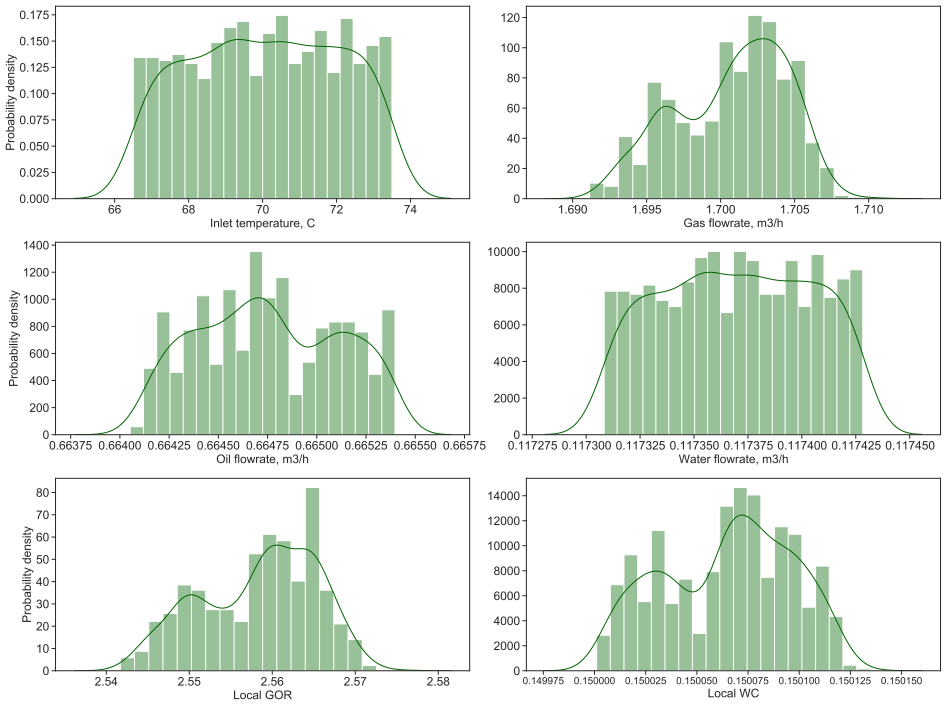

Figure 4.1: Case 1 - Sensitivity of wellhead GOR and WC with respect to 5% error in T_{BH} (WC=15% [@$T_{BH} = 70$])

cut (WC) for the considered flow is 30% at standard conditions and GOR is 153 $\frac{Sm^3}{Sm^3}$. As such, the results obtained in the simulations should be treated as the results obtained for a three-phase flow, but not for a two-phase flow. The main reason why the water phase was not considered is the fact that we assumed that the water phase will behave similarly to the oil phase, while the oil phase is typically of a higher interest for petroleum engineers. At the same time, since the water cut along well will not be constant, the paper would benefit from presenting the results for the water phase too. However, the results presented for the oil phase are still valid, as it is simulated within a three-phase flow.

As we presented the sensitivity of only oil and gas rates with respect to noise in measurements and heat transfer modelling, we, in principle, showed how the local Gas-Oil-Ratio at the wellhead changes with respect to these parameters. To check our assumption that the water phase would behave similarly to the oil phase, we conducted additional studies to see the dependency of water cut (WC) with respect to heat transfer processes in a well. Unfortunately, by the time of conducting such

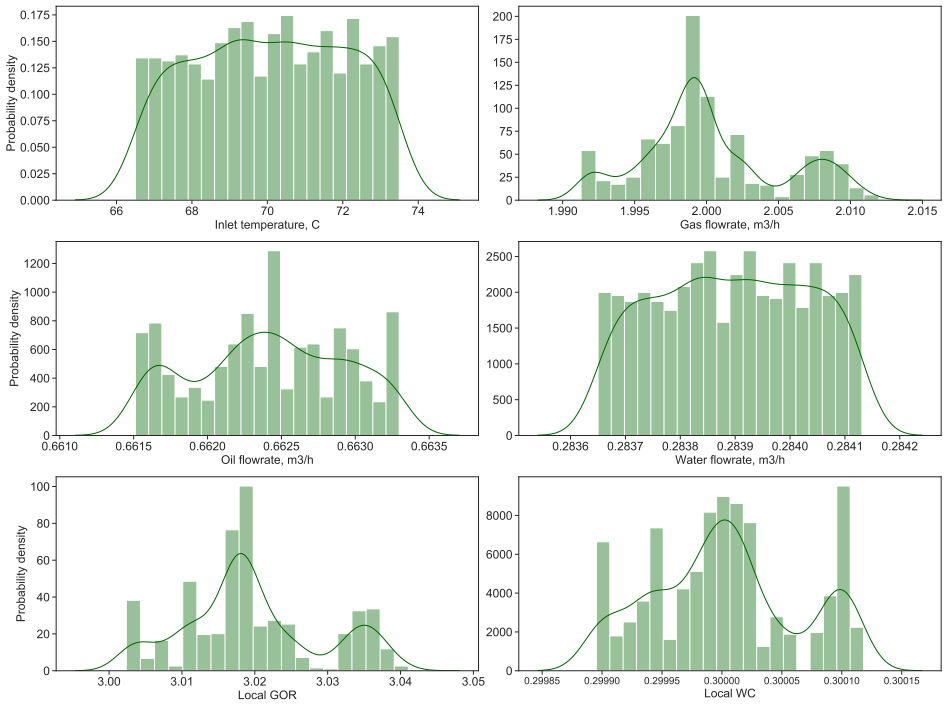

Figure 4.2: Case 2 - Sensitivity of wellhead GOR and WC with respect to 5% error in T_{BH} (WC=30% [@$T_{BH} = 70$])

studies, the licenses of the software used in the paper (OLGA) are not available to us. However, since in any case we considered the results from steady state simulations, we used a steady state model implemented in HYSYS and developed at Tulsa University (Zheng et al. (2016)). As in OLGA, the model also considers heat transfer modeling in a three-phase flow, as such the results can be compared qualitatively.

We consider a vertical well of 1000 m with the same hydrocarbon components as in Paper IV, with the bottomhole pressure of 100 bar and bottomhole temperature of 70°C and the constant heat transfer coefficient of 40 $\frac{kJ}{hm^2C}$. To test the effect of the temperature drop on WC, we study three case. For all the cases we consider a three-phase flow. In the flow, the inlet flowrates are fixed while other parameters are perturbed. In **Case 1**, for the given flowrates and bottomhole conditions, the wellhead water cut is equal to 15%, and we study how perturbations of the bottomhole temperature by 5% influence the wellhead values of GOR and WC. In **Case 2**, the same procedure is does as in Case 1, but for the flow with the wellhead

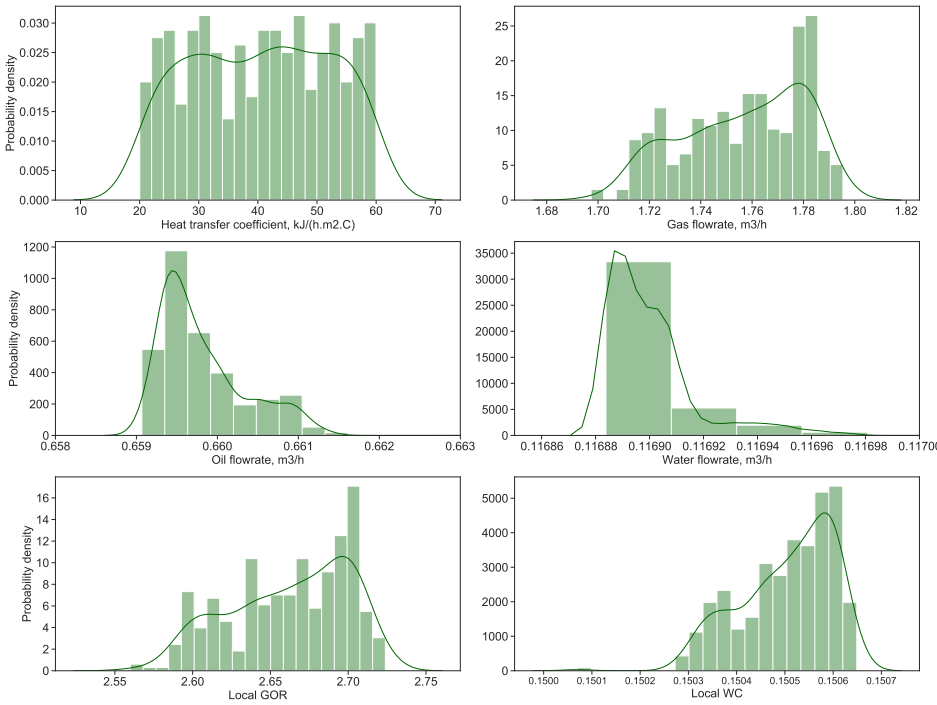

Figure 4.3: Case 3 - Sensitivity of wellhead GOR and WC with respect to heat transfer coefficient

water cut of 30%. By conducting this case, we see if the sensitivity of water cut with respect to the temperature drop noticeably changes with the water cut value itself. In **Case 3**, instead of fixing the heat transfer coefficient at 40 $\frac{kJ}{hm^2C}$, we take samples from a uniformly distributed values from the range of 20-60 $\frac{kJ}{hm^2C}$. In this way, we test how sensitive WC is to significant changes of the temperature drop along the well. To evaluate the sensitivity, we use the absolute change in values of WC and GOR relative to their means as follows:

$$Sensitivity = 100\% \left(\frac{y_{max} - y_{min}}{y_{mean}} \right) \tag{4.1}$$

Figure 4.1 shows the results for Case 1. From the figure we see that the WC value indeed changes with the change of the inlet temperature, but the change is very small and, in fact, smaller than for GOR. The GOR sensitivity is 1.34%, while the WC sensitivity is 0.09%. Similar results are obtained in Case 2 shown in

Figure 4.2. In this case, the GOR sensitivity is 1.28%, while the WC sensitivity is 0.07%. This means that for very different values of WC we see that its local value does not depend on temperature gradient modeling which means that we can relate the results obtained in Paper IV to the water flowrates as well. The results obtained in Case 3 (Figure 4.3) also agree with Case 1 and 2. We see a very small influence of the heat transfer coefficient on the water cut change at the wellhead.

While we see that the results presented in Paper IV can be, in general, transferred for the water flowrates and water cut, we believe that some other general conclusions in the paper can be improved. First of all, it is important to note that the simulations have been performed for a three-phase flow with the fixed composition. This means that the conclusions about the effect of drift and noise in sensor values are expected to be similar for similar flow conditions and fluid composition, while for a different flow composition the results might vary. For instance, in a case with a multiphase flow with a high GOR, we typically observe a stronger influence of temperatures on modeling results which can be caused by the high dependencies of gas densities on temperature. This means that more care might need to be taken for such wells when fitting a first principles VFM to the measured temperature values. As such, we would like to emphasize that more investigations are required for specific flow conditions and fluid properties while some of the approaches presented in the paper can be taken as guidelines to perform new evaluation studies of VFM.

References

Zheng, W., Zhang, H.Q., Sarica, C., et al., 2016. Unified model of heat transfer in gas/oil/water pipe flow, in: SPE Latin America and Caribbean heavy and extra heavy oil conference, Society of Petroleum Engineers.

4.3 Uncertainty Estimation of Mechanistic First Principles Models and Digital Twins Using Bayesian Machine Learning (Paper V)

Paper V describes applications of Bayesian Machine Learning for tuning first principles models based on a case study of a three-phase (oil, gas and water) pipe flow. The paper describes a method of quantifying the uncertainty of the tuned first principles models based on the uncertainties of the parameters of Bayesian Neural Networks. The main motivation for this paper was the fact that even complex first principles models are almost never sufficiently accurate to describe the real process due to complexity of modeled phenomena, as such they need to be tuned. The authors wanted to investigate capabilities of Bayesian Neural Networks for this task because such models allow to estimate the uncertainty of the tuned model. This can be very useful in practice, for instance, when the model starts deviating from the process measurements and the reason for this is not clear. In this case, the model uncertainty quantification might help to understand the need for model or sensor re-calibration. Apart from that, when the model predicts a certain parameter, it is, in general, useful for operators to know how certain the model is about its predictions to make accurate decisions to operate the process in a safe and reliable manner.

Bikmukhametov, T., and Jäschke, J. Uncertainty Estimation of Mechanistic First Principles Models and Digital Twins Using Bayesian Machine Learning. Submitted to Engineering Applications of Artificial Intelligence, 2020

Uncertainty Estimation of Mechanistic First Principles Models and Digital Twins Using Bayesian Machine Learning

Timur Bikmukhametov, Johannes Jäschke*

Dept. of Chemical Engineering, Norwegian University of Science and Technology (NTNU), NO-7491 Trondheim

Abstract

To operate process engineering systems in a safe and reliable manner, predictive models are often used in decision making. In many cases, these are mechanistic first principles models which aim to accurately describe the process. In practice, the parameters of these models need to be tuned to the process conditions at hand. If the conditions change, which is common in practice, the model becomes inaccurate and needs to be re-tuned. In this paper, we propose a framework which allows to tune first principles models to process conditions using two different types of Bayesian Neural Networks. Our approach estimates the expected values of the first principles model parameters but also quantify the uncertainty of these estimates. As an example, we chose a multiphase pipe flow process for which we constructed a three-phase steady state model based on the drift-flux approach which can be used for modeling of pipe and well flow behavior in oil and gas production fields with or without the neural network tuning.

Keywords:
Bayesian Neural Networks, Uncertainty Quantification, Machine Learning, First Principles Model, Digital Twins, Drift-flux model, Multiphase Flow

1. Introduction

Today, process operation decisions are increasingly made on the basis of process models. Traditionally, process models are derived from first principles such as mass, momentum and energy conservation laws. This approach is called first principles or mechanistic modeling (Pantelides and Renfro (2013)). The main advantage of these models is that they are built based on knowledge about the system and are understandable to the knowledgeable user. A conceptually different approach is based on using process date to learn a

*The authors gratefully acknowledge the financial support from the center for research-based innovation SUBPRO, which is financed by the Research Council of Norway, major industry partners, and NTNU.

*Corresponding author

Email addresses: timur.bikmukhametov@ntu.no (Timur Bikmukhametov), johannes.jaschke@ntnu.no (Johannes Jäschke)

model of the process (Rasheed et al. (2019)). Data-driven approaches of this kind become increasingly popular due to the progress in data handling, analytics and machine learning techniques.

In the recent years, mechanistic models of process plants and equipment together with machine learning and virtual reality technologies have formed the Digital Twin framework which may be used for monitoring of process conditions, equipment health and plant efficiency, and support critical decisions on plant operation quickly and effectively with minimal human intervention (Rasheed et al. (2019)). Digital Twins offer significant potential in operating cost reduction, however, they require in-time automatic or semi-automatic model recalibration to be successfully used in industrial systems (Rasheed et al. (2019)).

In all but the most trivial cases, first principles model parameters need to be tuned, such that the model predictions accurately match the plant. Such tuning can be conducted in experimental laboratories, onsite at a process plant or, in many cases, both options are required (Pantelides and Renfro (2013)). During operation, the predictive accuracy of the obtained models will depend on several factors. One factor is the measurement accuracy. Process measurements may drift over time, as such the model calculates its outputs based on wrong inputs, and the model accuracy drifts accordingly (Bikmukhametov et al. (2018)). Another important factor is that process conditions such as material or fluid properties may change over time and differ from the tuning conditions which may lead to inaccurate predictions and economic loss (Mazzour and Hodouin (2008), Amjad and Al-Duwaish (2003)). In addition, equipment in process plants often degrades over time which makes the predictive model of the equipment behavior inaccurate (Gorjian et al. (2010)). As such, it is very important to identify under which conditions the tuned mechanistic model becomes unreliable to use and needs recalibration, and this is the topic of the present paper.

One promising method to estimate the need for model recalibration and understanding its predictive capabilities is to quantify uncertainty and bias of model predictions. If the prediction uncertainty and/or bias is high, then the model recalibration or restructuring is required, because the produced estimates cannot be trusted.

In the literature, there are different contributions which report methods to quantify uncertainty of first principles models. One approach relies on checking sensitivities of model predictions with respect to the change in model parameters, typically referred as Sensitivity Analysis (Ratto et al. (2007), DiGiano and Zhang (2004)). In this approach, selected parameters are perturbed, the change of the model output is recorded and then the ratio of the output change to the parameter change is computed. Although easy to implement, this method does not consider the uncertainty of the data and model. Therefore, it estimates the sensitivity of the model with respect to the input parameters. The main result from such sensitivity analysis is the conclusion about the parameters to which the fitted mechanistic model is the most sensitive to, but not in general about how well the model matches the process.

A more informative approach about model uncertainty is based on the Bayesian framework. In this approach, the uncertainty of parameters is estimated based on the tuned model to the data using various methods. One approach is to use Markov Chain Monte Carlo (MCMC) method which computes the probability of the parameters via a poste-

rior parameter distribution over the proposed parameters' priors (Aldebert and Stouffer (2018), Leil (2014)). MCMC is a powerful concept of estimating unbiased posterior distributions, however, it may be very slow for many practical applications and accelerating MCMC methods is an active field of research (Robert et al. (2018)). When applied to parametric uncertainty estimation of mechanistic first principles models, this can be an issue, if, for instance, the mechanistic model needs a time consuming iterative procedure to be solved. Shrestha et al. (2009) addressed this problem by approximating MCMC results using neural networks, however, in this case, MCMC simulations still need to be performed.

In this paper, we propose to tune the parameters of the first principles model using Bayesian Neural Networks (BNNs). This is done by, first, learning the distribution of the neural network parameter values from the process data and then propagating this distribution through the first principles model to give a distribution of the model output. This is then used to quantify the first principles model uncertainty. As such, the main idea is to utilize uncertainty quantification capabilities of Bayesian Neural Networks when estimating first principles model parameters.

Previously in the literature, authors have adapted maximum likelihood neural networks for model parameter tuning, see the works by Psichogios and Ungar (1992), Ahmadi and Chen (2018), Anifowose et al. (2017), Klyuchnikov et al. (2019), Onwuchekwa et al. (2018), Kanin et al. (2019). However, using the maximum likelihood approach, it is not possible to estimate the uncertainty of the first principles model parameters, while our approach allows doing so.

For the training of BNNs, we build upon work by Blundell et al. (2015) who used variational approximations for Bayesian learning of neural networks and work by Gal and Ghahramani (2015) who introduced the concept of Markov Chain (MC) Dropout techniques for deep neural networks. We compare the performance of both approaches and give recommendations on the conditions for combining each type of Bayesian Neural Networks with first principles models.

As an example of the first principles model, we create a complex, space discretized model of a three-phase (oil, gas and water) flow in pipes which considers the slip effect and mass transfer between the gas and liquid phases. We show how the friction coefficient of this model can be tuned using a Bayesian Neural Network and how uncertainty of these estimates can be quantified using this approach. As the approach is scalable, it can be applied to systems of any size which is advantageous for Digital Twin technology which typically considers process plants of a large scale.

As such, the main contribution of this work is that we provide and exemplify a new flexible framework for uncertainty estimation of complex mechanistic first principles models. In addition, we discuss how the obtained results can be interpreted for the purpose of model/Digital Twins recalibration.

The paper is organized as follows. Section 2.1 introduces the proposed concept of tuning first principles models parameters by means of Bayesian Neural Networks. Section 3 describes the multiphase flow model which is used as the example of the first principles model to be tuned by BNNs and shows adaptation of the concept described in Section 2.1 for this model. In Section 5, we provide the simulation results and discuss them. In Section 6, we make conclusions from our work.

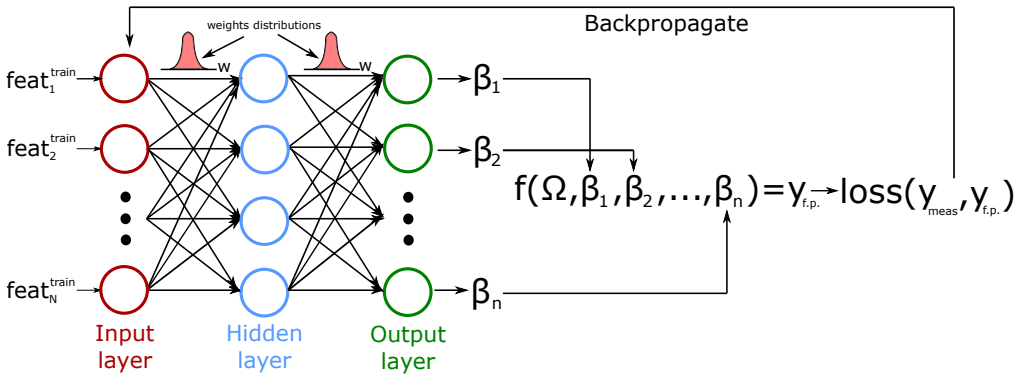

Figure 1: Training Bayesian Neural Networks for first principles models tuning

2. Proposed concept of parameter estimation of first principles models using Bayesian Neural Networks

2.1. General description of the proposed concept

The main idea of the proposed framework is similar to any first principles model tuning to data - select parameters to be tuned or introduce coefficients which are adjusted to get an accurate fit to the data. A schematic representation of this process is shown in Figure 1. The main difference between the maximum likelihood tuning is that we learn the distribution of weights and biases represented by the approximate variational distributions instead of single point estimates. We do this by two BNN models that are described in Section 2.3.2 and 2.3.3 below.

At the prediction (test) stage, shown in Figure 2, the test features are fed into the trained Bayesian Neural Network. Then, a specified number of samples from the trained distribution of weights and biases is taken. These sampled parameters produce distributions of the tuned first principles model parameters. As a result, a distribution of the modeled output by a mechanistic first principles model is obtained. From the distribution, the mean and variance can be calculated. The mean value will correspond to the maximum a posterior estimate of the variable while the variance will correspond to the prediction uncertainty.

It is important to note that the proposed approach considers the uncertainty of model parameters based on the training data and does not account for the uncertainty of the model structure. As such we assume that in order to apply this method, one should consider the model which is structurally correct such that it describes the general plant behavior well while may not consider all the complexities of the modeled phenomenon.

2.2. General form of first principles models

To describe the proposed framework of estimating parameters of first principles models in more detail, first, we define the general mathematical form of a steady state first principles model as:

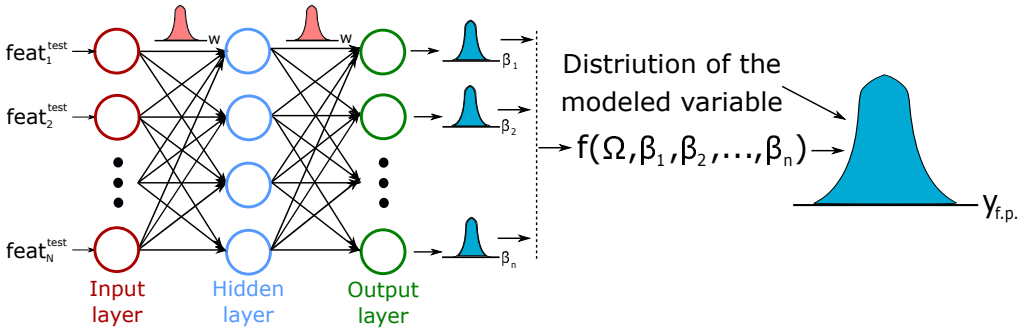

Figure 2: Prediction stage of Bayesian Neural Networks for predicting the mean and variance of the modeled variable

$$f(\Omega, B) = 0 \tag{1}$$

where $\Omega = [\omega_1, \omega_2, ..., \omega_n]^T$ denotes a vector of states of the process which is described by the model (e.g. pressure, temperature, fluid properties, etc.) and $B = [\beta_1, \beta_2, ..., \beta_n]^T$ denotes a vector of the first principles model parameters. Also, user dependent and known input variables will typically be present in the model, but we do not include them explicitly to keep the notation simple.

Let us further denote y_{meas} as a vector of process measurements. We assume that given a set of parameters B, a first principles model can produce an estimate of the process measurement y_{meas} when solved with respect to it, i.e.:

$$\hat{y}_{f.p.} = g(\Omega, B) \tag{2}$$

where $\hat{y}_{f.p.}$ is an estimate of y_{meas} obtained by solving the first principles model $f(\Omega, B)$ for Ω and evaluating the output equation $g(\Omega, B)$.

In case when the mechanistic model describes the process accurately, $\hat{y} \simeq y_{meas}$. This can be the case when the model structure is correct and the model parameters B are accurately tuned to the process data. In this work, we do not discuss the general framework of how to construct an accurate representation of the mechanistic first principles model. Instead, given a sequence of steady state process data $X = [(x^{(1)}, y^{(1)}), (x^{(2)}, y^{(1)})..., (x^{(n)}, y^{(n)})]$, we want to estimate the values of the parameters vector B and the uncertainty of the predictions based on the data.

2.3. Bayesian Neural Networks

2.3.1. Bayesian Learning Framework

Bayesian Neural Networks is a family of artificial neural networks whose weights are represented by distributions rather than by point estimates as in the conventional maximum likelihood approach (Neal (2012)). These distributions represent our beliefs about the values of the parameters. Bayesian learning of neural networks (and any other machine learning models) starts with defining prior distributions $P(W)$ of neural network

parameters, i.e. weights and biases. The prior distributions express our prior beliefs about the neural network parameters before we fit it to any data (Neal (2012)). In the learning process, the model parameters are updated according to the Bayes' rule:

$$P(W|X) = \frac{P(X|W)P(W)}{P(X)} \tag{3}$$

where X denotes the vector of observed data and the associated target variable (in case of this paper - measurement) $[(x^{(1)}, y^{(1)}), (x^{(2)}, y^{(1)})..., (x^{(n)}, y^{(n)})]^T$ and W denotes the vector of neural network parameters (weights and biases).

In Eq. 3, $P(W|X)$ is the posterior distribution of the model parameters which is a result of the update of our prior beliefs about them represented by $P(W)$ after fitting the model to the data. $P(X|W)$ is called a likelihood function which represents neural network predictions for a given set of parameters (weights and biases). $P(X)$ is the normalizing constant which ensures that the probability sums to one.

From the Bayes' rule we see that the learning process of model parameters is done in a natural way, such that we propose our beliefs about how the model should look like and then update it according to the observed data. Also, the main advantage of Bayesian learning is that, in addition to the maximum likelihood (or maximum a posterior) point estimate of the model parameters, we get uncertainty of model parameters. As the result, we are be able to estimate uncertainty of the target (modeled) variable during inference as the following:

$$\begin{aligned} &P(y^{(n+1)}|x^{(n+1)}, (x^{(1)}, y^{(1)}), ..., (x^{(n)}, y^{(n)})) \\ &= \int P(y^{(n+1)}|x^{(n+1)}, W)P(W|(x^{(1)}, y^{(1)}), ..., (x^{(n)}, y^{(n)}))dW \end{aligned} \tag{4}$$

where $(x^{(1)}, y^{(1)}), (x^{(2)}, y^{(1)})..., (x^{(n)}, y^{(n)})$ denote the observed data points and $x^{(n+1)}$ denotes the point for which the target variable is estimated.

The main disadvantage of the Bayesian approach for neural networks learning is that the probability distribution $P(X)$ is high dimensional and analytically intractable (Bishop (1997)). For this reason, various approximations of posterior parameter distributions $P(X|W)$ are used. In this work, we use variational inference (Blundell et al. (2015)) and Markov Chain (MC) Dropout (Gal and Ghahramani (2015)) approaches as approximations of the posterior distribution, which are described in the next sections in more detail. The main reason why these methods have been chosen is the fact that they can be used for big data sets in the context of process engineering systems, as such the methods proposed in this paper can be applied to many systems of interests.

2.3.2. Bayes by Backprop

One popular approach to approximate the exact posterior distribution of neural network parameters $P(W|X)$ is to use a variational approximation of it, as proposed by Hinton and Van Camp (1993) and further developed Graves (2011). The main idea is to use a variational distribution $q(W|\theta)$ on the weights parameterized by θ and find such parameters θ of the approximate distribution $q(W)$ which minimize the Kullback-Leibler (KL) divergence (which is a measure of distributions similarity), with respect to the exact posterior distribution $P(W|X)$ (Blundell et al. (2015)):

$$\theta^{\star} = \arg\min_{\theta} KL[q(W|\theta)||P(W|X)] = \arg\min KL[q(W|\theta)||P(W)] - \mathbb{E}_{q(W|\theta)}[logP(X|W)] \tag{5}$$

From Eq. 5, the resulting cost to be minimized is:

$$J(X, W, \theta) = KL[q(W|\theta)||P(W|X)] - \mathbb{E}_{q(W|\theta)}[logP(X|W)] \tag{6}$$

where cost function $J(X, W, \theta)$ is called a variational free energy (Blundell et al. (2015)).

Blundell et al. (2015) showed that the cost $J(X, W, \theta)$ can be approximated as:

$$J(X, W, \theta) \approx \sum_{i=1}^{n} q(w^{(i)}|\theta) - logP(w^{(i)}) - logP(X|w^{(i)}) \tag{7}$$

where $w^{(i)}$ denotes a weight sample from the variational posterior distribution $q(w^{(i)}|\theta)$.

This approach of training Bayesian Neural Networks is called the Bayes by Backprop (BBP) algorithm. At the inference stage of BBP, weight samples are drawn from the variational posterior distribution $q(W|\theta)$ which substitutes the exact posterior distribution $P(W|X)$ in Eq. 4. As a result, the mean estimate of the target variable as well as the uncertainty are estimated from the resulting approximated distribution $P(y^{(n+1)}|x^{(n+1)}, (x^{(1)}, y^{(1)}), ..., (x^{(n)}, y^{(n)}))$.

2.3.3. Markov Chain (MC) Dropout

The second approach to approximate the posterior distribution of the neural network parameters is Markov Chain Dropout. The theoretical foundation of Markov Chain Dropout is based on the fact that neural networks with applied dropout for each weight layer is mathematically equivalent to variational inference in the deep Gaussian Process. The derivation of the method is outside the scope of this paper and the interested reader is referred to the original article by Gal and Ghahramani (2015) and the appendix of the referred paper.

The outcome of Gal and Ghahramani (2015) derivations is that the exact posterior distribution of weights $P(W|X)$ can be approximated by an approximate variational distribution $q(W|\theta)$ via minimizing the following objective function:

$$J(X, W, p_{mc}) = -\frac{1}{N} \sum_{i=1}^{N} logP(x^{(i)}|w^{(i)}) + \frac{1 - p_{mc}}{2N} \|W\|^2 \tag{8}$$

where p_{mc} denotes the MC Dropout probability, $w^{(i)}$ denotes the sample drawn from the variational distribution $q(W|\theta)$.

The advantage of this method is that the loss expressed in Eq. 8 is the same as we would have had during training of a traditional maximum likelihood neural network using dropout.

At the inference time, the dropout probability is kept, as such we obtain the mean and the variance of the posterior distribution $P(y^{(n+1)}|x^{(n+1)}, (x^{(1)}, y^{(1)}), ..., (x^{(n)}, y^{(n)})$ as the following:

$$E(y) \approx \frac{1}{T}\sum_{t=1}^{T} P(x^{(i)}|w^{(i)}) \tag{9}$$

$$var(y) \approx \sigma^2 + \frac{1}{T}\sum_{t=1}^{T} P(x^{(i)}|w^{(i)})P(x^{(i)}|w^{(i)}) - E(y)^T E(y) \tag{10}$$

where T denotes the number of stochastic passes through the neural network,$E(y)$ - the expected value of the target variable, $var(y)$ - the variance of the produced estimates of the target variable, σ^2 - the data noise (irreducible error).

The part of Eq. 10 excluding σ^2 represent model (or epistemic) uncertainty which can be reduced if more data is collected and used for training, while σ^2 is the irreducible error and called aleatoric uncertainty.

3. First principles model description and solution method.

3.1. System description.

We consider a problem of pressure drop tuning of multiphase flows in pipes. More specifically, we study a three-phase multiphase flow model which aims to replicate a steady state multiphase flow behavior in oil and gas production systems. This is a complex phenomenon and has been an important research topic since 1950's. The first attempt to model multiphase flow pressure drop in pipes was based on empirical correlations proposed by Lockhart and Martinelli (1949). Nowadays, the research and industrial standard of modeling this phenomenon is based on first principles such as mass, momentum and energy equations supported by some lab or field correlations to close the mathematical set of equations. The mechanistic approach allows a much more accurate description of complex flow phenomena including dynamic flow situations such as severe slugging (Taitel (1986)).

Due to the complexity of multiphase flow phenomena, it is difficult to create such closure laws and empirical relations at the lab which accurately hold at field conditions. We consider OLGA (Bendiksen et al. (1991)) simulation results as the "true" field conditions. OLGA is the industrial standard of multiphase flow simulations, and we use it as a reference for data generation. The three-phase flow model developed in this work is used as the model which we would like to adjust to the "true" plant data generated by OLGA. Our first goal is to build a first principles model which produces relatively accurate results. However, it will not be able to exactly match the "true" plant data generated by OLGA due to different model formulation and different way of computing phase and mixture densities and viscosities which influence the friction loss values. To account for this inaccuracy between OLGA and our model, we use Bayesian Neural Networks which adjust the constructed model parameters and also estimate the uncertainty of the tuned predictions.

We selected a relatively simple plant setup to keep the discussion of the simulated phenomena under control. We model a straight horizontal pipe flow (see Fig. 3), such that pressure drop in the pipe is caused only by friction. Table 1 shows all the required boundary conditions which are constant in the training and test sets. We consider a

Figure 3: Straight pipeline plant setup used for case studies. The goal is to predict P_{in} given the following boundary conditions: Q_{gas}, Q_{liq}, T_{in}, P_{out}, T_{out}. When P_{in} is predicted, other parameters such as phase velocities or flow regimes can be identified.

Parameter	Value
Pipe length	1000 m
Pipe diameter (D_{pipe})	0.2 m
Hydraulic roughness (ϵ)	$3e^{-5}$ m
Outlet pressure (P_{out})	10 bar
Outlet temperature (T_{out})	25 °C
Inlet temperature (T_{out})	25 °C
Gas-oil ratio (GOR)	50 Sm^3/Sm^3
Water cut (WC)	0.3
Bubble point pressure (P_{bp})	50 bar
Bubble point temperature (T_{bp})	20 °C
Standard oil density ($\rho_{\bar{o}}$)	867 kg/m^3
Standard water density ($\rho_{\bar{w}}$)	1020 kg/m^3
Standard gas density ($\rho_{\bar{g}}$)	0.997 kg/m^3

Table 1: Fluid properties, boundary conditions and pipe dimensions use for case studies in the training and test sets

relatively short pipeline of 1000 m with small pipe diameter of 0.2 m to get a high pressure drop using high flowrate values. This allows avoiding long simulations during the training and tuning process and larger error between OLGA simulations and our model but does not affect the application procedure of the proposed concept.

In this work, the inlet and outlet temperatures are assumed to be equal, so the fluid flow is assumed to be isothermal. The outlet pressure is required to get the solution of the drift-flux model using SIMPLE integration scheme (Wang et al. (2016), Spesivtsev et al. (2013)) which we later discuss in the paper and the value for this pressure is kept at 10 bar. The fluid has a relatively low Gas-Oil-Ratio (GOR) and Water Cut (WC) values and typical values of standard gas, oil and water densities as well as bubble point pressure value.

3.2. The first principles model

In this section, we introduce the main part of the first principles model which is used as the example of the model to be tuned by Bayesian Neural Networks.

Fluid property	Correlation
Critical pressure (P_{crit})	McCain Jr et al. (1991)
Critical temperature (T_{crit})	McCain Jr et al. (1991)
Oil formation volume factor (B_o)	McCain Jr et al. (1991)
Water formation volume factor (B_w)	McCain Jr et al. (1991)
Gas compressibility factor (z)	Dranchuk et al. (1975)
Dead oil viscosity (μ_{doil})	Egbogah and Ng (1990)
Saturated oil viscosity (μ_{loil})	Beggs et al. (1975)
Gas viscosity (μ_{gas})	Lee et al. (1966)
Water viscosity (μ_{water})	McCain Jr et al. (1991)
Oil-gas surface tension (σ_{o-g})	Abdul-Majeed and Al-Soof (2000)

Table 2: Fluid properties correlations using within the Black Oil formulation

3.2.1. Fluid properties model

In order to model multiphase fluid flow motion in pipes, first, a model of the fluid properties at different conditions have to be created. There are two main approaches to model fluid properties of a petroleum liquid: compositional model and Black Oil (BO) model. In the compositional formulation, mass or molar fractions of the petroleum components are specified and then Equations of State are solved to compute the required fluid properties (Whitson et al. (2000)). In the Black Oil formulation, oil and gas are considered separately and their properties are computed using correlations which are based on several model properties such as solution gas-oil ratio, water cut, etc (Whitson et al. (2000)). The compositional approach can be generally more accurate and should be considered when a fluid composition is available. However, this is typically not the case and often only Black Oil properties are measured in the lab for petroleum calculations.

In this work, we use Standing Black Oil correlations (Standing et al. (1947)) for solution gas-oil ratio R_{so} and bubble point pressure P_{bp}. Standing correlations are suitable for the conditions we use in our problem, but in practice, other correlations which are more suitable for the conditions at hand can also be used and this will not change neither the solving procedure of the first principles models nor the tuning part using Bayesian Neural Networks.

Since we would like to achieve the results which are relatively close to OLGA simulation outcomes, we use fluid properties correlations of the OLGA Black Oil model which are mainly based on the work by McCain Jr et al. (1991). The summary of the used correlations are shown in Table 2.

Apart from that, we compute some of the properties based on the material balance. In particular, the formation liquid volume factor is computed as:

$$B_l = B_o\left(\frac{1}{1+WOR}\right) + B_w\left(\frac{WOR}{1+WOR}\right) \tag{11}$$

where B_l denotes the formation liquid volume factor and WOR - the water-oil ratio which is computed as $\frac{WC}{1-WC}$ where WC denotes the water cut.

Densities of oil, gas and water are also computed from the material balance:

$$\rho_{o,g,w} = \frac{\rho_{\bar{o},\bar{g},\bar{w}}}{B_{o,g,w}} \tag{12}$$

where $\rho_{o,g,w}$ denotes the oil, gas and water density respectively at local conditions, $\rho_{\bar{o},\bar{g},\bar{w}}$ - the oil, gas and water density respectively at standard conditions, $B_{o,g,w}$ - the oil, gas and water formation volume factor respectively at local conditions.

Mixture density and viscosity are computed based on the volumetric basis:

$$\rho_{mix} = \alpha_g \rho_{gas} + (1 - \alpha_g)\rho_{liq} \tag{13}$$

where ρ_{mix} denotes the mixture density and α_g - the gas volume fraction.

$$\mu_{mix} = \alpha_g \mu_{gas} + (1 - \alpha_g)\mu_{liq} \tag{14}$$

where μ_{mix} denotes the mixture viscosity.

The solution gas-liquid ratio R_{sl} is computed as:

$$R_{sl} = R_{so}\left(\frac{1}{1 + WOR}\right) \tag{15}$$

where R_{so} denotes the solution gas-oil ratio at local conditions.

Having computed the solution gas-liquid ratio R_{sl}, we can compute the liquid density based on the material balance:

$$\rho_{liq} = \frac{\rho_{\bar{g}} R_{sl} + \rho_{\bar{liq}}}{B_l} \tag{16}$$

where ρ_g denotes the gas density at local conditions, $\rho_{\bar{g}}$ - the water density at standard conditions, B_g - the gas formation volume factor at local conditions.

The described properties are used in computing mass and momentum balances for the multiphase flow mixture for given pressure and temperature conditions along the pipe.

Important note on densities and viscosities computation. As discussed above, the densities are computed based on the material balances. In OLGA, the software that simulates the true plant, the densities are computed differently.

In addition to the densities, we compute the mixture viscosity based on the volumetric balance, assuming homogeneous mixing between the phases. In OLGA, however, there are advanced options for computing the emulsion viscosities which are not based on the homogeneous mixing assumption. This influences the viscosity values which results in deviations of the friction losses values.

In this work, these simplifications are done intentionally in order to introduce additional error into computations which is then minimized by Bayesian Neural Networks and to mimic the real case, where the "true" model does not exist. To get a more accurate multiphase flow model, one may consider to compute densities and viscosities differently.

3.2.2. Mass and momentum balance formulation and discretization

There are two main approaches for modeling multiphase flows in pipes (Nydal (2012)): a two-fluid (or multi-fluid) model and drift-flux model. The two-fluid formulation is a more complex approach and considers mass and momentum equations for each fluid field such

as gas, oil and water separately. In addition, liquid droplets can also be considered as a separate fluid medium. Two leading commercial multiphase flow simulators in the oil and gas industry, OLGA and LedaFlow, use this approach (Bendiksen et al. (1991), Goldszal et al. (2007)).

The drift-flux formulation treats the multiphase flow fluid as a mixture which simplifies the modeling process. This results in one momentum equation for the mixture while the mass conservation equations are typically written separately for the gas and liquid fields (Holmås et al. (2011)). In our work, we consider the drift-flux model and then tune the model parameters such that the modeling outcomes are close to the ones produced by the two-fluid model from OLGA.

System of equations. We consider a steady state model, as such we do not include time derivatives into the equations. However, we do consider the mass transfer from the oil phase to the gas phase because gas bubbles out from oil when pressure decreases along the pipe. The mass transfer term is adopted from Andreolli et al. (2017). The resulting mass and mixture momentum balances are:

$$\frac{d(\alpha_g \rho_g u_g)}{dx} = -Q_o^{sc} \rho_g \frac{dR_{so}}{dx} \tag{17}$$

$$\frac{d\big((1-\alpha_g)\rho_{liq} u_{liq}\big)}{dx} = Q_o^{sc} \rho_g \frac{dR_{so}}{dx} \tag{18}$$

$$\frac{dP}{dx} = \frac{2\xi_{mix}\rho_{mix}u_{mix}^2}{D_{pipe}} + \rho_{mix} g sin(\psi) \tag{19}$$

where α_g denotes the gas volume fraction, u_g - the gas phase velocity, R_{so} - the solution gas-oil ratio, u_{liq} - the liquid phase velocity, Q_o^{sc} - the oil flowrate at standard conditions, P - the fluid pressure, u_{mix} - the mixture velocity, ξ_{mix} - the friction factor coefficient computed using mixture properties, D_{pipe} - the pipe diameter, g - the acceleration constant, ψ - the angle of the pipe relative to the horizontal plane.

To compute the system we need the following boundary conditions:

- inlet: liquid flowrate (Q_{liq}), inlet temperature (T_{in}) [in our case $T_{in} = T_{out}$ because we assume isothermal flow]
- outlet: outlet pressure (P_{out}), outlet temperature (T_{out})

In order to close the system of equations, the void fraction correlation is required which is used to compute the difference between the gas and liquid phase velocities and also linked with computing the local gas volume fraction (void fraction) in the pipe within the mass balance. In this work, we use a comprehensive flow pattern independent correlation by Bhagwat and Ghajar (2014) which shows an accurate performance for various conditions, flow regimes and fluid types. However, the model is not restricted to application of this correlation and other correlations can be used in search of a more accurate solution. Since in this paper our goal is to get a robust and physically feasible solution of the model and adjust it to the plant data, the solution accuracy is not essential. As such,

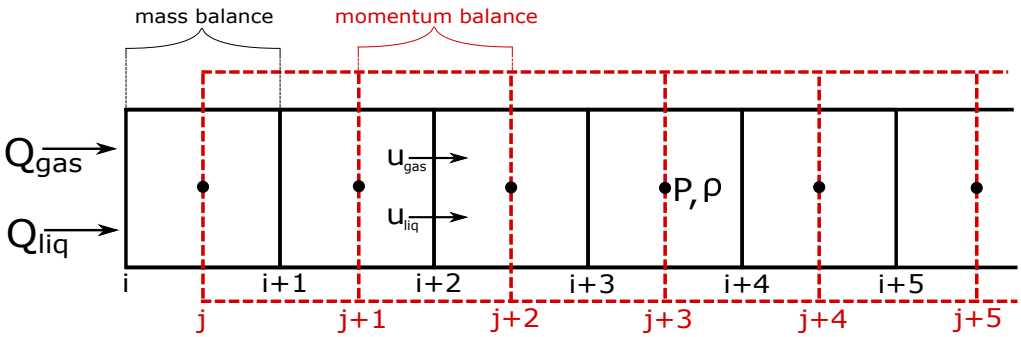

Figure 4: Staggered grid discretization scheme used to solve the system of equations of the drift-flux model

it is out of the scope of this paper to compare the performance of this correlation with other ones.

In order to compute the friction factor, we use the Colebrook equation with the mixture properties (Colebrook et al. (1939)):

$$\frac{1}{\sqrt{\xi_{mix}}} = -4log_{10}\left(\frac{1.256}{Re_{mix}\sqrt{\xi_{mix}}} + \frac{\epsilon}{3.7D_h}\right) \tag{20}$$

where Re_{mix} denotes the mixture Reynolds number ϵ - the hydraulic roughness, D_h - the hydraulic diameter (in our case $D_h = D_{pipe}$).

The Reynolds number in Eq. 20 is computed as follows:

$$Re_{mix} = \frac{\rho_{mix} u_{mix} D_{pipe}}{\mu_{mix}} \tag{21}$$

3.2.3. Discretization and numerical scheme.

Equations 17, 18, 19 are discretized using the control volume approach in a mesh with staggered grid. The discretization scheme is shown in Figure 4. The mass balances are solved within the black control volumes while the momentum balances are solved in control volumes shifted from the mass control volumes by half a mass control volume cell (shown in red). The scalar variables such as pressure, density, etc are computed in the middle of the control volumes (or at the faces of the momentum control volumes) while the velocity components computed at the at the mass control volume faces. This helps to avoid undesirable oscillating behavior of the solution of the pressure field as well as gives an opportunity to evaluate the velocities at the faces where they needed to compute advection terms of the equations, for example, $\alpha_g \rho_g u_g$ term (Yang et al. (2010)).

3.3. Model solving procedure

To solve Equations 17, 18, 19 within the staggered grid framework, we use Semi-Implicit Method for Pressure-Linked Equations (SIMPLE) with the first order upwind scheme for the advection terms of the mass conservation equations (Wang et al. (2016), Spesivtsev et al. (2013)). The general solution procedure is as follows:

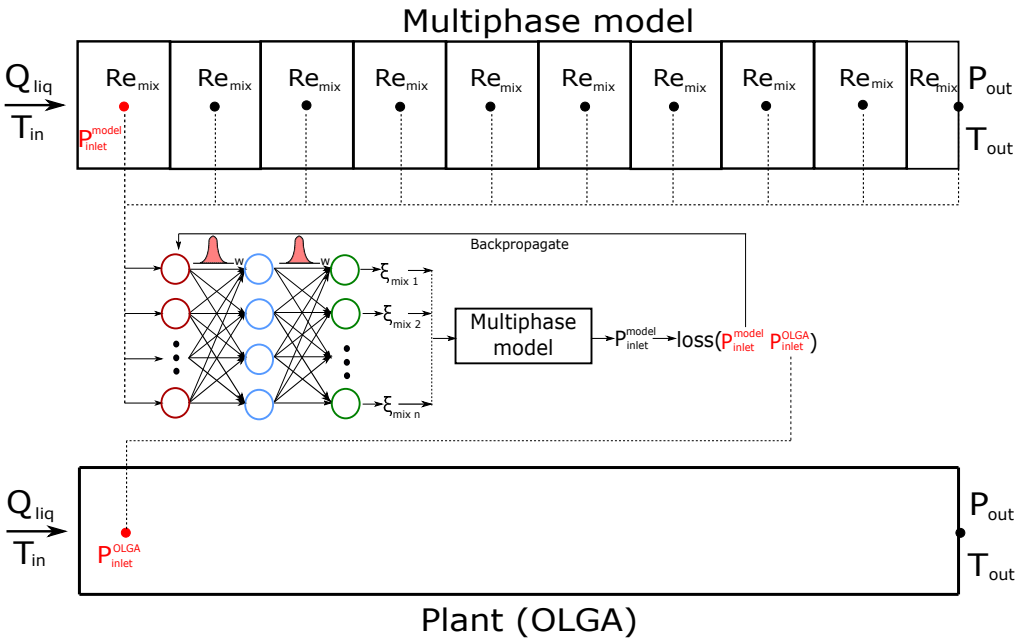

Figure 5: Training a Bayesian Neural Network for pressure drop tuning of multiphase flow in a pipe using measured inlet and outlet conditions

1. Initialize the pressure and temperature fields.
2. Compute required fluid properties at the initialized conditions.
3. Solve the mass balance equations.
4. Compute the velocity field.
5. Solve the momentum balance equation.
6. Compute the pressure field.
7. Compute the error between the newly computed pressure field and the guessed pressures.
8. If the pressure error is acceptable, solution is converged, if not - assign the new pressure field as the guessed pressure field (possibly with some relaxation factor) and start from Step 1.

4. Case study setup

4.1. Using Bayesian Neural Networks for tuning first principles model parameter to data

The training part of the tuning concept adaptation for the considered problem is shown in Figure 5. We selected the friction factor ξ_{mix} as the parameter to be tuned. To tune the friction factor, we divide the pipe into 10 control volumes and take the calculated Re_{mix} as features from each control volume. We selected Reynolds numbers Re_{mix} for the features because the friction factor ξ_{mix} was selected as a tunable parameter. From

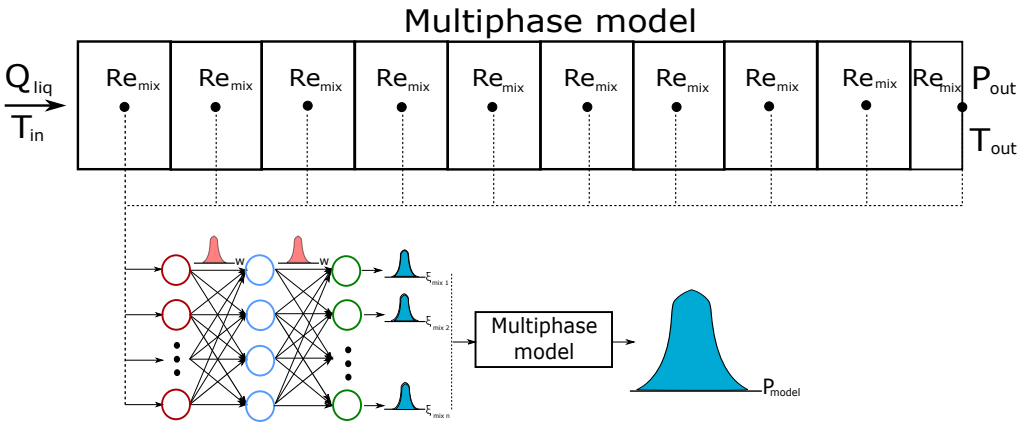

Figure 6: Prediction stage of Bayesian Neural Networks for predicting the mean and variance of the modeled variable

Eq. 20 we see that the friction factor is a function of Re_{mix}, as such we will try to find almost the direct correction mapping for the friction factor ξ_{mix}.

The computed friction factors from the BNNs are then inserted back to the first principles model to compute the pressure at the inlet of the pipe. The computed pressure is compared with the plant measurement produced by OLGA, and the neural networks weights and biases distributions are adjusted via backpropagation.

The reason why inlet pressure is selected to be the target variable used for BNNs tuning is the fact that in oil and gas production systems inlet and outlet pressures are typically measured using sensors, such that we can use it for first principles model adjustment. In our case, we use the outlet pressure as the boundary condition of the multiphase first principles model, while the inlet pressure is used as the tuning reference.

Figure 6 shows the inference stage of the trained BNN at the prediction (test) time. Here, the computed Re_{mix} at test conditions are inserted into the trained BNN, which produces distributions of the friction factors. Based on these distributions, the distribution of the inlet pressure is computed.

4.2. Case studies

Training set. One of the main goals of this work is to see if BNNs are able to estimate uncertainty correctly under different process conditions. To do that, we control the distribution of the conditions in the training and test sets such that we know when the test set is within the distribution of the training set and when it is not. For the process conditions to be changed, we selected the inlet liquid flowrates. We assume of 1440 training points available to us. These points are split unequally such as 90% correspond to high flowrate range values (between 0.15 and 0.25 m^3/s) and 10% correspond to low flowrate values (between 0.05 and 0.15 m^3/s). This is done in order to see if Bayesian Neural Networks produce different level of uncertainty for different flowrate ranges in the test set depending on the training set size of each range.

Parameter	Value/value range	Number of samples
Training set		
Inlet liquid flowrate (Q_{liq})	10% - [0.05 - 0.15] m^3/s	144
	90% - [0.15 - 0.25] m^3/s	1296
Test set, Case 1		
Inlet liquid flowrate (Q_{liq})	50% - [0.05 - 0.15] m^3/s	25
	50% - [0.15 - 0.25] m^3/s	25
Test set, Case 2		
Inlet liquid flowrate (Q_{liq})	50% - [0.05 - 0.15] m^3/s	25
	50% - [0.25 - 0.30] m^3/s	25

Table 3: Process conditions in the training and test sets

Test case studies. We consider two case studies and each case study is performed with two types of Bayesian Neural Network: trained by MC Dropout and by Bayes by Backprop. Table 3 shows the conditions for each case study together with the training set flowrate ranges.

In **Case 1**, we consider the same conditions in the training and test sets. We split the data of flowrate range equally between the ranges which are used in training: 50% for Q_{liq} = [0.05-0.15] m^3/s and 50% for Q_{liq} = [0.15-0.25] m^3/s. The values for training are taken from the uniform distribution within the specified ranges.

We test the model for 50 test points, 25 points per flowrate range (high and low). The values of the flowrates are taken randomly from the specified ranges. For each value the simulation is run 5 times. It is done in this way because it produces better visualization of the results while does not deteriorate any conclusions from it.

The idea of this case study is to test capabilities of BNNs to quantify uncertainty based on the amount of information in the training set. Since we have only 10% of the training set in the range of $[0.05 - 0.15]m^3/s$, our hypothesis is that the BNN will give a higher uncertainty when predicting the target variable. It is also interesting to see how in general a BNN behaves under the conditions which are within the training range.

In **Case 2**, we increase the high flowrate range from 0.25 up to 0.3 m^3/s in the test set data. We introduce the new range to the model, but we do not re-train it to update the BNNs parameters. This is done to see what is the bias and uncertainty levels of the predictions for these new conditions. Table 3 shows all the values important for the case studies to consider.

5. Results and Discussion

5.1. Case 1 results and discussion

In Case 1, the range of the inlet flowrates was the same as in the training set and the main idea behind this case was to see how BNNs quantify the uncertainty of the inlet pressure for high and low flowrate values with different number of training points for each flowrate range.

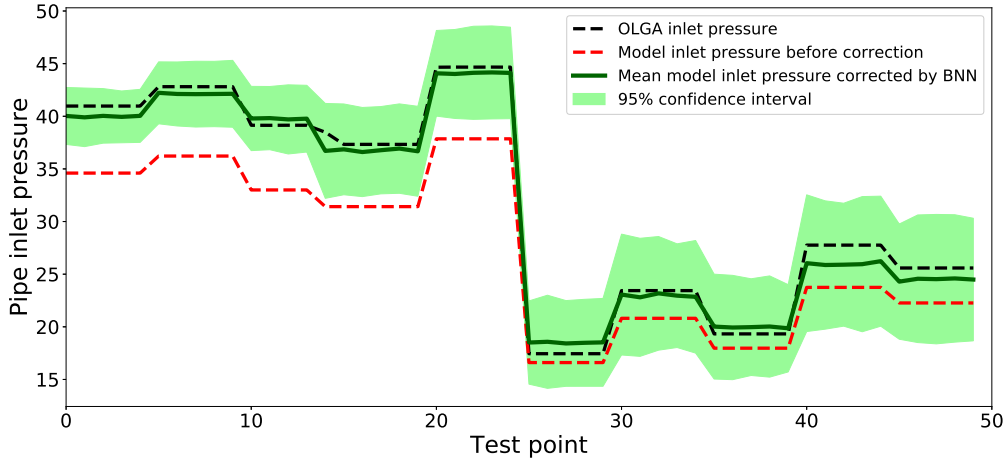

Figure 7: Estimated mean and 95% confidence interval of the corrected multiphase flow model using MC Dropout Bayesian Neural Network for Case 1.

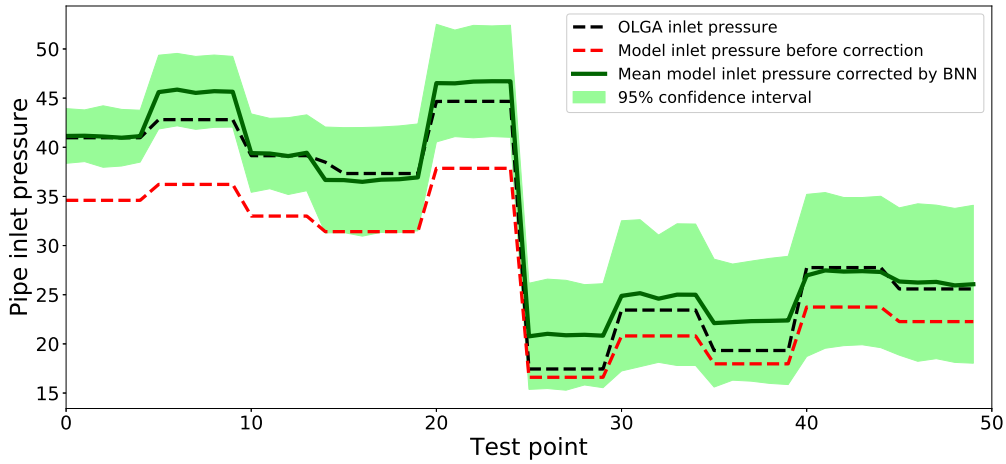

Figure 8: Estimated mean and 95% confidence interval of the corrected multiphase flow model using Bayes by Backprop Bayesian Neural Network Case 1.

Mean and uncertainty estimates. Fig. 7 and Fig. 8 show the results of the first principles model tuning process by BNNs in Case 1. We see that both BNN types are able to tune the first principles model such that the mean estimates of the inlet pressure produced by the hybrid (first principles + BNN) models are close to the plant (OLGA) pressures. This holds for both high inlet flowrates (high pressure values) and low inlet flowrates (low pressure values). However, the Bayes by Backprop BNN shows slightly worse performance in terms of the mean estimates on the low pressure values where the

Model	MAPE error		
	High flowrates	Low flowrates	Entire set
Untuned model	15.65%	10.10%	12.88 %
Model tuned with MC Dropout	1.79%	4.39%	3.09%
Model tuned with Bayes by Backprop	2.81%	8.84%	5.83%

Table 4: Mean absolute percentage errors between the model mean outcomes and the plant pressure values in Case 1

Model	95% confidence interval [in bar]		
	High flowrates	Low flowrates	Entire set
Model tuned with MC Dropout	3.52	5.27	4.40
Model tuned with Bayes by Backprop	4.26	6.95	5.61

Table 5: 95% confidence intervals produced by hybrid Bayesian models in Case 1

number of data points is small. Due to the small number of training points in that region, the guessed priors may not have been accurate enough to obtain good posterior estimates, so that it was difficult to tune the model in that region and in some cases the tuned model works worse than the untuned version. Table 4 shows the mean absolute percentage errors (MAPEs), computed using Eq. 22, produced by the untuned and tuned models for all flowrate ranges in Case 1. From the table we see that the errors within the high flowrate range values are smaller than for the low flowrate range for both BNNs.

$$MAPE = \frac{1}{N}\sum_{n=1}^{N}\left|\frac{y_{plant} - \hat{y}_{plant}}{y_{plant}}\right| \tag{22}$$

where N denotes the number of test points, y_{plant} - plant values of the measurement (in our case - OLGA inlet pressure), $\hat{y}_{plant}$ - estimated mean of the plant value by hybrid (first principles + BNN) or the untuned first principles model.

As for the uncertainty estimates level, in Fig. 7 and Fig. 8 we observe that the average uncertainty estimates for the low pressures are higher, than for the high pressure values. The values of the 95% confidence intervals are shown in Table 5. We see that the estimates of the confidence intervals produced by the different types of BNNs are quite similar, however, the BNN trained Bayes by Backprop produce higher uncertainty levels.

5.2. Discussion of Case 1 results

Our observations of the simulation results have been hypothesized prior to the training and confirmed at the results stage. For instance, the results confirmed that both BNN types are able to correctly qualitatively identify the uncertainty levels of the first principles models parameters (friction factors) based on the training size distributions. The distribution of the friction factors have been then introduced into the first principles models which resulted in the uncertainty level estimates of the inlet pressure values. The results also show that in the regions where BNNs have less prior information, they have less accurate interpolating capabilities, which resulted in less accurate mean estimates and larger uncertainty. On the other hand, we see that in most of the cases even a small training set was enough for the neural networks to adjust the first principles models to the plant conditions. However, this is mainly caused by the fact that no noise was introduced into the data. This has been done intentionally to prove the concept of tuning parameters by BNNs, rather than additionally challenge them to fit the data at hand. In general, more noisy data would result in the need of more tuning data.

Training difficulties of Bayes by Backprop algorithm. In general, the success of neural network training depends on the parameters (weights and biases) initialization. This is especially important for Bayesian Neural Networks because the poor prior distribution of the parameters will usually result in poor posterior, which in turn results in inaccurate and uncertain predictions.

Since the training procedure of the MC Dropout network is similar to conventional training, in this work we used the initialization procedure by He et al. (2015) which has been proven as a robust initialization technique. As for the Bayes by Backprop, we used the normally distributed priors of the neural network weights as suggested in the original paper by Blundell et al. (2015). However, in practice we observed that guessing a good prior is difficult and we met problems trying to find a suitable prior which results in a robust tuning, meaning that the guess prior had been leading to bad posteriors and poor simulation results.

To overcome the obstacles with tuning the Bayes by Backprop BNN, we initialized the priors close to the weights distributions produced by the tuned MC Dropout BNNs. This resulted in a relatively robust tuning procedure. However, to make it even more robust, we performed 3 samples of the weights per epoch to compute the approximated cost shown in Eq. 7, which resulted in a less stochastic behavior of the cost function and more robust tuning. Therefore, as a result of our investigations, we suggest a similar approach for guessing a good initial prior when performing first principles model tuning using the Bayes by Backprop algorithm.

One could argue that there is no point in creating a hybrid (first principles + BNN) model using the Bayes by Backprop algorithm if the MC Dropout is more robust in tuning. However, this may not always be the case and in the literature there are various examples when MC Dropout underestimated the uncertainties if compared to the Bayes by Backprop algorithm (Blundell et al. (2015)). In fact this is what we also observe in our case. Despite that the estimated uncertainty levels for both BNNs types are quite similar, the levels produced by Bayes by Backprop are larger (see Table 5) and in fact may be more accurate. As such, when the level of the hybrid model uncertainty is critical for the problem at hand, for instance for the subsequent use in robust optimization of

the process, one may consider using the Bayes by Backprop algorithm rather than MC Dropout.

Data noise and overfitting. One more important fact to discuss here is that we assumed that the plant measurements do not have noise which made it easier for the BNNs to tune the first principles model to the plant conditions. In real operation, this is typically not the case. This will most likely result in the fact that more measurement data will be required to tune the models accurately. Moreover, the tuning itself will be more difficult because data noise may cause overfitting. At the same time, a strong feature of Bayesian Neural Networks is the fact that they are less prone to overfitting than conventional maximum likelihood neural networks due to model parameter averaging. In addition, the data noise can be learned from the data. This can be done via selecting the noise level as the learnable BNN's parameter. This will result in the fact that the noise will be accounted when making mean and uncertainty estimates of the target variable.

5.3. Case 2 results and discussion

In Case 2, the range of the inlet flowrate was not the same as in the training set for the high flowrate range. As such, the main idea behind this case was to see how BNNs estimates the model bias and uncertainty when the plant process conditions change. In this case, the inlet flowrate is outside the training set, however, since we use the Reynolds numbers as the features, the feature distribution is not necessarily fully outside the training set.

Mean and uncertainty estimates. Fig. 9, Fig. 10, Table 6 and Table 7 show the results of the first principles model tuning process by BNNs in Case 2. From the figures and tables we see that where the process conditions do not change (low pressure values), the uncertainty level and the mean predictions error are low and in fact the same as in the Case 1 because the conditions are the same. This is not the same as for the high flowrate case. We see that in addition to the bias, the uncertainty level of predictions are several times larger than for the low flowrate cases and even worse than for the untuned model. This is true for both BNNs types.

Such results have been expected since the flowrate values which correspond to the high pressure values in Case 2 are outside the training range. This resulted to the fact that the difference between the mean estimates and the actuate plant values are high. But what is more important, we can see that the both BNNs types are able to correctly estimate the qualitative uncertainty levels depending on how far the test data points are from the training set, as we see that for the highest pressure value is uncertainty is the largest for both BNNs types. We discuss the usefulness and practical applicability of the obtained results in the next subsection.

5.4. Discussion of Case 2 results

Importance of uncertainty levels for monitoring of process system plants.

Process measurement drift/Non-observable process conditions change

The obtained results lead to very important conclusions from the process operations point of view. In many cases, the process measurements drift over time which is very difficult to identify in practice. Let us assume that the inlet pressure drifts over time and we are not aware of this situation. Having uncertainty estimates about our predictions

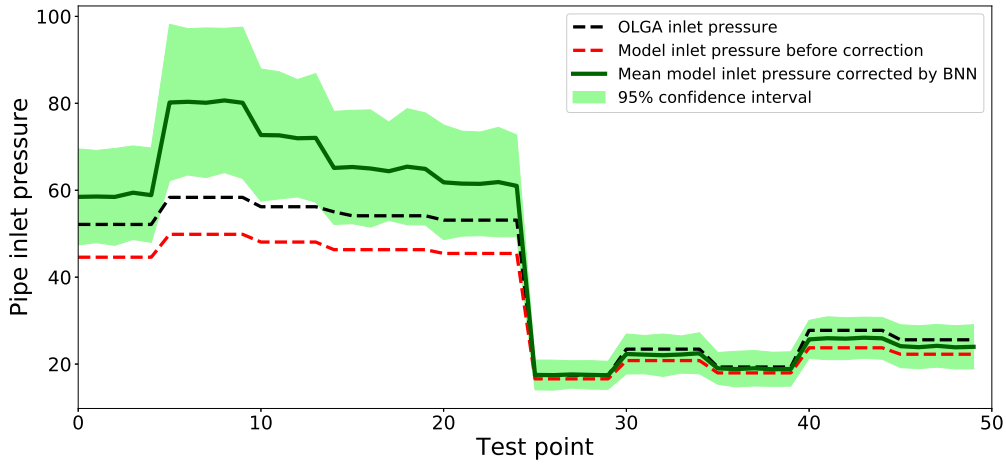

Figure 9: Estimated mean and 95% confidence interval of the corrected multiphase flow model using MC Dropout Bayesian Neural Network for Case 2.

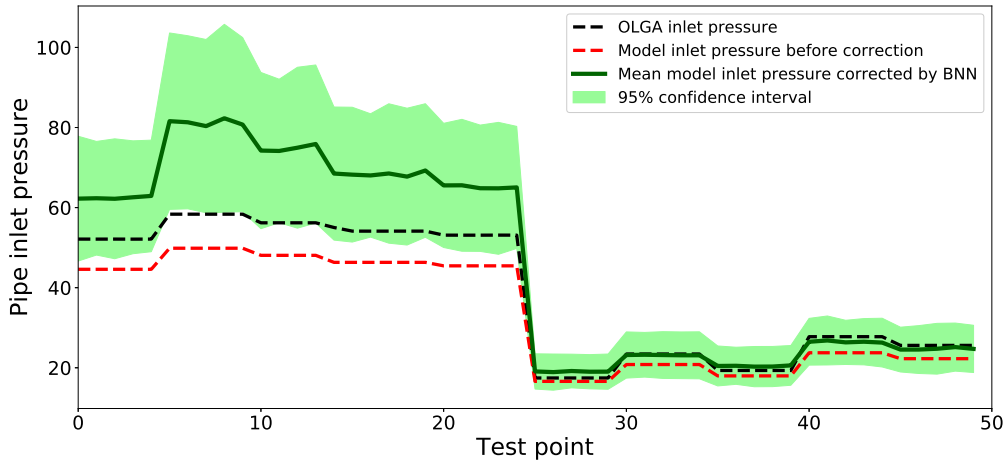

Figure 10: Estimated mean and 95% confidence interval of the corrected multiphase flow model using Bayes by Backprop Bayesian Neural Network Case 2.

will help us to identify the measurement drift. This is because, *assuming that we know the inlet flow conditions*, we know that the flow conditions have not change and for any particular point in time we get high confidence in our predictions (low uncertainty levels). At the same time, we see that the inlet pressure estimates deviates from the measurements. This will be a most likely caused by the fact that the process measurement drifted over time.

In addition, we may be able to identify other process condition changes. For instance,

Model	MAPE error		
	High flowrates	Low flowrates	Entire set
Untuned model	15.65%	10.10%	12.88 %
Model tuned with MC Dropout	22.58%	4.39%	13.48%
Model tuned with Bayes by Backprop	27.88%	8.84%	18.36%

Table 6: Mean absolute percentage errors between the model outcomes and the plant pressure values in Case 2

Model	95% confidence interval [in bar]		
	High flowrates	Low flowrates	Entire set
Model tuned with MC Dropout	13.49	5.27	9.38
Model tuned with Bayes by Backprop	17.6	6.95	12.28

Table 7: 95% confidence intervals produced by hybrid Bayesian models in Case 2

again, assuming the known flowrate measurements, we may see the deviation between the mean estimates of the proposed model and measurements. Knowing that the observed conditions have not changed, there is a possibility that non-observable process conditions change. In the multiphase flow pipeline, this can be for instance, wax and hydrate depositions which increased the friction loss and caused additional pressure drop. As such, hazardous situation can be avoided using the proposed methods with a much higher confidence that using just untuned non-bayesian first principles models.

The need for model recalibration There are less hazardous situations when Bayesian First Principles models can be effectively used. This is when we know that the observable process conditions changed over time and the bias and uncertainty levels of the models increased. This is the exact situation which we have provided in our work. We changed the inlet flowrate and observed that the difference between the referenced pressures and produced mean estimates became high for the high flowrate values and this difference has been also confirmed by the high uncertainty levels. This is a clear situation when the model needs recalibration, because the deviations and high uncertainties are caused by the fact that the model has not seen such process conditions before because the plant has ot been operated around this point. After recalibration the model can be used successfully again for the new conditions.

6. Conclusions

In this paper, we propose the general framework of tuning first principles models using Bayesian Neural Networks and show applications of such a framework based on tuning a steady state three-phase multiphase flow model. For the Bayesian Neural Networks training, we used variational approximation methods such as MC Dropout and Bayes by Backprop. The multiphase flow model consists of two main parts: fluid properties model represented by the Black Oil approach and the hydrodynamic drift-flux model solved by the SIMPLE numerical integration scheme over the staggered numerical grid.

We found that by tuning the first principles model using Bayesian Neural Networks, it is possible to adjust them to the seen process conditions such that the tuned model correctly represent the process. As such, the Bayesian Neural Networks were found to be a good tool for tuning the first principles models despite a relatively small dataset size. The main advantage of using the Bayesian Neural Networks was found to be the ability to correctly estimate the uncertainty level of predictions depending on the number of available training data points, such that for a smaller part of the training distributions, the produced level of uncertainties were higher. We also found that Bayesian Neural Networks are able to correctly identify the level of uncertainty when when the process conditions become outside the training range.

In addition, we discussed how the proposed method can be used to identify the measurement drift in a process plant, change of non-observable process conditions or when the model recalibration is needed. We found that the proposed methods can be of a great importance when making decisions during the monitoring of process engineering systems.

As for the difference between the Bayesian Neural Networks, we found that the ones trained with Bayes by Backprop algorithm produce larger uncertainty levels, slightly less accurate in terms of the mean estimates and are much harder to fit than the BNNs trained with MC Dropout algorithm. As an ad-hoc training approach, we proposed to first train an MC Dropout BNN, sample the weights and use it as a prior to the weights for Bayes by Backprop training.

In general, we believe that the first principles models tuned by Bayesian Neural Networks will become a great, robust and highly usable tool in the near future in process conditions monitoring. This is because the computational power increases over time which allows training deep Bayesian Neural Networks for any process at hand. In addition, such an approach will provide more degrees of freedom when making correct decisions to either change the measurement sensors, perform additional maintenance check and operation, for instance, pigging, or perform recalibration of Digital Twins models which represent a real time process plant behavior.

References

Abdul-Majeed, G.H., Al-Soof, N.B.A., 2000. Estimation of gas–oil surface tension. Journal of Petroleum Science and Engineering 27, 197–200.

Ahmadi, M.A., Chen, Z., 2018. Comparison of machine learning methods for estimating permeability and porosity of oil reservoirs via petro-physical logs. Petroleum .

Aldebert, C., Stouffer, D.B., 2018. Community dynamics and sensitivity to model structure: towards a probabilistic view of process-based model predictions. Journal of the Royal Society Interface 15, 20180741.

Amjad, S., Al-Duwaish, H.N., 2003. Closed loop identification with model predictive control: a case study, in: SICE 2003 Annual Conference (IEEE Cat. No. 03TH8734), IEEE. pp. 144–149.

Andreolli, I., Zortea, M., Baliño, J.L., 2017. Modeling offshore steady flow field data using drift-flux and black-oil models. Journal of Petroleum Science and Engineering 157, 14–26.

Anifowose, F.A., Labadin, J., Abdulraheem, A., 2017. Hybrid intelligent systems in petroleum reservoir characterization and modeling: the journey so far and the challenges ahead. Journal of Petroleum Exploration and Production Technology 7, 251–263.

Beggs, H.D., Robinson, J., et al., 1975. Estimating the viscosity of crude oil systems. Journal of Petroleum technology 27, 1–140.

Bendiksen, K.H., Maines, D., Moe, R., Nuland, S., et al., 1991. The dynamic two-fluid model olga: Theory and application. SPE production engineering 6, 171–180.

Bhagwat, S.M., Ghajar, A.J., 2014. A flow pattern independent drift flux model based void fraction correlation for a wide range of gas–liquid two phase flow. International Journal of Multiphase Flow 59, 186–205.

Bikmukhametov, T., Stanko, M., Jäschke, J., et al., 2018. Statistical analysis of effect of sensor degradation and heat transfer modeling on multiphase flowrate estimates from a virtual flow meter, in: SPE Asia Pacific Oil and Gas Conference and Exhibition, Society of Petroleum Engineers.

Bishop, C.M., 1997. Bayesian neural networks. Journal of the Brazilian Computer Society 4.

Blundell, C., Cornebise, J., Kavukcuoglu, K., Wierstra, D., 2015. Weight uncertainty in neural networks. arXiv preprint arXiv:1505.05424 .

Colebrook, C.F., Blench, T., Chatley, H., Essex, E., Finniecome, J., Lacey, G., Williamson, J., Macdonald, G., 1939. Correspondence. turbulent flow in pipes, with particular reference to the transition region between the smooth and rough pipe laws.(includes plates). Journal of the Institution of Civil engineers 12, 393–422.

DiGiano, F.A., Zhang, W., 2004. Uncertainty analysis in a mechanistic model of bacterial regrowth in distribution systems. Environmental science & technology 38, 5925–5931.

Dranchuk, P., Abou-Kassem, H., et al., 1975. Calculation of z factors for natural gases using equations of state. Journal of Canadian Petroleum Technology 14.

Egbogah, E.O., Ng, J.T., 1990. An improved temperature-viscosity correlation for crude oil systems. Journal of Petroleum Science and Engineering 4, 197–200.

Gal, Y., Ghahramani, Z., 2015. Dropout as a bayesian approximation. arXiv preprint arXiv:1506.02157 .

Goldszal, A., Monsen, J., Danielson, T., Bansal, K., Yang, Z., Johansen, S., Depay, G., et al., 2007. Ledaflow 1d: Simulation results with multiphase gas/condensate and oil/gas field data, in: 13th International Conference on Multiphase Production Technology, BHR Group.

Gorjian, N., Ma, L., Mittinty, M., Yarlagadda, P., Sun, Y., 2010. A review on degradation models in reliability analysis, in: Engineering Asset Lifecycle Management. Springer, pp. 369–384.

Graves, A., 2011. Practical variational inference for neural networks, in: Advances in neural information processing systems, pp. 2348–2356.

He, K., Zhang, X., Ren, S., Sun, J., 2015. Delving deep into rectifiers: Surpassing human-level performance on imagenet classification, in: Proceedings of the IEEE international conference on computer vision, pp. 1026–1034.

Hinton, G.E., Van Camp, D., 1993. Keeping the neural networks simple by minimizing the description length of the weights, in: Proceedings of the sixth annual conference on Computational learning theory, pp. 5–13.

Holmås, K., Løvli, A., et al., 2011. Flowmanager^{TM} dynamic: A multiphase flow simulator for online surveillance, optimization and prediction of subsea oil and gas production, in: 15th International Conference on Multiphase Production Technology, BHR Group.

Kanin, E., Osiptsov, A., Vainshtein, A., Burnaev, E., 2019. A predictive model for steady-state multiphase pipe flow: Machine learning on lab data. Journal of Petroleum Science and Engineering 180, 727–746.

Klyuchnikov, N., Zaytsev, A., Gruzdev, A., Ovchinnikov, G., Antipova, K., Ismailova, L., Muravleva, E., Burnaev, E., Semenikhin, A., Cherepanov, A., et al., 2019. Data-driven model for the identification of the rock type at a drilling bit. Journal of Petroleum science and Engineering 178, 506–516.

Lee, A.L., Gonzalez, M.H., Eakin, B.E., et al., 1966. The viscosity of natural gases. Journal of Petroleum Technology 18, 997–1.

Leil, T., 2014. A bayesian perspective on estimation of variability and uncertainty in mechanism-based models. CPT: pharmacometrics & systems pharmacology 3, 1–3.

Lockhart, R., Martinelli, R., 1949. Proposed correlation of data for isothermal two-phase, two-component flow in pipes. Chem. Eng. Prog 45, 39–48.

Mazzour, E.H., Hodouin, D., 2008. Measurement accuracy selection for designing observers of metallurgical plant performances, in: 2008 16th Mediterranean Conference on Control and Automation, IEEE. pp. 1478–1483.

McCain Jr, W., et al., 1991. Reservoir-fluid property correlations-state of the art (includes associated papers 23583 and 23594). SPE Reservoir Engineering 6, 266–272.

Neal, R.M., 2012. Bayesian learning for neural networks. volume 118. Springer Science & Business Media.

Nydal, O.J., 2012. Dynamic models in multiphase flow. Energy & Fuels 26, 4117–4123.

Onwuchekwa, C., et al., 2018. Application of machine learning ideas to reservoir fluid properties estimation, in: SPE Nigeria Annual International Conference and Exhibition, Society of Petroleum Engineers.

Pantelides, C.C., Renfro, J., 2013. The online use of first-principles models in process operations: Review, current status and future needs. Computers & Chemical Engineering 51, 136–148.

Psichogios, D.C., Ungar, L.H., 1992. A hybrid neural network-first principles approach to process modeling. AIChE Journal 38, 1499–1511.

Rasheed, A., San, O., Kvamsdal, T., 2019. Digital twin: Values, challenges and enablers. arXiv preprint arXiv:1910.01719 .

Ratto, M., Young, P., Romanowicz, R., Pappenberger, F., Saltelli, A., Pagano, A., 2007. Uncertainty, sensitivity analysis and the role of data based mechanistic modeling in hydrology. Hydrology and Earth System Sciences Discussions 11, 1249–1266.

Robert, C.P., Elvira, V., Tawn, N., Wu, C., 2018. Accelerating mcmc algorithms. Wiley Interdisciplinary Reviews: Computational Statistics 10, e1435.

Shrestha, D., Kayastha, N., Solomatine, D., 2009. A novel approach to parameter uncertainty analysis of hydrological models using neural networks. Hydrology and Earth System Sciences 13, 1235–1248.

Spesivtsev, P., Sinkov, K., Osiptsov, A., 2013. Comparison of drift-flux and multi-fluid approaches to modeling of multiphase flow in oil and gas wells. WIT Transactions on Engineering Sciences 79, 89–99.

Standing, M., et al., 1947. A pressure-volume-temperature correlation for mixtures of california oils and gases, in: Drilling and Production Practice, American Petroleum Institute.

Taitel, Y., 1986. Stability of severe slugging. International journal of multiphase flow 12, 203–217.

Wang, N., Sun, B., Wang, Z., Wang, J., Yang, C., 2016. Numerical simulation of two phase flow in wellbores by means of drift flux model and pressure based method. Journal of Natural Gas Science and Engineering 36, 811–823.

Whitson, C.H., Brulé, M.R., et al., 2000. Phase behavior. volume 20. Henry L. Doherty Memorial Fund of AIME, Society of Petroleum Engineers ....

Yang, C., Mao, Z.S., Wang, T., Li, X., Cheng, J., Yu, G., 2010. Numerical and Experimental Studies on Multiphase Flow in Stirred Tanks. volume 3. Bentham Science Publishers: Oak Park, IL, USA.

Chapter 5

Concluding remarks and recommendations for future work

5.1 Concluding remarks

The main objectives of this PhD work were to review the current methods of multiphase flowrate estimation, develop new approaches in this area and contribute to general approaches of combining machine learning and first principles models with a focus on oil and gas production systems and uncertainty estimation.

As the first step, a comprehensive literature review on multiphase flowrate estimation methods was performed. In the review, the following main points have been found:

- Currently, first principles-based approaches for multiphase flowrate estimation take the leading role, however, machine learning methods have a big potential to enhance, be combined or even replace them depending on the data availability.
- The current estimation methods still have a room for improvement because they still struggle with handling uncertainties in data used for model tuning, sensor measurements and model structures. This has to be addressed in research and development to make robust and accurate solutions.
- The general trend of the multiphase flowrate estimation methods development is positive and such approaches have the potential to replace physical multiphase flow meters in the near future. Currently, they can be successfully applied as a back-up system to hardware installations.

A major focus of this PhD work was concentrated on applications of machine learning methods and their combinations with first principles models towards accurate data-driven multiphase flowrate estimation solutions. Different approaches of combining machine learning with petroleum production physics have been tested together with various machine learning algorithms, e.g. neural network-based and regression tree-based ones. Based on the obtained results and many discussions with industrial experts, the following conclusions have been made:

- Machine learning models are very promising for multiphase flowrate estimation applications. This is particularly true for hybrid (machine learning + first principles) models.
- Even simple physical models introduced to machine learning models might enhance accuracy and explainability of the resulting data-driven solutions.
- Meta-modeling which combines different hybrid machine learning models creates the most accurate results among other combinations of machine learning models in case of multiphase flowrate estimation systems.

Finally, regarding the general applications of hybrid (machine learning + first principles) models with a focus on oil and gas systems and uncertainty estimation, two main approaches have been considered: sensitivity analysis of first principles models and Bayesian Machine Learning applied to first principles models. Different case studies have been considered such as increased measurement noise and drift, change in process conditions and unbalanced historical data for training Bayesian Machine Learning models. Based on these investigations, the following conclusions have been made:

- Accuracy of first principles multiphase flowrate estimation tools are very sensitive to measurement drift and relatively sensitive to measurement noise, while some simplifications can be made during the modeling process, for instance, in the thermodynamic part. As such, robust re-tuning process has to be performed regularly when measurement drift exists in the production system measurements.
- Bayesian Neural Networks are good tools for tuning first principles multiphase flow models to different process conditions and able to estimate uncertainties correctly depending on the historical distribution and the size of the data.

- Bayesian Neural Networks can be successfully used under changing process conditions of engineering systems in order to understand when there is a need to recalibrate the model or when there is a need to perform condition maintenance of the system.

Overall, throughout all the conducted work, we can see that accurate and physically meaningful combinations of machine learning and first principles models which also account for model uncertainties can create robust tools for multiphase flowrate estimation systems in oil and gas production fields. However, one needs to carefully select the right first principles models and machine learning algorithms depending on the data at hand as well as perform consistent tuning of the resulting hybrid models to achieve the best estimation results.

5.2 Recommendations for future work

Based on the conducted research work and the current research activity in the community of process and petroleum engineering, the following research directions can extend the work presented in this thesis:

- Considering dynamic Bayesian recurrent neural networks together with dynamic multiphase flow models. With this approach, it is potentially possible to accurately describe dynamic multiphase flow behavior using unsteady production data. This will allow to get valuable insights on how to operate the field in challenging dynamic conditions and estimate uncertainties of the resulting predictions.

- Extending the work conducted on Bayesian Neural Networks for tuning multiphase flow pipe models to the entire production system and investigate formal criteria under which model recalibration is required or when non-observable process conditions change and there is a need for condition maintenance.

- Extending the work on combining non-Bayesian machine learning methods and physics of process engineering systems and investigate how these models can be used under limited data criteria and how to perform transfer learning in such regression problems, such that the model from one well can be applied to another well with minimal model re-training.